STUDY OF CORRELOGRAMS OF DIESEL ENGINE PARAMETERS

by

MOHAMMAD REZA MODARRES-RAZAVI

B.Sc., D.I.C., M.Sc.

Thesis submitted for the degree of

Doctor of Philosophy

of the

University of London

June 1978

Thermal Power Section,
Department of Mechanical Engineering,
Imperial College of Science & Technology,
London SW7 2BX.

ABSTRACT

This work seeks to discover the influence of fuel injection system characterizing parameters (such as the starting time of injection and the quantity of fuel injected) on the cycle-to-cycle variations of cylinder pressure development for a naturally aspirated direct injection diesel engine.

The main contribution of this work is the development of a "dynamic modelling" concept, utilizing an engine performance prediction model. By this means, it was possible to analyse the response of an engine to small perturbations of the injection system parameters over a number of consecutive cycles.

The functional dependence of the fuel injection system characterizing parameters on the maximum rate of cylinder pressure rise, peak cylinder pressure and the angle of occurrence of the maximum rate of cylinder pressure rise was determined and the results are discussed in terms of the problem of cyclic dispersion in engines. On the basis of this analysis, it was shown that variations in injection system characteristics have a noticeable effect on the cycle-to-cycle combustion variabilities.

The statistical behaviour of various characterizing parameters of the combustion and fuel injection system were studied in terms of their histograms and correlograms for both the experimental and theoretically predicted results. Consequently, a distinct correlation has been found between the variations in the fuel injection system and the engine performance at high speed and low load conditions.

ERRATA

Correction	Mistake	Page	Line
electronic system	electronic device	35	4
radially	radically	51	11
have no effect	have not effect	53	4B
are non-linearly	are not linearly	59	3
introducing	introudcing	61	4
heat release	head release	68	2B
the mode of	the model of	87	3B
DAC	ADC	122	3
hierachical	hierachal	125	2B
(τ, $\hat{P}$ and $d\hat{P}$)	(τ, $\hat{P}$, $d\hat{P}$ and $\theta(d\hat{P})$)	151	9B
ratio	ration	160	1B
is haphazard, is	is haphazard and is	191	19
$\overline{\sigma^2}$ =	$\overline{\sigma_i^2}$ =	195	1AT
$log\ \overline{\sigma^2}$ =	$log\ \overline{\sigma_i^2}$ =	"	2AT
$\overline{\sigma^2}$ =	$\overline{\sigma_i^2}$ =	196	1AT
$log\ \overline{\sigma^2}$ =	$log\ \overline{\sigma_i^2}$ =	"	2AT
$\overline{\sigma^2}$ =	$\overline{\sigma_i^2}$ =	197	1AT
$log\ \overline{\sigma^2}$ =	$log\ \overline{\sigma_i^2}$ =	"	2AT
low load condition	low speed condition	216	9
dynamic	static injection, dynamic	231	13
$+ \sum \dot{Q}_i +$	$+ \sum Q_i +$	257	7
$+ \frac{1}{M} \sum \dot{Q}_i -$	$+ \frac{1}{M} \sum Q_i -$	"	12
$r_o = Y \tan \theta$	$r_o = T \tan \theta$	266	12
equation (A3.8)	equation (A3.10)	267	4
t_ω	t_W	267	8,10,15
Figure A3.2	Figure R5	269	7
$< 2S/D_v$	$< 25/D_v$	278	5
frustum	frustrum	"	6
height h is	height is	"	"
175 atm	170 atm	283	5B
$\hat{G}_k$ =	$\tilde{G}_k$ =	298	1
$n - m$	$N - m$	300	10 & 13
n	N	"	14

ACKNOWLEDGEMENTS

I would like to express my sincere gratitude to my supervisors, Professor W. Murgatroyd and Dr R.D. Wing, who gave so generously of their time, assistance and valuable advice to all stages of the work.

I would like to thank Dr N. Watson and Dr M. Marzouk for providing the original computer program and useful suggestions and remarks.

Thanks are also due to the technical staff of the Thermal Power Section, especially to Mr R.D. Bloxham for his assistance with the electronic hardware, and Dr T.F. Jones for his assistance in teaching the low level language (MACRO).

I am also very grateful to Miss E.A. Quin for her conscientious typing of the manuscript.

I would like to express my gratitude and my deep respect to my parents, who supported me and encouraged me in all aspects during the period of my studies.

CONTENTS

	Page
Abstract	2
Acknowledgements	3
Contents	4
Glossary of Symbols	9
List of Figures	18
CHAPTER 1 : INTRODUCTION	27
1.1 : Introduction & Objectives	27
1.2 : Organisation of the Thesis	30
CHAPTER 2 : LITERATURE SURVEY	32
2.1 : Introduction	32
2.2 : Cycle-to-Cycle Variation in Spark Ignition Engines	34
2.2.1 : Data processing techniques	44
2.2.2 : Characterizing parameters	44
2.2.3 : Empirical models	46
2.2.3.1 : Barton, Lestz & Meyer model	47
2.2.3.2 : Winsor & Patterson model	50
2.2.4 : Effect of different variables on cyclic variations	52
2.2.5 : Causes of the cycle-to-cycle variations	56
2.3 : Cycle-to-Cycle Variations in Diesel Engines	57
2.4 : Conclusion	59

		Page
CHAPTER 3 :	THEORETICAL ANALYSES	61
3.1 :	Introduction	61
3.2 :	Dynamic Modelling	62
3.3 :	Diesel Engine Simulation Program	67
3.3.1 :	Physical description	69
3.3.2 :	Governing relationships	72
3.3.3 :	Analysis procedure	77
3.4 :	Diesel Engine Combustion	79
3.4.1 :	Combustion models	82
3.4.2 :	Marzouk model	86
3.4.3 :	Ignition delay	92
3.5 :	General Remarks	103
CHAPTER 4 :	APPARATUS & MEASUREMENT TECHNIQUES	106
4.1 :	Introduction	106
4.2 :	Test Bed	108
4.2.1 :	The engine	108
4.2.2 :	The brake	113
4.2.3 :	Transducers	113
4.2.4 :	Differentiator	116
4.2.5 :	Digitiser	119
4.2.6 :	Speed and torque controller	120
4.2.7 :	On-line data logger	122
4.2.8 :	Off-line data logger	122
4.2.9 :	Interface	123
4.2.10 :	Computer	124
4.3 :	Control and Data Logging Software	124

		Page
4.3.1 :	Control logging software	127
4.3.2 :	Data logging software	129
4.3.2.1 :	PERFU2 program	129
4.3.2.2 :	AVESTD program	135
CHAPTER 5 :	STATISTICAL RESULTS	148
5.1 :	Introduction	148
5.2 :	Diesel Engine Time-Series	149
5.2.1 :	Engine measurements for correlations tests	151
5.2.2 :	Discussion of correlation measurements	154
5.2.2.1 :	Statistical parameters	155
5.2.2.2 :	Histograms	161
5.2.2.3 :	Auto-correlograms	169
5.2.2.4 :	Cross-correlograms	172
5.2.3 :	Properties of random data	178
5.2.3.1 :	Stationarity, ergodicity, normality and periodicity of random data	180
5.2.3.2 :	Run test	183
5.2.3.3 :	Homogeneity of variances	191
5.3 :	Dynamic Modelling Results	198
5.3.1 :	Perturbing input data	199
5.3.2 :	Planning of tests	203
5.3.3 :	Discussion on the predicted results	206
5.3.4 :	Analysis and comparison of predicted and experimental results	221
5.4 :	The Behaviour of the Characterizing Parameters	231

Page

5.4.1 : Characterizing parameters of the fuel injection process 231

5.4.1.1 : Starting angle of injection (dynamic injection) 232

5.4.1.2 : Quantity of injected fuel 235

5.4.1.3 : Duration of injection 236

5.4.2 : Characterizing parameters of the combustion process 238

5.5 : General Discussion of the Results 245

CHAPTER 6 : CONCLUSIONS 248

6.1 : Introduction 248

6.2 : Conclusions 249

6.3 : Suggestions for Future Work 252

APPENDICES

Appendix A1: Formulae for Internal Energy and Gas Constant 254

Appendix A2: Calculation of Apparent Rate of Heat Release 257

Appendix A3: The CAV Model 264

Appendix A4: Description of Optimization Program for the Modification of Ignition Delay Correlation 272

Appendix A5: The Procedure for Finding the Specific Heat Coefficient 276

Appendix A6: Effective Valve Area Calculations 278

Appendix B1: Specifications of the Engine 283

Appendix B2: Specifications of the Transducers 285

		Page
Appendix B3:	Specifications of the Amplifiers	287
Appendix B4:	Program Listings	288
Appendix C1:	Statistical Definitions	292
Appendix C2:	Regression Analysis	299
References		312

GLOSSARY OF SYMBOLS

a	:	regression constant
a_1, a_2, a_3	:	empirical constants in ignition delay correlation
a_t	:	white noise
A	:	mass of air entrained (gr)
$AC_r(x)$	:	auto-correlation coefficient of x at lag r
A/F	:	air/fuel ratio
A_b	:	flame front area (in^2)
A_g	:	geometric flow area (for inlet and exhaust valves) (in^2)
A_i	:	area exposed of the heat transfer surface i to the gas (in^2)
A_m	:	minimum valve flow area (in^2)
$A_{l,i}$	:	instantaneous values of linear area (in^2)
b	:	regression coefficient
c_1, c_2, c_3	:	shape coefficients in Wolfer formula
$cd1, cd2$	:	constants of diffusion burning function
$cp1, cp2$	:	constants of premixed burning function
$cw1, cw2$	:	shape coefficients of Wiebe formula
$CC_r(x,y)$	:	cross-correlation between x and y at lag r
C_d	:	coefficient of discharge
C_3	:	constant
d_c	:	critical distance during which the flame speed is sensitive to the local velocity (in)
$\hat{dm}_{fb}$	:	maximum rate of fuel mass burning ($lbm/^oCA$)
$dM_{fb}/d\theta$	:	the fuel mass burning rate with respect to the crank angle ($lbm/^oCA$)
$\hat{dP}$	:	maximum rate of cylinder pressure rise ($psi/^oCA$)
dW	:	work calculated from an increment of the PV diagram

D : cylinder bore (in)

D_i : diffusivity constant (cm^{-1})

D_n : nozzle hole diameter (cm)

DFR : degree of freedom due to regression

DFD : degree of freedom about regression

e_a : standard error for applied method

E : expansion ratio

E_r : air entrainment ratio

f : fuel/air ratio

f_s : stoichiometric fuel/air ratio

f : frequency (Hz)

f_c : cut-off frequency (Hz)

f_i : number of degrees of freedom

$f(U)$: increase in S_b as a function of the gas velocity U

F : equivalence ratio

F_τ : variance ratio for τ

F_w : constant related to the wall jet

$F(OV)$: function of operating variables

$FBR_p(\alpha)$: premixed fuel burning rate

$g(\overline{U}_i)$: function of average velocity at ignition

$\tilde{G}$: raw power spectral density

$\hat{G}$: smoothed power spectral density

h : time interval between samples (sec)

h_f : enthalpy of the fuel (Btu/lbm)

h_i : instantaneous heat transfer coefficient for surface i (chu/ft^2 ^{0}K sec)

$h(A/F)$: function of air/fuel ratio

$H(\hat{dP})$: histogram of maximum rate of cylinder pressure rise

HV : higher heating value (Btu/lbm)

ID : ignition delay (ms)

k : ratio of the turbulent flame speed to the turbulent velocity

k : integer number sample period shift

Kt : Kurtosis

l : length of connecting rod (in)

L : valve lift (in)

m : maximum lag number

m_f : quantity of fuel injected (lbm)

m_j : mass flow through surface j (lb/sec)

m_t : total mass flow into a cylinder (lb/sec)

M : molecular weight

M : mass in the system (lbm)

M : Bartlett criterion

M_o : mass prior to fuel addition (lbm)

M_a : mass of micromixed air (gr)

M_f : mass of micromixed fuel (gr)

MSR : mean square value (due to regression)

MSD : mean square value (about regression)

n : number of cylinders

n : heat capacity ratio

N : total number of sample products

N : engine speed (rpm)

N_1 : number of (+)

N_2 : number of (-)

P : total pressure in the system (psi)

$\overline{P}$: mean cylinder pressure during cycle (psi)

$\hat{P}$: peak cylinder pressure (psi)

P_{inj} : injection pressure (atm)

P_m : arithmetic mean of cylinder gas pressure during delay (psi)

Q : volume flow in wall jet (cm^3/sec)

Q : heat transfer (Btu)

$\dot{Q}_i$: rate of heat transfer through surface i (Btu/sec)

r : run variable

r : crank radius (in)

r : radius of wall jet front from axis (cm)

R : gas constant (Btu/lbm ^oR)

$\hat{R}_r$: estimate of auto-correlation at lag r

s : sum of square deviation errors

S_b : laminar burning velocity (ft/sec)

$S(X)$: standard deviation of variable X

$S(t_b^*)$: standard deviation of total burn time (sec)

Sk : skewness

SSR : sum of explained error (due to regression)

SSD : sum of unexplained error (about regression)

SST : total error

t : time since beginning of injection (sec)

t_b : initial burn duration (sec)

t_c : critical time; that is, time of burn to the critical distance (sec)

t_o : initial reference time in wall jet (sec)

t_{oc} : the time for one engine cycle (720^oCA)

t_p : injection period (^oCA)

t_w : current reference time in wall jet (sec)

t_Y : time for impingement (sec)

T : averaging time

T : gas temperature of the system (^{o}R)

T_i : average surface temperature (^{o}R)

T_{inj} : cylinder gas temperature at injection point (^{o}K)

T_m : arithmetic mean of cylinder gas pressure during the delay (^{o}K)

T_s : sample period

U : gas velocity (cm/sec)

U : velocity of fluid (ft/sec)

U : specific internal energy of the system (Btu/lb)

V : volume of the system (in^3)

V_b : volume of the burned gases (in^3)

$V_{e,i}$: instantaneous values of cylinder volume (in^3)

V_{cyl} : swept volume (in^3)

V_f : jet front velocity (cm/sec)

V_f : flame velocity (ft/sec)

V_{ig} : cylinder volume at ignition point (in^3)

V_p : mean piston speed (ft/sec)

W : jet front velocity on the wall (cm/sec)

W_t : total engine indicated work (ft.lb/cyl)

x : ratio of fuel burned at any instant to total fuel present

x : independent variable

$\overline{x}$: average of sample variable x

$\hat{x}$: maximum value of sample variable x

Y : impingement distance (cm)

y : dependent variable

y : penetration of free jet front (cm)

y_c : computed dependent variable

z : ratio of gas density relative to air at NTP

$\tilde{Z}_{t-1}$: previous value of the process

Greek Symbols

α : dimensionless time function

β : mode of burning proportionality factor

β : quantity of fuel injected as a perturbing parameter (lbm)

γ : specific heat ratio

δ : jet thickness on wall (cm); injection duration

ε : error

θ : cone half angle (degree)

θ_i : crank angle at ignition point (^{o}CA BTDC)

$\theta(\hat{P})$: the crank angle at which $\hat{P}$ occurs (^{o}CA ATDC)

μ_r : mean value of run variable

ρ_a : gas density in cylinder (gr/cm^3)

ρ_{ic} : mixture density at intake valve closure

σ_a : standard deviation for applied method

$\hat{\sigma}_b$: standard error of regression coefficient

$\sigma_{d\hat{P}}$: standard deviation of $d\hat{P}$

σ^2 : variance

τ : dynamic injection (^{o}CA BTDC)

χ^2 : statistical chi-squared variable

Ω_e : engine speed

Subscripts

a : subscript denoting the applied method; air

b : burning or burned

c : cylinder

co : computed

cr : critical

c : cut-off

d : discharge

ds : downstream

e : exhaust manifold

e : end of burning

f : fuel

fb : fuel burned

f,d : diffusion fuel burning

f,p : premixed fuel burning

f,t : total fuel burning

g : gas

i : induction manifold

i : index subscript (e.g. designated to instants between inlet valve closed to instant of ignition occurrence)

ic : intake valve closure

ig : corresponds to time of ignition

inj : corresponds to time of injection

k : subscript denoting the mode of combustion

n : subscript denoting the normal method

o : one engine cycle.

p : piston

r : run

s : steam

us : upstream

v : valve

w : wall

Y : impingement

o : initial (prior to fuel addition)

Superscripts

$\dot{}$	:	derivative of that function with respect to time
$\hat{}$	:	peak; estimated
$\bar{}$	:	mean
$\tilde{}$	:	raw
*	:	no dissociation
*	:	total

Abbreviations

ABDC	:	after bottom dead centre
ADC	:	analogue digital converter
AROH	:	apparent rate of heat release
ATDC	:	after top dead centre
BBDC	:	before bottom dead centre
BMEP	:	brake mean effective pressure
BTDC	:	before top dead centre
CA	:	crank angle
CI	:	compression ignition
CO	:	carbon monoxide
CTCV	:	cycle-to-cycle variation
CV	:	coefficient of variation
dc	:	direct current
DAC	:	digital analogue converter
DCA	:	degree of crank angle
DI	:	direct injection
DPA	:	distributor pump model A
EVC	:	exhaust valve closing
EVO	:	exhaust valve opening

FMEP	:	friction mean effective pressure
H_2	:	hydrogen
HC	:	hydrocarbon
IC	:	internal combustion
ID	:	ignition delay
IMEP	:	indicated mean effective pressure
IVC	:	inlet valve closing
IVO	:	inlet valve opening
N_2	:	nitrogen
NADI	:	naturally aspirated direct injection
NAG	:	Numerical Algorithm Group
NO	:	nitric oxide
O_2	:	oxygen
OV	:	operating variables
ROB	:	rate of burning
SA	:	spark advance
SI	:	spark ignition
TDC	:	top dead centre

LIST OF FIGURES

			Page
Figure 3.1	:	Diagram of dynamic modelling	65
Figure 3.2	:	Engine thermodynamic system	70
Figure 3.3	:	Fuel burning rate distribution	89
Figure 3.4	:	Cumulative mass of fuel burnt and heat released	89
Figure 3.5	:	Simulation program predicted results at given operating conditions	93
Figure 3.6	:	Comparison of ignition delay formulae with the aid of experimental data	96
Figure 3.7	:	Mean cylinder temperature, mean cylinder pressure and ignition delay as functions of BMEP	99
Figure 3.8	:	Ignition delay and dynamic injection as a function of BMEP	101
Figure 3.9	:	Comparison of predicted and experimental results at given operating conditions	105
Figure 4.1	:	Hardware system of Perkins control engine	109
Figure 4.2	:	The Perkins 4.236 diesel engine test bed	110
Figure 4.3	:	The computer, interface, ADC, multiplexor and monitoring devices	111
Figure 4.4	:	Injector characteristics	112
Figure 4.5	:	Operating limits for engine and dynamometer; fixed torque/speed test points	114
Figure 4.6	:	Voltage to frequency sawtooth signal and its differentiated signal by differentiator	118
Figure 4.7	:	Calibration curve for differentiator	118

			Page
Figure 4.8	:	Motored cylinder 1 test for finding the location of TDC	121
Figure 4.9	:	Software architecture for diesel engine	126
Figure 4.10	:	Perkins software system flowchart	128
Figure 4.11	:	Signals, sampling and timing diagram for PERFU2	131
Figure 4.12	:	Block diagram of subroutine PERFU2	132
Figure 4.13	:	PERFU2 Macro program flowchart (analysis)	134
Figure 4.14	:	Typical output of sample data analysis (histograms)	137
Figure 4.15	:	Typical output of sample data analysis (auto-correlograms)	138
Figure 4.16	:	Typical output of sample data analysis (cross-correlograms)	139
Figure 4.17	:	Signals, sampling and timing diagram for cylinder 2 (AVESTD)	140
Figure 4.18	:	Block diagram of program AVESTD	142
Figure 4.19	:	AVESTD Macro program flowchart (analysis)	143
Figure 4.20	:	Typical plot of sampling by AVESTD	147
Figure 5.1	:	Typical sample data for $\hat{P}$, $d\hat{P}$ and τ at low load-low speed conditions	150
Figure 5.2	:	Typical sample data for $\hat{P}$, $d\hat{P}$ and τ at low load-high speed conditions	150
Figure 5.3	:	Typical sample data for $\hat{P}$, $d\hat{P}$ and τ at high load-low speed conditions	152
Figure 5.4	:	Typical sample data for $\hat{P}$, $d\hat{P}$ and τ at high load-high speed conditions	152
Figure 5.5	:	Two of the typical sample data discarded	153

		Page
Figure 5.6	: Histograms for τ, $\hat{dP}$, $\theta(\hat{dP})$ and $\hat{P}$ at a speed of 2500 rpm and a load of 6.18 mkp	157
Figure 5.7	: Auto-correlograms of τ, $\hat{dP}$, $\theta(\hat{dP})$ and $\hat{P}$ at a speed of 2500 rpm and a load of 6.18 mkp	158
Figure 5.8	: Cross-correlograms of τ & $\hat{dP}$, τ & $\theta(\hat{dP})$, and τ & $\hat{P}$ at a speed of 2500 rpm and a load of 6.18 mkp	159
Figure 5.9	: Bimodal distribution obtained from the combination of two normal distributions	162
Figure 5.10	: Histogram of dynamic injection at a speed of 2750 rpm and a load of 5 mkp operating conditions	162
Figure 5.11	: (a) Histogram of maximum rate of cylinder pressure rise indicating a probable presence of periodic components	164
	(b) Histogram of maximum rate of cylinder pressure rise indicating normal distribution	164
Figure 5.12	: Histograms of τ, $\hat{P}$, $\hat{dP}$ and $\theta(\hat{dP})$ at Test 13	165
Figure 5.13	: Histograms of τ, $\hat{P}$, $\hat{dP}$ and $\theta(\hat{dP})$ at Test 19	166
Figure 5.14	: Histograms of τ, $\hat{P}$, $\hat{dP}$ and $\theta(\hat{dP})$ at Test 43	167
Figure 5.15	: Histograms of τ, $\hat{P}$, $\hat{dP}$ and $\theta(\hat{dP})$ at Test 49	168
Figure 5.16	: Distorted bell-shaped distribution obtained from two normal distributions	169
Figure 5.17	: Cross-correlation coefficient (zero order) between τ and $\hat{dP}$ as a function of speed for various torques	174
Figure 5.18	: Cross-correlation coefficient (zero order) between τ and $\hat{dP}$ as a function of brake power for various speeds	175

Page

Figure 5.19 : Mean value, standard deviation and coefficient of variation for dynamic injection against brake power for different speeds 176

Figure 5.20 : Mean value, standard deviation and coefficient of variation for maximum rate of cylinder pressure rise against brake power for different speeds 177

Figure 5.21 : Ensemble of series for defining stationarity and ergodicity 180

Figure 5.22 : Auto-correlation and spectral density of τ and $\hat{dP}$ at Test 13 184

Figure 5.23 : Auto-correlation and spectral density of τ and $\hat{dP}$ at Test 17 185

Figure 5.24 : Auto-correlation and spectral density of τ and $\hat{dP}$ at Test 18 186

Figure 5.25 : Auto-correlation and spectral density of τ and $\hat{dP}$ at Test 19 187

Figure 5.26 : Dynamic modelling prediction results at Test 49A when generated random values of τ are used as perturbing parameter 200

Figure 5.27 : Dynamic modelling prediction results at Test 49A' when experimental values of τ are used as perturbing parameter 200

Figure 5.28 : Dynamic modelling prediction results at Test 19A when generated random data for τ are used as perturbing parameters 204

Page

Figure 5.29 : Dynamic modelling prediction results at Test 19B when generated random data for m_f are used as perturbing parameters 205

Figure 5.30 : Dynamic modelling prediction results: τ and m_f perturbing simultaneously by generated random values 207

Figure 5.31 : Dynamic modelling prediction results. Experimental values for τ used as perturbing parameters at given operating conditions 208

Figure 5.32 : Significance of reduced interval in dynamic modelling modelling prediction results when perturbed values were small 210

Figure 5.33 : Dynamic modelling prediction results at Test 43B when generated random values for m_f are used as perturbing parameters 211

Figure 5.34 : Generated random values for τ as a perturbing parameter for given operating conditions 212

Figure 5.35 : Generated random data for m_f as a perturbing parameter for given operating conditions 213

Figure 5.36 : Experimental data for τ as a perturbing parameter for given operating conditions 214

Figure 5.37 : Experimental data for given operating conditions 215

Figure 5.38 : Different functional dependences for x and y 217

Figure 5.39 : Effect of different curvature of functional dependences on the output histograms 220

Figure 5.40 : Experimental data presented graphically to show $F(d\hat{P},\tau)$, $F(\theta(d\hat{P}),\tau)$, $F(\hat{P},\tau)$ and $F(\theta(d\hat{P}),\tau)$ 222

Page

Figure 5.41 : Linear regression for $d\hat{P}$, $\theta(d\hat{P})$ and $\hat{P}$ against τ at a speed of 2500 rpm and a load of 6.38 mkp 224

Figure 5.42 : (a) Cross-correlogram between predicted values of $d\hat{P}$ and generated values for τ at Test 19A 229

(b) Cross-correlogram between predicted values of $d\hat{P}$ and minus values of experimental data for τ at Test 19A' 229

(c) Cross-correlogram between predicted values of $d\hat{P}$ and generated values of τ when both τ and m_f were perturbed simultaneously at Test 19C 230

Figure 5.43 : Histogram of dynamic injection at an engine speed of 2500 rpm and an engine load of 10 mkp 234

Figure 5.44 : Variation of the maximum rate of heat release to the duration of injection 237

Figure 5.45 : Experimental results at low load-low speed conditions indicating the existing correlation between different combustion characterizing parameters 239

Figure 5.46 : Experimental results at low load-high speed conditions 240

Figure 5.47 : Experimental results at high load-low speed conditions 241

Figure 5.48 : Experimental results at high load-high speed conditions 242

Figure 5.49 : Dynamic modelling prediction results for low load-high speed. Correlations between different combustion characterizing parameters 244

			Page
Figure A2.1	:	Typical unsmoothed diagrams for showing the shock waves on rate of cylinder pressure rise diagram	260
Figure A2.2	:	Effect of different degree of smoothing on the rate of cylinder pressure rise diagram	262
Figure A2.3	:	Experimental results at given operating conditions. Apparent rate of burning obtained by the Borman method	263
Figure A3.1	:	Fuel spray free jet and wall jet air entrainment model	264
Figure A3.2	:	Comparison between predicted (CAV model) values and experimental results for the rate of heat release and cumulative heat release at given operating conditions	270
Figure A5.1	:	Typical cylinder pressure diagram	276
Figure A6.1	:	Position of standard type valve for different lift	279
Figure A6.2	:	Effective valve area for inlet and exhaust valves	282

LIST OF TABLES

			Page
Table 3.1	:	A number of published ignition delay correlations	95
Table 3.2	:	Ignition delay, mean cylinder pressure, mean cylinder temperature and specific heat ratio at different operating conditions	100
Table 4.1	:	Output of sample data analysis (statistical parameters)	136
Table 5.1	:	Output of sample data analysis at a speed of 2500 rpm and a load of 6.18 mkp (statistical parameters)	156
Table 5.2	:	Percentage points of run distribution	189
Table 5.3	:	Typical values of run test	190
Table 5.4	:	F-test for variability of variances	192
Table 5.5	:	Bartlett test	195
Table 5.6	:	Bartlett test	196
Table 5.7	:	Bartlett test	197
Table 5.8	:	Tabulated mean value and standard deviation of τ and m_f	202
Table 5.9	:	Classified correlation coefficient for different tests	226
Table 5.10	:	Comparison of predicted and experimental coefficients of variation	227
Table A2.1	:	Volumetric efficiency against engine speed	259

			Page
Table C2.1	:	Regression analysis for Test 19A (generated values for τ)	304
Table C2.2	:	Regression analysis for Test 19AP (experimental values for τ)	306
Table C2.3	:	Regression analysis for Test 19C (generated values for τ and m_f)	308
Table C2.4	:	Regression analysis for Test 19E (experimental data)	310

CHAPTER 1

INTRODUCTION

1.1 INTRODUCTION & OBJECTIVES

Previous methods for increasing the thermal efficiency of an engine (such as increasing the compression ratio and the development of more efficient combustion chambers) have been constrained by such factors as noise, emissions, power-to-weight ratio, and expense. This has directed research towards further perfection of existing designs rather than radical changes and attention has thus been directed towards improvement of cyclic variation in internal combustion engines (IC engines). The term "cyclic variation" refers to the fact that in IC engines the cylinder pressure during combustion does not identically repeat from cycle to cycle at any given operating condition. This cycle-to-cycle variation (CTCV) is an important engine malfunction which gives rise to various problems, such as unsteadiness of power output (surge), loss of efficiency, reduction in economy and reliability, increased exhaust emissions, and significantly increased engine noise. Improvement of excessive surge and roughness noise brought the first incentive for research in cyclic variation, because these were not tolerable in passenger cars. Later, the control of exhaust emissions played a greater rôle in studies of this topic after the introduction of restrictive legislation for passenger car exhaust emissions. Since the early fifties, the cyclic variation problem has attracted the attention of many researchers. In 1960, Soltau wrote that, had maximum pressure in all cycles remained equal to that of the highest pressure, a gain of 10% in power output would have been realized. Hence, an understanding of the cause of CTCV in IC engines is clearly valuable in the study of many aspects of engine performance and exhaust

emissions.

Early studies of cyclic variation were mainly concerned with spark-ignition engines (SI engines), as it was thought that in the case of diesel engines only insignificant variation would exist as a result of the different nature of combustion in these engines. However, Wing (1975) demonstrated that CTCV in naturally aspirated direct injection (NADI) diesel engines exists to a surprisingly large extent and he investigated its effect on the nitric oxide emissions.

Available literature on cyclic variation shows that most of the work has been related to SI engines, not only because of the high degree of variation due to the nature of combustion in which a flame propagates in a homogeneous fuel/air mixture, but also because of the wide application of these engines in passenger cars where smoothness of running and low noise are of commercial importance.

Fuel economy has recently brought the use of diesel engines in passenger cars into prominence. Some diesel engine problems (surge, roughness and exhaust emission) which were not regarded as important in many industrial applications, are now attracting more attention.

A general study of cyclic variation in NADI diesel engines, and particularly its effect on nitric oxide formation, was first carried out in the Thermal Power Section of Imperial College employing a computer controlled diesel engine facility (Wing & Murgatroyd (1972); Modarres-Razavi (1973); Pires (1973); Wing (1975)). The statistical analyses carried out on certain possible engine parameters engendering these variations raised a demand for further research in this subject.

On the basis of these studies, it was shown that fuel injection variations are the dominant cause of cyclic variation in NADI diesel engines. Therefore, an accurate knowledge of the inter-relation of

injection system characteristics (i.e. starting angle of injection* or quantity of fuel injected) and CTCV in a NADI diesel engine has become this author's main task.

The work presented in this thesis attempts to analyse the experimental correlation existing between injection system characteristics (mainly starting angle of injection which was previously shown as the most significant parameter) and the cylinder pressure development characteristics (i.e. maximum rate of cylinder pressure rise, peak cylinder pressure, time of occurrence of the maximum rate of cylinder pressure rise) at different operating conditions. Furthermore, a simulation program is presented which correlates injection system parameters with the CTCV in order to interpret the correlograms obtained from experimental results. The simulation program models the combustion for a large number of consecutive cycles and employs either artificial or experimental values of the fuel injection parameters for each cycle instead of using mean values of those parameters, as is the case with most combustion models.

This "dynamic† modelling" will therefore be a useful tool with which to compare experimental results and to investigate the influence of

---

* The terms "starting angle (time) of injection", "timing of injection" and "dynamic injection" have been used in previous literature to describe the angle at which injection occurs. In this work, the term "starting angle of injection" was used except where the setting injection time (static injection) and actual injection time (dynamic injection) were discussed.

† "Dynamic" is used in the sense that these programs take account of the injection characteristic for each cycle instead of using a mean value.

variation of certain parameters on the predicted correlation results. Having analysed the correlograms, histograms and the other statistical terms pertinent to the predicted and experimental values, a physical explanation was made of certain extraordinary results obtained (i.e. the negative correlation between starting time of injection and the maximum rate of cylinder pressure rise at high brake horsepower). The present technique also provides an assessment of the validity of using mean values in combustion simulation programs, the normal practice of engine designers, instead of considering the changing variables in the non-linear diesel engine combustion process. Furthermore, the functional relationship between CTCV of various characterizing parameters of the combustion and fuel injection system characteristics are established.

1.2 ORGANISATION OF THE THESIS

The present chapter serves as an introduction to this thesis. As one aspect of this study is concerned with cycle-to-cycle variations in diesel engines and variations of the fuel injection system parameters, a literature survey of the previous works on cyclic variations in both petrol and diesel engines is given in Chapter 2. In this chapter, the effect on cyclic variation of different operating parameters and all other significant variables has been reviewed. Emphasis has been particularly focused on the effect of injection system characteristics on cylinder pressure oscillation and subsequently on exhaust emissions. Critical discussion of previous work presents the justification necessary for the assumptions made in this work.

The dynamic modelling technique has been created for studying the effect of injection system characteristics on diesel engine combustion and also the effect of one cycle on later cycles. A description of this

original technique and discussion of the principal assumptions made are given in Chapter 3. The diesel engine simulation program based on the "filling and emptying" concept, and the combustion model based on the fuel burning rate approach which involves the two functions presenting the pre-mixed and diffusion burning, are also described in this chapter. The justification for the choice of this particular model is presented, and a description of another model given in Appendix A3.

In Chapter 4, a brief description of the computer controlled test bed, details of instrumentation and the data acquisition system has been provided. As the computer controlled test bed data acquisition system in general are described elsewhere (Bloxham et al (1972); Jones & Wing (1975)), details are given only of differences from the system used in previous studies.

A description and comparison of the results obtained from statistical analysis of the predicted and the experimental data are presented in Chapter 5. The auto-correlation, histogram, power spectral density, and appropriate cross-correlation of each set of data are presented. Discussion of the results follows the description of each represented test and the reasons for differences between the predicted and experimental data are also examined.

A general conclusion and discussion of the contribution made by this thesis and a plan for further research on this subject are provided in Chapter 6.

The appendices following the main parts contain information which is not directly essential to an understanding of the main text, but provide a more detailed analysis of some relevant problems.

CHAPTER 2

LITERATURE SURVEY

2.1 INTRODUCTION

For a long time the improvement of internal combustion engine efficiency, reliability, steady power output, engine roughness, exhaust gas emission, and cost of building has been the objective of many studies. In the early stages, these improvements - especially the increase in thermal efficiency - have been mostly achieved by increasing the compression ratio, employing better quality fuel, and more efficient combustion chambers. The incentive for more research has been growing as the result of problems such as air pollution in cities (e.g. smog in Los Angeles and Tokyo) and the resulting introduction of new legislation limiting the exhaust emission of vehicles. Although potential gains become smaller as the theoretical limit is approached, the new design criteria of low exhaust emission are now even more challenging than the other parameters.

At present, one of the important and unsolved problems in internal combustion engines is the unsteady power output which is termed as "surge". It has been known for many years that power fluctuation is mainly caused by the fact that the combustion process differs from cycle to cycle and from cylinder to cylinder. In other words, cylinder pressure development is a random function during the combustion period and peak pressure values often differ by as much as 30% for spark-ignition engines (Patterson (1966)). This cyclic variation exists under all engine operating conditions (Vichnievsky (1955)). If combustion variations can be eliminated, smoother and more steady power will be obtained, leading to an economy increase of 10%-20%, as well as an appreciable reduction in the

exhaust emissions and the engine noise (Patterson (1966)).

Since the magnitude of the combustion variations in spark-ignition engines are noticeably higher than those in the diesel engine due to the different nature of combustion, most of the work and documentation in this field relates to spark-ignition engines (Vichnievsky (1955); Soltau (1960); Curry (1963); Patterson (1966); Karim (1967); Cole & Mirsky (1968); Peters & Borman (1970); Barton, Kenemuth, Lestz & Meyer (1970); Hansel (1970,1971); Tanuma, Sasaki, Keneko & Kawasaki (1971); Barton, Lestz & Meyer (1971); Matsuoka, Yamaguchi & Umemura (1971); Burgett, Leptich & Sangwan (1972); Winsor & Patterson (1973); Milkins, Watson, Goldsworthy & Hallworth (1974); Chen & Krieger (1974); Watson, Goldsworthy & Milkins (1976)). Nevertheless, the existence of significant cyclic variations in a direct injection diesel engine under certain operating conditions and revelation of the effect of these variations on the exhaust emissions (Wing (1975)), has raised interest for more profound research in diesel engines. On this ground, the effect of different engine operating parameters on the cyclic variations and the causes of these cycle-to-cycle variabilities are to be studied.

Several different characteristics of cylinder pressure record (i.e. the peak cylinder pressure, the maximum rate of cylinder pressure rise, the indicated work per cycle, the maximum torque, etc.) have been studied by different researchers to assess the combustion variations. The variation of these parameters have been viewed absolutely or relatively as a percentage of their mean values and, therefore, a certain amount of confusion has been introduced on this account.

Since combustion variation results from apparently random events, it is necessary to sample a large number of cycles from each cylinder in order to accurately determine the magnitude of the cyclic variation.

A survey of previous work on cycle-to-cycle variations in spark-ignition engines follows as these give valuable guidance in understanding the nature of cyclic variations in compression-ignition engines, since (i) some similarities exist between these two processes, and (ii) the techniques and instrumentation used to study both engine types are virtually identical.

2.2 CYCLE-TO-CYCLE VARIATION IN SPARK-IGNITION ENGINES

The previous works relating to different aspects of the cycle-to-cycle variations in spark-ignition engines can be classified as follows:

I. Testing the effect of different operating variables on the extent of cyclic combustion variation.
II. Studying the engine defects, such as knocking combustion and engine roughness, in relation to cycle-to-cycle variations.
III. Finding the causes of the cycle-to-cycle variations.
IV. Studying the exhaust emission and the means of reducing it.
V. Non-specified category.

I. Vichnievsky (1955), Soltau (1960), Patterson (1966), Karim (1967), Peters & Borman (1970), and Barton et al (1970) all started by investigating the effect of different engine parameters on the cyclic combustion variations aiming to discover the causes of the cylinder pressure fluctuation and the means of preventing it. However, they only succeeded in showing the influence of some variables on the cycle variations, and failed to find out the causes of these variations. The basic difference between all these works is the use of different instrumentation, data processing techniques, number of samples (which

itself is limited by the data processing techniques), engine and cylinder pressure characterizing parameters (different characterizing parameters have been discussed in Section 2.2.2).

Using an electronic device, Vichnievsky sampled about 500 cycles and thus studied the cyclic (peak pressure) variations statistically. He showed that:

(a) Cyclic variations always exist, regardless of the engine operating conditions or the fuel type.

(b) The chemical nature of the fuel affects the burning velocity during the whole combustion phase, and especially has an appreciable influence on the standard deviation of the peak cylinder pressure.

(c) The mixture strength has an important effect on the peak pressure cyclic variation.

(d) Spark timing is not entirely responsible for the combustion dispersion. (It has been previously thought that the cycle-to-cycle variations are caused by the changes in the spark timing due to the variation of the drive or distributor mechanism.)

By employing photographic recording techniques, Soltau examined the effect of every working variable on the combustion variations using mostly 10-12 cycles. The variables studied in this research were: ignition system characteristic (spark timing, spark energy, spark plug, electrode shape, type of ignition, number of ignition sources, spark plug position), air/fuel ratio, fuel, compression ratio, exhaust gas dilution, air movement, heat release, squish turbulence, flame propagation, and

cylinder head wall temperature. In this study, Soltau concluded that those parameters which increased the rate of cylinder pressure rise can usually cause a reduction in the cyclic variations at the peak cylinder pressure, and that the deviations in peak pressure and indicated mean effective pressure were both caused by differences in the heat release rate from cycle to cycle. He also showed that, during the burning process, the only factor which remains reasonably constant in every cycle is the duration of the second stage of combustion. (The combustion process has been divided by him into three defined phases: firstly, the delay period between the occurrence of the electric spark and the start of a stable flame front; secondly, the stage of propagation of the flame front; and, thirdly, the phase during which most of the heat is released.)

Patterson sampled nearly 2000 cycles and employed a statistical analyser in order to examine the effect of several operating variables (swirl and turbulence, mixture preparation, ignition system, fuel distribution, exhaust residual) on the extent of cyclic dispersion in a multi-cylinder engine. Based on some unreported hot-wire velocity measurements in the combustion chamber of a motored engine, and on the premise that the engine speed or the mixture motion has a significant effect on the combustion rate in a constant volume system, Patterson indicated that the major cause of the combustion rate variation is the mixture velocity differences that exist in the cylinder near to the spark plug at the time of ignition. He suggests a possible mechanism to support his postulation by hypothesizing that combustion rate is affected by velocity gradients through wrinkling and distortion of the flame front. His description of the causes of the cyclic variations is, however, based on conjecture rather than theory. Finally, he showed that the extent of variations can be reduced by increasing the average combustion rate.

Employing a photographic recording technique and using a similar engine to that previously used by Soltau, Karim sampled 100 cycles and studied quantitatively the effect of some engine operating variables on the extent of cyclic variations (such as charge mixture strength, type of fuel, spark ignition characteristic, concentration of diluents in the charge, the degree of throttling, the cylinder water jacket temperature). He showed that the histogram of peak pressure constructed from a sample of 400 cycles should not necessarily follow a normal distribution. Although his results were presented in a quantitative form, they were sufficient only to confirm the previous conclusions.

Peters & Borman studied the effect of cyclic pressure changes and engine variables on the mass burning rate, and analytically showed:

(a) The low pressure cycles were initially those of the slow burning cycles.

(b) Although there are large cyclic cylinder pressure variations in the actual engine data, the differences in the work output of various cycles are negligible.

A statistical analysis of the peak pressure, the maximum rate of cylinder pressure rise and the angles at which the peak pressure and the maximum rate of cylinder pressure rise occur were carried out by Barton, Kenemuth, Lestz & Meyer. Using a magnetic tape recording facility, they sampled batches of 200 samples and showed that there exist significant differences in the standard deviation of the four pressure development parameters at different engine operating conditions. For the first time in the history of this topic, they employed correlation techniques to show the statistical relation between each pair of parameters or consecutive

cycles. (They used the auto-correlation coefficient to show the exhaust residual effect from the previous combustion cycle. Previous investigators, such as Soltau, Patterson and Karim, studied the same effect on the basis of firing every other cycle.) Their conclusions are summarised as follows:

(a) The combustion process variation does not depend on any other combustion cycle but only on the intake, the compression and the combustion process of each individual cycle.

(b) The cross-correlation coefficient indicates a one-to-one linear association between the peak cylinder pressure and the maximum rate of cylinder pressure rise.

(c) The average flame speed changes, the cyclic variation of the flame speed and the phasing of the combustion process are the most important parameters affecting the engine output variations.

(d) The engine variables having the most significant effect on the combustion variations are those affecting the intake process (that is, the speed effect and the changes in the intake preparation).

The effect of different engine parameters on the extent of cycle-to-cycle combustion variations has been discussed in Section 2.2.4.

II. Curry (1963) investigated abnormal combustions, especially the characteristics of the knocking process in spark-ignition engines. He showed that the average burning rate of knocking cycles is significantly

greater than the average burning rate of the non-knocking cycles, throughout the entire cycle.

Andon & Marks (1964) studied engine roughness and the means of improving it. They discovered that the objectionable low frequency rapping sound is caused by uneven intensity noise bursts which vary in amplitude from cycle to cycle and cylinder to cylinder. The structural vibrations which cause the "roughness noise" can be eliminated by reducing the rate of cylinder pressure rise during the combustion. Retarding the ignition timing is not generally a satisfactory solution to avoid the "roughness noise" problem because of the large power and economy loss it causes. With a stiffer engine structure, higher burn rates can be used without generating roughness noise; however, appreciable gains are only achieved by elimination of the cylinder-to-cylinder and cycle-to-cycle variations.

The importance of their achievements in finding the existing inter-relations between the cycle-to-cycle combustion variations and other engine problems (such as knocking combustion, noise and vibrations) is in no doubt. But, because these studies were not directly related to the cyclic variations, they did not provide an answer to the question "What are the causes of cycle-to-cycle combustion variations?".

III. Cole & Mirsky (1968), Hansel (1970), Barton et al (1971), Matsuoka et al (1971), and Winsor & Patterson (1973) all based their work on the Patterson (1966) conjecture that "... the major cause of combustion rate variation is the mixture velocity variations that exist within the cylinder near the spark plug at ignition.". They tried to correlate the mixture motion variations to the cyclic combustion variations.

Cole & Mirsky used a constant volume cylindrical bomb as the

first order simulation of the spark-ignition engine combustion process to examine the suspected influence of the mixture motion on the cyclic combustion variations. They showed that:

(a) The sensitivity of the flame kernel to the disturbance can be attributed to the size of these disturbances.

(b) The rate of pressure rise increases approximately linearly with the mixture jet velocity and the width of the mixture jet has some effect on the rate of pressure rise.

Hansel presented a semi-quantitative model for describing the cycle-to-cycle variation of the peak cylinder pressure in spark-ignition engines by utilizing turbulent combustion theory. In this model, the maximum variation in peak cylinder pressure (arising from the variation in the flame propagation time) is assumed to be proportional to the variation in mass burning rate of the kernel (caused by the interaction of the kernel with the turbulent flow). He showed that the cyclic variation in peak cylinder pressure is primarily a function of the air fuel ratio and random variation in turbulence intensity. However, this semi-quantitative model may only provide a reasonable prediction for lean mixture ratios.

Barton, Lestz & Meyer developed an empirical model for correlating the cyclic cylinder gas motion and the combustion variations of a spark-ignition engine. The correlation was obtained by using a model which was originally based on the assumption that the time required to burn the same initial volume of the charge in each cycle was only a function of the gas velocity. They measured the velocities and their variations at the spark location of a motored engine with a platinum hot-film anemometer, and attempted to relate these velocity variations to the combustion

variations. However, they could only demonstrate a known correlation between the mean velocity and its variations.

Matsuoka, Yamaguchi & Umemura followed a similar objective. From the statistical data and the analytical study, they showed that some correlations exist between the combustion speed, flow velocity, and the mixture ratio. They also showed that the time of occurrence of peak cylinder pressure is a useful means for indicating the trend of the mean combustion period. However, their data were only sufficient to display the existence of this relationship and therefore do not yield a quantitative conclusion.

Winsor & Patterson developed a simple model in order to describe the probable relation between the variations in the combustion duration and the mixture velocity. This model postulates a critical flame radius increment where the mixture motion variations near the spark electrodes create the cyclic combustion variations. With the help of this model, they showed that the combustion variation can be reduced if the critical distance, which is believed to be a function of the eddy size, becomes smaller. Also, a reduction in the coefficient of variation of the mixture velocity reduces the combustion variations.

The model has been developed under certain conditions assuming an isotropic turbulence near TDC during the combustion period and, therefore, it is not longer valid when the effect of swirl on combustion variations becomes an appreciable factor (description of these two models can be found in Section 2.2.3).

Previous research has further shown that a major source of cycle-to-cycle variations is attributed to mixture velocity variations in the region of the spark plug during a short period after ignition. However, the precise nature of these mixture velocity fluctuations, whether

small scale turbulences or larger eddy sizes, is not yet well understood.

IV. Tanuma et al (1971), Burgett et al (1972), Milkins et al (1974), and Watson et al (1976) have all studied the effect of cyclic combustion variations on the exhaust emission level. They also provided some information for selecting ignition systems, increasing mixture turbulence and designing the combustion chamber configuration to optimize the engine emission levels and smoothness of engine operation. Lean mixture combustion as a solution for reducing the exhaust emissions (because of its low concentration of CO and NOx) has brought new problems of its own (i.e. degraded specific fuel consumption, rough engine operation and increased HC emissions which are caused by misfiring and cycle-to-cycle combustion variations).

Tanuma, Sasaki, Keneko & Kawasaki worked on the following problems: the possibility of extending the lean limit; improving the engine performance with an extremely lean mixture; reducing the exhaust emission without sacrificing the smoothness of engine operation. Therefore, they concluded that the lean limit can be extended by modifying the ignition system (the gap width, the centre electrode diameter, the gap projection of the spark plug and the increase in spark ignition), increasing the mixture turbulence, and improving the mixture condition (i.e. uniformity and temperature). Smooth operation of the engine can be maintained even at retarded spark timing if the above modifications are applied and hot intake air to the engine is provided. Furthermore, a substantial reduction in the exhaust emissions can also be achieved.

Burgett, Leptich & Sangwan have studied the effects of spark plug and ignition system design on the engine performance. They showed that the extended gap between location, wider gap size and higher spark energy

level are the most significant parameters which affect the cyclic combustion variation and unburned hydrocarbons, especially under very lean mixtures.

Milkins, Watson, Goldsworthy & Hallworth measured the exhaust emissions (CO, HC, O_2, H_2 and N_2) as a function of the burning time using a single cylinder spark-ignition engine. They showed the existence of a significant and regular variation of CO and HC with combustion timing. They also proved that reducing the cycle-to-cycle variation improves the overall CO and HC emissions, particularly for very lean mixtures.

Watson, Goldsworthy & Milkins, in another paper, revealed that the nitric oxide is extremely sensitive to the combustion time, whilst CO and HC are less sensitive but may show significant variations under certain operating conditions.

V. There are certain other works which are difficult to classify. These are as follows:

Karim & Sarpal (1975) studied the response of cyclic pressure variations to the small perturbations in operating parameters in an auto-igniting engine. They showed that the thermal rather than kinetic nature of the residuals is a more effective contributor to cyclic dispersion in auto-igniting engines with hydrogen as fuel.

Chen & Krieger (1976) presented a method of calculating properties of the frozen nitric oxide concentration formed during consecutive cycles of spark ignition. Despite their interesting methods, they were unable to arrive at any significant conclusions.

2.2.1 Data Processing Techniques

The nature of the cyclic variation in internal combustion engines is random. Therefore, any reliable quantitative assessment requires a considerable number of records to be obtained. The number of records that can be examined manually is limited by the effort involved and the extent of confidence interval required. The practical difficulties of measurement, especially the recording of cyclic combustion variations, has played the restrictive rôle in the research history of this type.

Since the photographic recording of oscilloscope records has become possible, this technique was employed in many works, such as Soltau (1960), Curry (1963), and Karim (1967). Later, this technique was replaced by a magnetic tape recording and, therefore, the number of possible recordings and the measurement accuracy were increased (Patterson (1966) used 2000 cycles). The latest recording technique to become viable is the use of on-line computer for real-time data analysis and reduction (Bloxham et al (1972)), a description of which may be found in Chapter 4.

2.2.2 Characterizing Parameters

In a brief review of research history on the measurements of cyclic variations, we have shown that, up to the present time, various characterizing parameters have been employed as yardsticks to quantify the combustion cyclic variations. The peak cylinder pressure (Vichnievsky (1955)), the maximum rate of cylinder pressure rise (Patterson (1966)), the indicated mean effective pressure (Soltau (1960)), the time for the flame front to travel across the chamber (Watson et al (1976)), etc., are among the possible characterizing parameters which can be used. The choice between these parameters requires consideration of the following

premises:

(a) The ease and accuracy of their measurements.

(b) The percentage change of these parameters from cycle to cycle.

(c) The general ability of the parameters to describe the combustion process.

Patterson (1966) showed that for spark-ignition engines the maximum rate of cylinder pressure is, no doubt, the most reasonable indicator of the combustion variations. On the other hand, the output quantities (such as torque, work and power) should not be employed as the combustion yardsticks, since their variations are immeasurably small and far removed from the combustion process. Moreover, the time for the flame front to travel across the chamber is more difficult to measure compared to the relatively easy and accurate measurement of the peak cylinder pressure and the maximum rate of cylinder pressure rise. The two remaining parameters (the peak pressure and the maximum rate of cylinder pressure rise) are directly related to the combustion process and, therefore, can be used as indicators of the cyclic variations. Peak pressure as the measured parameter reflects the piston motion and the integral of the charge burnt. It is related to the combustion process in a somewhat complex manner and, therefore, for the case of small variations in the angle at which the peak pressure occurs, it is a reasonable parameter by which to represent the cyclic variations. The rate of cylinder pressure rise is related to the combustion rate and the piston velocity and, therefore, when the piston velocity is low (namely TDC), it is an ideal parameter for measurements of the combustion variations.

As a point of departure, many researchers selected the cylinder peak pressure because it had been previously used as a measurement of cyclic variations in internal combustion engines, and since it generally denotes the most feasible parameter for designers, operators and investigators. On the other hand, the maximum rate of cylinder pressure rise is a more sensitive indicator of the cyclic variations since, mathematically speaking, the higher the order of derivative of a given function, the greater is its sensitivity to changes in the function.

The more recent studies (Barton et al (1970,1971), and Matsuoka et al (1971)) considered the effect of the three or four different parameters, namely, the peak pressure, $\hat{P}$, the maximum rate of cylinder pressure rise, $\hat{dP}$, and the crank angles at which $\hat{P}$ and $\hat{dP}$ occur, $\theta(\hat{P})$ and $\theta(\hat{dP})$, respectively. Barton et al (1970) showed that there exists a one-to-one linear association between $\hat{P}$ and $\hat{dP}$ in spark-ignition engines.

The cyclic variation* reported in different studies are presented either absolutely or as a percentage of their mean values. The percentage of mean (coefficient of variation), the dimensionless quantity used by Karim (1967), is a more informative parameter because it relates variations of the standard deviations to variations of the mean values (CV = standard deviation/mean value).

2.2.3 Empirical Models

In this section, the two models which have been developed by

---

* The cyclic variation of each parameter has been described as either the standard deviation or the maximum deviation between the highest and lowest values of that parameter. In this work, the first definition has been employed to indicate the degree of cyclic variation.

Barton, Lestz & Meyer (1971) and Winsor & Patterson (1973) are discussed. These models mainly attempt to relate the cyclic combustion variations to the mixture velocity and its variations.

2.2.3.1 Barton, Lestz & Meyer model

This model basically postulates that the variations in the time required to burn 5% of the fuel are responsible for the cyclic variation of the pressure development. They called this period of time the initial burn duration, t_b. Having measured the four quantities, $\hat{P}$, $d\hat{P}$, $\theta(\hat{P})$, $\theta(d\hat{P})$, and studied the calculated statistic of these variables, they showed that the following relation between the standard deviations and the averages of $\hat{P}$ and $\theta(\hat{P})$ is a valid assumption:

$$\frac{S(\hat{P})}{S(\theta(\hat{P}))} = \frac{\partial \bar{\hat{P}}}{\partial \bar{\theta}(\hat{P})} \tag{2.1}$$

when all engine variables are constant, except spark advance.

Therefore, the standard deviation of $\theta(\hat{P})$ can be used as a measure of the standard deviation of the initial burn duration.

They considered that the cylinder volume is divided into two regions: the unburned mixture region, and the burned product region. The rate of change of burned volume is expressed by the following relation, which is similar to that used by Eschenback & Agnew (1958) for constant volume combustion bombs:

$$\frac{dV_b}{dt} = A_b S_b E f(U) \tag{2.2}$$

where V_b = volume of the burned gas

A_b = flame front area

S_b = laminar burning velocity

E = expansion ratio = $(T_b M_u)/(T_u M_b)$

$f(U)$ = increase in S_b as a function of the gas velocity U

The following assumptions and postulations have been made for this model:

(a) An hemispherical burning shell of radius r_b.

(b) The expansion ratio, E, and the laminar burning velocity, S_b, are kept constant, disregarding the small effect of pressure and temperature increase due to piston motion for the first few degrees after ignition.

(c) The velocity U, and thus $f(U)$, remain constant.

(d) In a short period after the ignition, the volume fraction and the fuel mass fraction burned are linearly related (Curry (1963)).

(e) A linear regression between initial burn duration, velocity and their variations can be obtained:

$$t_b - \overline{t}_b = CC(t_b,U) \frac{S(t_b)}{S(U)} (U - \overline{U}) \tag{2.3}$$

(f) The cross-correlation between the initial burned duration and the gas velocity is equal to one:

$$CC(t_b,U) = 1 \tag{2.4}$$

On the basis of the above assumptions, and performing some mathematical steps, equation (2.2) can be rewritten as follows:

$$\left(\frac{E\ S_b}{V^{1/3}}\right)_i \left(\frac{S(t_b)}{S(U_i)}\right) = \frac{C_3}{f^2(U)} \frac{df(U)}{dU} = C_3\ g(\overline{U}_i) \qquad (2.5)$$

Substituting the approximate relationship of the expansion ratio, the laminar burning velocity, and the polytropic process expression for the compression stroke up to ignition in equation (2.5), the following correlations can be obtained:

$$F(OV) \frac{S(t_b)}{S(U_i)} = C_3\ g(\overline{U}_i) \qquad (2.6)$$

$$F(OV) = \frac{h(A/F)}{\rho_{ic}^{0.4}\ (A/F)^{0.33}} \qquad (2.7)$$

where $F(OV)$ = function of operating variables

$h(A/F)$ = function of air/fuel ratio

ρ_{ic} = mixture density at intake valve closure

Equations (2.6) and (2.7) describe the Barton et al model which indicates that, if the gas velocity variations are the cause of initial burn duration variations, a high correlation should exist between measured values of $F(OV).(S(t_b))/(S(U_i))$ and measured values of $\overline{U}_i$. In order to verify these relations experimentally, the values of $S(t_b)$, $S(U_i)$, $\overline{U}_i$ and $F(OV)$ were obtained at different engine conditions and thereby the correlation between the quantities of $log\ [F(OV)(S(t_b)/S(U_i))]$ and $log\ (\overline{U}_i)$ evaluated, using least squares linear regression. Thence, a correlation of about 0.975 was acquired, confirming the hypothesis that gas velocity variations in the vicinity of spark at the time of ignition result in variations of the initial burn duration, and consequently cycle-to-cycle variation of the combustion process.

On the basis of their model, Barton et al concluded that:

(a) The cycle-by-cycle combustion variations in an SI engine are the result of the gas velocity variations in the vicinity of the spark plug at the time of ignition.

(b) The gas velocity variations cause the variations in the initial burn duration.

(c) A quantitative measurement of the extent of the cyclic burn duration is the standard deviation of the angle of occurrence of the maximum cylinder pressure.

(d) The initial burn duration variations and the phasing of the combustion process determine the extent of the cycle-to-cycle maximum pressure variations.

(e) The temporal pressure development characteristic, $\theta(\hat{P})$, is associated with the cause of the cyclic variations, while the magnitude of $\hat{P}$ is the result of the initial burn duration variations and the combustion process after the duration of initial burn.

High correlation between initial burn duration variations and cycle-to-cycle variations in spark-ignition engines suggests that, if a similar correlation exists in diesel engines, the cycle-by-cycle variability is related to the first phase of combustion in diesel engines.

2.2.3.2 Winsor & Patterson model

The model postulates that the average flame speed is only sensitive to the local turbulent velocity when the flame radius lies

in a certain range, d_c. All disturbances leading to the cyclic combustion variations are assumed to occur during this critical period, and also the velocity variations are the sole cause of combustion variations; therefore:

$$S(t_b^*) = S(t_c) = \left(\frac{d\bar{t}_c}{dU}\right) S(U) \tag{2.8}$$

where $S(t_b^*)$ = standard deviation of burn time

$S(t_c)$ = standard deviation of critical time period

$S(U)$ = standard deviation of turbulent velocity

To indicate the combustion period and its variations, the rate of pressure rise was used. The gas velocity measurements were obtained using a hot-wire anemometer oriented vertically, radically and tangentially. Thereby, it was shown that the turbulence near TDC was isotropic and the turbulent velocity increased linearly with speed. Moreover, it was indicated by Curry (1963) that the flame speed in SI engines increases linearly with the engine speed; therefore, they assumed that the flame speed is a linear function of the turbulent velocity:

$$V_f = k\,U \tag{2.9}$$

where k is a constant dependent on the fuel/air ratio, residual gas concentration, and other mixture conditions.

Also, it was postulated that both the turbulent velocity and the flame speed have certain average values during the critical period in each cycle:

$$d_c = V_f\, t_c \tag{2.10}$$

Assuming the critical distance to be constant, and by differentiating from equation (2.10), we have:

$$\frac{dt_c}{dU} = -\frac{d_c}{V_f^2}\frac{dV_f}{dU} \tag{2.11}$$

Statistically: $$\overline{V}_f^2 = \overline{V}_f^2 + S^2(V_f) \tag{2.12}$$

Substituting equations (2.11), (2.9) and (2.12) into equation (2.8), we have:

$$S(t_b^*) = \frac{d_c}{\overline{V}_f}\frac{S(U)/\overline{U}}{1 + (S(U)/\overline{U})^2} \tag{2.13}$$

Using the approximation $\overline{V}_f = D/\overline{t}_b^*$, equation (2.13) can be solved for the critical distance, thus:

$$d_c = D\frac{S(t_b^*)}{\overline{t}_b^*}\frac{1 + (S(U)/\overline{U})^2}{S(U)/\overline{U}} \tag{2.14}$$

The above equation, which describes the model, shows an inverse relationship between the burn-time variation and the flame speed. Also, it can be realized that the combustion variations would decrease if the critical distance, which is believed to be a function of eddy size, becomes smaller.

High correlation between critical time variations and cyclic combustion variations in SI engines suggests that, if a similar relation exists in diesel engines, the premixed combustion variations will be related to cyclic combustion variability.

2.2.4 Effect of Different Variables on Cyclic Variations

Engine cyclic variations are the direct consequence of

variations in the progress of the combustion process and the rate of net energy released by combustion. Therefore, any effect of each engine variable should be viewed in terms of the following considerations:

(a) The phasing of combustion with respect to the piston motion.
(b) The average flame speed and its variations.
(c) The net rate of energy released and the total net energy available per cycle.

Because of various approaches to the problem, and various operating conditions used, some conflicting ideas on which variables are important exist. The effects of most working variables on cycle-to-cycle variations in SI engines have been well documented (Soltau (1960); Patterson (1966); Karim (1967); Barton et al (1970); Burgett et al (1972)). Below, the effects of some of these variables are reviewed.

I. Ignition system characteristics: The parameters of the ignition system, considered in various works, are mainly spark timing, spark energy, spark plug electrode shape, type of ignition, number of ignition sources, spark plug position, spark duration, peak secondary current, gap size, electrode size, and surface gap spark plug. In the previous literature, it has been generally agreed that the spark timing and the spark plug position have only an insignificant effect, and the spark energy and the spark plug electrode shape have not effect on the cycle-to-cycle combustion variations. However, the work of Burgett & Leptich (1972) on the effect of spark plug and ignition system design performance showed that:

(a) By increasing the spark duration, the peak secondary current and gap size, the cyclic combustion variation becomes smaller, and thus an improvement of the hydrocarbon (HC) concentration can be achieved.

(b) By increasing the diameter of electrode size, the cycle-to-cycle variation, and consequently the concentration of hydrocarbons, becomes greater.

(c) Among the various tip configurations of the plugs, the standard air gap has the best performance for minimum HC concentration.

Employing several simultaneous ignition sources results in more rapid burning, and therefore improves the peak cylinder pressure repeatability. This can be argued as:

i) The second stage of combustion is accelerated.

ii) The average delay period tends to be constant.

II. Air/fuel ratio: Air/fuel ratio has an important effect on the cyclic variation. The most stable combustion process occurs at an air/fuel ratio of about 10-13. As the mixture becomes richer or weaker, the coefficient of variation increases. In particular, the changes are sharper in the case of weak mixtures.

III. Fuel: There is a definite relationship between the type of fuel used and the cycle-to-cycle variations. Generally, those fuels having a more rapid rate of burning are less prone to give wide differences

in combustion development. Soltau (1960) indicated that all the hydrocarbons exhibit similar fluctuations, while town gas (rapid burning) only shows slight variations.

Although the means of fuelling has no significant effect on these variations, the direct injection of fuel into the combustion chamber aggravates the repeatability of the combustion process. This phenomenon can be caused by an insufficient period for the fuel to mix with the air charge. Nevertheless, it should be emphasised that fuels generally have little influence on the cycle-to-cycle variations.

IV. Compression ratio: A greater compression ratio increases the average flame speed; however, because of combustion phasing, a higher average flame speed adversely affects the cyclic variations. Variations of the combustion process significantly increase if the compression ratio becomes greater. This is due to combustion phasing and the variations in flame speed which are due to the higher density and temperature. At high compression ratios, the cyclic variations decrease due to better scavenging, and hence smaller exhaust gas dilution which has a detrimental effect on cyclic variability.

V. Exhaust gas dilution: Although the exhaust gas dilution is a significant factor compared to the increase in charge temperature and pressure, its effect on cyclic variation remains small. By increasing the concentration of the diluents in the charge, the coefficient of variation becomes greater.

VI. Swirl and turbulence: An increase in the swirl or turbulence improves the cyclic variations. This phenomenon mainly arises through

the flow disturbances occurring during the induction and due to the piston movement which smears and wrinkles the flame kernel, thus increasing the flame front area.

VII. Water jacket temperature: An increase of the cylinder water jacket temperature causes a reduction in the extent of the cyclic variations; however, its influence on the cycle-by-cycle combustion variations is negligible.

VIII. Engine speed: By increasing the engine speed, the average flame speed becomes greater as the spark advance changes. This is accompanied by higher flame speed variations. Greater combustion variation due to the higher speeds arises as a result of the variations of the mixture motion.

IX. Throttling: Throttling the charge affects the combustion repeatability. Generally, as the degree of throttling becomes greater, the coefficient of variation increases.

X. Fuel distribution: A high percentage of the variation from cylinder to cylinder is attributed to the fuel distribution.

The higher cyclic variation itself results in a reduction of the thermal efficiency and an increase of the exhaust gas emission, mechanical and thermal stress, and the noise level and vibrations.

2.2.5 Causes of the Cycle-By-Cycle Variations

The pressure development is a result of the release of chemical

energy (i.e. the combustion process) and is influenced by the engine variables and the piston motion. Thus, the combustion process may vary from cycle to cycle. Soltau (1960) showed that the fluctuations in the peak pressure and IMEP are caused by the differences in the rate of heat release from cycle to cycle. He indicated that the time between the ignition and the formation of a stable flame front is the principal variable from cycle to cycle, while the time required for the flame to travel across the combustion chamber after stabilization does not play an important rôle in the cyclic variations.

It is generally agreed that most of the working variables may, to a greater or lesser extent, affect the cyclic variations; however, they do not necessarily cause the deviations. The effect of these variables has been discussed in the previous section. It must be mentioned that any operating variables which are not repeated exactly from cycle to cycle have an influence on the progress of the combustion process, and can be attributed as a case of these variations. For example, the variations of the spark timing due to the variation of the drive or distributor mechanism is responsible for about 10% of these variations (Patterson (1966)). Variation of the mixture velocity in the vicinity of the spark plug which is caused by the intake process and the piston movements are the main cause of cyclic variations.

Random dispersion in the charge quality from cycle to cycle - whether as a result of poor mixing due to an incomplete evaporation of the fuel or any inconsistent cylinder scavenging - is also one of the important factors causing the cycle-to-cycle variations.

2.3 CYCLE-TO-CYCLE VARIATIONS IN DIESEL ENGINES

There is little literature on cycle-to-cycle variations in diesel

engines. This is mainly due to the different nature of diesel combustion which yields a smaller coefficient of variation relative to the variations in spark-ignition engines.

In SI engines, the combustion is a process of propagation of the flame from the ignition point through the chamber and, therefore, it is a function of thermal and kinetic histories of the premixed fuel/air charge before and after ignition. Every variation in any of these factors would affect the combustion process without any rectification. On the other hand, the combustion process in diesel engines does not depend on its initiation at a specific point, but rather on the most favourable point for auto-ignition. The overall process of combustion is not noticeably affected unless the entire level of the charge preparation is changed. In diesel engines, ignition is spontaneous and an appreciable volume of the premixed fuel and air burns quickly. This accounts for the relative freedom of the compression ignition engine from cyclic variations. It can be argued that the injection system characteristics, which affect the charge preparation and consequently the occurrence of ignition, is one of the main sources of cyclic variation in diesel engines (Wing (1975)).

Certain established parameters which influence the cyclic variability in spark-ignition engines may be similarly applied to diesel engines. These variables are as follows: the preparation of the charge and its influence on flame propagation rate, duration of burning, the turbulence of the mixture in the cylinder, air/fuel ratio, exhaust gas dilution, and injection system characteristics (injection timing, duration of the fuel injection, quantity of fuel injected).

Wing (1975) showed that appreciable cyclic variation in a direct injection diesel engine can be detected (a coefficient of variation up to 30% for $\hat{dP}$ was found). He concluded that:

(a) The maximum rate of pressure rise is a reasonable indicative measure for studying combustion irregularities in diesel engines.

(b) $\hat{P}$ and $\hat{dP}$ are not linearly correlated to each other, contrary to the case of spark-ignition engines.

(c) A strong correlation exists between the starting time of injection and the maximum rate of cylinder pressure rise at low and medium power. This correlation is sensitive to the fuel temperature.

(d) Residual effects do not play any significant rôle in cycle-to-cycle variations.

(e) Although the cyclic variation in diesel engines affects the formation of NO concentration in the exhaust emission, its influence is insignificant over most of the operating range of the engine.

2.4 CONCLUSION

Considerable similarity exists between the analytical techniques and instrumentation used for studying the cyclic variation in both spark-ignition engines and compression-ignition engines, and the study of the effects of different working variables on the cyclic variations in spark-ignition engines facilitates the study of similar relationships in diesel engines when analogous phenomena are found. The results obtained for spark-ignition engines can then be brought into play as a basis for the postulations necessary for the study of diesel engines.

The development of empirical models in spark-ignition engines has been based on the idea of an existing relation between initial burn duration variations and the cyclic combustion variations (Model A), or

between critical time variations and the cyclic variations (Model B). If a similar relation exists for diesel engines, it is likely to be concerned with premixed combustion variations. Furthermore, injection system characteristics affect the charge preparation and consequently the cyclic variations in diesel engines (Wing (1975)). These arguments lead to the postulation that variations in the fuel injection process are the major source of cyclic variations in diesel engines. The simulation model presented in this work will therefore be based on the probable relationship between these two processes (injection and combustion processes).

CHAPTER 3

THEORETICAL ANALYSES

3.1 INTRODUCTION

"Dynamic modelling" was investigated by introducing known perturbations of the injection system parameters to the performance prediction program of Marzouk (1976). This program is based on the quasi-steady "filling and emptying" concept for predicting DI diesel engine performance.

The aim of employing such a technique is to study the influence of variations in injection system characteristics on cyclic variations in the combustion process. The essential novelty of the statistical approach used in this study is that each engine cycle is treated as the realisation of a random experiment. Specifically, the cylinder pressure as a function of crank angle is considered as a stochastic process, and the injection system parameters (i.e. the starting angle of injection, the quantity of fuel injected) are considered to be random variables associated with random experiments.

The stochastic process of combustion is approximated by a single degree of randomness expression with the starting time of injection or the quantity of fuel injected as the characterizing random variable. Hence, all relevant thermodynamic variables, such as pressure, temperature and chemical composition, being somehow related to the characterizing random variable, are also stochastic processes associated with the random experiment. By employing this method, the statistical properties of the variables which characterize the combustion processes were calculated. Moreover, the method can be used to calculate the statistical distribution of the exhaust emissions (i.e. frozen nitric oxide concentration which is not readily measured from cycle to cycle), and to determine the different

parameters contributing to cyclic variations in IC engines, particularly for cases which cannot be established by a direct experiment.

Classical methods of dealing with the nature of the system (dynamic characteristics) based on deterministic perturbations of the input, such as steps, impulses and sinusoidal input functions, have not always been successful (Harland et al (1969)). This is because the response of the system may be masked by uncontrollable random disturbances collectively referred to as noise. Therefore, a random form of perturbations was used in this study to consider a more realistic form of variation and also to defuse the effect of noise disturbances.

The dynamic modelling, the simulation program predicting the performance of DI diesel engines and the combustion model employed are discussed and presented in this chapter. The procedure for correlating the constants of the dynamic model to the experimental results used in a preliminary investigation is described in the appendices* to this chapter.

3.2 "DYNAMIC MODELLING"

"Dynamic modelling", as a technique which deals with the cyclic variation problem theoretically, has recently attracted the attention of some researchers working on this subject.

Karim & Sarpal (1975) analytically studied the rôle of small perturbations in operating parameters on the cyclic pressure variation in an auto-igniting engine fuelled with hydrogen over a number of consecutive cycles. They showed that, with hydrogen as a fuel, the thermal conditions rather than the kinetic nature of the residuals is the more effective

---

* The appendices to Chapters 3, 4 and 5 are denoted by A1, A2, ..., B1, B2, ..., and C1, C2, ..., respectively.

contributor to cyclic dispersion. In their studies, the influence of any of the operating parameters are examined by perturbating their values by a small factor, either over one cycle or periodically over a number of cycles. As a result, they did not employ the random form of perturbation that one expects in real processes.

Chen & Krieger (1976) calculated the probability density function of the nitric oxide concentration using the functional relationship of the frozen nitric oxide concentration with cylinder pressure. The functional relationship was achieved by creating a set of consecutive cylinder pressure-crank angle data which gave the statistical properties of the cylinder pressure of spark-ignition engines at a normal condition. The cylinder pressure was approximately evaluated by assuming a stochastic process with one degree of randomness, and taking the peak cylinder pressure from the experimental results as the characterizing parameter of this process. The data were then fed into the combustion and nitric oxide kinetic models.

Apart from the method presented for studying the statistical distribution of the frozen nitric oxide, their results and conclusion (that the cyclic variation in spark-ignition engines has an insignificant effect on the average formation of nitric oxide in the exhaust) are not comprehensive since the whole work was limited to a single operating condition.

Ghobadian (1976) investigated the effect of putting perturbations in the form of hypothetical sine or random waves either on the flame nucleus which controls the combustion timing or on the flame factor which determines the turbulent flame speed with all other engine variables constant. His conclusion was in confirmation with the previous results, where a small cyclic variation in combustion initiation timing in SI

engines has shown little effect on cyclic variation. Conversely, the turbulence variation from cycle to cycle had a major effect on the cylinder pressure cyclic variation.

The present model was set up to investigate analytically the response of a DI diesel engine to small perturbations of the operating variables (mainly the fuel injection system parameters) over a number of consecutive cycles. The results are then discussed in terms of the problem of cyclic dispersion in engines. For this reason and those mentioned in Section 1.1, the DI diesel engine performance prediction program based on the "filling and emptying" approach was employed. The schematic diagram of this technique is shown in Figure 3.1.

The effect of one cycle on the next was analysed by employing the engine variables calculated at the end of each cycle as the initial conditions for the next calculation (this process is shown by line number 4 in the scheme). The analysis was carried out over a range of 100 successive cycles at each test point. In the present dynamic modelling system, some assumptions were made either to simplify or to provide a suitable simulation model possessing maximum simplicity and reasonable accuracy with a minimum of parameters and constants for this work.

In order to study the effect of all possible engine variables logically, the model permits a change in one variable at a time, and thus attempts to fix all other variables at constant value during every cycle. However, in a special case, two variables, τ and m_f, were changed simultaneously and, as will be described, a more reasonable result was achieved.

As shown by the dotted line in the scheme (Figure 3.1, line number 5), the effect of the engine drive on the injection system was not considered. However, when experimental values were used to provide the perturbations,

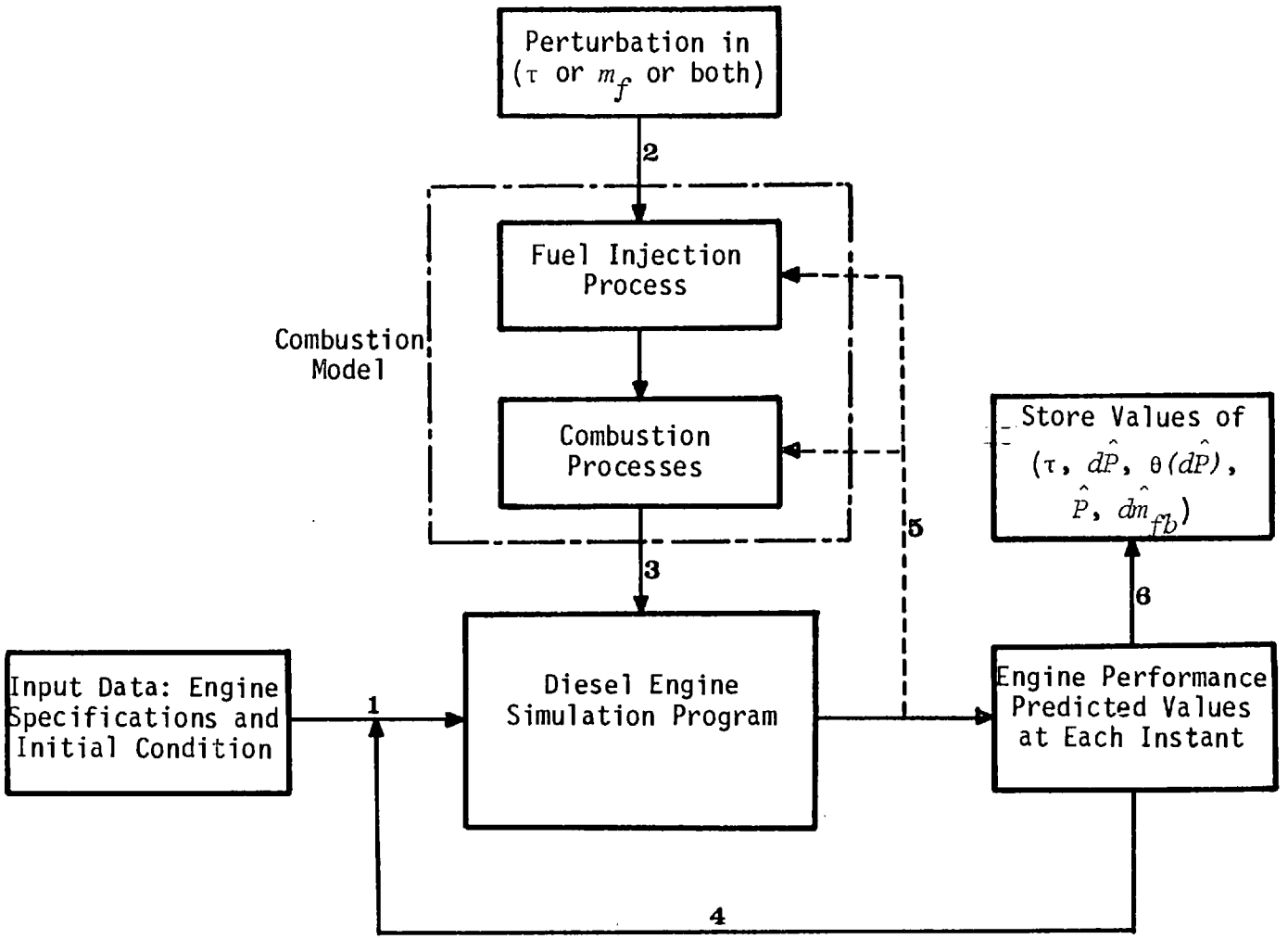


Figure 3.1: Diagram of dynamic modelling

this effect was taken into account to some extent. As a result, the correlation existing between the variation of the drive and the variation of the injection system characteristic was not considered thoroughly. This aspect could be studied by coupling the injection pump to an electric motor (instead of driving the pump from the engine itself), and hence variation of the injection system parameters due to variations of the engine drive would be eliminated.

All coefficients employed in the model were assumed to remain constant, while the perturbations were introduced. This assumption is reasonable only when the perturbations in the system are small.

The system was fed by two sets of input: one to set the engine variables and the initial conditions for the first cycle, and the other to vary the fuel injection system parameters for each cycle. These two sets of input to the system are shown by line number 1 and number 2 in the scheme. Line number 6 shows the output of the system where five variables were stored and later analysed for every engine cycle at each test point, these being:

(a) Injection system variable parameters:

τ = starting angle of injection (degree of crank angle (DCA) before top dead centre (BTDC))

m_f = quantity of fuel injected (pound mass per cycle per cylinder)

(b) $\hat{dP}$ = maximum rate of cylinder pressure rise (PSI/DCA)

(c) $\theta(\hat{dP})$ = location of $\hat{dP}$ (DCA/ATDC)

(d) $\hat{P}$ = peak cylinder pressure (PSI)

(e) $\hat{dm}_{fb}$ = maximum rate of burning (LB/DCA)

The two characterizing parameters of the fuel injection system in the combustion model are the starting angle of injection, τ, and the amount of fuel injected, m_f. At each operating condition, the mean values of these parameters used in the program correspond to the values obtained by experiments. The perturbations put on each parameter are either measured experimentally or generated by a random number subroutine having normal distributions, specified mean and standard deviation values (G05AEF, NAG library subroutine (1977)).

3.3 DIESEL ENGINE SIMULATION PROGRAM

Steady state performance prediction programs are employed in a wide variety of applications, especially for design purposes, for example:

(i) Prediction of component temperature and cylinder pressure diagrams for thermal and stress analyses.

(ii) Parametric studies with the objective of optimizing certain design concepts, e.g. valve timing.

(iii) Its application in "dynamic modelling" for different studies.

In order to simulate the engine processes, it is helpful to delineate the various models describing different processes taking place in the diesel engine. These processes are as follows:

(a) The properties of the working gas.

(b) The combustion process.

(c) The heat transfer.

(d) The gas flow through the inlet and outlet ports.

(e) The scavenging process.

(f) The inlet manifold.

(g) The exhaust manifold.

(h) The engine friction losses.

In setting up these models, some assumptions and simplifications must be introduced in order to construct the mathematical representations of each phenomenon.

The simulation program of Marzouk (1976), based on the direct injection diesel engine model, is here briefly described. The description is made under the three following topics:

(i) Physical description: the concept of different physical processes taking place in a diesel engine as the basis of the model.

(ii) Governing relationships: conservation and state equations relevant to the combustion concept, the hypotheses and the pertaining correlations used in the model.

(iii) Analysis procedure: the method adopted for solving the differential equations.

The original program, called IMCOENG (Marzouk & Watson (1976)), can predict the performance of naturally aspirated and turbo-charged diesel engines. Here, only the part used in the present study will be reviewed.

In order to predict the behaviour of diesel engines with altered operating conditions by means of cycle simulations, a basic knowledge of the rate of heat release is necessary. For mathematical representation of the results, the actual head release diagrams were replaced by simplified "Marzouk model" heat release diagrams which are based on the

fuel burning rate approach and have the same beginning and duration of combustion.

3.3.1 Physical Description

The original program was written by Marzouk (1976) to predict the performance of the naturally aspirated and turbocharged direct injection diesel engines, although only the parts concerning the former are discussed in this section. The mathematical model for the simulation program is obtained by hypothetically dividing the engine into several thermodynamic systems (cylinders, inlet and each branch of exhaust manifolds). The thermodynamic analysis of gas flow can be applied for each control volume individually and these control volumes are coupled by heat and/or mass transfer. Following the previous researchers, this concept is called the "filling and emptying" model. The DI diesel engine model is concerned with the properties of the gas flow contained in a cylinder, inlet and exhaust manifold, as represented in Figure 3.2.

The thermodynamic model is valid for all control volumes and it is assumed that there exists a thermodynamic equilibrium and an ideal gas behaviour at all times. It is also assumed that the control volumes contain an homogeneous mixture of air and combustion products at every instant. Phenomena such as temperature, entropy, fuel/air ratio gradients, pressure waves, non-equilibrium compositions, fuel vaporization before and during combustion, are thus ignored in this model. The required polynomial fits for the properties of equilibrium combustion products, including dissociation, for lean fuel-air mixtures ($F < 1$), were taken from Krieger & Borman (1966); and also for rich mixture products ($1 < F < 1.6$), data were taken from data published by the General Electric Company (1955). The formulae describing the thermodynamic properties of

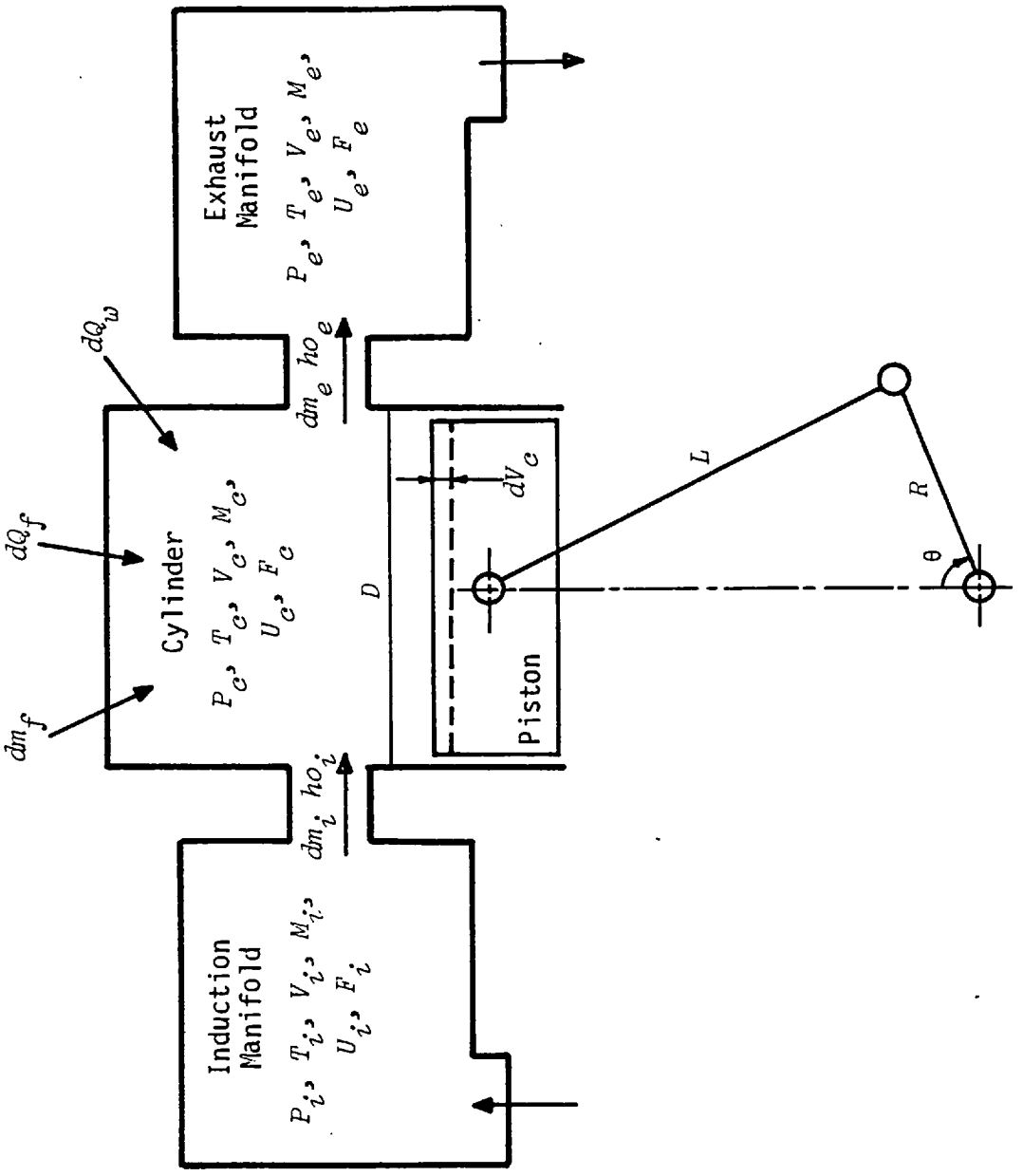


Figure 3.2: Engine thermodynamic system

the products of combustion of air and diesel fuel (assumed to be $C_n H_{2n}$) are given in Appendix A1.

All the control volumes are treated as quasi-steady open thermodynamic systems. By this is meant a system which reacts under unsteady conditions, at each instant of time, in the same manner as under steady conditions. Thus, the gas constant, enthalpy, internal energy and the partial derivatives of these with respect to temperature, pressure and equivalence ratio can be calculated at every instant required. The largest error in the property evaluation occurs during combustion when the charge is inhomogeneous in both temperature and composition and may not be in chemical equilibrium. For simplification, inlet and exhaust manifolds are also considered as control volumes (like cylinders) rather than a complex arrangement of pipes.

The combustion model is constructed of semi-empirical equations based on the fuel burning rate approach and considers separately two functions: premixed burning and diffusion burning. This model is discussed in more detail in Section 3.4.2.

Models for heat transfer are usually dependent upon empirical gas side heat transfer coefficients. None of these correlations are based on data which incorporate measured rates of radiation heat transfer with the air motion. For simplicity, Eichelberg's correlation (1939) was used in this program.

The flow through the engine ports is calculated by employing the quasi-steady flow approximation which assumes steady flow equations and steady flow coefficients at each instant. The effect of pressure wave propagation through the ports has been neglected.

3.3.2 Governing Relationships

The basic equations used in the simulation program are as follows:

(a) The energy equation for an open thermodynamic system is:

$$\frac{d(MU)}{dt} = -P\dot{V} + \sum_i \dot{Q}_i + \sum_j h_j \dot{m}_j \qquad (3.1)$$

where M = mass in the system (control volume)

U = specific internal energy of the system

h_j = total specific (stagnation) enthalpy of the mass entering or leaving the system through surface j

P = total pressure in the system

$\dot{V}$ = rate of volume change of the system

$\dot{Q}_i$ = rate of heat transfer through surface i

$\dot{m}_j$ = rate of mass flow through surface j

This equation is applicable to any control volume (cylinder or manifold) and states that the rate of change of internal energy in the system is equal to the sum of the rates at which energy leaves the system due to work ($-P\dot{V}$), due to heat transfer ($\sum_i \dot{Q}_i$), and due to mass transfer ($\sum_j h_j \dot{m}_j$). This equation can be solved for $\dot{T}$ in terms of known quantities by combining it with the following relationships.

(b) The mass quantity equation:

$$\dot{M} = \sum_j \dot{m}_j \qquad (3.2)$$

which shows the rate of change of mass in every control volume equals the rate at which mass flows in or out. The continuity equation for fuel is:

$$\dot{M}_f = \sum_j \dot{m}_{f,j} \tag{3.3}$$

(c) Thermodynamic property relationships:

$$U = U(T,P,F) \tag{3.4}$$

$$R = R(T,P,F) \tag{3.5}$$

(d) Equation of state for ideal gases:

$$P\,V = M\,R\,T \tag{3.6}$$

where R = gas constant.

(e) Equivalence ratio is defined by:

$$F = \frac{f}{f_s} \tag{3.7}$$

where f = fuel/air ratio

f_s = stoichiometric fuel/air ratio

(f) By using the above relationships with some manipulation, equation (3.1) can be solved for $\dot{T}$ and gives:

$$\dot{T} = \frac{\psi_1 - \frac{P}{\psi_3}\frac{\partial U}{\partial P}\left[\frac{\dot{M}}{M} - \frac{\dot{V}}{V} + \frac{\dot{F}}{R}\frac{\partial F}{\partial R}\right] - \dot{F}\frac{\partial U}{\partial F}}{\frac{\partial U}{\partial T} + \frac{\psi_2}{\psi_3}\frac{P}{T}\frac{\partial U}{\partial P}} \tag{3.8}$$

where:

$$\psi_1 = -RT\frac{\dot{V}}{V} + \frac{1}{M}\left(\sum_i \dot{Q}_i + \sum_j h_j \dot{m}_j - U\dot{M}\right) \tag{3.9}$$

$$\psi_2 = 1 + \frac{T}{R}\frac{\partial R}{\partial T} \tag{3.10}$$

$$\psi_3 = 1 - \frac{P}{R}\frac{\partial R}{\partial P} \tag{3.11}$$

(g) Heat transfer: Instantaneous heat transfer rates were computed according to:

$$\dot{Q}_i = h_i A_i (T_i - T_g) \tag{3.12}$$

where $\dot{Q}_i$ = instantaneous heat transfer rate from surface i

h_i = instantaneous heat transfer coefficient for surface i

A_i = area exposed of the heat transfer surface i to the gas

T_i = average surface temperature of the heat transfer surface i

T_g = bulk gas temperature

(h) Heat transfer coefficient: From the many correlations existing for heat transfer coefficients, the Eichelberg formula (1939) was employed:

$$h_i = 8.06 \times 10^{-5} \sqrt[3]{V_p}\sqrt{P\,T} \tag{3.13}$$

where h_i = heat transfer coefficient (chu/ft^2.^{o}K.sec)

P = gas pressure (atm)

T = gas temperature (^{o}K)

V_p = mean piston speed (ft/sec)

(i) The expression for the rate of mass flow of an ideal gas through a flow area is given by equation (3.14) which is based on quasi-steady and standard compressible flow relationships:

$$\dot{m} = A_g C_d P_u \sqrt{\frac{2\gamma}{(\gamma - 1) R_u T_u} \left[\left(\frac{P_d}{P_u}\right)^{2/\gamma} - \left(\frac{P_d}{P_u}\right)^{(\gamma+1)/\gamma} \right]} \qquad (3.14)$$

where A_g = geometric flow area

C_d = coefficient of discharge

P_u, T_u, R_u = stagnation pressure, stagnation temperature, and the specific gas constant at upstream conditions

P_d = stagnation pressure downstream

γ = specific heat ratio based on upstream conditions

When sonic conditions prevail, the pressure ratio in equation (3.14) is the critical value given by:

$$\left(\frac{P_d}{P_u}\right)_{cr} = \left(\frac{2}{\gamma + 1}\right)^{\gamma/(\gamma-1)} \qquad (3.15)$$

Below this critical ratio, no increase in volumetric flow is possible.

(j) Event timing and engine geometry:

$$\frac{d\theta}{dt} = \Omega_e \qquad (3.16)$$

$$V_{c,i} = \frac{\pi}{4} D^2 r \left(\frac{l}{r} + 1 - \cos\theta - \sqrt{\frac{l}{r} - \sin^2\theta}\right) + V_{TDC} \qquad (3.17)$$

$$A_{l,i} = \pi D r \left(\frac{l}{r} + 1 - \cos\theta - \sqrt{\frac{l}{r} - \sin^2\theta}\right) + A_{l,TDC} \qquad (3.18)$$

where $V_{c,i}$ = instantaneous values of cylinder volume

$A_{l,i}$ = instantaneous values of linear area

D = cylinder bore

r = crank radius

l = length of connecting rod

(k) The valve flow area is given as a numeric function of crank angle:

$$A_{v,n} = A_{v,n}(\theta) \qquad (3.19)$$

(l) Engine friction is given by Chen's correlation (1965):

$$FMEP = 13.7896 + 0.005\,\hat{P} + 1.0858\, r \times \Omega_e \qquad (3.20)$$

where $FMEP$ = friction mean effective pressure

(m) Engine performance equations:

$$\text{Volumetric efficiency} = \frac{m_t \times \overline{T} \times R}{\overline{P} \times V_{cyl}} \qquad (3.21)$$

where m_t = total mass flow into a cylinder

$\overline{T}$ = mean cylinder temperature during cycle

$\overline{P}$ = mean cylinder pressure during cycle

$$IMEP = \frac{W_T}{n \times V_{cyl}} \tag{3.22}$$

where W_T = total engine indicated work

n = number of cylinders

V_{cyl} = swept volume

$$BMEP = IMEP - FMEP \tag{3.23}$$

where $BMEP$ = brake mean effective pressure

$IMEP$ = indicated mean effective pressure

$$ISFC = \frac{m_f}{W_T} \tag{3.24}$$

where $ISFC$ = indicated specific fuel consumption

m_f = total fuel injected

3.3.3 Analysis Procedure

The program designed for predicting the performance of DI diesel engines comprised of several subroutines (MAIN, INPUT, ETHERM, FBR, PERFOR, GEOMET, HT, RFLOW) (Marzouk & Watson (1976)). The main program, which is called MAIN, initializes variables, controls step size, calls the other subroutines and prints the output. The INPUT subroutine is designated for reading the data and is called by MAIN. The input data consist of those which determine the operating conditions and the physical description of the engine.

ETHERM, which is called by MAIN, calculates the thermodynamics of the next step for all control volumes, and solves the differential equation (3.8) with the help of other governing relationships. The general form of these equations are:

$$\frac{dX_i}{dt} = g_i\,(X_1, X_2, \ldots, X_n, t) \quad , \quad i = 1, 2, \ldots, n \tag{3.25}$$

which satisfy the periodicity conditions:

$$X_i(t) = X_i(t + t_o) \quad , \quad i = 1, 2, \ldots, n \tag{3.26}$$

where t_o = the time for one engine cycle.

In order to solve these differential equations on a digital computer, the predictor-corrector method (Euler formula (Conte (1965))) is used. The predictor-corrector method allows an estimate of errors incurred at each step. This step error estimation ability, the speed and the stability of this method constitute a great advantage over the Runge-Kutta methods. With the predictor formula (the Euler formula), which is the first approximation obtained by:

$$X_i(t + \Delta t) = X_i(t) + \Delta t\, g_i\,(X_i(t), \ldots, t) \tag{3.27}$$

The corrector formula (equation (3.28)) will then use the predictor result to compute the second approximation; that is:

$$X_i(t+\Delta t) = X_i(t) + \frac{\Delta t}{2}\left[(g_i(t), \ldots, t) + g_i\,(X_i(t+\Delta t), \ldots, t+\Delta t)\right] \tag{3.28}$$

By using the result of equation (3.28) over again in the

corrector formula, an iteration procedure evolves. After each iteration, the difference between the last two values of X_i is compared with a specified error limit. If the difference is within the given limit, the last value of X_i is accepted and the computational procedure moves to the next point.

PERFOR subroutine calculates the overall cycle performance and prints the output. FBR calculates the instantaneous fuel burning rate during the combustion. PROP is called either by MAIN or ETHERM, and calculates the thermodynamic properties of the mixture in accordance with equations (A1.1) to (A1.12) in Appendix A1. GEOMET calculates the engine geometry, the instantaneous values of cylinder volume (equation (3.17)), the valve area (equation (3.19)), and so on. HT is called by ETHERM, and calculates the heat transfer using equations (3.12) and (3.13). RFLOW calculates the instantaneous value of mass flow rate through the values from equation (3.14).

The selection of initial conditions reduces the computing time, although with almost any initial condition, the program will converge. The program is run for a specified number of cycles (100 cycles) and uses the results from the previous cycles as starting data for the next. Although the original program is written for multi-cylinder diesel engines, the program was modified to calculate conditions at cylinder no. 1 only to save computational time.

3.4 DIESEL ENGINE COMBUSTION

In principle, diesel combustion is distinguished by initially the heterogeneous distribution of the fuel and air in the combustion chamber, compression ignition, and continuous mixing throughout the period in which combustion occurs.

When fuel is injected at a high pressure through a nozzle into the hot air of the combustion chamber of a diesel engine, a spray of small droplets should form. These droplets do not ignite immediately, although the air temperature is well above the ignition temperature of the fuel (Pedersen & Qvale (1974)). The time elapsed between the injection of the first droplets into the combustion chamber and the formation of ignition nuclei is known as the ignition delay period. The length of this period is very important, since it affects the subsequent combustion processes, the mechanical and thermal stresses, and noise and exhaust emissions. Pre-ignition processes in a diesel engine can be classified into physical and chemical processes. These processes overlap each other, but they can be examined separately for a better understanding of the phenomenon. The physical part consists of the following processes taking place in the cylinders: the spray disintegrates and forms into droplets; the liquid fuel evaporates due to the heat; and the diffusion of the vapour into the air forms a combustible mixture. This physical part of ignition delay commences at the time of dynamic injection and lasts until the formation of a combustible mixture. The chemical process is mainly the decomposition of the heavy hydrocarbons into the lighter compositions and is ensued by pre-ignition chemical reactions between the decomposed compositions and oxygen. The chemical part can be defined as the time elapsing from the instant that a suitable mixture has been formed until the appearance of the hot flame.

In a detailed study of the ignition delay in DI diesel engines, Henein & Bolt (1972) have shown that the pre-ignition chemical reactions, rather than the physical processes, are the dominant rate-controlling processes.

The following description of the nature of combustion processes in

diesel engines is based on that of Austen & Lyn (1960).

The combustion process is divided into three phases: the first phase (premixed combustion) is associated with a period of rapid combustion which lasts only a few degrees of crank angle (5^{o} to 7^{o} CA). During this phase, the fuel, which is evaporated and mixed with air during the delay period will ignite and burn with a non-luminous flame. The second stage corresponds to the main period of heat release lasting for about 40^{o} of crank angle. The burning rate decays in this phase, and the fuel jet burns with a luminous, highly turbulent diffusion flame. Normally, about 80% of the total heat is released in these two stages. In the final period, the remaining fuel burns at a very low rate, so that the third phase may extend throughout the entire expansion stroke. The details of the combustion chamber geometry, the fuel injection characteristics and the fuel-air mixing influence the shape but do not appear to change the character of the combustion diagram significantly.

As described above, combustion in compression-ignition engines is a complex process starting from the start of dynamic injection to the end of combustion. This comprises of different processes, such as fuel atomization, evaporation, mixing, and chemical kinetics. These processes are usually inter-related, but in a relatively unknown manner (Gee & Karim (1966)). In principle, it is possible to consider all of these processes in one model, but the computations involved will be too lengthy to permit their inclusion in a "dynamic modelling" simulation program. The objective is, therefore, to choose a model having maximum simplicity and reasonable accuracy with a minimum number of parameters and constants. Two different models (CAV model (Khan, Greens & Whitmore (1972)) and the Marzouk empirical model (Marzouk (1976))) were carefully studied and the latter was adopted for the dynamic modelling. The details of these models

and the reasons for choosing them are given in the following sections.

3.4.1 Combustion Model

Construction of a mathematical model for describing the diesel engine combustion process provides a useful tool to perform a parametric study of the effect of various engine variables (such as equivalence ratio, compression ratio, engine speed, etc.) on the performance of the engine. The accuracy of the model can be tested with an experimentally obtained pressure time trace.

Although there are still many fundamental problems involved in forming an accurate combustion model, the need for such a model has led several investigators to develop a number of hypothetical models which incorporate various simplifying assumptions. The art of combustion modelling in diesel engines has been developed mainly on the basis of different methods of calculating the heat release diagram. These models are mainly divided into five categories:

(i) Constant pressure combustion model: This is one of the most primitive model, since it assumes that the diesel engine combustion occurs at constant pressure. Obert (1970) furnished an example of this type of combustion, where his calculations are based on an ideal diesel cycle. His assumptions are unrealistically far from the actual process.

(ii) The second method uses combustion pictures similar to those of Rassweiler & Withrow (1938) to determine the approximate mass burning rate. A high degree of empiricism is invoked by this method which limits its applicability.

(iii) The third technique uses experimental values for pressure-time data in order to calculate mass burning rates. In these models, the working fluid is assumed to have uniform properties determined by chemical equilibrium. An imaginary fuel or an apparent heat added to the working fluid progressively increases its energy and fuel/air ratio. By the first law of thermodynamics, a relationship between cylinder pressure and the apparent rate of heat release is then obtained:

$$HR = dW + dU + dQ \tag{3.29}$$

where HR = heat released by combustion

dW = work calculated from an increment of the PV diagram

dU = change of internal energy

dQ = heat transfer to the surroundings

The most convincing presentation of these models was by Krieger & Borman (1967). A brief description of their method is given in Appendix A2 as it is used to calculate the apparent rate of heat release in this study.

The main disadvantage in using the apparent rate of heat release (which is based on an imaginary fuel addition rate) is that it attributes no physical relationship to the fuel injection rate.

(iv) Burning rate models based on the injection rates: These models, which relate the apparent rate of burning to the injection system characteristics, fall into two main categories: (a) models based on single droplet burning; (b) models based on fuel-air mixing.

(a) These models were based on the consideration of single droplet burning and were applied with a limited degree of success. The studies of Shipinski, Uyehara & Myers (1969) were based on a similar approach. This method explicitly represents the processes of fuel injection, vaporization, ignition and combustion. However, by assuming a single droplet burning approach, the calculation does not take into account the distribution or stratifications of mixture products as determined by the jet mixing process.

(b) The model proposed by Grigg & Syed (1969) was based on the assumption that diesel combustion is strongly controlled by the mixing of fuel and air. The air entrainment into the spray was therefore calculated by using the Schweitzer penetration formula (1938). In their model, the turbulent mixing of fuel and air was determined by an empirical model and the rate of burning was calculated from an empirical Arrhenius type formula, giving the apparent heat release rate. It is important to note that the process of droplet evaporation was not considered in these models. The more advanced form of these models were developed by Shahed et al (1975).

(v) The fifth category consists of analytical burning rate functions which describe the pattern of the apparent rate of burning. The Wiebe (1956) function is the most common expression of such kind, and is defined by:

$$X = \frac{M_{fb}}{M_{ft}}(\alpha) = 1 - exp\left[-cw1\ (\alpha)^{cw2}\right] \qquad (3.30)$$

where X = the ratio of fuel burned at any instant to total fuel present

$cw1, cw2$ = shape coefficients

α = dimensionless time function = $(\theta - \theta_i)/(\theta_e - \theta_i)$

θ_i = crank angle at ignition

θ_e = crank angle at which burning ends

The derivative of Wiebe's function is a smooth curve for the rate of heat release and is given by:

$$AROH = C \times cw1 \times cw2 \times \alpha^{(cw2-1)} \exp\left[- cw1\ \alpha^{cw2}\right] \qquad (3.31)$$

where $AROH(\alpha)$ = smoothed rate of heat release

C = $(m_f (HV)\ 1000)/(\theta_e - \theta_i)$

m_f = weight of fuel per cycle

A knowledge of the heat release is a prerequisite for predicting the operational characteristics of the engine with the aid of real cycle simulation. To date, many attempts have been made to describe the combustion process by constructing theoretical models. However, these models do not provide an accurate basis to compute the rate of heat release solely from the engine geometry. In view of these problems, the choice of a model for the heat release calculations is generally determined by the accuracy desired and is naturally restricted by the permitted length of computations involved.

To begin with, among various combustion models studied, the CAV model was assumed to produce a reasonable approximation to the DI

diesel engine rate of heat release (the description of this model and some necessary modifications to the model constants are given in Appendix A3). For this work, it was found that this model was not entirely satisfactory and it was eventually replaced by Marzouk's model which provided a better accuracy over all operating conditions. In general, the CAV model yielded a reasonably accurate cumulative heat release. However, the main inaccuracy in the model was that the predicted rates of heat release were very different from the real values at some operating conditions. In particular, a predicted high second hump in the rate of heat release diagram does not agree with the apparent rate of heat release obtained for naturally aspirated diesel engines. The main advantage of the CAV model over the Marzouk model is in the relation between the injection system characteristics and the combustion process. In this model, all the injection system parameters contribute to the combustion pressure development, while, in the case of the Marzouk model, the relation between the fuel injection system and the combustion process are determined only by the starting angle of injection, τ, and the quantity of fuel injected, m_f.

3.4.2 Marzouk Model

This is an empirical model based on the fuel burning rate approach and was developed by Marzouk (1976) to simulate the combustion process during steady-state conditions.

In this model, the combustion process is assumed to start at the dynamic injection and the heat generation calculated following the computed ignition delay period. The ignition delay was evaluated by modifying the constants of Wolfer's formula (1938) to match the particular engine considered. The ignition delay is given by:

$$ID = c_1 \exp (c_2/T_m)/P_m^{c_3} \tag{3.32}$$

where P_m = arithmetic mean of cylinder gas pressure during the delay

T_m = arithmetic mean of cylinder gas temperature during the delay

c_1, c_2, c_3 = empirical constants

The combustion process was assumed to comprise two different burning modes: "premixed burning" and "diffusion burning". Each of these mechanisms were described by analytical functions. The two modes are assumed to start at the ignition point and, after the premixed fuel-air mixture is burnt, the burning continues in the form of diffusion burning. Thus, the instantaneous rate of burning can be mathematically expressed as the sum of two components:

$$\frac{dM_{f,t}}{d\theta} = \frac{dM_{f,p}}{d\theta} + \frac{dM_{f,d}}{d\theta} \tag{3.33}$$

where $dM_f/d\theta$ = the fuel mass burning rate with respect to the crank angle

θ = crank angle

and the subscripts t, p, d denote the total, the premixed, and the diffusion, respectively.

The mode of burning proportionality factor was introduced in this model to define the share of fuel burnt in each of the two different modes. By definition, the model of burning proportionality factor, β, is the ratio of cumulative fuel consumption due to premixed burning, $M_{f,p}$, to the total amount of fuel injected per cycle, $M_{f,t}$; that is:

$$\beta = \frac{M_{f,p}}{M_{f,t}} \tag{3.34}$$

where:
$$M_{f,t} = M_{f,p} + M_{f,d} \tag{3.35}$$

Substituting equations (3.33) and (3.34) in equation (3.35), the non-dimensional form of fuel burning rate can be obtained as:

$$FBR_t(\alpha) = \beta\, FBR_p(\alpha) + (1 - \beta)\, FBR_d(\alpha) \tag{3.36}$$

where $FBR_k(\alpha) = \dfrac{(dM_{f,k}(\alpha)/d\theta).(\theta_e - \theta_i)}{M_{f,k}}$ $(k = t, p, d)$ denotes the non-dimensional burning rate distribution for k mode

α $= (\theta - \theta_i)/(\theta_e - \theta_i)$

θ_i = crank angle at ignition point

θ_e = crank angle at the end of combustion

The mode of burning proportionality factor is a function of ignition delay and the equivalence ratio of trapped mass. Marzouk found the following equations to be the most suitable approximation of these two processes:

$$FBR_p(\alpha) = cp1\ cp2\ \alpha^{cp1-1}\ (1 - \alpha^{cp1})^{cp2-1} \tag{3.37}$$

$$FBR_d(\alpha) = cd1\ cd2\ \alpha^{cd2-1}\ exp\ (-\ cd1\ \alpha^{cd2}) \tag{3.38}$$

where $cp1$, $cp2$, $cd1$, $cd2$ are shape factors.

Figure 3.3 illustrates the total fuel burning rate distribution which consists of the sum of two dimensionless distribution components weighted by the mode of burning proportionality factor.

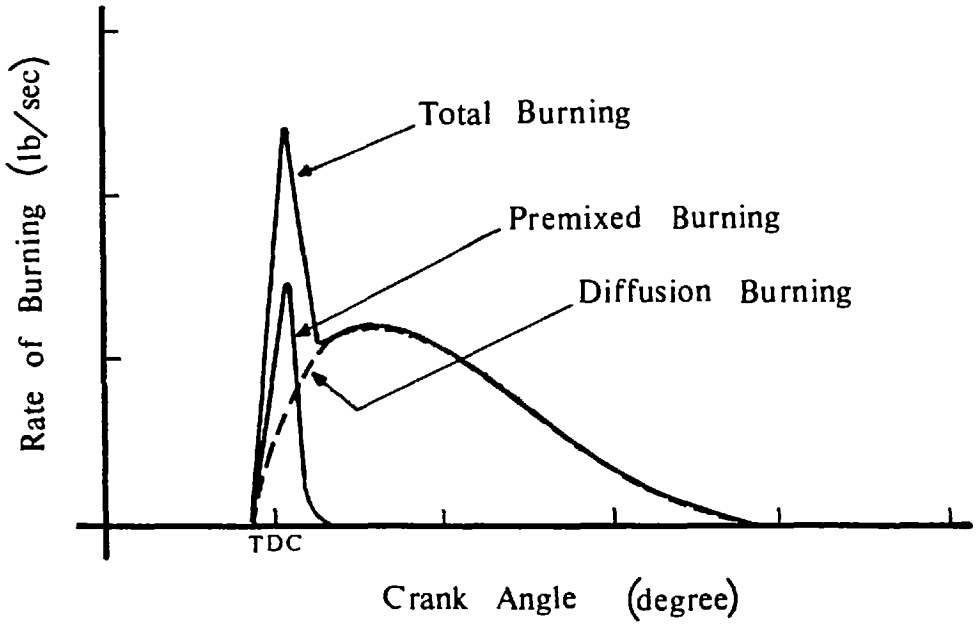


Figure 3.3: Fuel burning rate distribution

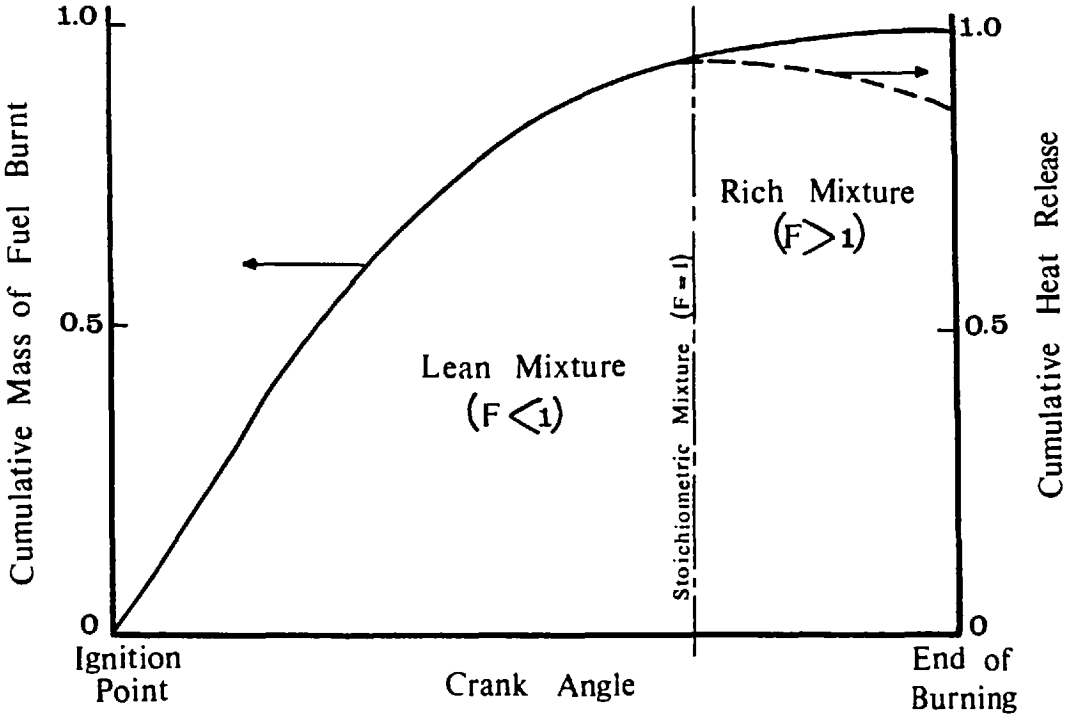


Figure 3.4: Cumulative mass of fuel burnt and heat release

The relationship between the fuel burning rate and heat release is based on the assumption of thermodynamic and chemical equilibrium, and is linear for lean mixtures ($F < 1$) in the absence of dissociation. But, in the case of rich mixtures ($F > 1$), or occurrence of dissociation, the amount of reacting fuel would result in a reduction in the cumulative heat release (Figure 3.4).

As shown in Figure 3.3, for a large value of *cp2*, the first function, giving the premixed burning, indicates a very steep rise and decay in the burning rate diagram. This is similar to the sharp peak of rate of burning measured in the actual premixed burning. In the model, the time of occurrence of the peak value can be controlled by the value of *cp1*. The area under the first distribution of premixed burning should be equal to unity, as:

$$\int_0^1 FBR_p(\tau) = \left[1 - (1 - \tau^{cp1})^{cp2}\right]_0^1 = 1$$

The second equation, which is similar to the Wiebe function, was selected to represent the diffusion burning. Thus, the model accounts for the changes in burning rate at various operating conditions by correlating β, *cp1*, *cp2*, *cd1*, *cd2*, F and ID constants to the required operating conditions of the engine.

The following equations represent Marzouk's combustion model (for calculating rate of heat release) for the Leyland engine (Marzouk (1976)):

$$ID = 3.52 \frac{e^{2100 \cdot 8/T_m}}{p_m^{1 \cdot 0218}} \tag{3.39}$$

$$\beta = 1.0 - 0.9259 \frac{F_o^{0 \cdot 3708}}{ID^{0 \cdot 2613}} \tag{3.40}$$

$$cp1 = 2.0 + 1.25 \times 10^{-8} (ID \times \Omega_e)^{2.4} \quad (3.41)$$

$$cp2 = 5000.0 \quad (3.42)$$

$$cd1 = \frac{14.2}{F_o^{0.644}} \quad (3.43)$$

$$cd2 = 0.791 (cd1)^{0.2477} \quad (3.44)$$

where F_o = trapped equivalence ratio

ID = ignition delay (ms)

The Marzouk model was used to predict the fuel burning rate diagram for the Perkins 4.236 direct injection diesel engine using the aforementioned correlations for computing the constants of this model. It was found that the prediction of ignition delay calculated from equation (3.39) largely deviates from the experimental data. This is because the modified Wolfer equation employed in the model was given for a turbo-charged diesel engine which has a relatively shorter ignition delay due to higher charge density. Bearing this in mind, the constants for the ignition delay correlation were modified by an optimization program, using the experimental results obtained for ignition delay over different operating conditions. Having modified the ignition delay correlation, and by a slight alteration of the mode of burning proportionality factor, the Marzouk model produced a relatively accurate rate of heat release diagram for most operating conditions. The best values of the mode of burning proportionality factor for the four operating conditions (Test 13, Test 19, Test 43, and Test 49) were found experimentally by trial and error.

Figure 3.5 demonstrates typical predicted results using the simulation program for the cylinder pressure diagram, rate of cylinder pressure diagram, rate of burning and cumulative fuel burned at 1000 rpm and 20 mkp.

3.4.3 Ignition Delay

The importance of ignition delay on the initial rate of pressure rise, and hence on combustion behaviour of a diesel engine, is emphasized in many publications (Lyn & Valmains (1966); Henein & Bolt (1967); Andree & Pachernegg (1969); Pedersen & Qvale (1974)). Lyn & Valmains (1966) studied the effects of physical factor on ignition delay. They described the effect of engine operating variables (such as speed and load) on the ignition delay as a function of a change in certain primary factors, such as injection pressure, compression temperature, pressure, and air velocity. In general, the duration of ignition delay is attributed to the chemical and physical properties of the fuel, the temperature and pressure of compressed air, the degree of fuel atomization, the nature and degree of swirl, and combustion wall temperature.

Ignition delay comprises the physical delay (the time between dynamic injection and the formation of combustible mixture) and chemical delay (the time elapsed from the starting of the process of breaking heavy hydrocarbons to the lower ones until the ignition occurs). Because of the overlapping of these two processes, the difficulty remains in measuring accurately the relative duration of each process.

The chemical delay increases rapidly with decreasing temperature and slightly decreases as pressure rises. The physical delay period also increases by employing lower injection pressure, lower turbulence, and lower compression temperature. Among the different

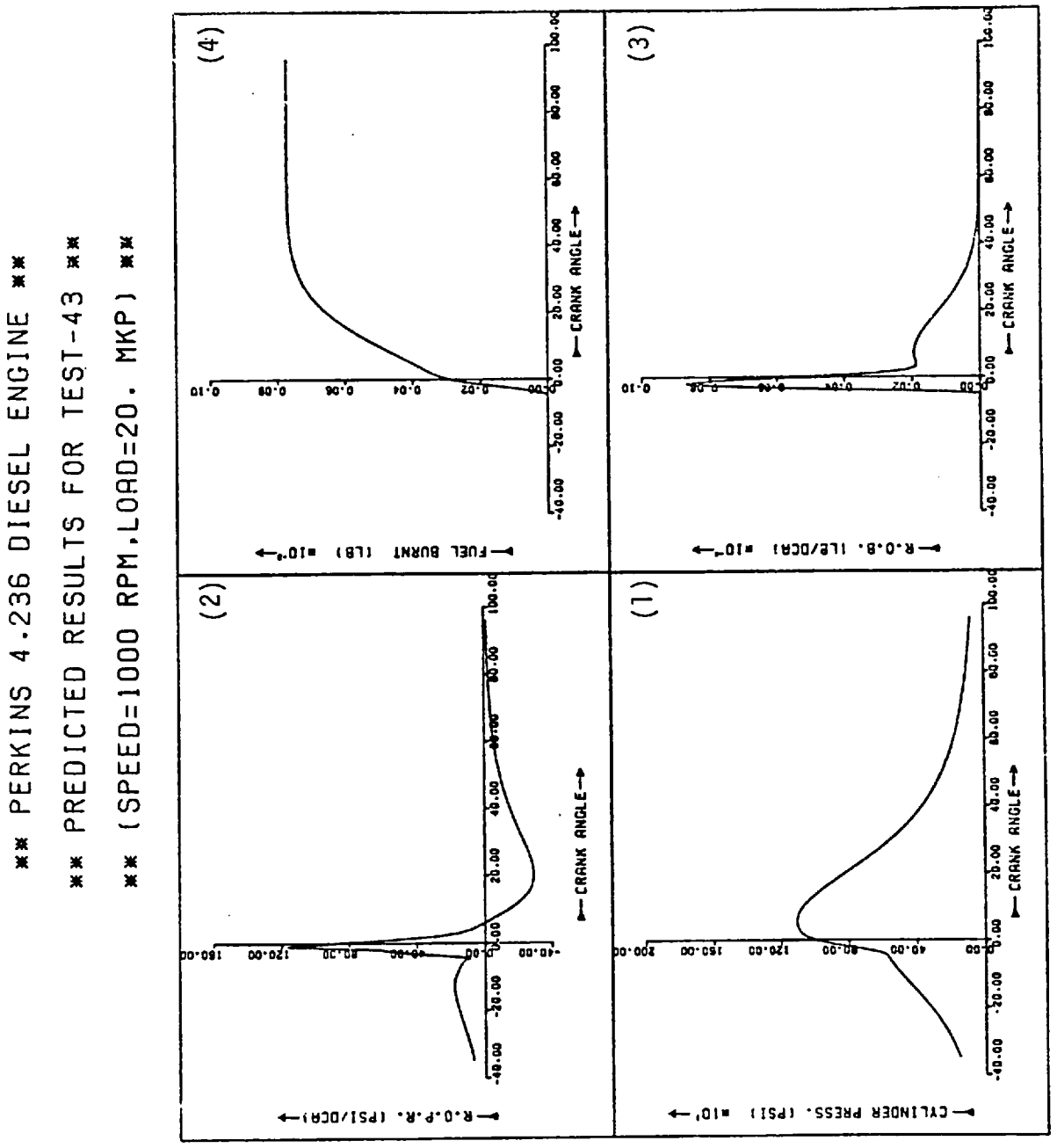


Figure 3.5: Simulation program predicted results for:

(1) Cylinder pressure diagram

(2) Rate of cylinder pressure diagram

(3) Rate of burning diagram

(4) Cumulative mass of fuel burnt diagram at given operating conditions

correlations obtained for describing ignition delay, the Wolfer (1938) formula (equation (3.32)) is one of the most prominent, and is based on a purely chemical process.

Although certain models are developed to describe the physical part of ignition delay (Pedersen & Qvale (1974)), and all investigators recognize the existence of the physical period, nevertheless, correlations based on purely chemical processes are still in common use. This is because these correlations can be simply modified for the measured values of total ignition delay with good accuracy. Hence, some investigators have attempted to correlate the constant values appearing in equation (3.32) to the experimental values obtained from the engine under test. As a result of this, several different values were obtained for the constants of Wolfer's formula, although, reportedly, similar fuels were used. Table 3.1 shows different correlations for ignition delay obtained by various workers.

Figures 3.6(a) and (b) show the experimental values of the ignition delay versus the theoretical predictions based on Wolfer (1938), Schmidt (1938), Zimmerman (1962), and Marzouk (1976) correlations. Clearly, a large deviation exists between the measured and predicted values for all the theoretical models applied and even larger deviations were found when Sitkei (1963) and Rögener (1949) correlations applied.

As the predicted values of ignition delay at some operating conditions deviated from the true values when each of the mentioned correlations were employed, it was decided to evaluate the coefficients (c_1, c_2 and c_3) of equation (3.32) on the basis of the experimental values measured on the Perkins diesel engine.

The optimization in describing the best values of c_1, c_2 and c_3 over a wide range of operating conditions was achieved by solving a set

TABLE 3.1

A Number of Published Ignition Delay Correlations

Investigator	Correlation
Schmidt (1938)	$ID = \frac{0.0646}{P^{1.08}} \exp\left(\frac{6330}{T}\right)$
Wolfer (1938)	$ID = \frac{0.429}{P^{1.19}} \exp\left(\frac{4650}{T}\right)$
Zimmerman (1962)	$ID = \frac{0.392}{P^{1.05}} \exp\left(\frac{4650}{T}\right)$
Marzouk (1976)	$ID = \frac{3.52}{P^{1.0218}} \exp\left(\frac{2100.8}{T}\right)$
Sitkei (1963)	$ID = 0.5 + \frac{0.133}{P^{0.7}} \exp\left(\frac{37564.8}{R\,T}\right) + \frac{4.63}{P^{1.8}} \exp\left(\frac{37564.8}{R\,T}\right)$
Rögener (1949)	$ID = \frac{8.027 \times 10^{-9}}{P^{0.66}} \exp\left(\frac{15100}{T}\right) + \frac{0.487 \times 10^{3}}{P^{1.82}} \exp\left(\frac{-1400}{T}\right)$
Tsao et al (1970)	$ID = \left(\frac{8.48}{P_{inj}} + 0.415\right)\left[\left(-\frac{20.17}{T_{inj}} + 0.0222\right) N + \left(\frac{26361.1}{T_{inj}} - 26.66\right) + \left(0.0018\,T_{inj} - 1.45\right)\left(\frac{1000 - N}{60}\right)\right]$

where: ID = ignition delay (ms); T = mean cylinder temperature during delay (^{o}K); T_{inj} = cylinder temperature at injection point (^{o}K); P = mean cylinder pressure during delay (bar); P_{inj} = cylinder pressure at injection point (bar); N = engine speed; R = universal gas constant = 8.314 (kJ/k mole ^{o}K).

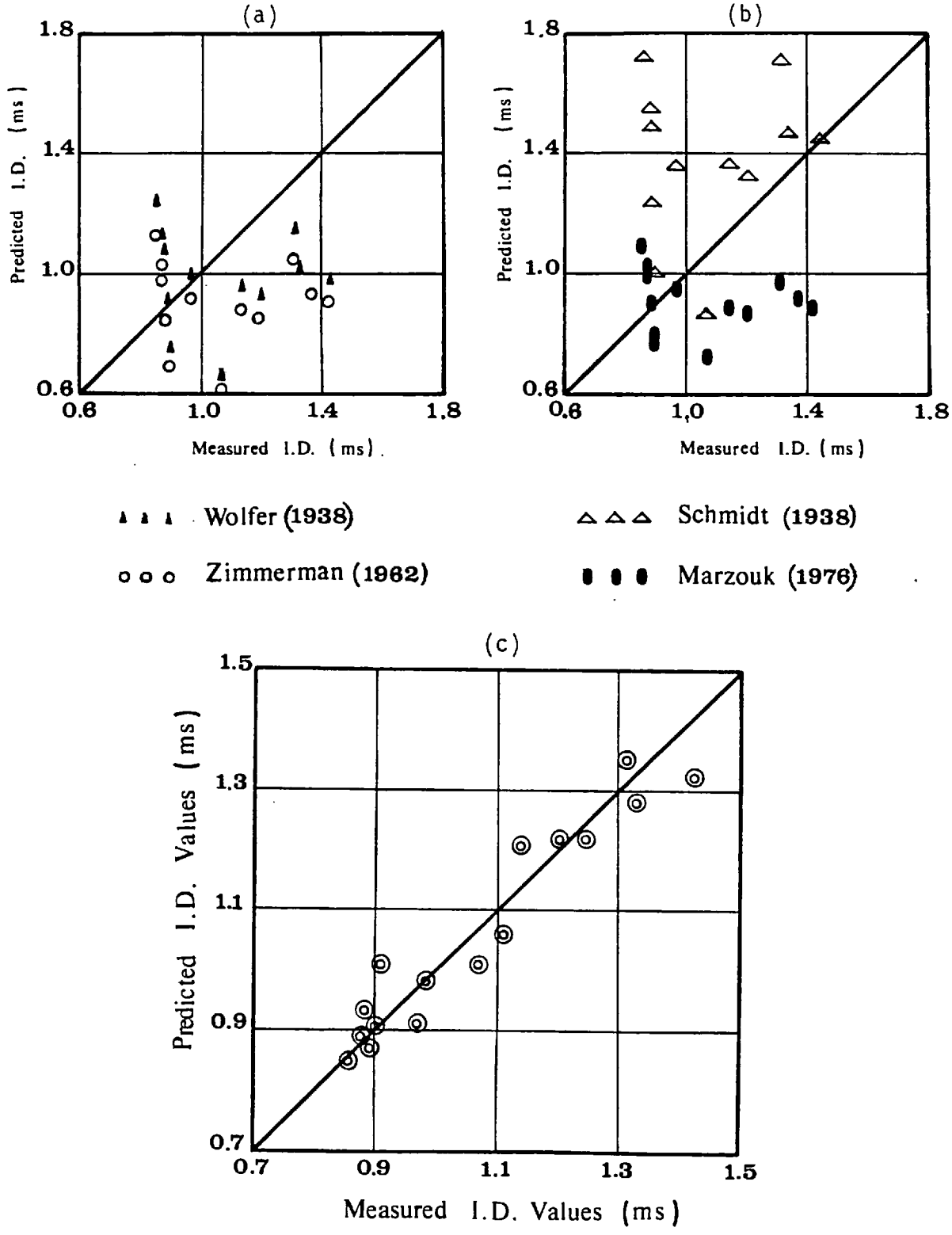


Figure 3.6: Comparison of ignition delay formulae with the aid of experimental data

of three linear equations (the details are given in Appendix A4).

The experimental values of ignition delay were found by obtaining the dynamic injection and ignition points. These were achieved by the aid of AVESTD, a program to read and record the needle-lift diagram, fuel-line pressure diagram, cylinder pressure diagram, the rate of cylinder pressure diagram, and also to compare with the data provided by Watson & Marzouk (1974). The starting time of injection was taken from both the needle-lift diagram and the fuel-line pressure diagram (at the instant of maximum rate of fuel-line pressure rise). The ignition point was read from the rate of heat release diagram and compared with the initial rate of cylinder pressure rise due to the combustion described by the rate of cylinder pressure diagram.

The mean cylinder pressure between dynamic injection and ignition point was found experimentally, employing the cylinder pressure diagram. The mean cylinder temperature during this period was calculated analytically, using the following equation:

$$T_m = \frac{1}{2 - n} = \frac{T_{ig} V_{ig} - T_{inj} V_{inj}}{V_{ig} - T_{ig}} \qquad (3.45)$$

where T_m = mean cylinder temperature during delay

T_{ig} = temperature at ignition

V_{ig} = cylinder volume at ignition instant

T_{inj} = temperature at injection

V_{inj} = cylinder volume at injection instant

n = specific heat capacity heat ratio

Equation (3.45) is derived by integrating the cylinder temperature over the period between the injection and ignition points, assuming a polytropic

process (that is, $PV^n = constant$, where P and V are the pressure and volume of gas inside the cylinders during the compression process, respectively). The value of n (specific heat capacity ratio) was also calculated from the cylinder pressure diagram for different operating conditions with the aid of:

$$n = \frac{ln\ C \sum_{i=1}^{m} ln\ V_i - \sum_{i=1}^{m} ln\ V_i\ ln\ P_i}{\sum_{i=1}^{m} ln\ V_i^2} \qquad (3.46)^*$$

where $C = P_1 V_1^n = P_2 V_2^n = \ldots P_i V_i^n = constant$

P = cylinder pressure

V = instantaneous cylinder volume

i = index designated to instants between inlet valve closed to instant of ignition occurrence

The results obtained for ignition delay, mean cylinder pressure, mean cylinder temperature and n (heat capacity ratio) are demonstrated graphically in Figure 3.7 and tabulated in Table 3.2 for different operating conditions. Figure 3.8 illustrates the ignition delay in terms of crank angle and dynamic injection for the same operating conditions. In these figures, all variables are plotted as a function of brake mean effective pressure for different speeds.

Having calculated the ignition delay, mean cylinder pressure and mean cylinder temperature for the whole range of operating conditions, and by applying them in the optimization program (see Appendix A4), the following values were found for the coefficients of Wolfer's type formula

---

* The method of derivation of this formula is given in Appendix A5.

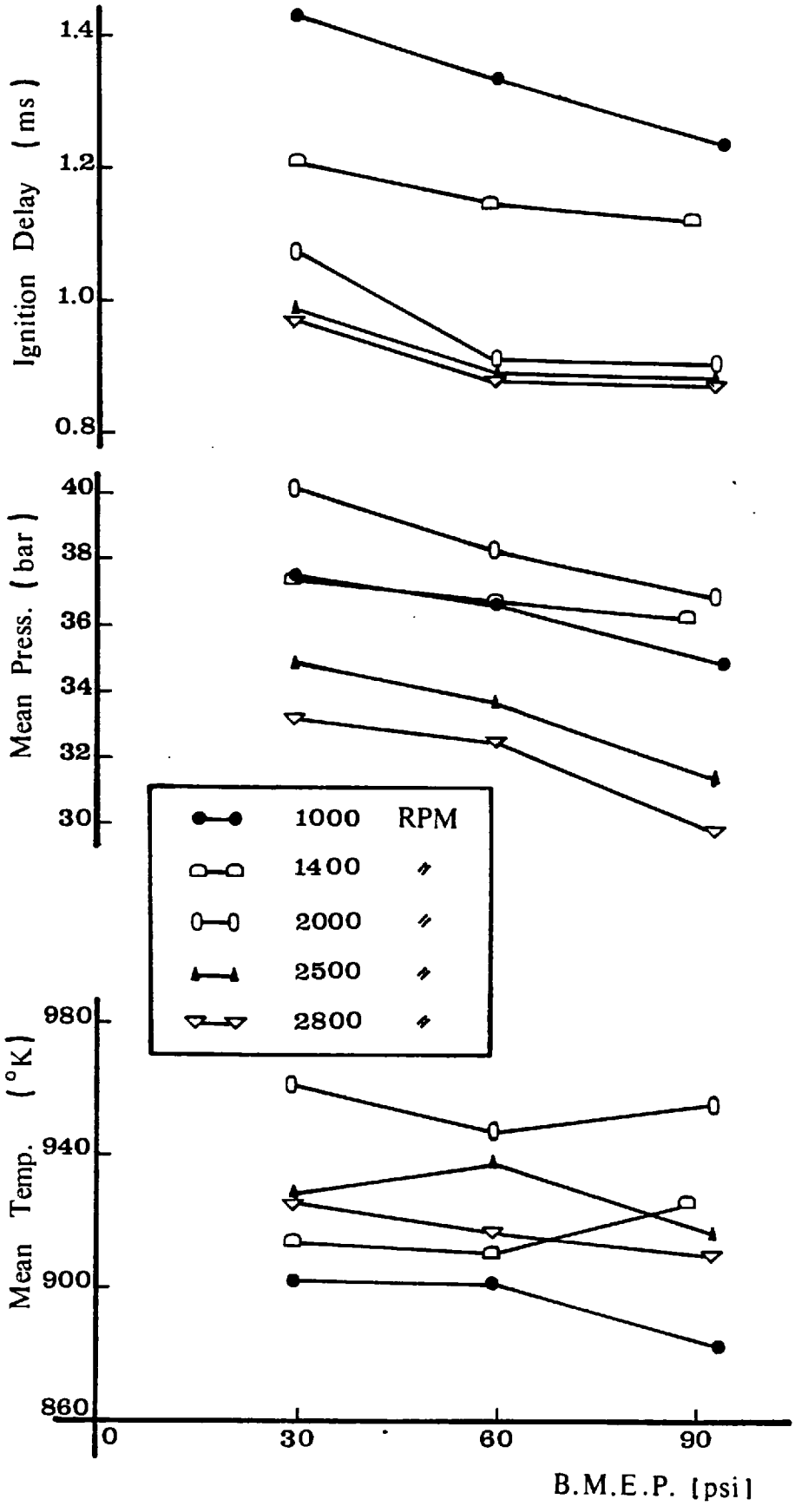


Figure 3.7: Mean cylinder temperature, mean cylinder pressure and ignition delay as a function of BMEP

TABLE 3.2

Test Number	Ignition Delay (ms)	Speed (rpm)	Mean Cylinder Temperature (^{o}K)	Mean Cylinder Pressure (bar)	Specific Heat Ratio
1	1.425	1000.0	902.995	37.590	1.309
2	1.202	1400.0	913.292	37.461	1.270
3	1.075	2000.0	961.189	40.120	1.274
4	0.987	2500.0	928.453	34.869	1.278
5	0.970	2800.0	926.233	33.244	1.355
6	1.330	1000.0	901.728	36.6B3	1.289
7	1.140	1400.0	910.674	36.909	1.221
8	0.908	2000.0	947.812	38.311	1.242
9	0.890	2500.0	938.046	33.700	1.281
10	0.881	2800.0	917.441	32.501	1.302
11	1.310	1000.0	886.548	35.680	1.187
12	1.119	1400.0	926.751	36.337	1.283
13	0.900	2000.0	955.023	36.930	1.225
14	0.880	2500.0	916.620	31.460	1.264
15	0.869	2800.0	910.519	29.882	1.224

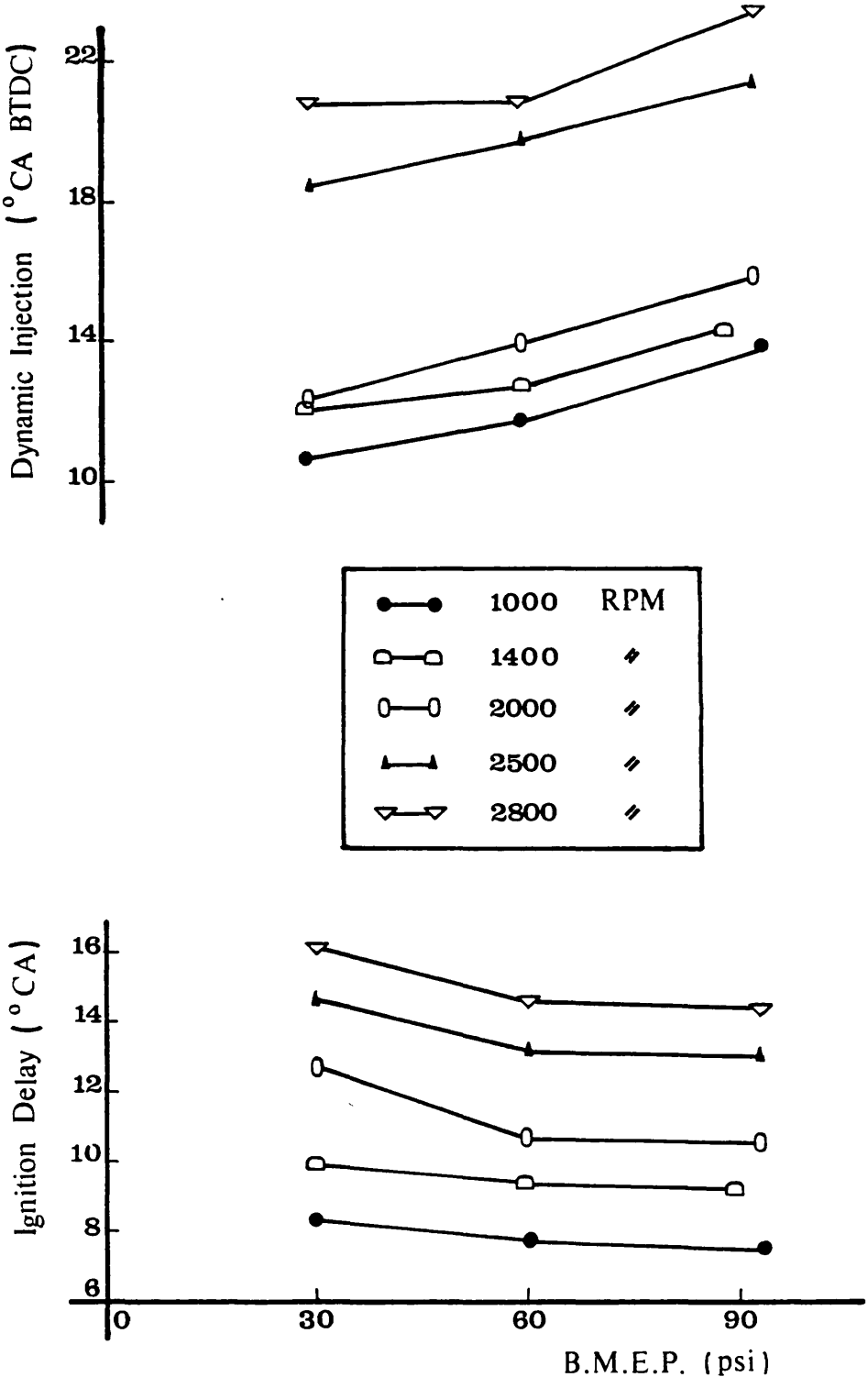


Figure 3.8: Ignition delay and dynamic injection as a function of BMEP

for ignition delay:

$$c_1 = 0.5532 \times 10^{-5} \quad , \quad c_2 = 5640.5 \quad , \quad c_3 = -1.692$$

If these values are inserted in the Wolfer's equation, the ignition delay computed is reasonably satisfactory. This has been shown graphically in Figure 3.6(c) in which the predicted and experimental values are compared. The mean error estimated is 4.3% and, for the most severe condition, the error does not exceed 11% of the experimental values.

An apparently odd point about the correlation obtained here is the negative sign for the coefficient c_3 which is in contrast with all other correlations reported elsewhere (Wolfer (1938); Schmidt (1938); Zimmerman (1962); Marzouk (1976)). This can, however, be explained by considering the nature of the DPA rotary fuel injection pump which was employed on the engine under test. The characteristics of this pump, as shown in Howes (1969), is that the static injection time varies with speed of the engine as a result of the speed advance device. In a DPA rotary pump, the injection is advanced by increasing the engine speed, and therefore the mean pressure between the dynamic injection and ignition point may decrease with the engine speed under certain conditions. Figure 3.7 shows the mean cylinder pressure and the mean cylinder temperature versus the engine powers and, as demonstrated, they are not monotonic functions of speed and load. This phenomenon is in contrast with all the aforementioned formulae obtained for different engine pumps in common use, since they assume a constant static injection time. Bearing this in mind, a monotonical increase of mean cylinder pressure due to the increase of speed and load will be expected for these pumps (e.g. for the jerk pump, see Marzouk (1976)). The other reason for

obtaining a negative coefficient of c_3 is due to the variation of dynamic injection as a result of the variation of load. Figure 3.8 illustrates how dynamic injection advances with increasing load for different speeds.

As far as it is known, there is no reference describing the characteristics of the DPA rotary fuel injection pump, so the validity of the numerical values obtained for the coefficient of the Wolfer formula cannot be compared. However, the reasonably accuracy achieved for predicting the ignition delay justifies the application of the correlation described with confidence.

3.5 GENERAL REMARKS

Examination of the combustion pressure under normal conditions shows that there is a large cycle-to-cycle variation in the combustion. This variation complicates the experimental procedure necessary for evaluating the burnt gas composition and its relation to particular operating conditions. Experimental results thus represent average values of a number of different cycles for comparison with predicted values.

The engine computer control and data acquisition facility (which are discussed in more detail in the following chapter) were used to record the average of 128 cycles of cylinder pressure, needle-lift, fuel-line pressure, and the rate of cylinder pressure rise with standard deviation of cycle-to-cycle variation in cylinder pressure development. These data were used to obtain dynamic injection, ignition delay, mean cylinder pressure during delay and also the rate of heat release diagram by Krieger & Borman's method (1966). This method and the numerical analysis solution for solving the relevant equations are presented in Appendix A2. These diagrams were taken into account when comparing the theoretical predictions of different methods and to modify the constants of different models

corresponding to real situations.

Apart from engine specifications supplied by the manufacturer, some supplementary data were needed which were not available at the time of analysis. These data were found through experiments or assumed on the basis of other engine data. For example, the following data were supplied by Perkins: valve timing, mean cylinder head temperature, mean piston crown temperature, mean linear temperature, etc. Inlet manifold volume, volume and heat transfer area of exhaust manifold, dynamic injection, end of combustion, and weight of fuel per cycle per cylinder were either measured or calculated. Effective inlet and exhaust valve areas were calculated from valve lift diagrams, and coefficients of discharge were taken from Kastner, William & White's data (1968). The description of the method and the diagrams of the effective inlet and exhaust valve areas versus the crank shaft are presented in Appendix A6.

The starting time of injection, ignition delay, quantity of fuel injected, rate of heat release, and cumulative heat release were measured or calculated for some operating conditions and compared with other available data (for example, Marzouk & Watson (1974) which contains data useful in modifying the combustion model coefficients).

Figure 3.9 is a typical plot of the comparison between predicted values obtained by the simulation program with experimental results for Test TR13 at a speed of 1000 rpm and a load of 5 mkp operating conditions.

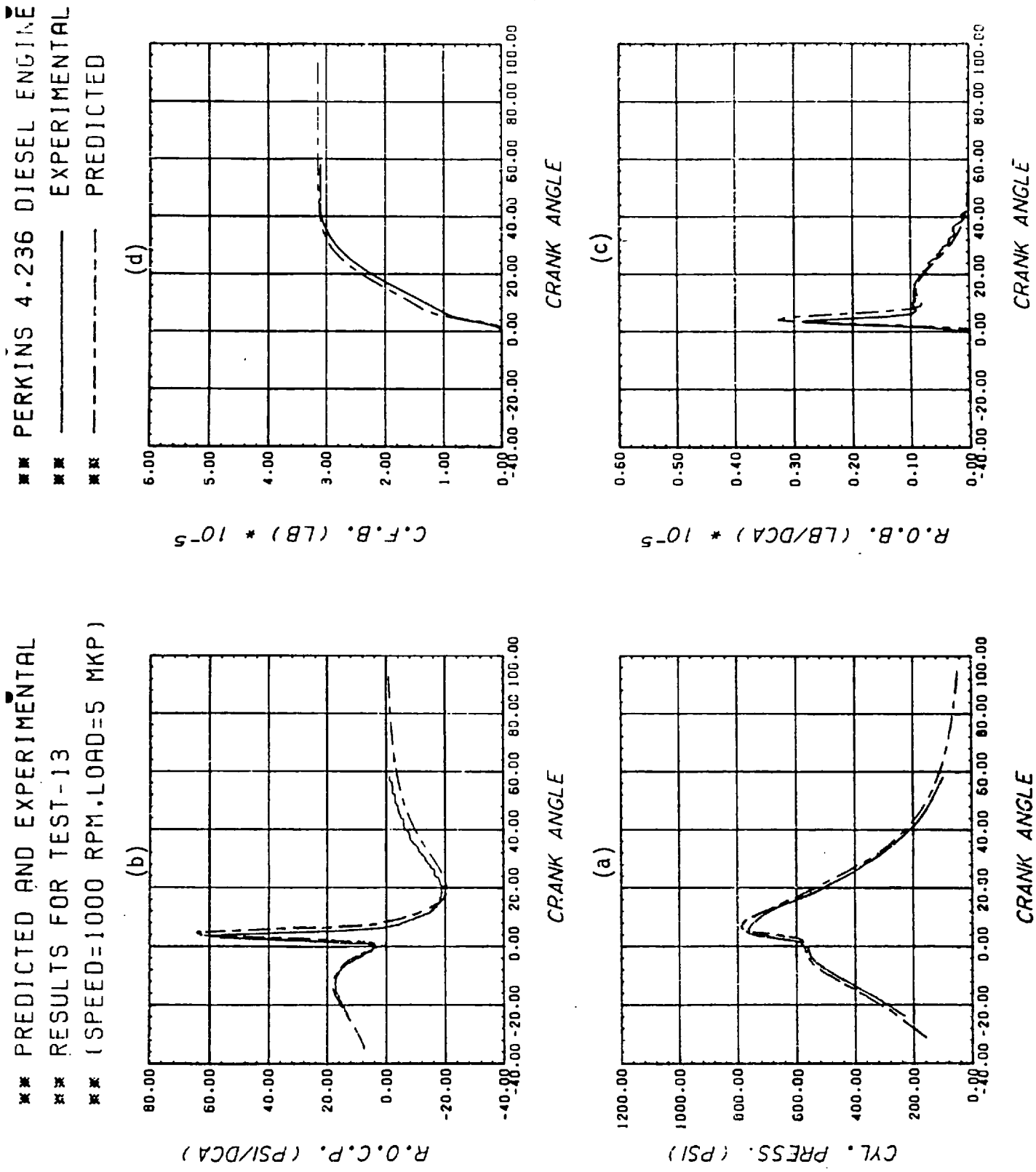


Figure 3.9: Comparison of the predicted values by the diesel engine simulation program and experimental results at given operating conditions:

(a) Cylinder pressure diagram

(b) Rate of cylinder pressure rise diagram

(c) Rate of burning

(d) Cumulative mass of fuel burnt

CHAPTER 4

APPARATUS AND MEASUREMENT TECHNIQUES

4.1 INTRODUCTION

Technological advances in electronic instruments have played an important rôle in the history of research in internal combustion engines by improving the speed and accuracy of engine measurements. The instrumentation for engine research and development includes not only devices for measuring pressure, temperature, speed, etc., but also control systems for setting test conditions, recording and analysing data.

It is beyond the scope of this thesis to give details of all the instrumentation employed in this work, since (i) such information is well documented elsewhere, and (ii) in this particular study, it is sampling techniques rather than the instruments themselves which are of importance in these statistical and correlation tests. In any digital instrumentation system, the rate of sampling of each parameter must be chosen from statistical requirements. In general, the minimum number of samples required depends on the variability inherent in the data which itself is a function of engine operating conditions and system noise level. For example, the random nature of cylinder pressure development requires that a large number of samples be recorded during the combustion period. Consequently, the development of the recording system has played an important rôle in the study of cycle-to-cycle variation in internal combustion engines. Due to the limitations of recording sufficient cycles and the difficulty of accurate analysis of film recording, photographic recording of oscilloscope records (employing a single frame camera, continuous film, or a drum camera) has been superseded by magnetic tape recording. The basic advantage of a digital recording system is in the

data processing method which is then carried out by software rather than hardware, providing greater flexibility and increased capability compared to the analogue system. A further improvement has been achieved by employing a mini-computer on-line with the engine for the following reasons:

i) Maximum elimination of human intervention.

ii) Rapid assessment of instrument errors so that tests are not abortive.

iii) Reduction of tedium in testing.

iv) Exploration of engine performance under conditions which are not possible with a conventional test bed (transient response of turbocharged diesel engines).

v) Facility of computer programming to define accurately the set point of analogue controllers at the engine and to check desired steady-state conditions.

vi) Precise timing of events, immediate availability of results and overall accuracy throughout the system.

vii) Possibility of preliminary analysis of data to be conducted during breaks in the data sampling. Also permits acquisition of large statistical samples with excellent repeatability of experiments.

The computer controlled engine test facility at Imperial College was designed for direct digital control of engine speed and brake torque. Secondary variables (coolant and oil temperature) are controlled locally. The extent of direct digital control is limited by the computer characteristics (speed and core memory), software capability and data

requirements.

This chapter includes a brief description of the computer controlled test bed facility, further details of which may be found in Bloxham et al (1972). The computer software specially written to carry out data logging is also described.

4.2 TEST BED

The computer controlled test facility is shown schematically in Figure 4.1. It consists of an eddy-current dynamometer and test bed, multiplexed analogue to digital converter (ADC), a specially built interface and a PDP-15 computer. Figures 4.2 and 4.3 give different views of the test bed and instrumentation.

4.2.1 The Engine

The engine used in all these tests was a Perkins 4.236 diesel, 4 cylinder, direct injection machine, naturally aspirated and of 3.86 litre capacity. The fuel pump is a CAV distributor (DPA) type, as described by Howes (1969) and Khan & Green (1975). Injector rack position of the fuel pump is controlled by a stepping motor which provides 400 steps over the operating range.

The injectors are of the multi-hole (four) nozzle type with maximum needle lift of about 0.28 mm and nozzle opening pressure of about 175 atm. Figure 4.4 shows the characteristics of the injectors used on the Perkins 4.236 diesel engine.

The detailed specifications of the engine are given in Appendix B1.

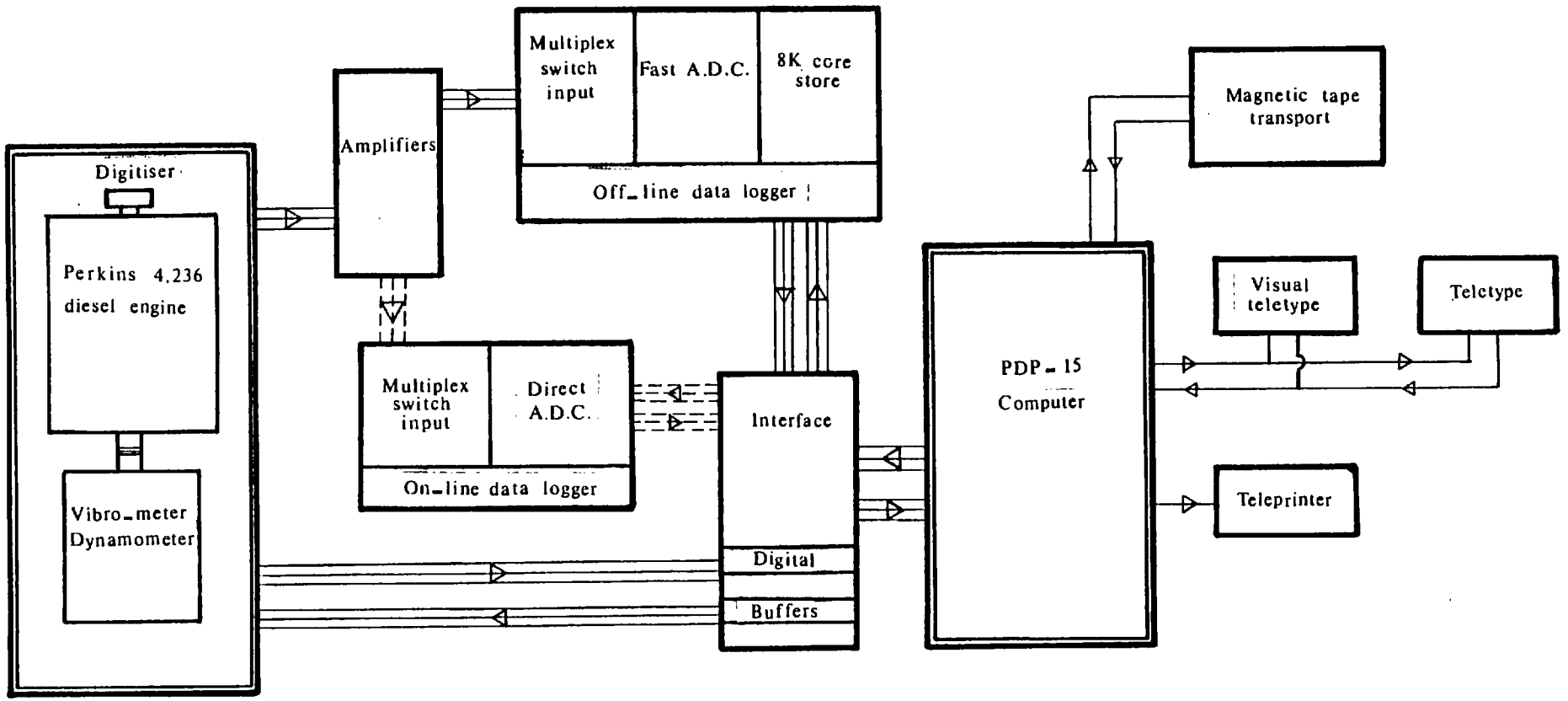
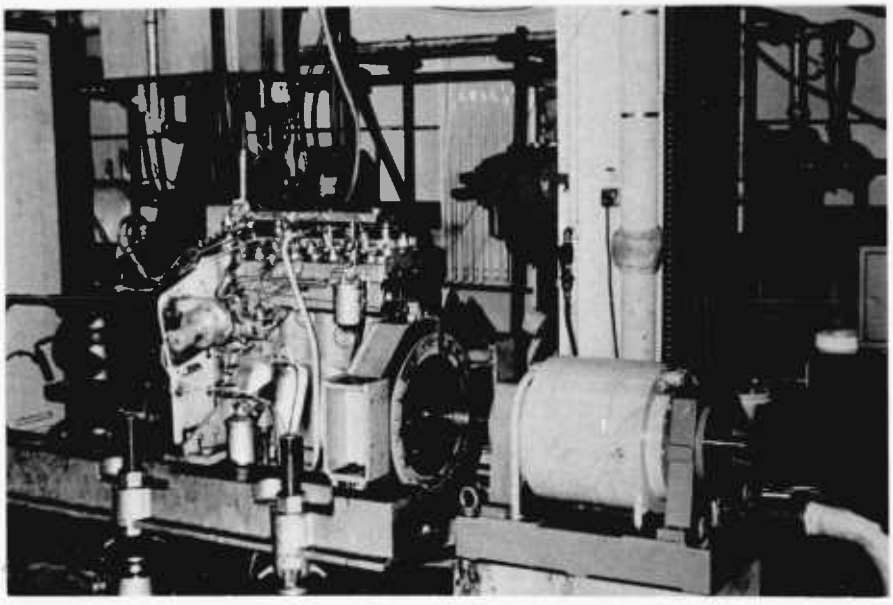


Figure 4.1: Hardware system of Perkins control engine and connections of the engine instrumentation to the computer

(a)



(b)

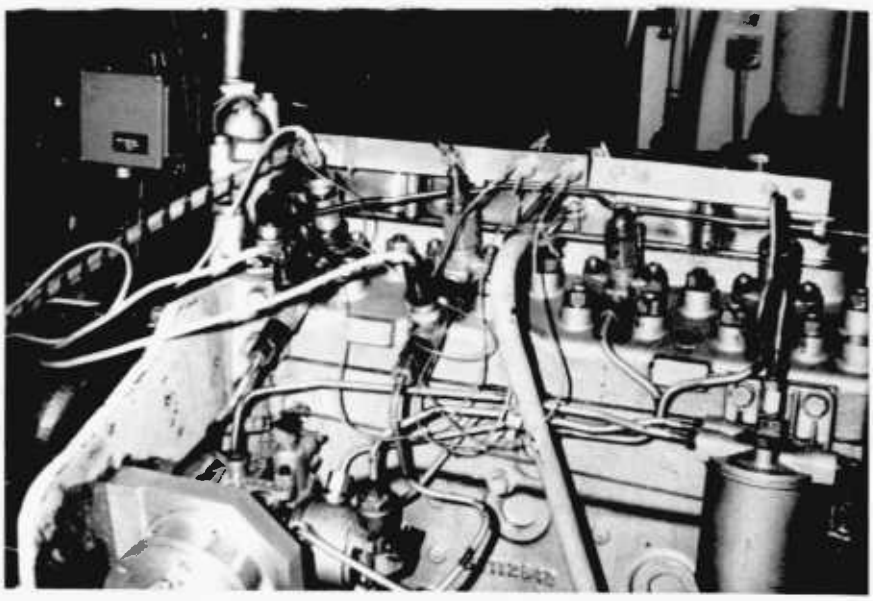
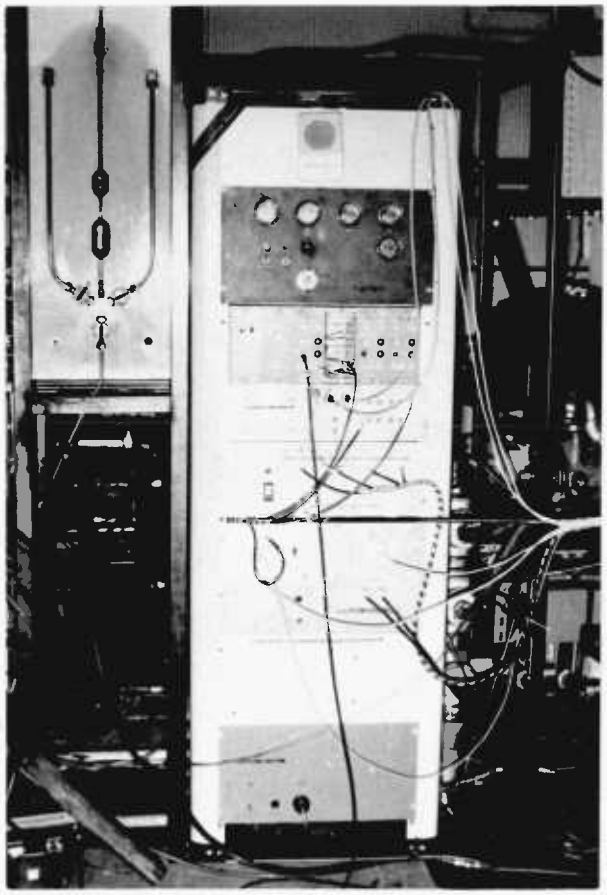


Figure 4.2: (a) The Perkins 4.236 diesel engine test bed

(b) The piezo-electric, strain gauge and inductive transducers mounted on the engine

(a)



(b)

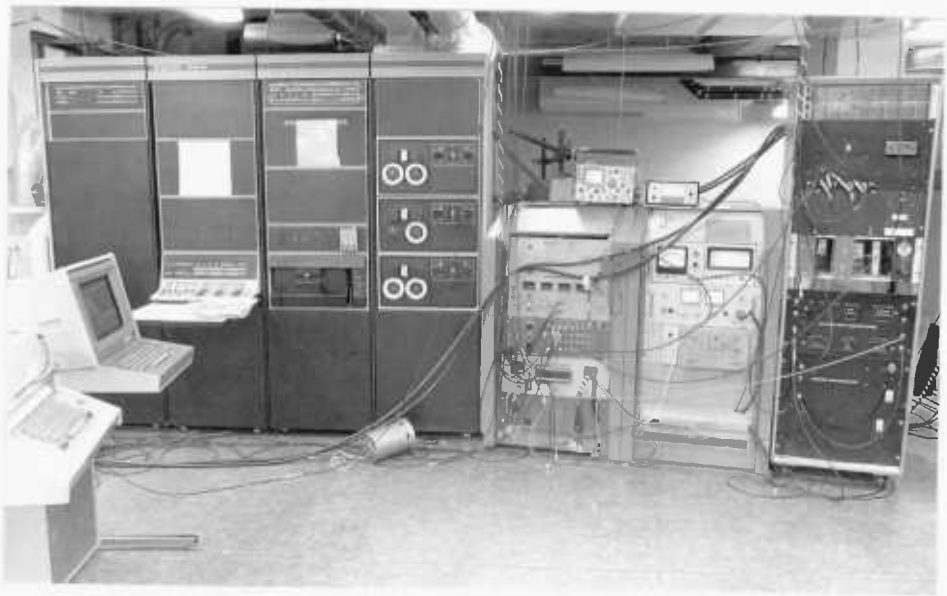


Figure 4.3: (a) Engine control and monitoring equipment (panel of amplifiers and power supply units)

(b) The computer, interface and on-line and off-line data loggers

Type of nozzle	:	DBLL 150 S 6507, XK
Maximum needle lift	:	0.28 mm
Specific weight of fuel	:	0.82 gr/cm^3
Fuel temperature	:	40^{o}C

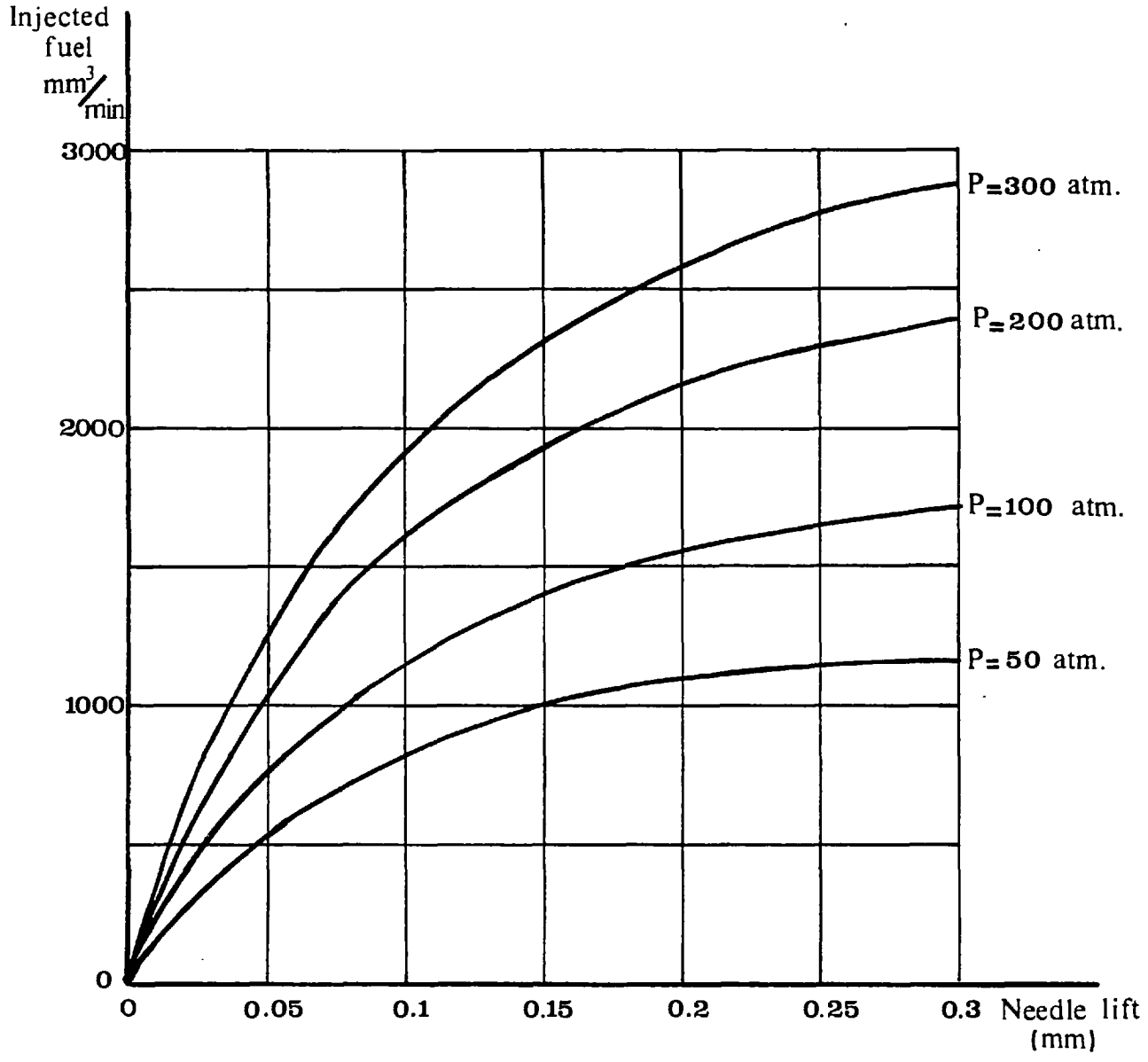


Figure 4.4: Injector characteristics

4.2.2 The Brake

The eddy-current dynamometer manufactured by the Vibro-Meter Corporation is coupled to the engine for power absorption. The dynamometer has a rapid overall response (0.3 ms for a change in output voltage from zero to the maximum voltage at maximum load) due to its low rotor inertia and thyristor drive unit. The required load is fed from the computer via a digital/analogue converter (DAC), a three-term control and linearization amplifier (proportional, integral, differential) and a thyristor drive unit to the dynamometer. A strain gauge bridge positioned inside the dynamometer accurately provides a continuous read-out of brake torque.

Heat generated due to the power dissipation is absorbed by cooling water which passes through the stator jacket. Figure 4.5 illustrates the operating limits for both the engine and the dynamometer.

4.2.3 Transducers

The two major requirements for any transducers are invariant calibration and fast response time. With pressure transducers (either piezo-electric type or strain gauge), the first requirement is hard to achieve but the fast response time can be easily met. With temperature transducers, contrarily, the first requirement is simpler to achieve than the latter. Displacement transducers can be constructed having fast response times and approximately invariant calibration; however, much care is needed to set up the device initially.

Two piezo-electric (quartz) transducers manufactured by Vibro-Meter (AVL) were installed in the head of two cylinders of the engine (cylinders number one and two) in order to measure cylinder pressure directly. The temperature of the transducers was maintained approximately

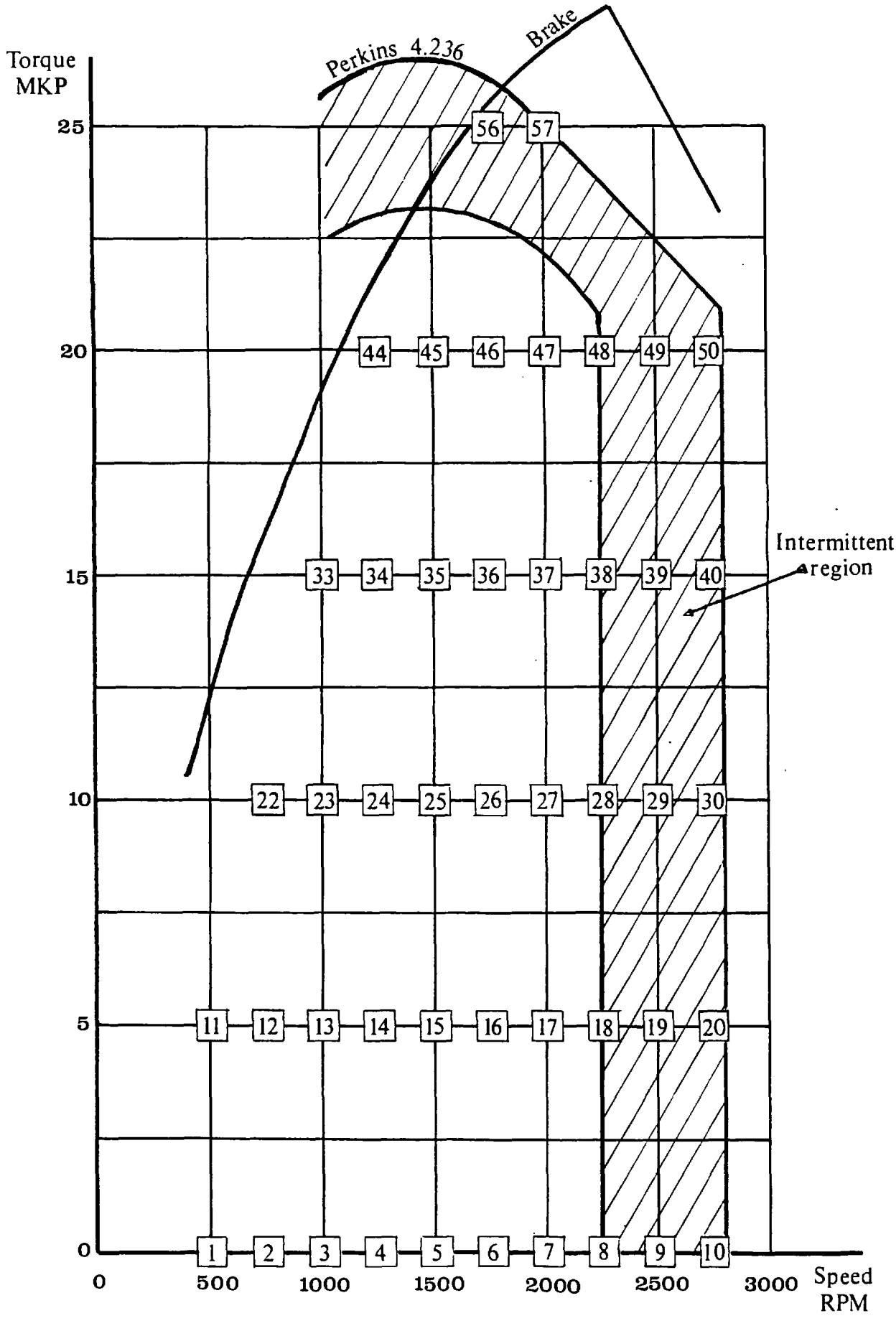


Figure 4.5: Operating limits for engine and dynamometer; fixed torque/speed test points

constant by circulating cooling water. This not only reduces the temperature drift but increases transducer life. However, high frequency noise created by the cooling water limits its flow rate. Overheating of the piezo-electric transducer can result in the breakage of some quartz elements or reduced sensitivity. If the piezo-electric transducer is located in the combustion zone, it may suffer from the thermal shocks, as shown by Brown (1967). Although these types of transducer are very small in size, they are generally of high stiffness and robust for these difficult circumstances. The other advantages of these transducers are their high frequency response (100 kHz) and linear operating range. On the other hand, the drift at zero position and the weak resistance to thermal shock are their main disadvantages. The output signal of these transducers, which is proportional to the pressures inside the cylinders, is sent to the ADC via charge amplifiers.

Two strain gauge line pressure transducers with plain passages manufactured by Vibro-Meter were used. These transducers are insensitive to mechanical stresses and vibrations, having wide and linear operating ranges and high accuracy (± 0.1%). The output signals of the transducers were fed into operational differential amplifiers in order to produce the fuel-line pressure analogue signals suitable for the ADC. Further details of the pressure transudcers and appropriate amplifiers are given in Appendix B2. The pressure transducers were calibrated by dead weight tester. Gain of the amplifiers was measured by a variable bridge designed specifically for this work.

To measure the injector needle position during the injection period, inductive displacement transducers were employed. To mount these transducers on injectors, some slight modifications were found to be necessary.

The inductive transducers consist of two coils forming a half-bridge circuit. A Ferrite slug is attached to the needle spindle by an aluminium rod. The inductance change produced at the half-bridge terminals due to movement of the Ferrite in the coils is proportional to the needle lift position. The signals generated by these inductive transducers were fed to carrier amplifiers.

High quality amplifiers were necessary for the following reasons, as Fisher & Macey (1975) reported:

i) Linear amplification: most of the transducer outputs for this application are low level signals in the range of ± 10 mV, whereas the ADC range is ± 5 V.

ii) Isolation from ground currents which could otherwise distort the data.

iii) Signal filtering is advantageous in controlling electrical and mechanical noise.

iv) Gain and attenuation adjustments: provide more application flexibility and easier calibration.

v) Low output impedance and high driving power: satisfies the dynamic interface requirements of the ADC.

4.2.4 Differentiator

In the present work, one of the important variables to be studied was the rate of cylinder pressure rise. Previous experience showed that digital differentiation of the cylinder pressure diagram using the computer was restricted by electronic (digitisation) noise and rounding errors. Therefore, it was necessary to obtain a smooth rate of

cylinder pressure rise by employing an analogue differentiator. Roughness of the cylinder pressure diagram itself arises from random high frequency oscillations, amplifier noise and thermal shock waves.

The differentiator was calibrated by an accurate ramp signal generator. The calibration was carried out on the same computer and conversion equipment to eliminate further errors. Figure 4.6 illustrates a typical sampled voltage-frequency saw-tooth signal with its differentiated signals, and Figure 4.7 shows the calibration curve for the differentiator. This calibration curve is plotted by obtaining the slopes of various saw-tooth signals and their differentiated signals.

The frequency response of the differentiator determines the degree of smoothness of signals provided by this device. A slower response results in a higher degree of smoothness as the device then filters high frequency oscillations due to noise and thermal effects.

The time lag in frequency response of the differentiator is found to be about 0.63 ms. Comparison of the time between sample pulses at 1000 rpm (t = 60/1000 × 1024 = 0.0585 ms) and at 2800 rpm (t = 60/2800 × 1024 = 0.0209 ms) with this time lag indicates that the differentiator response is too slow, so the maximum rate of cylinder pressure rise obtained will be under-valued. Moreover, this low response of the differentiator produces a shift in the differentiated signals (see Figure 4.20). It is essential, however, that this time lag remains greater than the time between two pulses at all conditions, otherwise the differentiator cannot filter the undesirable frequencies which are usually observed in the main signal, and consequently the differential signals will not be smoothed.

Because of the importance of this factor (slow response of the differentiator) at high speeds, a numerical differentiating technique was

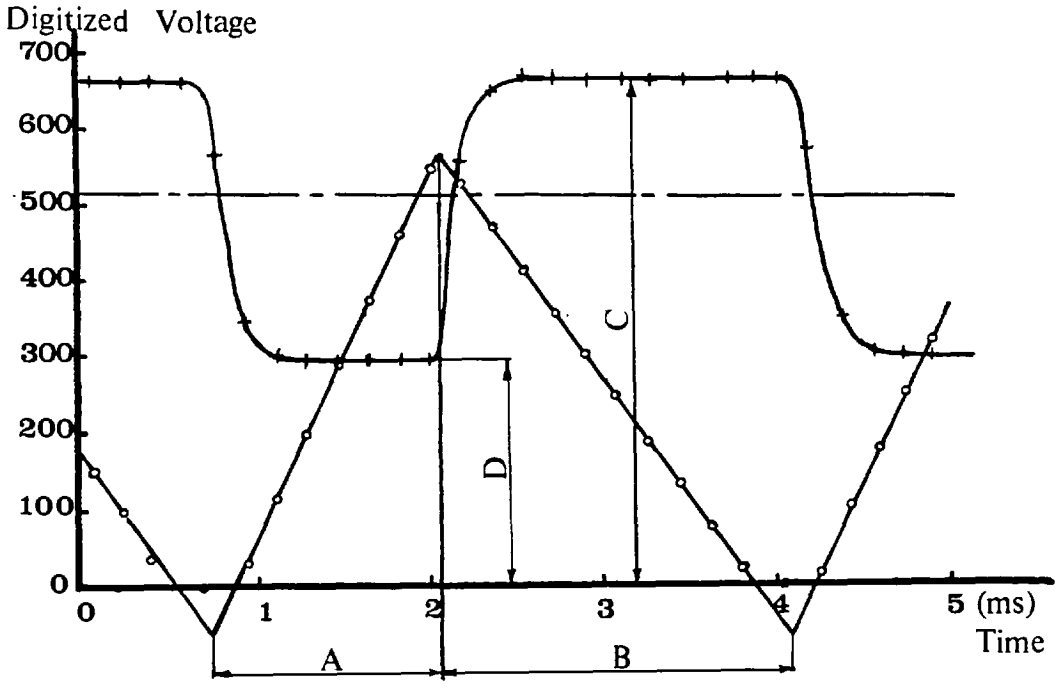


Figure 4.6: Voltage to frequency sawtooth signal and its differentiated signal by differentiator

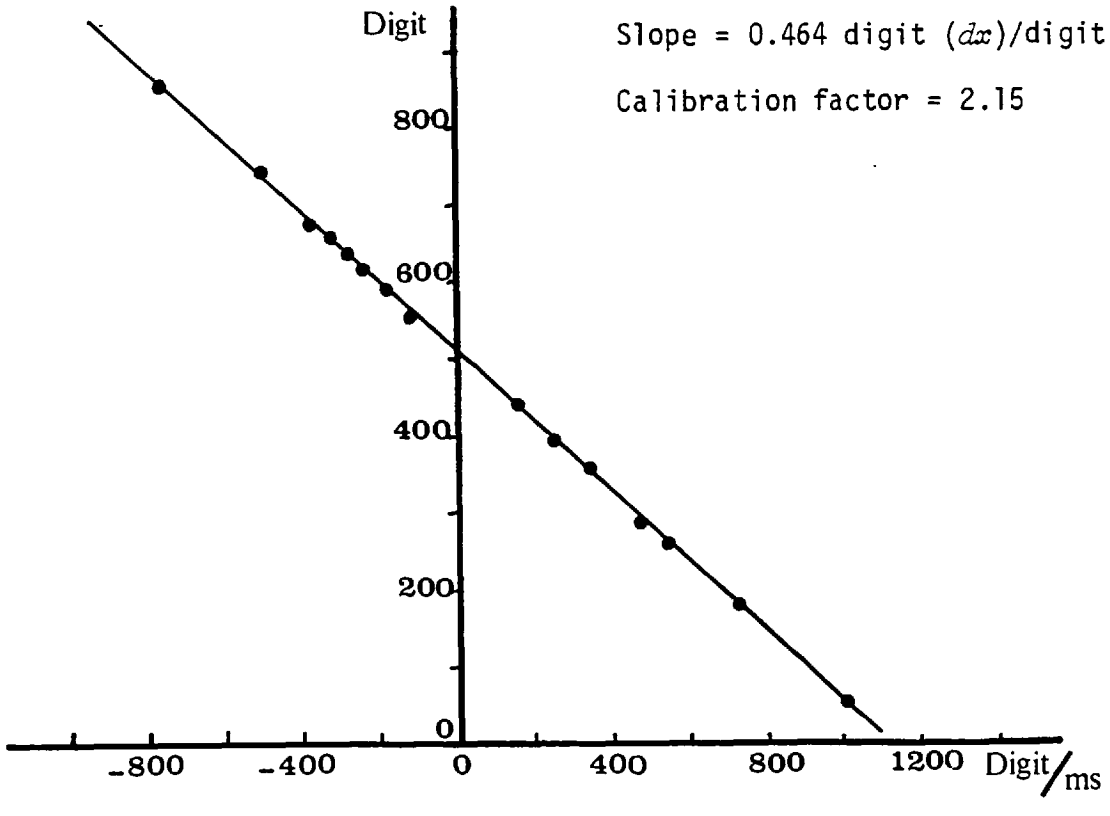


Figure 4.7: Calibration curve for differentiator

employed using spline functions (Streit & Borman (1971)).

To apply the spline function, the mean values and standard deviations of the cylinder pressure diagram are to be computed. However, the use of the spline function requires statistical analysis of a number of consecutive cycles. Therefore, when this analysis was available (by using program AVESTD, as described in Section 4.3.2.2), the spline function was used to obtain a smooth rate of cylinder pressure rise diagram, otherwise when analysis of individual cycles was required, the spline function could not be applied for smoothing the rate of cylinder pressure rise diagram. Under these conditions, the problem can be overcome by utilizing a differentiator in the hardware circuit. The program PERFU2 in Section 4.3.2.1 shows the application of the differentiator in the statistical study of engine characterizing parameters.

4.2.5 Digitiser

In order to start the experiment at precisely fixed trigger points in each cycle, to determine accurately the speed of the engine, and to measure the exact position of crank angle, an optical shaft encoder (a Moiré fringe incremental digitiser manufactured by Ferranti Limited) was employed. The digitiser was coupled directly to the engine crank shaft by an axially flexible but torsionally stiffened coupling. This device provided two different pulse signals: a gate pulse produced at each revolution, and digitiser pulses produced every 1/4096 of a revolution. (N.B. For many experiments, only 1024 pulses per revolution were employed, as sampling at approximately $1/3^{o}$ crank angle intervals was usually sufficient.)

The gate pulses also provided rapid and accurate measurement of engine speed by timing the interval between these pulses using a 25 kHz

crystal clock.

The digitiser pulses provided exact measurements of crank angle position and governed data sampling rates. Transducer signals (cylinder pressure, fuel-line pressure, needle lift) were fed into the ADC to be sampled in synchronization with these digitiser pulses. To define the position of TDC in relation to the marker pulses, the engine was run under different conditions with cylinder (1) motored. The mean cylinder pressure diagrams were recorded for 128 cycles and the maximum was assumed to occur at TDC. Figure 4.8 shows the needle lift, fuel-line pressure, cylinder pressure and rate of cylinder pressure diagrams at 1500 rpm and 5 mkp. (All diagrams correspond to the motored cylinder number 1.)

4.2.6 Speed and Torque Controller

(a) Speed controller: A stepping motor connected by reduction gearing to the injector pump is used to control engine speed, this being part of the speed control loop involving also the optical digitiser for speed measurement and the computer as controller.

In the digital speed buffer, the number of clock pulses between two gate pulses is stored and up-dated each engine cycle. The computer reads this number as the real engine speed and compares it with the speed required in the test. It then evaluates the number of steps and the direction of rotation of the stepping motor in order to achieve the desired speed. After defining the number of steps and the direction needed, the computer transfers this information to a binary counter where logic circuitry executes the operation. The number of steps executed is recorded in the counter. An electronic latch in the system monitors the number of steps executed and prevents possible interference of further commands given by the computer before completing the previous job.

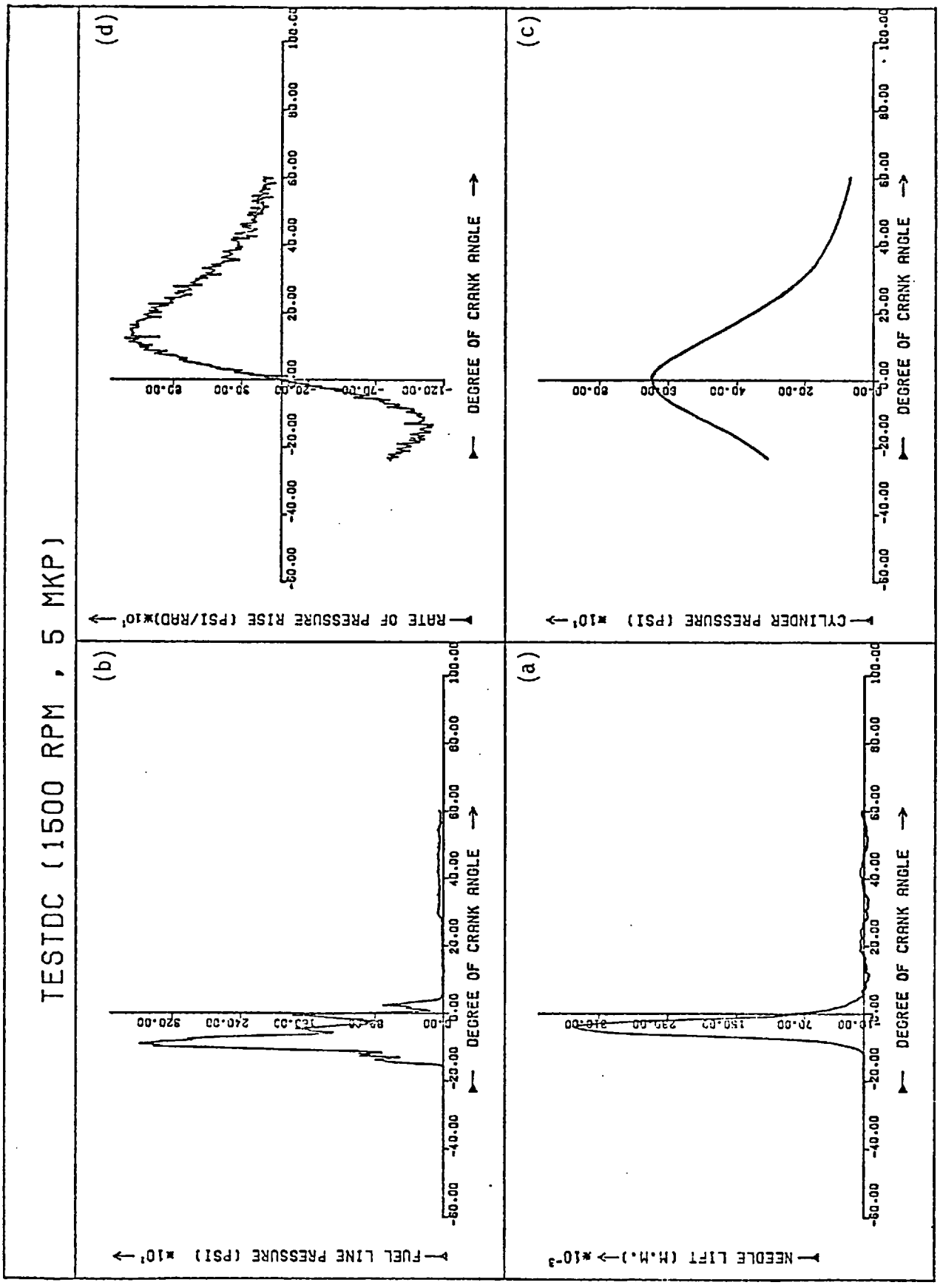


Figure 4.8: Motored cylinder 1 test for finding the location of TDC:

(a) Needle-lift diagram
(b) Fuel-line pressure diagram
(c) Cylinder pressure diagram
(d) Rate of cylinder pressure diagram

(b) Torque controller: The instrumentation used for setting the load consists of a brake excitation unit, three-term controller, linearization amplifier, torque meter, torque buffer and ADC. This system controls the torque independent of engine speed. The brake excitation unit which controls the brake load is a voltage stabilizer regulated by a thyristor. A stabilized DC current is fed to the stator coils of the dynamo-meter in order to maintain a constant magnetic field. The control and linearization amplifier minimizes variations in load owing to thermal variations or engine speed changes, and also compensates for non-linearities existing between brake torque and excitation current. The required torque determined by the computer is fed to this control amplifier via a 10-bit DAC.

4.2.7 On-Line Data Logger

The on-line data logger is basically a medium speed 10-bit ADC with an input voltage of - 5 to + 5 volts.

Sampling was carried out in synchronization with the digitiser pulses, and therefore the conversion rate was dependent on engine speed. The maximum rate of conversion was 40 kHz and the conversion characteristic was approximately linear with a relative accuracy of ± 0.05%.

A fast multiplex switch was employed, which gave the ADC 32 channel capability, channel switching being directly controlled by the computer.

4.2.8 Off-Line Data Logger

For combustion and fuel injection experiments, it was necessary to employ a much faster data conversion facility than that described above. The off-line system consists of a high speed ADC with up to 8 channel

input multiplexing and an 8 K word memory which allows the data to be temporarily stored. In brief, the off-line data logger consists of an ADC having a 1.2 μs conversion time with a 0-10 V input range, a 1, 2, 4 or 8 channel multiplexor, and an 8 K word store rotating memory.

The process of data logging was as follows: The computer was programmed to initiate recording with an instruction for clearing the memory and the sample counter. The multiplexing sequence was then selected and the sample counter set to the required count. Once initiated, the data logger read the input data and stored them in the memory, sampling being controlled by digitiser pulses. During sampling the computer was free to be used for other operations. Finally, after completion of data logging, the computer transferred the data from the ADC memory to its own core memory.

4.2.9 Interface

Communications between the computer and the engine test bed are effected by a purpose-built logic interface. These logic circuits provide the necessary electronic conversions between the computer's own logic system on one side and the various test bed electronic systems on the other. They include analogue to digital and digital to analogue conversions, and all operating command conversions, for example:

- Flag testing and setting
- Multiplex switching
- Engine speed buffer up-dating and reading
- Stepping motor actuation, ..., etc.

The interface includes registers for parameters such as engine

speed, torque requirement, etc. The information in these buffers are continuously up-dated and always available for data input and control functions.

4.2.10 Computer

A PDP 15 digital computer (manufactured by the Digital Equipment Corporation) was employed for the computer controlled engine test bed. This computer has 16 K words of core storage, an 18-bit word length, and a 0.8 μs cycle time. Peripheral devices include a 256 K word fixed disc, three small magnetic tape transports, a paper tape punch, paper tape reader, a teleprinter, a serial printer and a visual display unit.

Standard software included compilers for Fortran IV, Macro and Focal. The Fortran IV high level language was limited in its application due to the large storage requirement in such a small computer. Conversely, the Macro low level language employed the available storage with much greater efficiency, and also minimized computing time when employed effectively. Therefore, data logging software (which was employed on-line with the engine) was written in Macro, whereas programs for calculating the statistical terms (which were only used for off-line data processing and analysis) were written in Fortran IV because of easier programming. The computer was thus employed as an on-line engine controller and data acquisition system, and also for all off-line data analysis.

4.3 CONTROL AND DATA-LOGGING SOFTWARE

The main on-line functions of the computer were to control the engine and to acquire, and partly analyse, data with accurate timing of events.

The software architecture for the computer-controlled IC engine is

shown in Figure 4.9 and has been reported by Bloxham et al (1972). This framework was decided after a structural study of the software requirements which concluded that:

i) The software should be capable of carrying out different types of tests and of being used on different engine types.

ii) Any modifications could be easily adopted and tested while the original versions continued to be ready for normal operation.

iii) Any new subprogram written for any part of the system could be easily integrated within the whole system.

iv) It should be possible to simulate the equipment under development.

v) It should be possible to develop several versions of programming to find out the best alternatives.

vi) Simplicity, flexibility and rational segmentation of the software to reduce the development efforts are desirable.

In writing the software, the following were also considered:

vii) Core requirement of the software.

viii) Execution time of each program or part of a program.

ix) Maximum usage of conversational mode to give maximum assistance to the computer operator.

For these reasons, an assembly of separately compiled modules written in Macro (machine code) was decided as the program structure. These programs have a common data transfer link with all other modules. Each module performs one basic function in general, and hierarchal structure optimises the transfer of command from module to module.

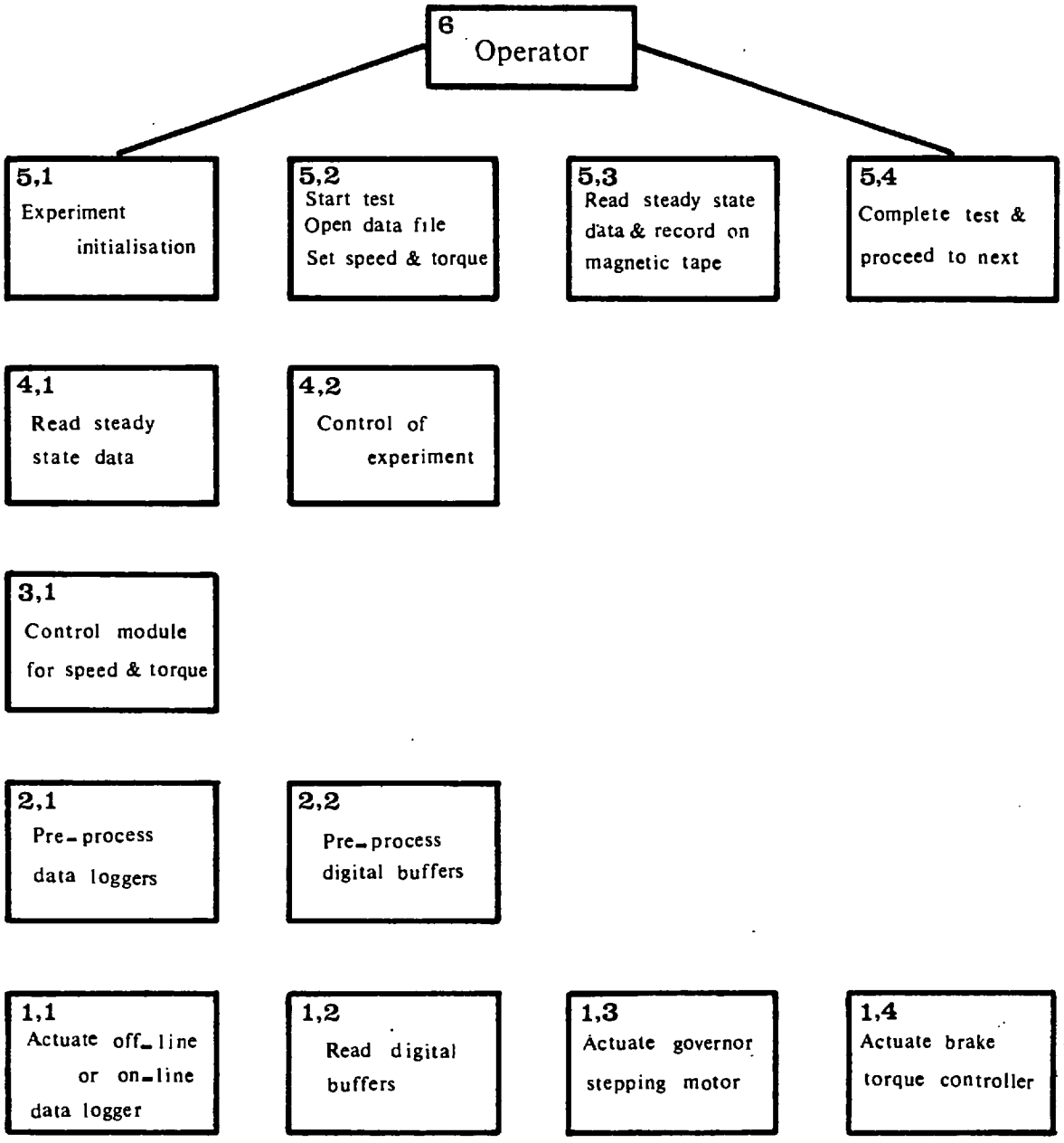


Figure 4.9: Software architecture for the diesel engine

The control software for the statistical study of diesel engines are described in the subsequent section. As will be shown, when a number of similar experiments are carried out, a combination of certain modules in a program is preferable (such as PERSYS, Perkins software system (Wing & Murgatroyd (1972))).

4.3.1 Control Logging Software

The programs used for continuous control of torque and speed were originally written by Wing & Jones (1972). Figure 4.10 illustrates the software system flowchart for the statistical study of cyclic variation on the Perkins 4.236 engine. The tasks of these programs are: the reception of operating instructions; the actuation of engine controls in order to reach the required test conditions; and the determination of the acceptability of steady-state conditions prior to logging data.

PERSYR (the new version of PERSYS, written by Wing (1972)) was the main program for controlling the Perkins 4.236 diesel engine. The operating conditions were set by inputs on the teletype keyboard by the operator. Each operating condition used was specified by a reference code number, as shown in Figure 4.5. It should be mentioned that, although these programs were normally used at the test points shown in Figure 4.5, the programs had sufficient flexibility to be modified for any required brake and torque. The subroutines called by the main program for controlling the engine speed and torque were:

PER31 - Controls the engine speed and torque in response to commands received from the operator input (Module - 3,1).

PER22 - Processes readings of engine speed from the digital buffers (Module - 2,2).

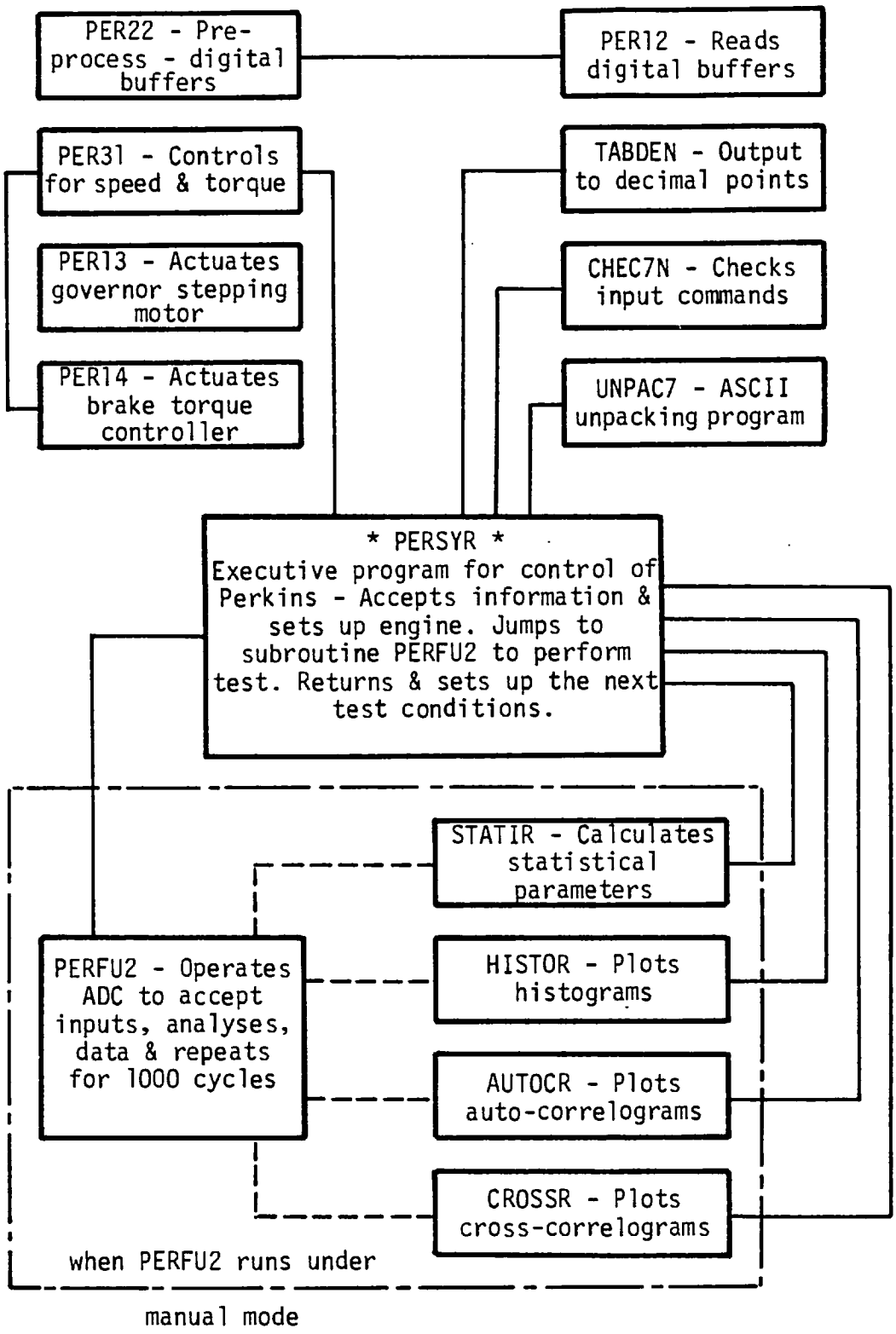


Figure 4.10: Perkins software system flowchart

PER12 - Checks for probable spurious results and reads the number of clock pulses between two consecutive gate pulses (Module - 1,2).

PER13 - Actuates the stepping motor on the injection pump rack for controlling engine speed (Module - 1,3).

PER14 - Provides output to the digital/analogue converter for setting the dynamometer load (Module - 1,4).

UNPAC7 - ASCII unpacking program. Converts teletype input commands to octal numbers in format required.

CHEC7N - Directs numeric input commands to relevant control modules.

In addition to the above control subroutines, a test management routine (in this case named PERFU2) was required for test initiation, sequencing and data logging. Further subroutines were used to calculate statistical and correlation parameters (STATIR, HISTOR, AUTOCR, CROSSR, etc.).

4.3.2 Data Logging Software

In this section, two test operation routines (PERFU2, AVESTD) will be briefly described. The statistical and correlation subroutines will not be explained in detail here, but are documented in Wing & Murgatroyd (1972).

4.3.2.1 PERFU2 program

PERFU2 is a subprogram invoked by the main program which operates the fast ADC to accept inputs from different transducer signals in synchronization with the digitiser, partly analyses the measurements, and repeats this operation for 1000 cycles. In brief, the program is planned to read 480 values each in a four channel mode data

acquisition of fuel-line pressure, cylinder pressure, fuel-line pressure again and rate of cylinder pressure rise, the sampling rate being 4096 pulses per revolution. Figure 4.11 illustrates the sampling and timing diagrams of the PERFU2 program. As shown schematically in this figure, the sampling zone begins approximately from 25^{o} crank angle before top dead centre to 15^{o} crank angle after top dead centre, so that the peak cylinder pressure, the maximum rate of cylinder pressure rise and dynamic injection are all included. The location of the zone can, however, be modified by the counter delay units. In the present test, 480 samples were recorded in this zone. The results were then analysed in order to produce the four physical quantities required during the idle time. The block diagram of subroutine PERFU2 is presented in Figure 4.12.

After reading the data from each cycle, the program evaluates the starting angle of injection, τ, the maximum rate of cylinder pressure rise, $\hat{dP}$, the time of occurrence of the maximum rate of cylinder pressure rise, $\theta(\hat{dP})$, and the peak cylinder pressure, $\hat{P}$. In this program, the dynamic injection was calculated from the fuel-line pressure diagram as the time of occurrence of the maximum rate of fuel-line pressure if it satisfied the nozzle opening pressure. This is because the starting angle of injection normally occurs at the maximum rate of fuel-line pressure rise but, in some special cases, the maximum rate of fuel-line pressure rise may occur at lower pressures than the nozzle opening pressure. Hence, the program checks whether the fuel-line pressure at the time of occurrence of the maximum rate of fuel-line pressure rise is higher than the anticipated value (experiment has shown the value of about 1.4 times greater than the fuel-line residual pressure would be a good value). If the condition is not met, the time of occurrence of the maximum rate of fuel-line pressure would be accepted as the starting time of injection, τ.

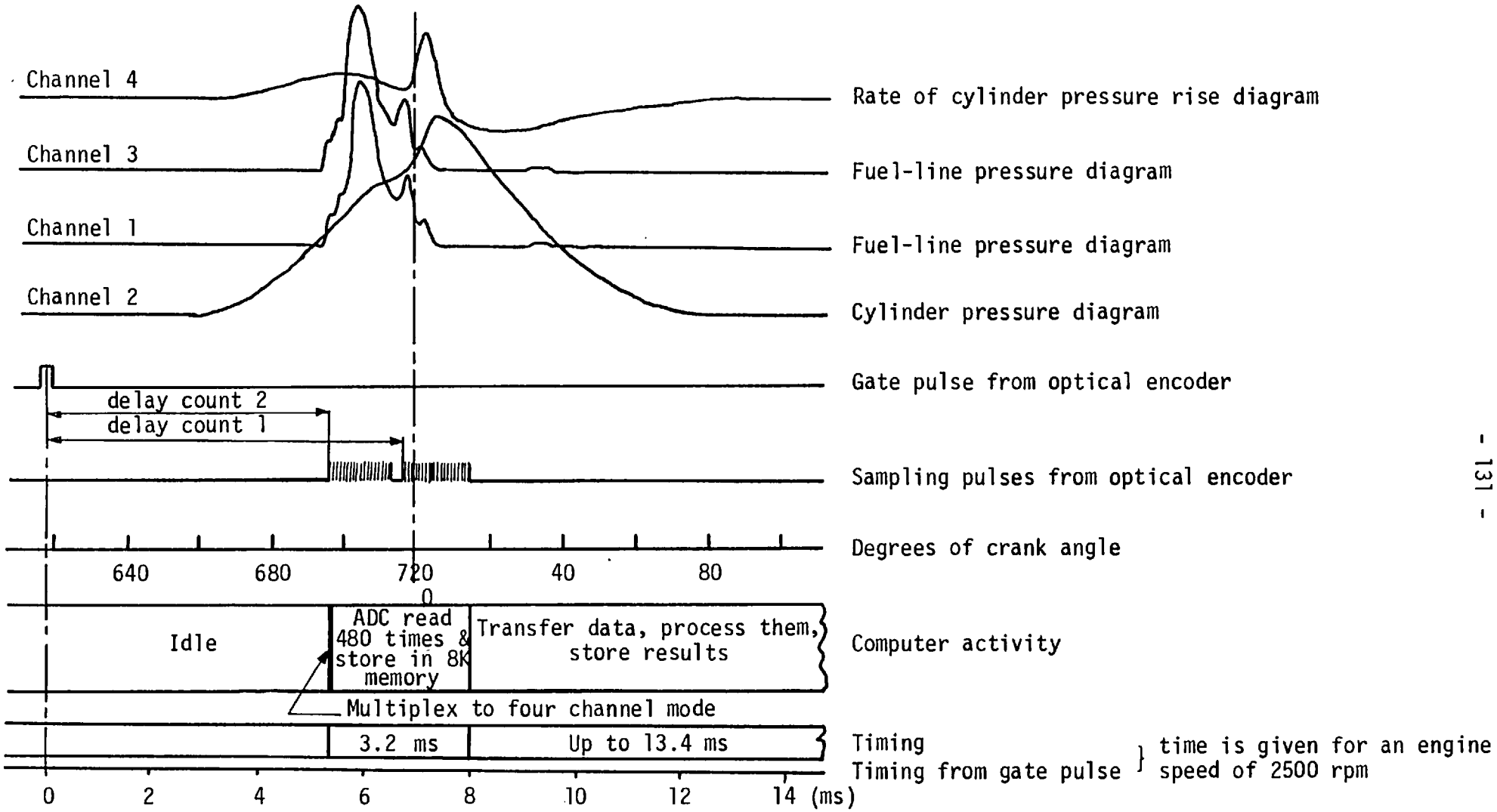


Figure 4.11: Signals, sampling and timing diagram for cylinder 1 (PERFU2)

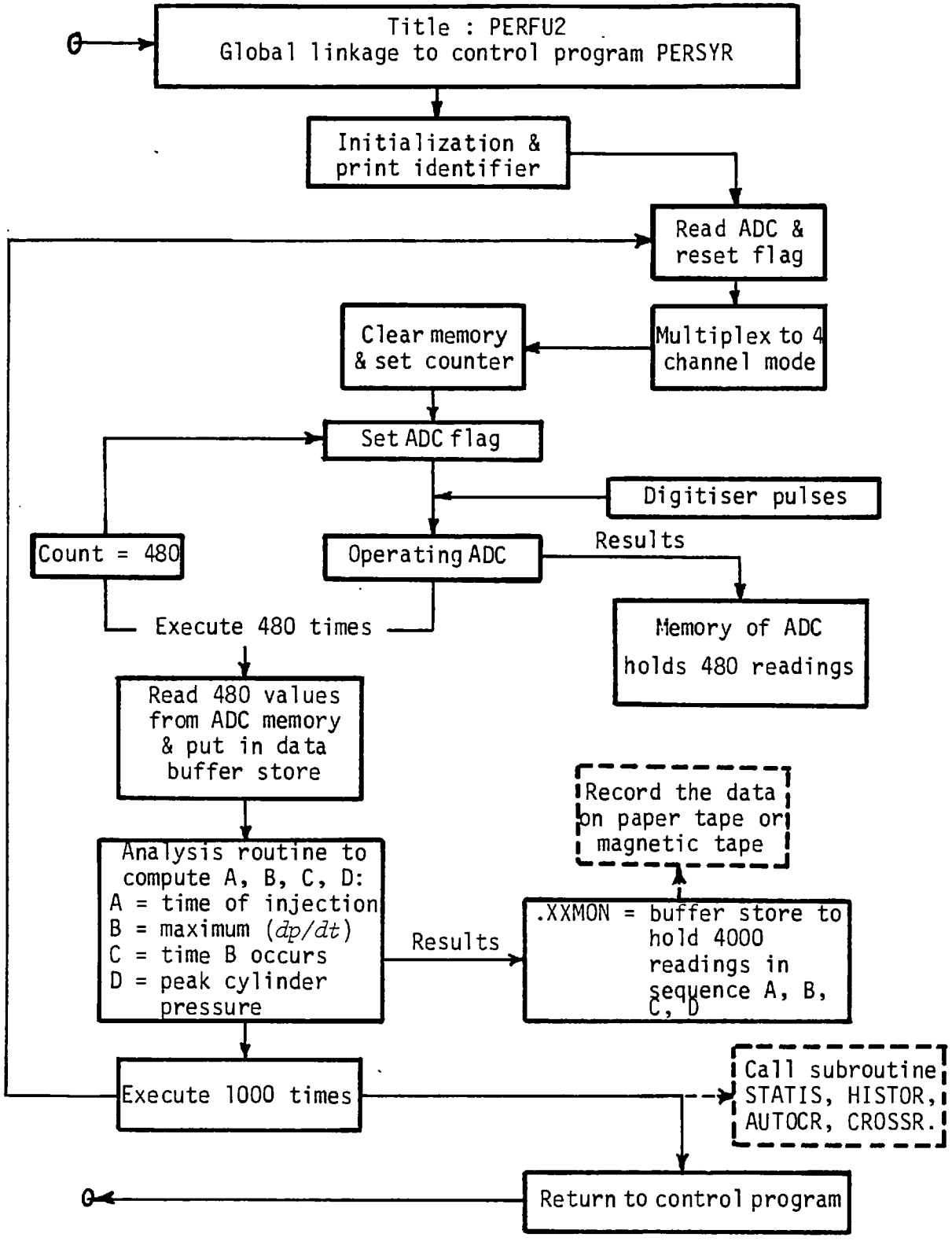


Figure 4.12: Block diagram of subroutine PERFU2

Otherwise, the program continues to search further for the next maximum rate of fuel-line pressure which satisfies the above condition. All timings (i.e. the starting time of injection or the time of occurrence of the maximum rate of cylinder pressure rise) were measured relative to a marker pulse on the optical shaft encoder on the crank shaft. This marker pulse was fixed at 28^{o} before TDC to provide an angular reference point. The flowchart of the analysis part of PERFU2 Macro program is given in Figure 4.13.

Under some low loading conditions, the maximum rate of cylinder pressure rise due to combustion may be smaller than the maximum rate of cylinder pressure due to compression. In finding the maximum rate of cylinder pressure rise due to combustion, the program should neglect the preceding maximum rate of cylinder pressure rise during the compression period. This can be done by skipping the 60 first values of the rate of cylinder pressure rise containing the possible $\hat{dP}$ at compression period. It should be mentioned that if the maximum rate of cylinder pressure due to combustion occurs during the compression process, this maximum will not be neglected.

After putting the four variables in the blank common locations, the program executes similar processes for another 999 engine cycles. Thus, a batch of 4000 locations of blank common for τ, $\hat{dP}$, $\theta(\hat{dP})$, and $\hat{P}$ values will be created.

The analysis of these data is then performed by calling subroutines STATER, HISTOR, AUTOCR, and CROSSR which calculate and present the statistical and correlation parameters in the form of histograms and correlograms. If data are satisfactory*, they are recorded on punched

---

* By satisfactory data, we mean a series of data which can be repeated and approximately populated as a normal distribution bell shape.

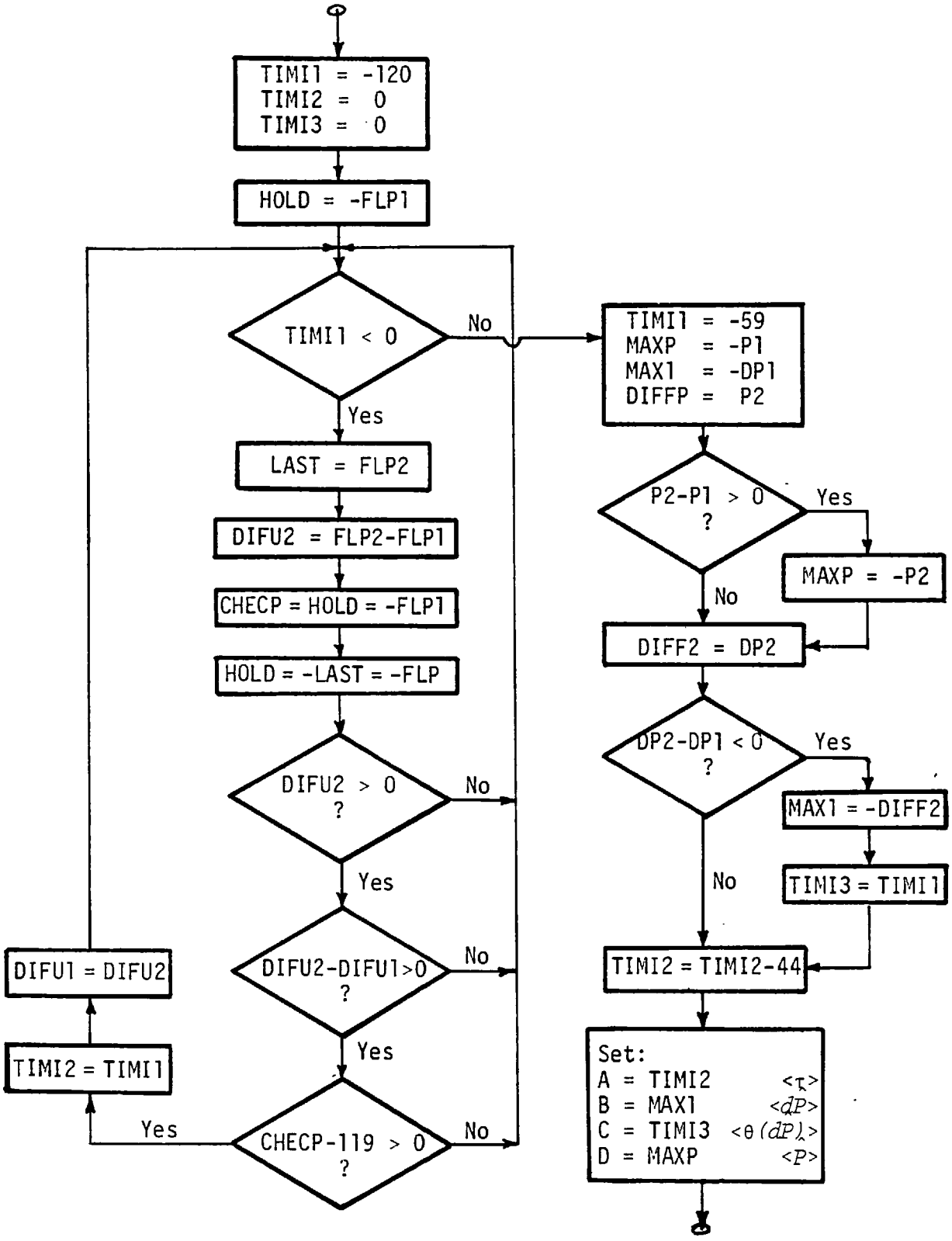


Figure 4.13: PERFU2 Macro program flowchart (analysis)

paper tapes for further applications and later access. Table 4.1 and Figures 4.14, 4.15 and 4.16 are typical samples of the computer output for execution of PERFU2 as an operating routine. The program listing of PERFU2 is also presented in Appendix B4.

4.3.2.2 AVESTD program

This program operates the fast ADC to accept inputs from different transducer signals in synchronization with the digitiser. It uses four channel mode data acquisition from cylinder pressure, rate of cylinder pressure rise, fuel-line pressure and needle lift, respectively. The program reads 960 values of these signals alternately at a rate of 4096 pulses per revolution. Hence, the values of each signal will be recorded at a rate of 1024 pulses per revolution (approximately three values in every degree of crank angle). Figure 4.17 presents the sampling and timing diagram of the AVESTD program. As is shown in this figure, the sampling zone starts approximately from 25^{o} crank angle before top dead centre to 60^{o} crank angle after top dead centre, and thus only covers a section of compression and combustion processes.

The program calculates the arithmetic means of cylinder pressure, rate of cylinder pressure rise, fuel-line pressure and needle lift diagrams over 128 successive cycles. Cycle average attenuates any random high frequency oscillations, electronic noise, etc. The program also calculates the standard deviation of the cylinder pressure diagram for two reasons. Firstly, these standard deviations are used to smooth the cylinder pressure diagrams, and secondly, by using the program to calculate the standard deviation of a large number of cylinder pressure diagrams, particularly during the intake stroke, it checks the base-line shift (or drift) of the piezo-electric pressure transducers or any other

TABLE 4.1: Output of Sample Data Analysis (Statistical Parameters)

(Speed = 1000 rpm; Load = 6.18 mkp)

A = Dynamic injection (τ)

B = Maximum rate of cylinder pressure rise ($\hat{dP}$)

C = Location of B ($\theta(\hat{dP})$)

D = Peak cylinder pressure ($\hat{P}$)

A= -51	B= 469	C= 8	D= 365
A= -51	B= 461	C= 8	D= 364
A= -51	B= 469	C= 8	D= 363
MAXIMUM			
A= -47 ,	B= 475 ,	C= 11 ,	D= 373
MINIMUM			
A= -52 ,	B= 445 ,	C= 6 ,	D= 358
MEAN			
A= -49.34 ,	B= 462.4 ,	C= 7.959 ,	D= 365.8
VARIANCE			
A= 1.074 ,	B= 19.38 ,	C= 0.3278 ,	D= 5.884
STANDARD DEVIATION			
A= 1.036 ,	B= 4.402 ,	C= 0.7265 ,	D= 2.426
STANDARD ERROR			
A= 0.3277E-01,	B= 0.1392 ,	C= 0.2297E-01,	D= 0.7671E-01
SKEWNESS			
A=-0.4228E-01,	B=-0.3387 ,	C= 0.2501 ,	D=-0.7188E-01
KURTOSIS			
A= 2.651 ,	B= 3.074 ,	C= 3.314 ,	D= 3.050

Ranges			Number of Occurrences
-52-	-51	:*	10
-51-	-50	:************	133
-50-	-49	:*************************	275
-49-	-48	:**********************************	385
-48-	-47	:***************	165
-47-	-46	:***	32
-46-	-45	:	0
-45-	-44	:	0
-44-	-43	:	0
-43-	-42	:	0

Histogram for starting angle of injection, H(τ)

445-	448	:	3
448-	451	:	4
451-	454	:**	18
454-	457	:********	76
457-	460	:**************	132
460-	463	:************************	235
463-	466	:****************************	268
466-	469	:******************	177
469-	472	:******	58
472-	475	:*	8

Histogram for maximum rate of cylinder pressure rise, H($\hat{dP}$)

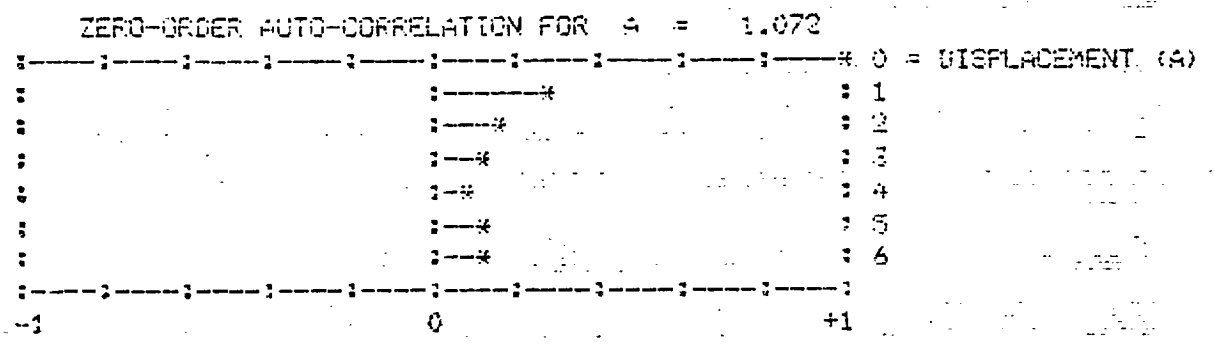
6-	7	:*	9
7-	8	:************************	238
8-	9	:**	557
9-	10	:******************	178
10-	11	:**	17
11-	12	:	1
12-	13	:	0
13-	14	:	0
14-	15	:	0
15-	16	:	0

Histogram for location of $\hat{dP}$, H($\theta(\hat{dP})$)

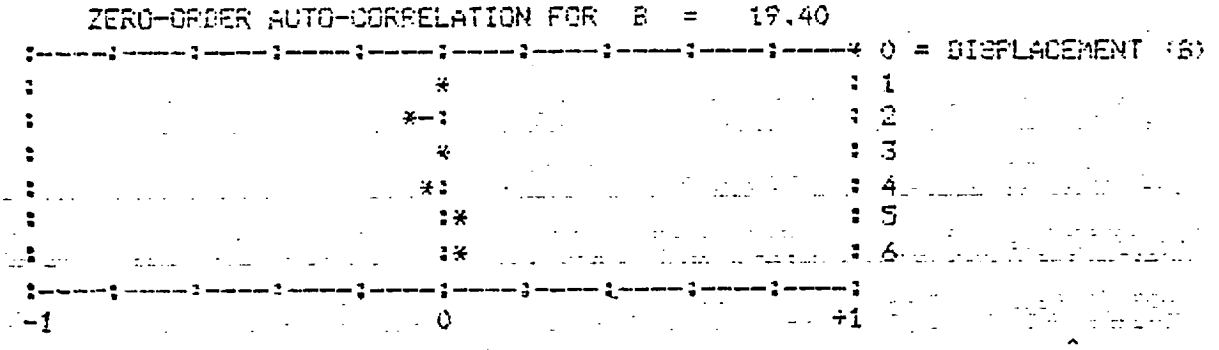
358-	360	:*	6
360-	362	:***	33
362-	364	:**********	116
364-	366	:******************************	287
366-	368	:*******************************	292
368-	370	:*********************	212
370-	372	:****	44
372-	374	:*	10
374-	376	:	0
376-	378	:	0

Histogram for peak cylinder pressure, H($\hat{P}$)

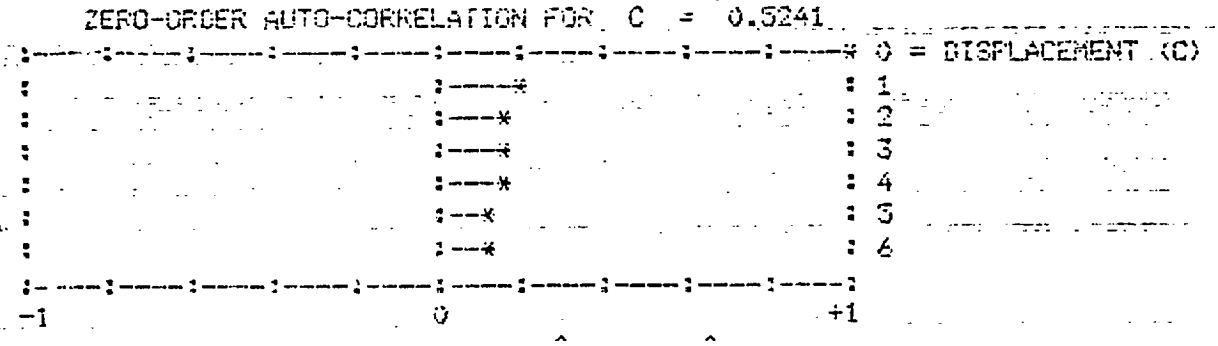
Figure 4.14: Output of sample data analysis (histograms)
(speed = 1000 rpm; load = 6.18 mkp)



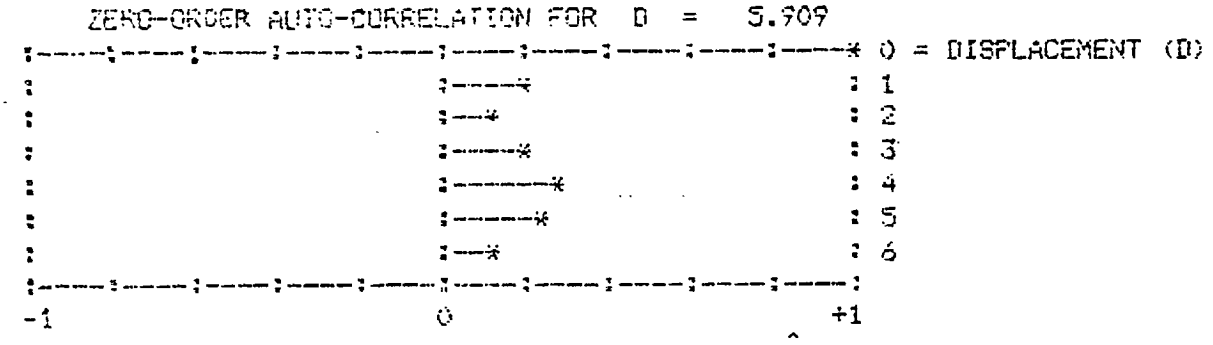
Auto-correlogram for starting angle of injection, AC(τ)



Auto-correlogram of maximum rate of cylinder pressure rise, AC($\hat{dP}$)



Auto-correlogram of location of $\hat{dP}$, AC($\theta(\hat{dP})$)



Auto-correlogram of peak cylinder pressure, AC($\hat{P}$)

Figure 4.15: Output of sample data analysis (auto-correlograms)
(speed = 1000 rpm; load = 6.18 mkp)

CROSS-CORRELATION FUNCTION FOR A/B, $CC(\tau, \hat{dP})$

```
:----:----:----:----:----:----:----:----:----:----:      DISPLACEMENT
:                         *                        :-6    0.1969E-01
:                        *:                         -5   -0.2260E-01
:                         :*                       :-4    0.4062E-01
:                         :*                        -3    0.2980E-01
:                         *                        :-2    0.3978E-02
:                         :*                        -1    0.3664E-01
:                         :-*                      : 0    0.8059E-01
:                         :*                         1    0.2409E-01
:                         *                        : 2    0.1751E-02
:                         *                         3    0.1981E-01
:                         *                        : 4   -0.1104E-01
:                         *                         5   -0.1184E-01
:                         *                        : 6    0.1799E-01
:----:----:----:----:----:----:----:----:----:----:
-1                        0                        +1
```

CROSS-CORRELATION FUNCTION FOR A/C, $CC(\tau, \theta(\hat{dP}))$

```
:----:----:----:----:----:----:----:----:----:----:      DISPLACEMENT
:                         :-*                      :-6    0.9073E-01
:                         :-*                       -5    0.7189E-01
:                         :*                       :-4    0.3620E-01
:                         :--*                      -3    0.1046E+00
:                         :--*                     :-2    0.1204E+00
:                         :----*                    -1    0.1805E+00
:                         :--------*               : 0    0.3361E+00
:                         :-----*                   1    0.2051E+00
:                         :---*                    : 2    0.1424E+00
:                         :--*                      3    0.1110E+00
:                         :--*                     : 4    0.1303E+00
:                         :-*                       5    0.6619E-01
:                         :-*                      : 6    0.9356E-01
:----:----:----:----:----:----:----:----:----:----:
-1                        0                        +1
```

CROSS-CORRELATION FUNCTION FOR A/D, $CC(\tau, \hat{P})$

```
:----:----:----:----:----:----:----:----:----:----:      DISPLACEMENT
:                       *-:                        :-6   -0.9691E-01
:                       *-:                         -5   -0.6815E-01
:                      *--:                        :-4   -0.1052E+00
:                       *-:                         -3   -0.8640E-01
:                       *-:                        :-2   -0.6652E-01
:                      *--:                         -1   -0.1001E+00
:                  *------:                        : 0   -0.2878E+00
:                       *-:                         1    -0.9130E-01
:                        *:                        : 2   -0.5496E-01
:                        *:                         3    -0.2902E-01
:                        *:                        : 4   -0.3333E-01
:                        *:                         5    -0.3629E-01
:                        *:                        : 6   -0.4610E-01
:----:----:----:----:----:----:----:----:----:----:
-1                       0                        +1
END OF PRINTOUT ** PROCEEDING TO NEXT TEST
```

Figure 4.16: Output of sample data analysis (cross-correlograms)
(speed = 1000 rpm; load = 6.18 mkp)

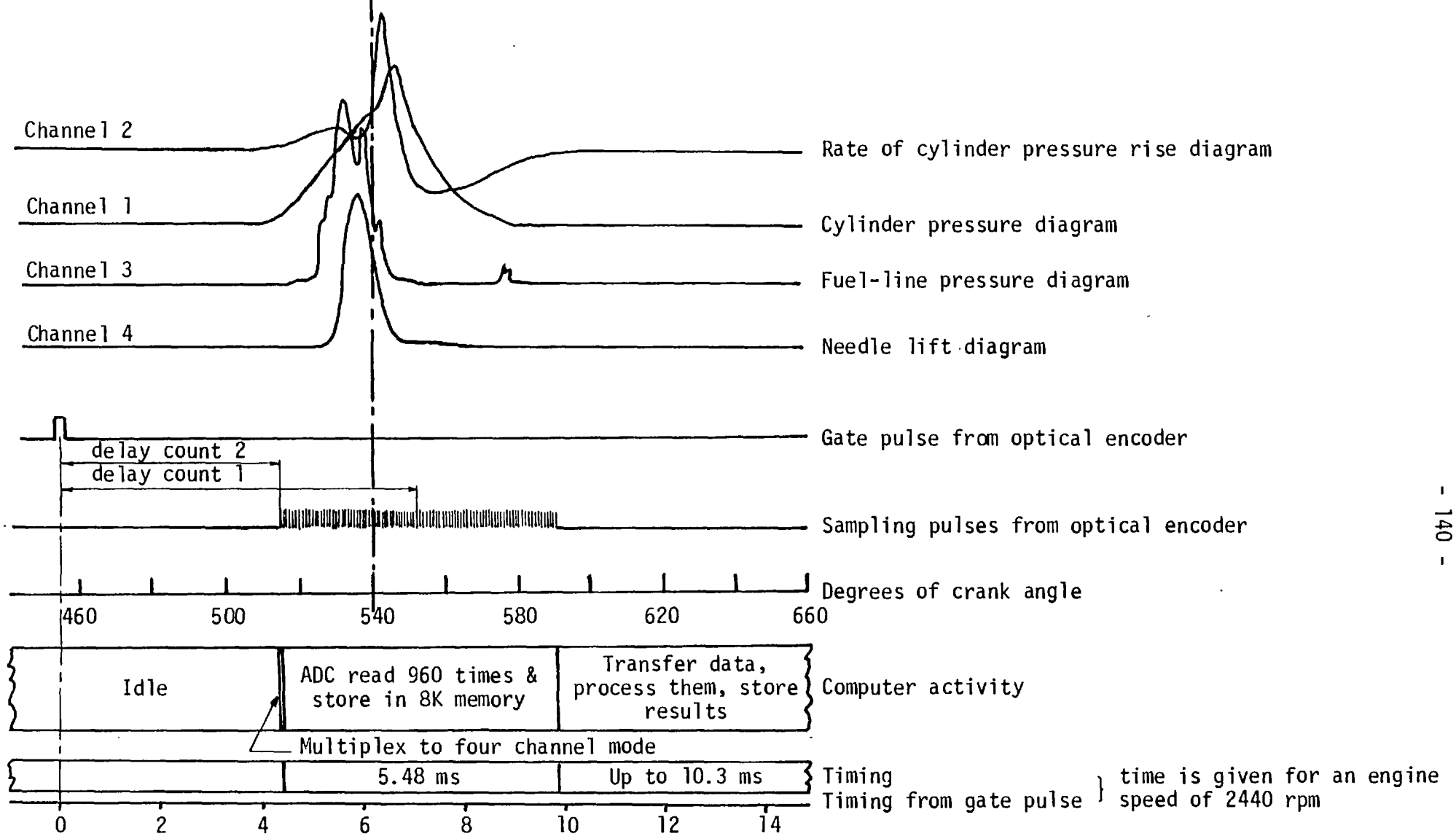


Figure 4.17: Signals, sampling and timing diagram for cylinder 2 (AVESTD)

transducer defects. In general, a high standard deviation indicates that some drifting exists. This technique reported by Marzouk & Watson (1976) suggests abandonment of the test if the standard deviation of the cylinder pressure exceeds 7 kN/m^2 ($\simeq$ 1.02 psi) during the compression stroke. However, this number was found to be small to be met for the Perkins engine under the test, the reason may be in the application of different methods employed for calculating the standard deviation which will be discussed later.

The block diagram and flowchart of the AVESTD are given, respectively, in Figures 4.18 and 4.19. The following procedure for calculating standard deviation is adopted mainly in order to simplify programming as well as to increase the accuracy of the calculated data with consideration of core memory limitation. The program reads and calculates the means of 128 cylinder pressures, rates of cylinder pressure rise, fuel-line pressures and needle lift diagrams. Having calculated the average at every cylinder pressure position, it proceeds to read another 128 cycles to calculate the standard deviation for every point, assuming that the second groups of data have the same cyclic averages. The advantage of this method is simply to reduce the core requirement from approximately N*M to 2*M (where N = number of cycles, and M = the number of recordings). The application of this method is restricted to the case of stationary conditions where the mean values remain unvaried. Therefore, after setting the engine at the desired condition, the validity of the postulation would be verified experimentally over the number of cycles required. The present work has shown that this assumption is approximately correct. Nevertheless, it can be shown theoretically that, even when the mean values change slightly, the technique is more accurate than the normal procedure. This can be easily shown by comparing the

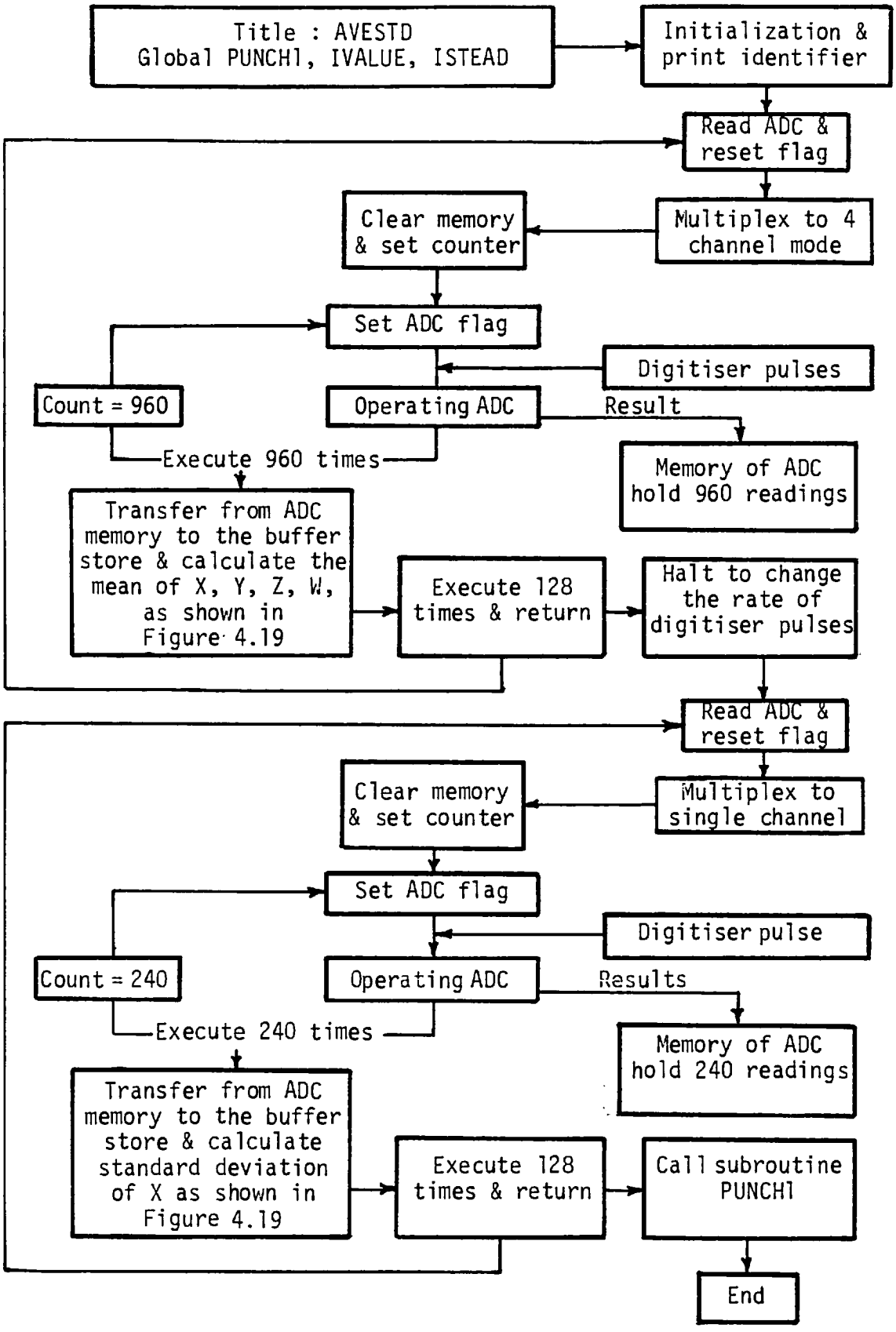
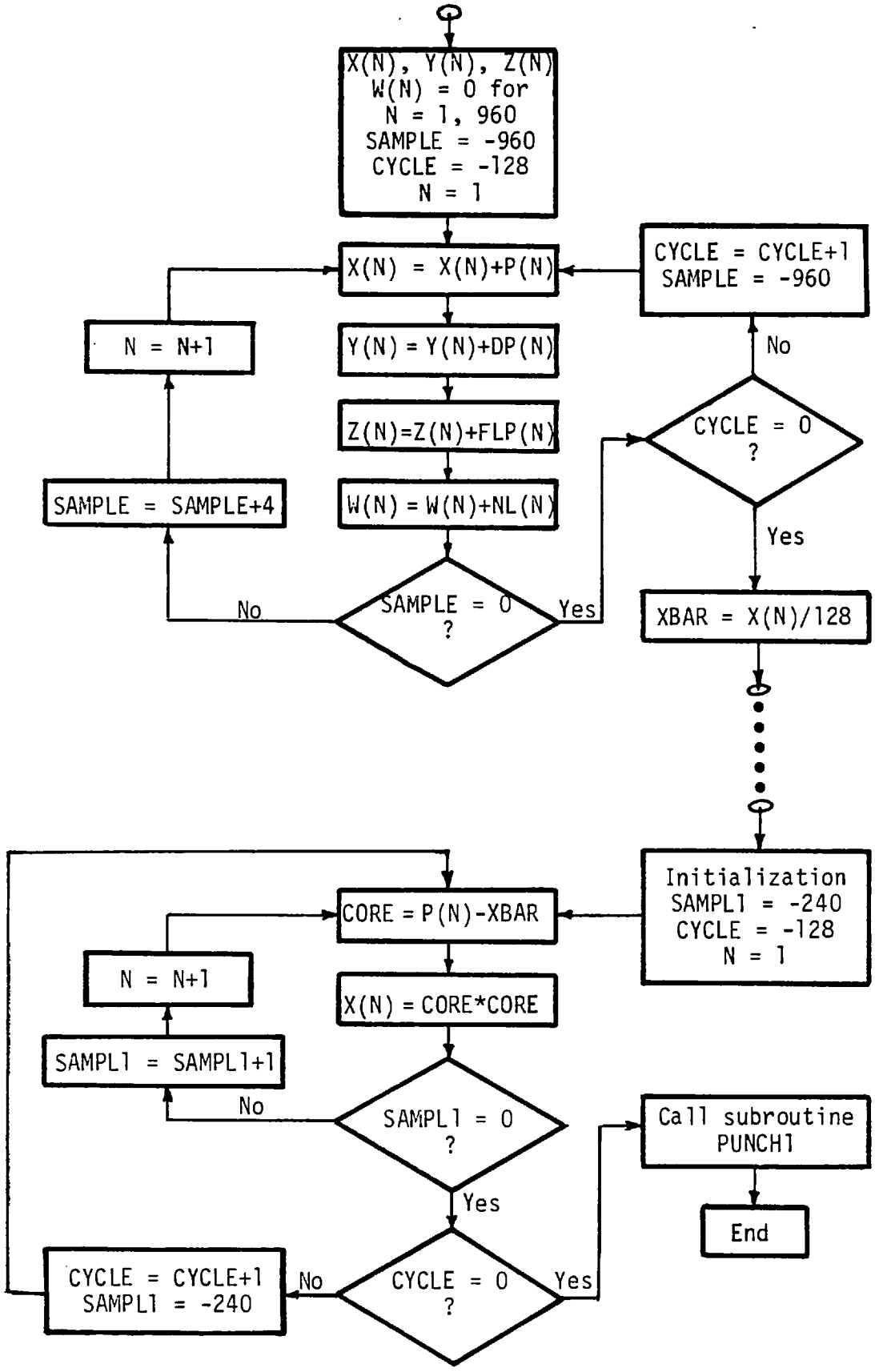


Figure 4.18: Block diagram of program AVESTD

Figure 4.19: AVESTD Macro program flowchart (analysis)



standard errors of the two methods.

By statistical definition, we have:

$$\bar{x} = \frac{1}{N} \sum_{i=1}^{N} x_i \tag{4.1}$$

$$\sigma^2 = \frac{1}{N-1} \sum_{i=1}^{N} (x_i - \bar{x})^2 \tag{4.2}$$

$$e = \frac{\sigma}{\sqrt{N}} \tag{4.3}$$

where $\bar{x}$ = arithmetic mean

σ = standard deviation

e = standard error

N = number of samples

If the mean value shifts by b, from equations (4.1) and (4.2), the new standard deviation is given by:

$$\bar{x}_1 = \bar{x} + b \Rightarrow \sigma_1^2 = \sigma^2 + b^2 \tag{4.4}$$

$$e_1 = \frac{\sigma_1}{\sqrt{N_1}} = \left(\frac{\sigma^2 + b^2}{N_1}\right)^{\frac{1}{2}} \tag{4.5}$$

Increases in the number of samples employed not only reduces the standard error but also decreases the deviation b from the mean value, $\bar{x}$. By comparing the standard errors of the two different procedures:

$$e_{a1} = \left(\frac{\sigma_a^2 + b^2}{N_1}\right)^{\frac{1}{2}} \tag{4.6}$$

$$e_n = \frac{\sigma_n}{\sqrt{N}} \tag{4.7}$$

where e_{a1} = standard error for applied method

e_n = standard error for normal method

For having better accuracy, e_{a1} should be less than e_n, so:

$$\text{for } e_{a1} < e_n \Rightarrow \frac{\sigma_a^2 + b^2}{N_1} < \frac{\sigma_n^2}{N} \tag{4.8}$$

$$b < (\sigma_n^2 \frac{N_1}{N} - \sigma_a^2)^{\frac{1}{2}} \tag{4.9}$$

This inequality shows the number of cycles necessary to satisfy the preceding method. (Putting N = 50 cycles and N_1 = 128 cycles, and assuming the equal standard deviation for both cases, $\sigma_a = \sigma_n$.) We have:

$$b < 1.249\ \sigma_a \tag{4.10}$$

If the above inequality does not hold, this test will be abandoned and the further acquisition of data will be necessary.

Because, in the second reading, only the cylinder pressure is needed, the program is written to be interrupted before the new set of samples is taken. The operator can then change the rate of pulses from 4096 per revolution to 1024 per revolution, reading the cylinder pressure values alone in a single channel mode.

At the end of the program's operation, there will be a batch of 1200 locations of blank common, consisting of the following values:

(a) The first 240 values are the arithmetic means of the cylinder pressure diagram.

(b) The second 240 values are the arithmetic means of the

rate of cylinder pressure rise diagrams.

(c) The third 240 values are the arithmetic means of the fuel-line pressure diagrams.

(d) The fourth 240 values are the arithmetic means of the needle lift diagrams.

(e) The last 240 values are the standard deviation of the cylinder pressure diagrams corresponding to the same mean values of cylinder pressure diagrams presented in the first batch of 240 values.

Figure 4.20 is a typical plot of the values obtained by the AVESTD program for test TR18 at a speed of 2250 RPM and a load of 5 mkp operating condition.

It is also important to note that for every experiment, the test should not start immediately after firing the engine since thermal drift must be avoided. After monitoring the data, if they were satisfactory, the punched paper tape from them would be obtained for further analysis.

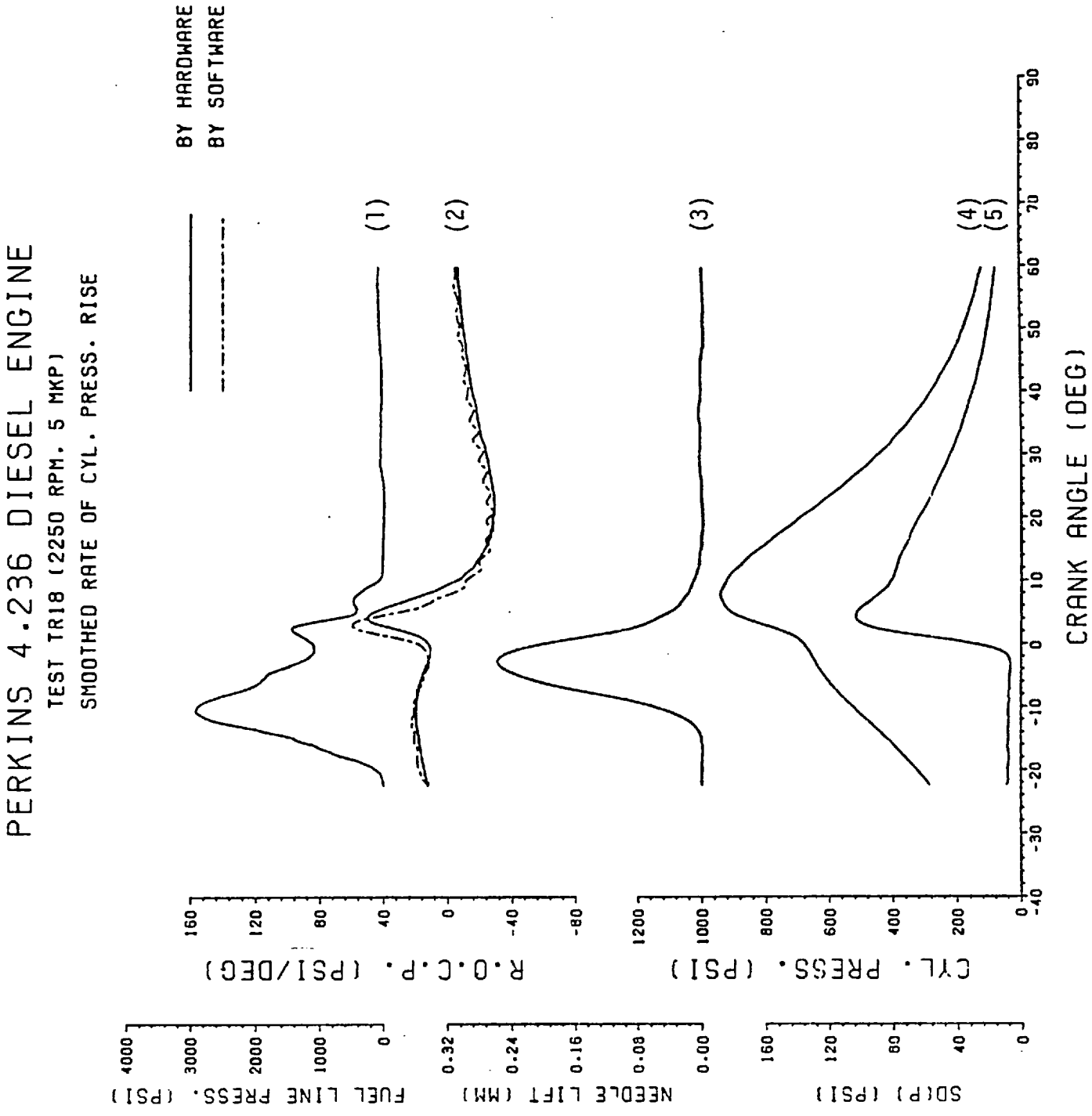


Figure 4.20: Typical plot of sampling by AVESTD:

(1) Fuel-line pressure diagram

(2) Rate of cylinder pressure rise diagram

(3) Needle lift diagram

(4) Cylinder pressure diagram

(5) Standard deviation of cylinder pressure diagram

CHAPTER 5

STATISTICAL RESULTS

5.1 INTRODUCTION

This chapter commences with an evaluation of diesel engine parameters as time-series and an explanation of tests carried out to classify these parameters as random data. The results obtained from the experiments and the prediction program at selected operating conditions are presented and compared with each other. Analysis of the engine data as a time-series assists in the specification of the nature of these time-series, and thus in the interpretation of certain statistical results (e.g. correlograms, histograms, etc.). The study of correlograms involving diesel engine time-series relies on analogy with the correlograms of well known stochastic processes (time variant sequences characterized by statistical properties). As the experimental results tended not to produce mathematically definable statistics, there are many instances where no more than visual comparison of distributions, correlations, and spectral analyses is possible. The definition of statistical terms and calculation procedures are presented in Appendix C1.

Correlation analysis (relating to the degree of dependence between pairs of values) and regression analysis (concerning the nature of the relationship between them if any exists) are applied and the results presented in this chapter. Different methods employed for testing the data over the sample period (tests of normality, stationarity, etc.) and the variability of variances (by the F test and the Bartlett test) are presented. Moreover, certain recorded sample data from the engine, which were discarded as undesirable, are also presented to show the validity and effectiveness of applying different methods in revealing the abnormality of data.

5.2 DIESEL ENGINE TIME-SERIES

A diesel engine time-series means a succession of data values resulting from the engine processes. It was noted that in all recorded engine parameters, successive data values in each time-series were related in some way to other values in the same time-series, and in some cases (cross-correlation) to those in other time-series (Heizman (1970)). These relationships may be deterministic or statistical. Time-series analyses of these relationships can lead to a better understanding of engine processes.

Investigations of cycle-to-cycle variation in engines assume that each engine cycle characterizing variable constitutes a random physical phenomenon. This means that neither the values of these characterizing variables repeat each other every cycle nor do their variations follow specific rules of any deterministic nature. This realization can easily be proven by recording samples of the variable over a finite time interval. Figure 5.2 shows typical sample data for $\hat{P}$, $\hat{dP}$ and τ plotted for successive cycles. Visual inspection indicates a degree of cross-correlation, although this is not apparent at all operating conditions. Such variables are usually related to each other in a highly complex manner, so that these relationships - buried in a random form - cannot be easily recognized unless the degree of correlation is sufficiently high. With the help of statistical techniques such as cross-correlation, these dependences can be revealed more accurately. It should be mentioned that the variations under consideration are at least several times greater than the accuracy of the measurements, and thus they are intrinsic properties of the engine process rather than the result of measurement inadequacies. On this basis, characterizing parameters such as peak cylinder pressure, maximum rate of cylinder pressure rise, time of occurrence of $\hat{P}$ and $\hat{dP}$, cylinder

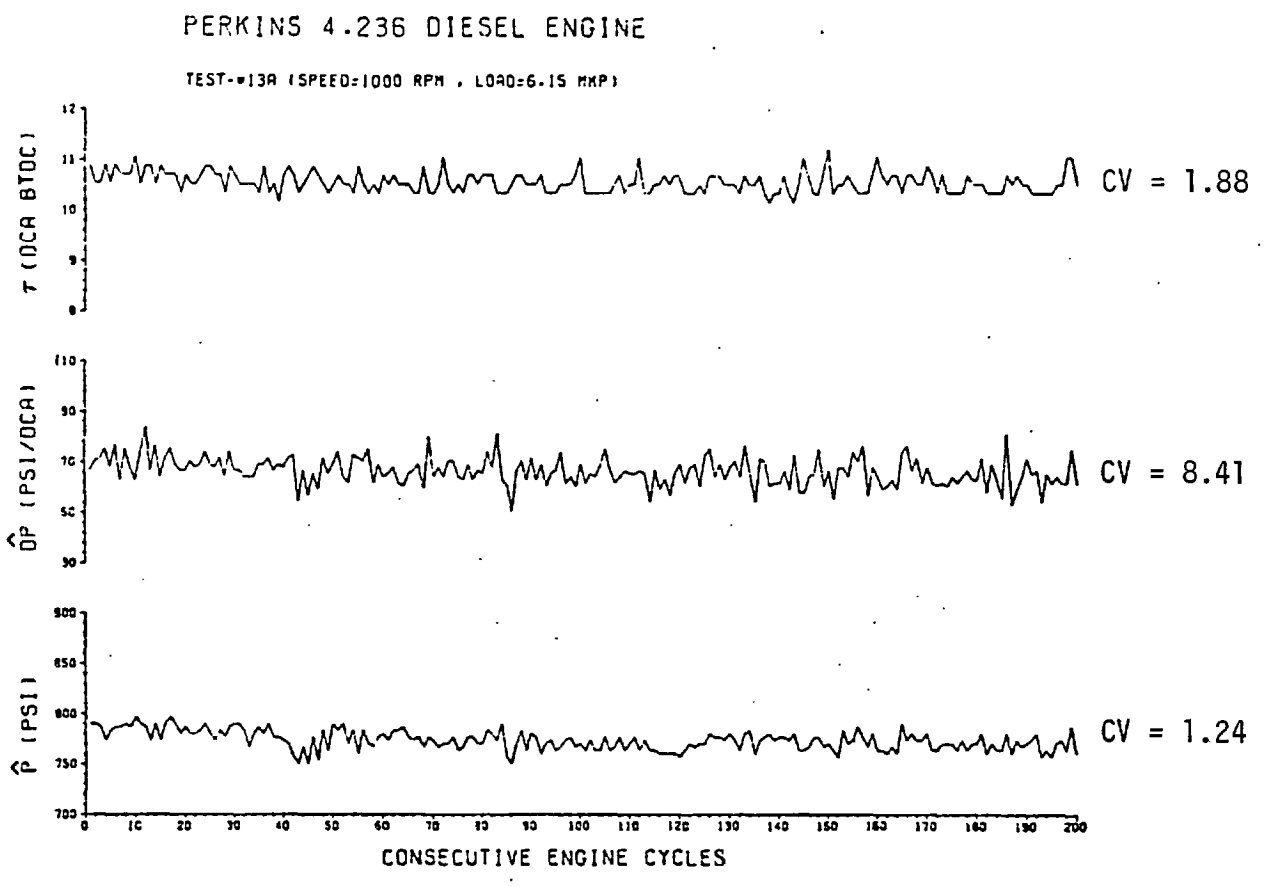


Figure 5.1: Typical sample data for $\hat{P}$, $\hat{dP}$ and τ at low load-low speed conditions

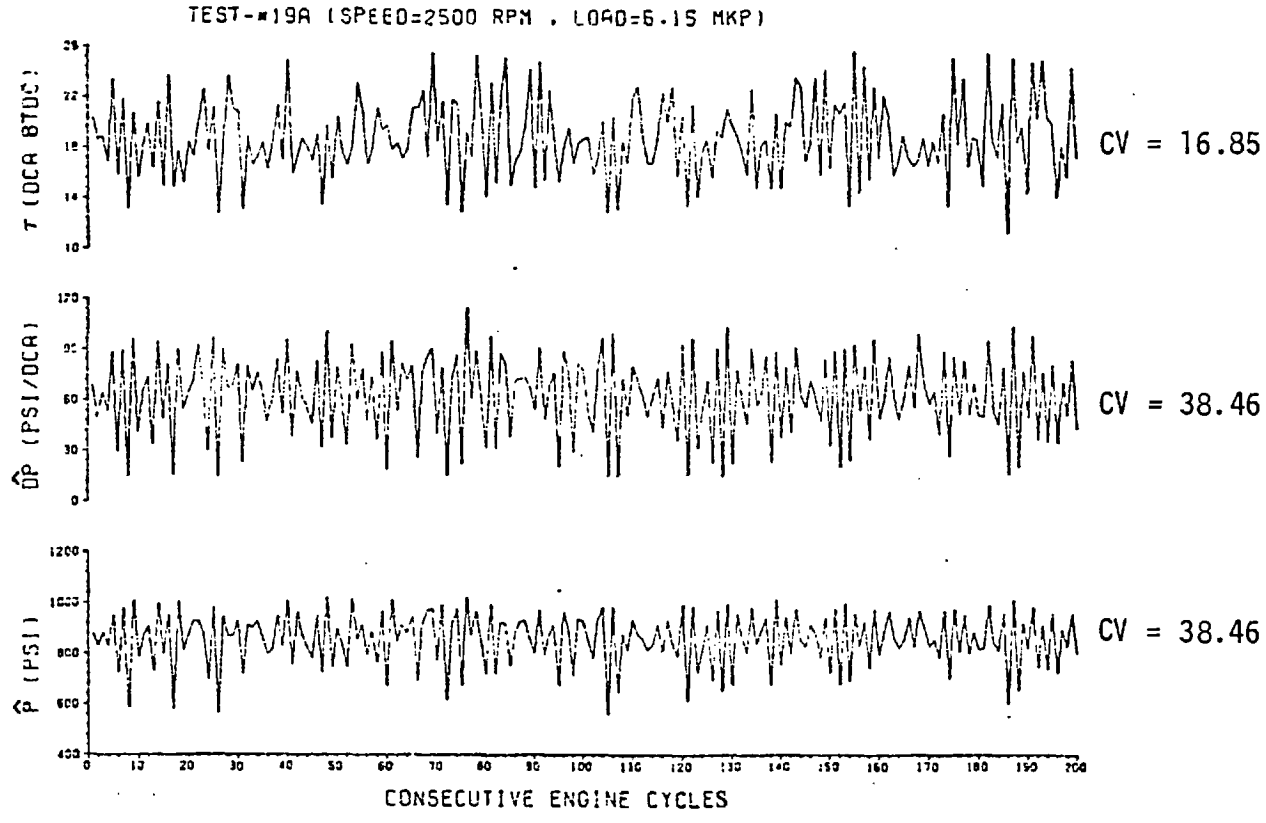


Figure 5.2: Typical sample data for $\hat{P}$, $\hat{dP}$ and τ at low load-high speed conditions

pressure development, temperature and equivalence ratio, ignition delay, fuel injection parameters, and other similar variables were treated as random variables and characterized by their statistical and probabilistic properties.

5.2.1 Engine Measurements for Correlation Tests

In order to carry out correlation tests on different characterizing parameters of injection and combustion processes, values of the desired parameters need to be obtained for large numbers of consecutive cycles. Some of the variables commonly used in such investigations are as follows: the peak cylinder pressure, $\hat{P}$; the angle of occurrence of the peak cylinder pressure, $\theta(\hat{P})$; the maximum rate of cylinder pressure rise, $\hat{dP}$; the angle of occurrence of maximum rate of cylinder pressure rise, $\theta(\hat{dP})$; the starting angle of injection, τ; the duration of injection, δ; the amount of injected fuel, m_f; etc.

Variables such as τ, $\hat{P}$, $\hat{dP}$ and $\theta(\hat{dP})$ were measured over 1000 cycles using the PERFU2 program previously described in Chapter 4. Therefore, a batch of 4000 values containing the successive values of the aforementioned parameters was set up during each test. Figures 5.1 to 5.4 show these parameters (τ, $\hat{P}$, $\hat{dP}$ and $\theta(\hat{dP})$) for some 200 consecutive cycles at low load-low speed, low load-high speed, high load-low speed, and high load-high speed operating conditions, respectively.

For certain forms of abnormality, visual presentation of data over a large number of consecutive cycles provides a useful means of detecting any oddness in the data. Figure 5.5(a) is the example of abnormal data in which $\hat{dP}$ values were truncated at a constant magnitude of 1023 (ADC number). Figure 5.5(b) shows another form of abnormality in the data in which some sporadic errors (distinguished by extremely deviated

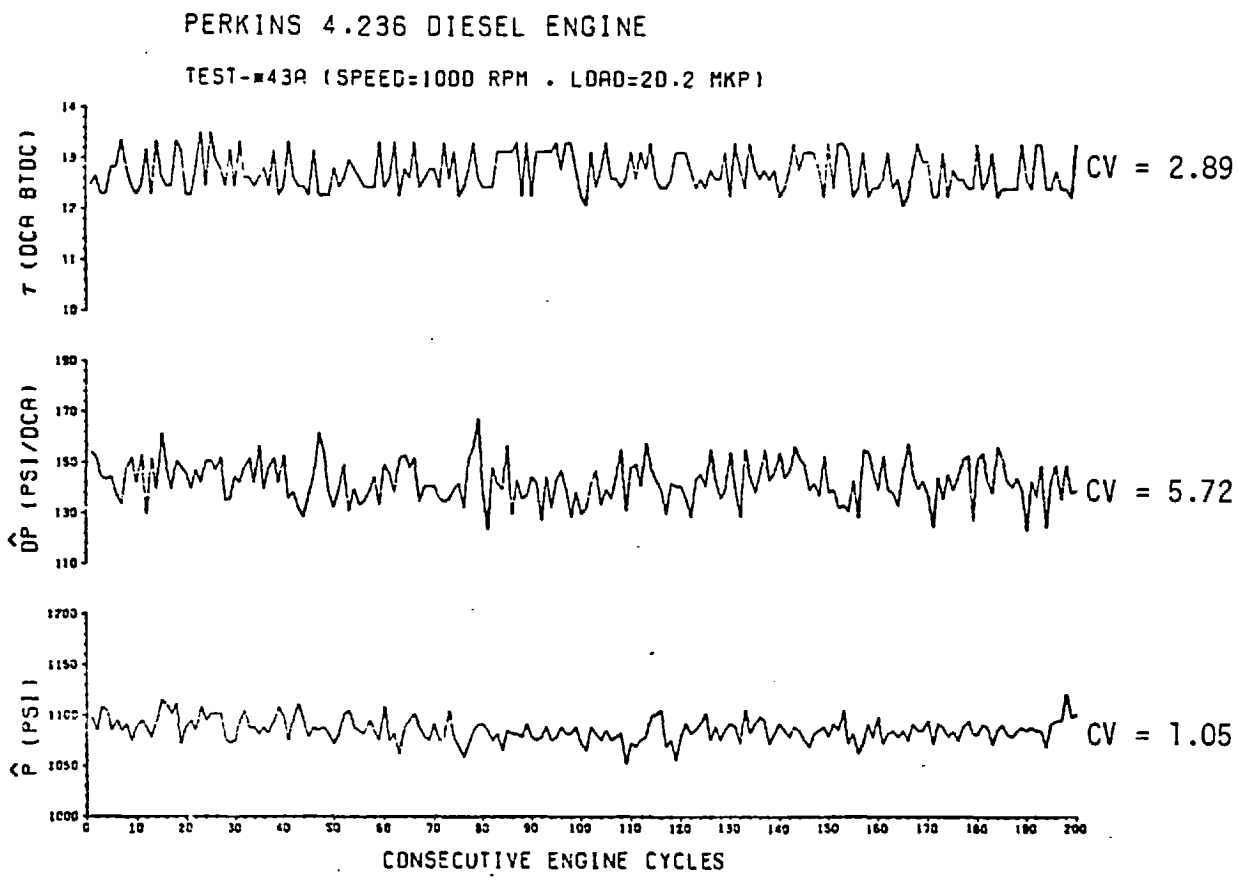


Figure 5.3: Typical sample data for $\hat{P}$, $\hat{dP}$ and τ at high load-low speed conditions

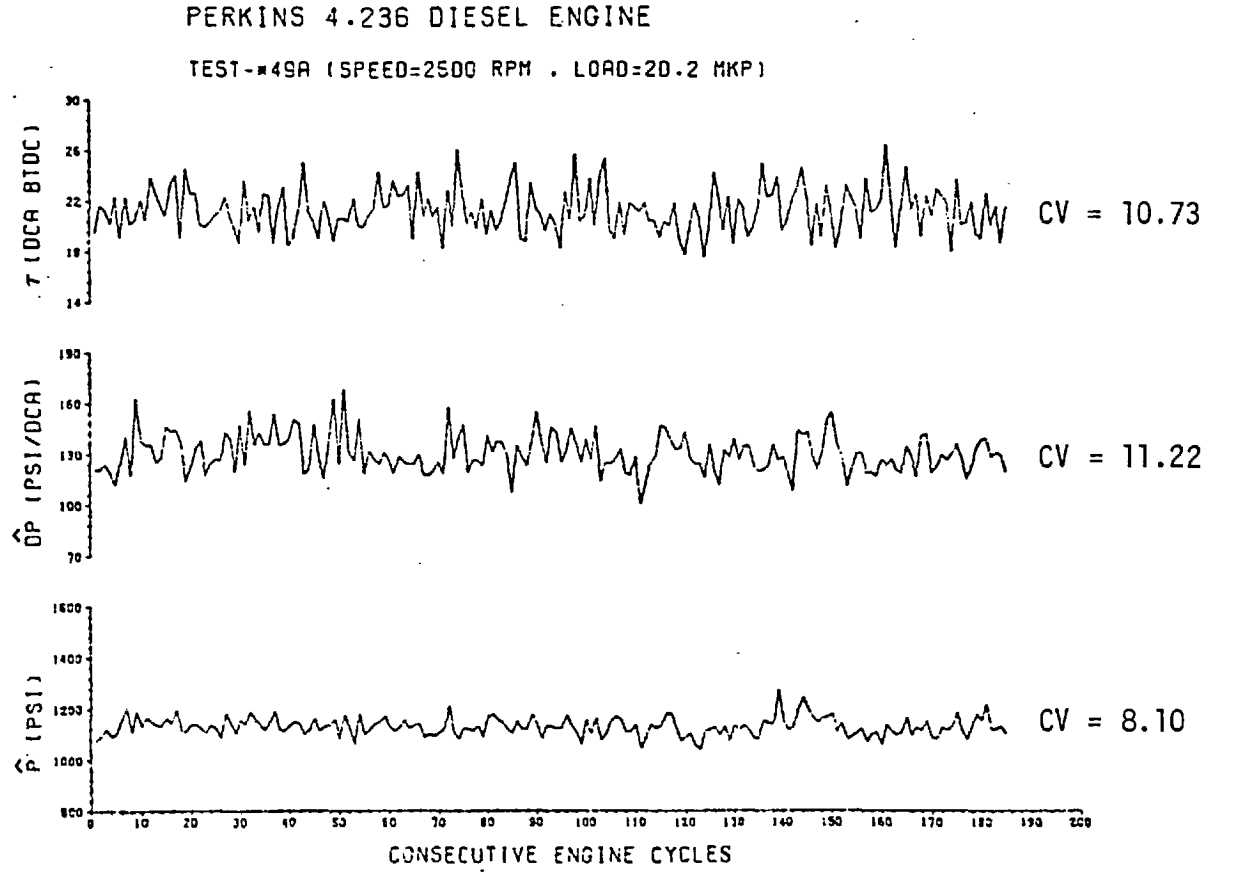


Figure 5.4: Typical sample data for $\hat{P}$, $\hat{dP}$ and τ at high load-high speed conditions

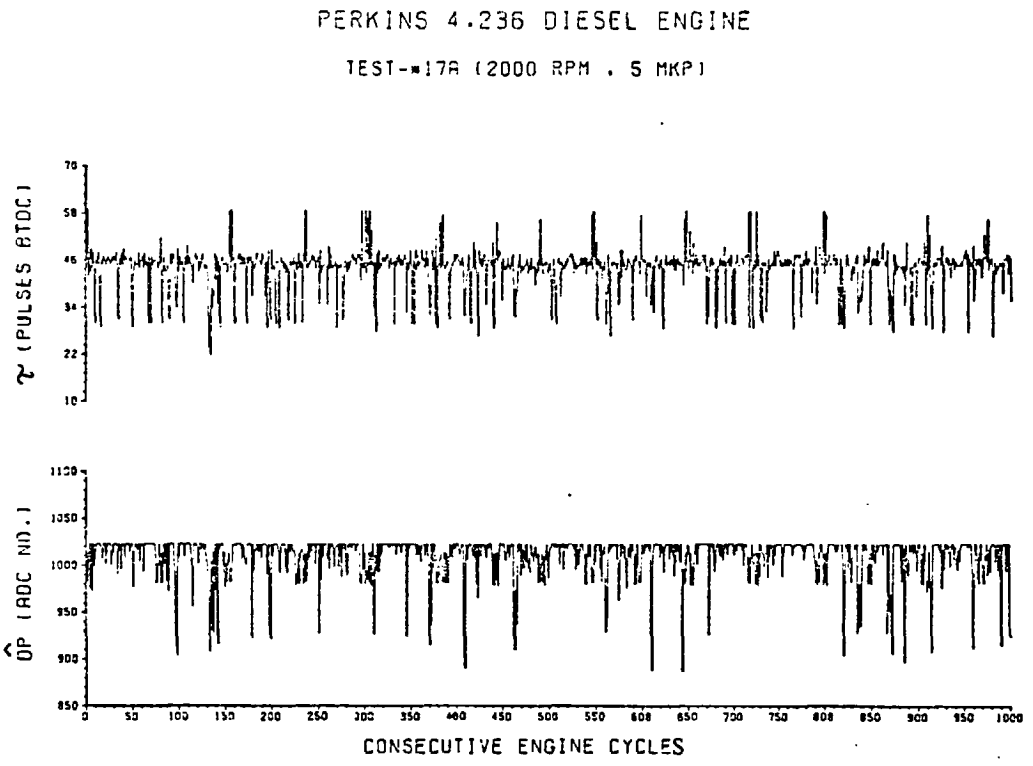


Figure 5.5(a): Sampled data for $\hat{dP}$ and τ at given operating conditions indicating abnormal data

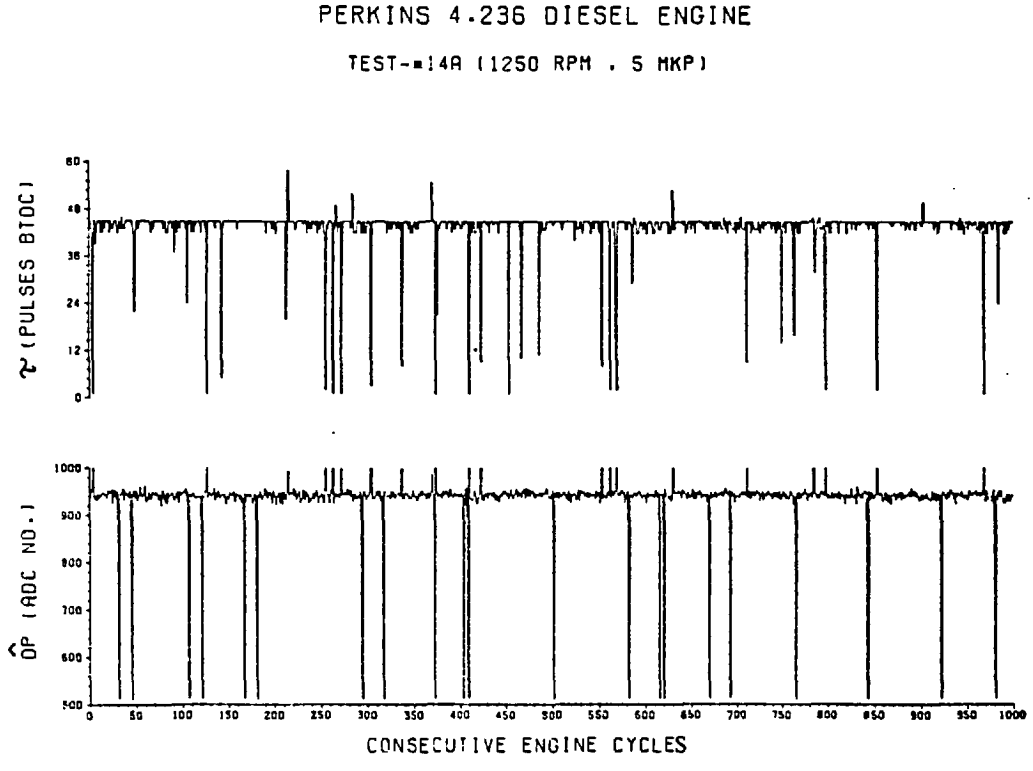


Figure 5.5(b): Sampled data for $\hat{dP}$ and τ at given operating conditions indicating abnormal data

values from the normal pattern) in τ and $\hat{dP}$ are exhibited. A similar common error (truncated at a constant value of less than 1023), often observed when evaluating $\hat{dP}$ by using the PERFU2 program, happened when the cylinder pressure threshold was not suitably adjusted for the operating conditions under test. As was previously described in Section 4.3.2.1, this problem arises only in conditions where the maximum rate of cylinder pressure rise due to combustion is smaller than the maximum rate of cylinder pressure rise due to compression.

Each set of data was then analysed in terms of their statistical properties, an underlying feature of which is the distribution function. Systematic analysis of the results was carried out for every set of data. This included the calculation of statistical properties such as maximum value, mean value, minimum value, variance, standard deviation, standard error, skewness, Kurtosis, histogram plot and relevant correlograms (either auto-correlation or cross-correlation). Figures 4.14 to 4.17 in the previous chapter demonstrate typical output of such systematic analysis of the sampled data.

5.2.2 Discussion of Correlation Measurements

From Figures 5.1 to 5.4, it can be seen that by increasing engine speed, the variability of the parameters $\hat{P}$, $\hat{dP}$ and τ increases, so that the effect of cycle-to-cycle variation is more crucial at higher speeds, especially at low load conditions. For example, Figure 5.2 demonstrates a high correlation between τ (injection characterizing parameter) and $\hat{dP}$ (combustion characterizing parameter). From Figures 5.1 to 5.4, one may conclude that for a cyclic variation analysis, the maximum rate of cylinder pressure is generally a better characterizing parameter than the peak cylinder pressure since a higher coefficient of

variation is obtained.

Table 5.1, with Figures 5.6 to 5.8, displays the interesting nature of data at a condition which exhibits the highest degree of correlation between the injection system variabilities and the engine cycle-to-cycle variations. Values presented for the statistical parameters of τ and $\theta(\hat{dP})$ are shown in terms of the number of pulses after TDC, where each pulse represents approximately $1/3^{o}$ of crank angle:

$$\frac{N_c}{N_p} = \frac{360}{1024} = 0.351^{o} \text{ CA/pulse}$$

where N_c = number of degrees of crank angle in one revolution

N_p = number of pulses in one revolution

The negative sign of dynamic injection implies that it occurred before TDC. Similarly, the values of $\hat{P}$ and $\hat{dP}$ presented in terms of the digital output, which were directly read from ADC. The change to conventional units has not been attempted as it was not required for the statistical analysis.

5.2.2.1 Statistical parameters

The frequency distribution of peak cylinder pressure, maximum rate of cylinder pressure rise, angle of occurrence of maximum rate of cylinder pressure rise, and dynamic injection were examined by calculating the statistical parameters of these variables (mean, standard deviation, skewness, Kurtosis, etc.). These statistical parameters not only summarize, or describe, data in a meaningful manner, but also generalize about a large amount of possible data from small amounts of available data to facilitate the application of statistical approaches to

TABLE 5.1: Statistical Parameters at a Speed of 2500 rpm and a Load of 6.18 mkp

A = Dynamic injection (τ)
B = Maximum rate of cylinder pressure rise ($d\hat{P}$)
C = Location of B ($\theta(d\hat{P})$)
D = Peak cylinder pressure ($\hat{P}$)

	A	B	C	D
	A=-110	B= 376	C= 6	D= 408
	A=-180	B= 416	C= 10	D= 368
	A=-101	B= 388	C= 7	D= 408
MAXIMUM	A= -59	B= 488	C= 39	D= 469
MINIMUM	A=-145	B= 271	C= -20	D= 311
MEAN	A= -102.3	B= 387.2	C= 10.61	D= 402.8
VARIANCE	A= 271.7	B= 2172.	C= 40.45	D= 881.5
STANDARD DEVIATION	A= 16.48	B= 46.61	C= 6.360	D= 29.69
STANDARD ERROR	A= 0.5213	B= 1.474	C= 0.2011	D= 0.9389
SKEWNESS	A=-0.3168	B= 0.2410	C= 1.959	D=-0.5232
KURTOSIS	A= 2.570	B= 2.308	C= 10.37	D= 2.833

Ranges			Number of Occurrences
-145-	-136	:***	32
-136-	-127	:*****	49
-127-	-118	:**********	104
-118-	-108	:***************	125
-108-	-100	:**********************	202
-100-	-91	:**********************	214
-91-	-82	:******************	172
-82-	-73	:*********	80
-73-	-64	:***	25
-64-	-55	:	1

Histogram of starting angle of injection, $H(\tau)$

271-	293	:*	6
293-	315	:**	24
315-	337	:**************	125
337-	359	:*****************	152
359-	381	:*****************	164
381-	403	:*****************	161
403-	425	:**************	150
425-	447	:**********	88
447-	469	:********	70
469-	491	:*******	60

Histogram of maximum rate of cylinder pressure rise, $H(\hat{dP})$

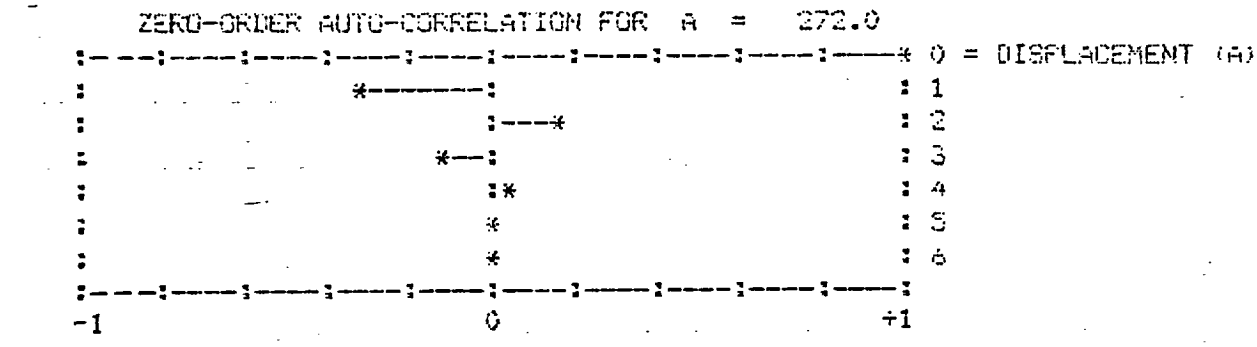
-20-	-14	:	1
-14-	-8	:	0
-8-	-2	:	0
-2-	4	:******	56
4-	10	:**********	428
10-	16	:**********	359
16-	22	:**********	123
22-	28	:*	10
28-	34	:	0
34-	40	:**	23

Histogram of location of maximum rate of cylinder pressure, $H(\theta(\hat{dP}))$

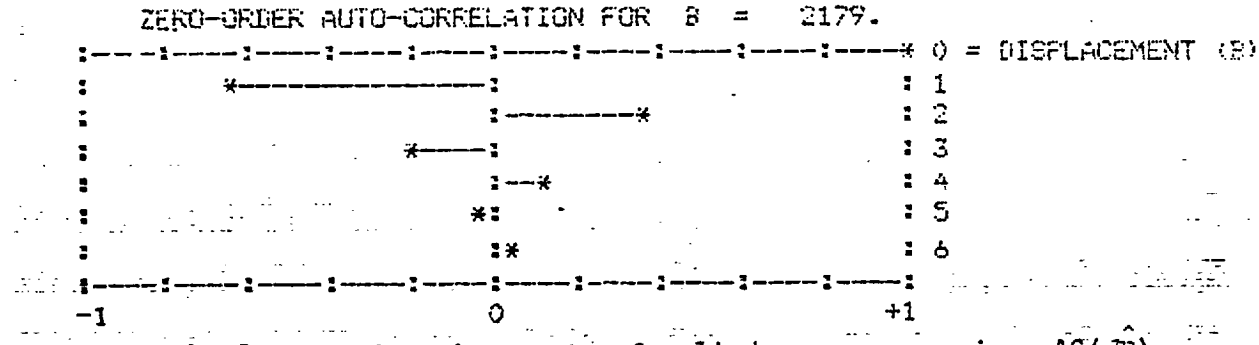
311-	327	:*	11
327-	343	:**	19
343-	359	:*******	63
359-	375	:********	73
375-	391	:****************	152
391-	407	:**********************	195
407-	423	:**********************	193
423-	439	:**********************	187
439-	455	:**********	104
455-	471	:	3

Histogram of peak cylinder pressure, $H(\hat{P})$

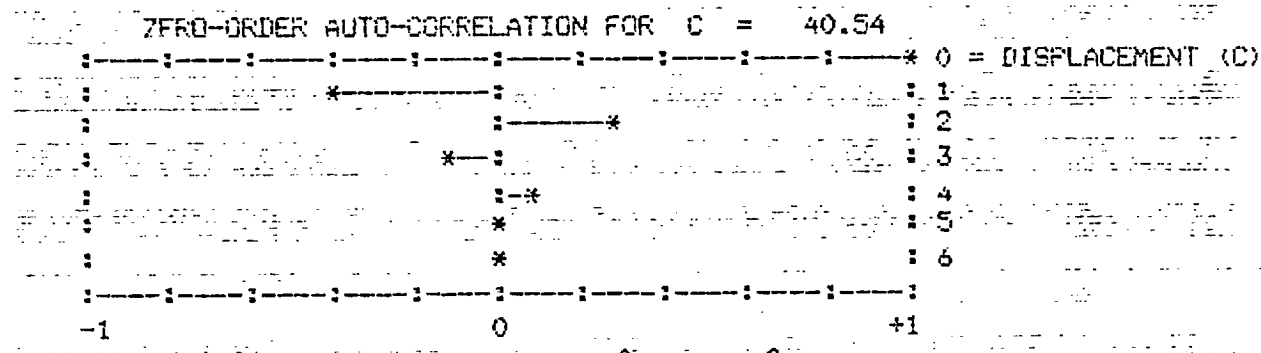
Figure 5.6: Histograms for τ, $\hat{dP}$, $\theta(\hat{dP})$ and $\hat{P}$ at a speed of 2500 rpm and a load of 6.18 mkp



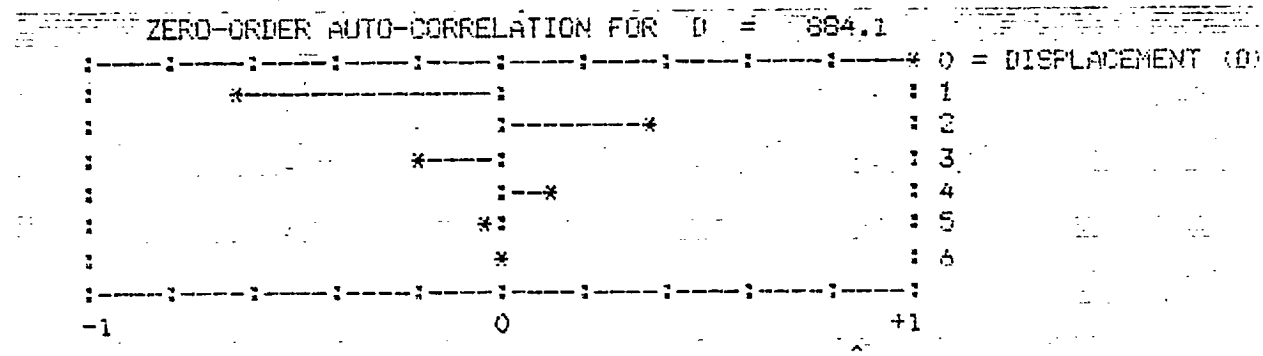
Auto-correlogram for starting time of injection, AC(τ)



Auto-correlogram of maximum rate of cylinder pressure rise, AC($\hat{dP}$)



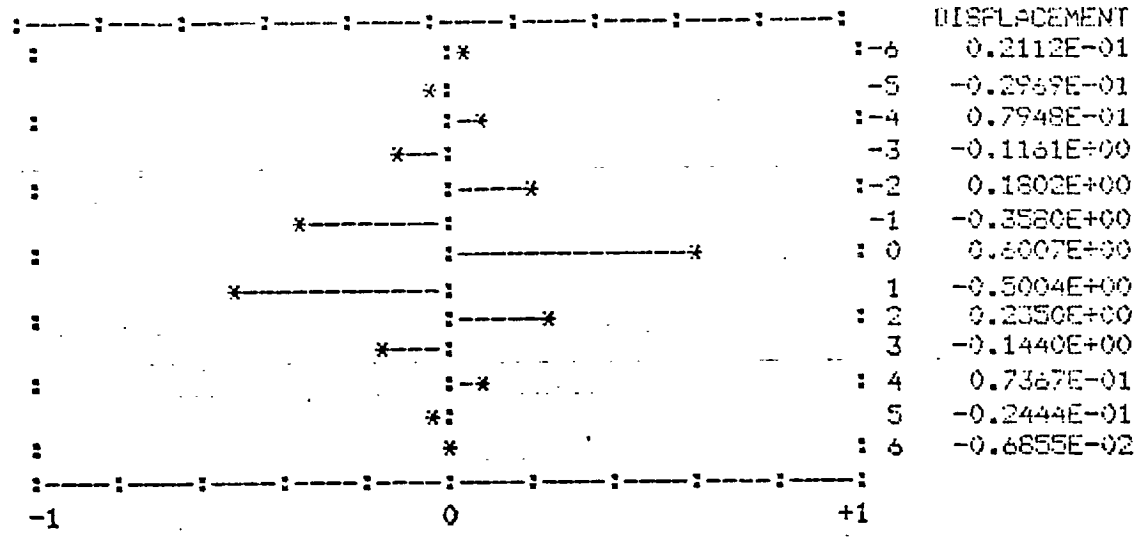
Auto-correlogram of location of $\hat{dP}$, AC($\theta(\hat{dP})$)



Auto-correlogram of peak cylinder pressure, AC($\hat{P}$)

Figure 5.7: Auto-correlograms of τ, $\hat{dP}$, $\theta(\hat{dP})$ and $\hat{P}$ at a speed of 2500 rpm and a load of 6.18 mkp

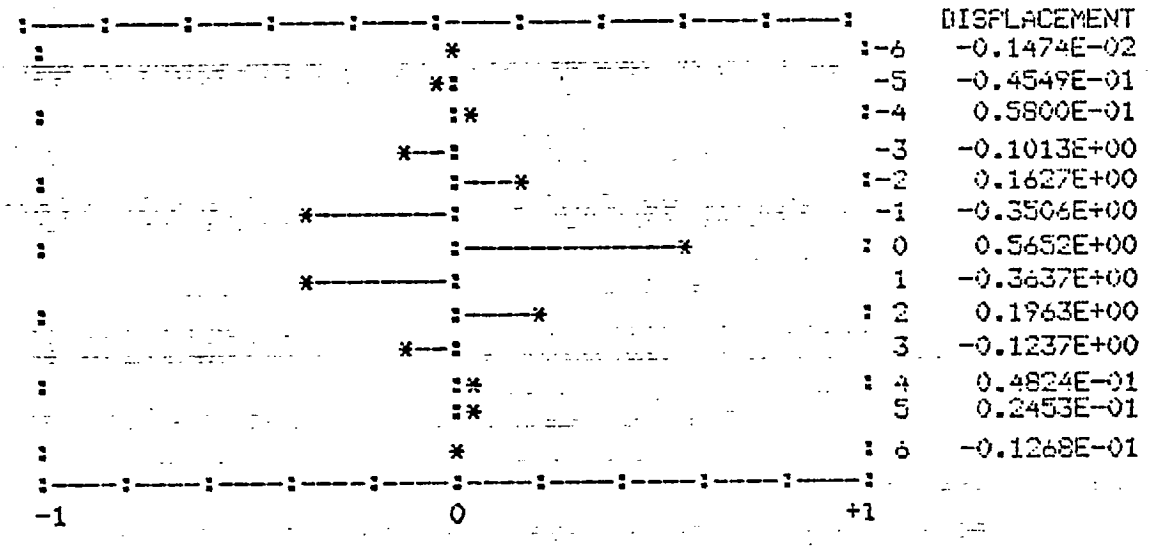
CROSS-CORRELATION FUNCTION FOR A/B, $CC(\tau, \hat{dP})$



	DISPLACEMENT
-6	0.2112E-01
-5	-0.2969E-01
-4	0.7948E-01
-3	-0.1161E+00
-2	0.1802E+00
-1	-0.3580E+00
0	0.6007E+00
1	-0.5004E+00
2	0.2350E+00
3	-0.1440E+00
4	0.7367E-01
5	-0.2444E-01
6	-0.6855E-02

-1 0 +1

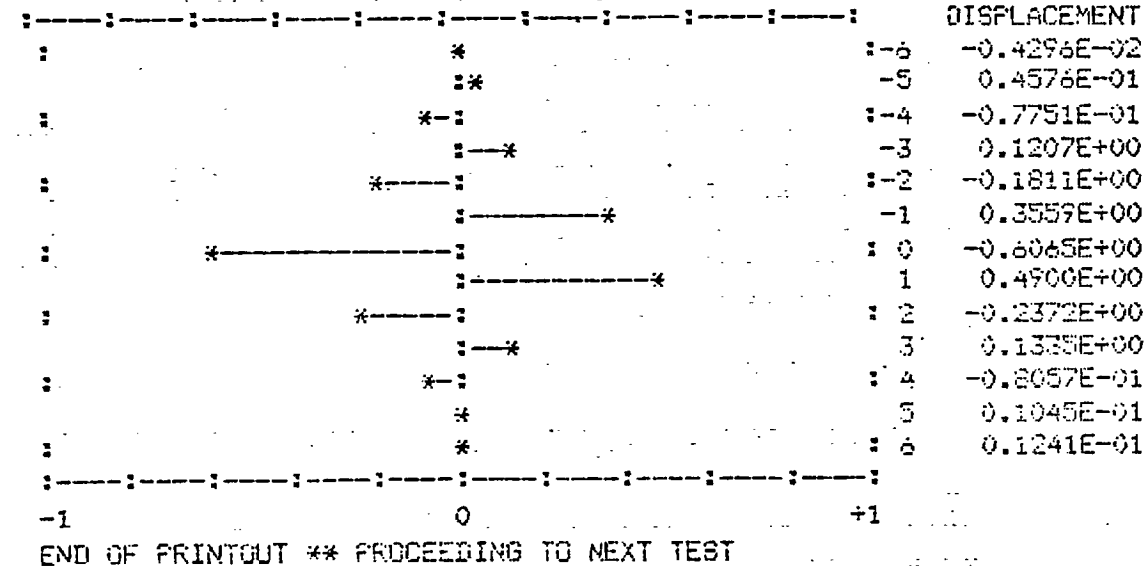
CROSS-CORRELATION FUNCTION FOR A/C, $CC(\tau, \theta(\hat{dP}))$



	DISPLACEMENT
-6	-0.1474E-02
-5	-0.4549E-01
-4	0.5800E-01
-3	-0.1013E+00
-2	0.1627E+00
-1	-0.3506E+00
0	0.5652E+00
1	-0.3637E+00
2	0.1963E+00
3	-0.1237E+00
4	0.4824E-01
5	0.2453E-01
6	-0.1268E-01

-1 0 +1

CROSS-CORRELATION FUNCTION FOR A/D, $CC(\tau, \hat{P})$



	DISPLACEMENT
-6	-0.4296E-02
-5	0.4576E-01
-4	-0.7751E-01
-3	0.1207E+00
-2	-0.1811E+00
-1	0.3559E+00
0	-0.6065E+00
1	0.4900E+00
2	-0.2372E+00
3	0.1335E+00
4	-0.2057E-01
5	0.1045E-01
6	0.1241E-01

-1 0 +1

END OF PRINTOUT ** PROCEEDING TO NEXT TEST

Figure 5.8: Cross-correlograms between τ & $\hat{dP}$, τ & $\theta(\hat{dP})$, and τ & $\hat{P}$, at a speed of 2500 rpm and a load of 6.18 mkp

the simulation models. Therefore, these statistics were chosen to indicate whether significant differences exist between the frequency distribution of these variables and those of a normal frequency distribution. Since a normal frequency distribution would indicate random occurrence of peak cylinder pressure, dynamic injection, maximum rate of cylinder pressure rise, etc., any deviation from the normal curve could indicate cause for the fluctuations. If the value of skewness and Kurtosis are close to zero and three, respectively, the characterizing parameter fluctuation is random and also does not depend on the previous values of the same parameters or, more specifically, on the conditions in any other cycle, but rather on the intake, compression and combustion of each individual cycle.

A preliminary study of the dynamic injection statistical parameters showed that the generalization of dynamic injection, being normally populated around its mean value, was a rational assumption over most engine operating conditions. The tabulation of calculated statistics of the measured characterizing parameter ($\hat{P}$, $\hat{dP}$, $\theta(\hat{dP})$ and τ) at an engine speed of 2500 RPM and a load of 6.18 mkp (Test 19A) is presented in Table 5.1.

The coefficients of variation (CV) of different characterizing parameters were calculated and used as yardsticks for comparing the variability of injection and combustion process. These CV values are presented on the curves in Figures 5.1 to 5.4. Although this CV has the advantage of being dimensionless, it is also sensitive to the mean value, which may create a form of erroneous judgement of the variations for some characterizing parameters (i.e. the occurrence angle of the maximum rate of cylinder pressure rise may vary from 5^{o} crank angle BTDC to 10^{o} crank angle ATDC and, therefore, as the mean value becomes closer to top dead centre, the ration between standard deviation and mean

value becomes more invalid).

5.2.2.2 Histograms

This is another common method to display frequency distributions of the data graphically.

From the visual presentation of the histograms (Figure 5.6), the frequency distributions for each sample are compared with known distributions (especially Gaussian distributions) and the possible skewness and peakedness of the distribution are determined. (For normal or Gaussian distributions, the skewness is zero and the Kurtosis is 3.00.) The study of histograms of these parameters reveals that a normal bell-shaped distribution with a small degree of skewness is likely to be obtained at most conditions, and thus one can assume a normal distribution for these samples with relative confidence. Any samples exhibiting an odd distribution were discarded and the test repeated until a near Gaussian set of samples were obtained. A frequent form of irregular distribution obtained was the bimodal type which almost certainly originated from the combination of two normal distributions, as shown in Figure 5.9. Figure 5.10 shows a distribution of this kind for dynamic injection at an engine speed of 2750 RPM and a load of 5 mkp. As demonstrated, the injection parameter (timing of the maximum rate of fuel-line pressure) oscillates between two values, only one being the true value for τ. In order to avoid the occurrence of such phenomena, the value of CHECP in program PERFU2 had to be adjusted during the experiment to cause the program to disregard the first maximum rate of fuel-line pressure as a real dynamic injection time.

The other form of abnormality in histograms may arise from the presence of periodic components in the sampled data. Figure

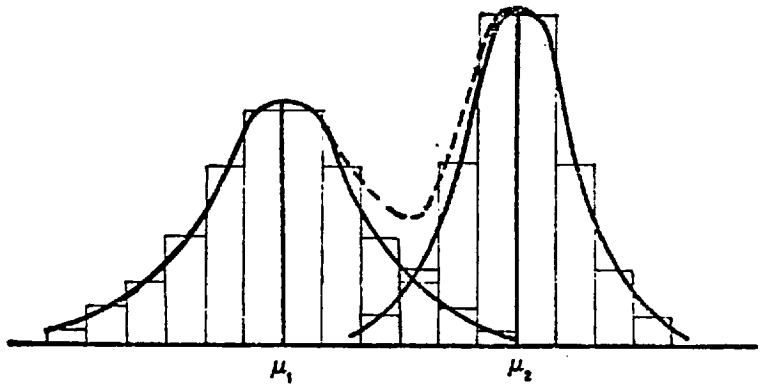


Figure 5.9: Bimodal distribution obtained from the combination of two normal distributions

Ranges			Number of Occurrences
10 -	14	:*	: 8
14 -	18	:****	: 38
18 -	22	:**********	: 115
22 -	26	:**********	: 114
26 -	30	:********	: 79
30 -	34	:*****	: 54
34 -	38	:******************	: 180
38 -	42	:**********************	: 210
42 -	46	:****************	: 164
46 -	50	:****	: 38

Figure 5.10: Histogram of dynamic injection at a speed of 2750 rpm and a load of 5 mkp

5.11(a) shows the histogram of $\hat{dP}$ sampled at 2000 RPM and 5 mkp which contains a periodic component. It will be shown in later sections that the autocorrelation and spectral density analyses are the most certain way of detecting such periodic oscillations.

Figures 5.12 to 5.15 demonstrate histograms of τ, $\hat{P}$, $\hat{dP}$ and $\theta(\hat{dP})$ for different operating conditions (low load-low speed; low load-high speed; high load-low speed; high load-high speed).

An abnormality in the histogram of a combustion characterizing parameter ($\hat{dP}$), especially in the form of skewed distribution, may have an important physical significance.

One of the characterizing features of knocking combustion in internal combustion engines is the occurrence of an excessive rate of cylinder pressure rise during combustion. From the study of the indicator diagrams obtained for petrol and high speed compression ignition engines, Judge (1967) concluded that a smooth, "knockless" combustion is secured only for a rate of cylinder pressure rise of less than 30 psi/^{o}CA, whilst beyond a pressure rate of about 100 psi/^{o}CA, a distinct knocking combustion occurs. In between these limits, there may appear occasional knocking. It is worth mentioning that Judge's analysis does not account for the effects of the fuel injection system and engine design.

From the above observation, the abnormality of the histogram of the maximum rate of cylinder pressure rise, $\hat{dP}$, obtained for Test 19A (Figure 5.13) (speed = 2500 RPM and load = 6.18 mkp) compared to that for a normal bell-shaped distribution can be described. Since the variation of $\hat{dP}$ in the present experimental analysis lies between 15 psi/^{o}CA and 110 psi/^{o}CA (Figure 5.2), two different forms of knocking and non-knocking combustion may be present. Therefore, the histogram of $\hat{dP}$

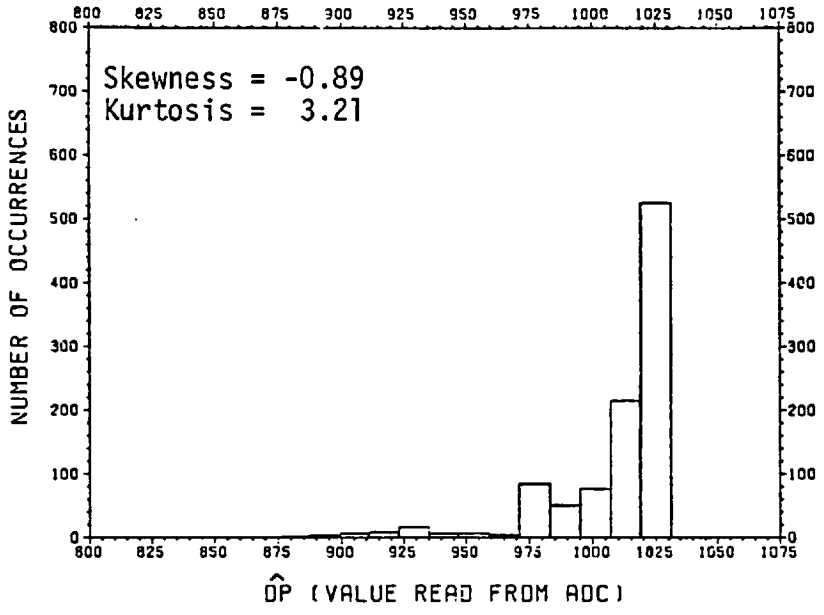


Figure 5.11(a): Histogram of maximum rate of cylinder pressure rise indicating a probable presence of periodic components

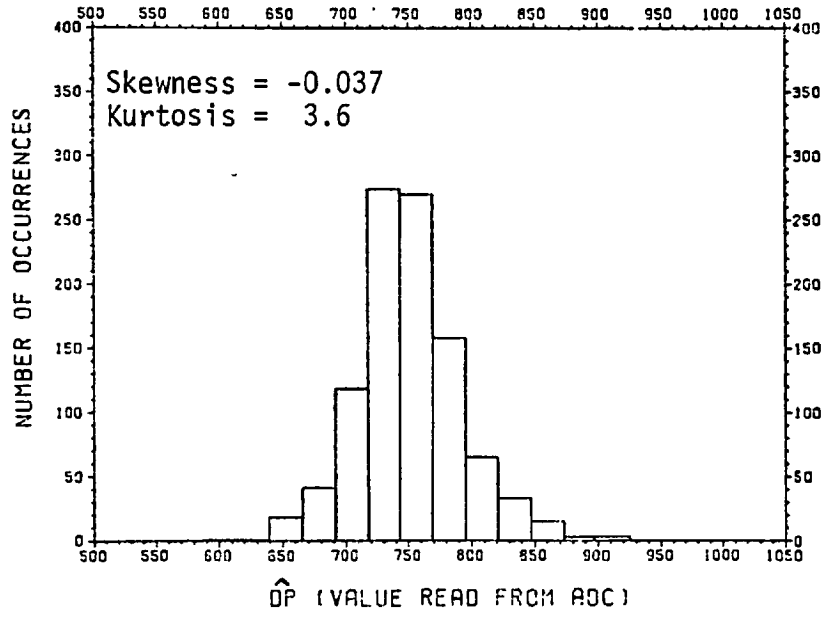


Figure 5.11(b): Histogram of maximum rate of cylinder pressure rise indicating a normal distribution

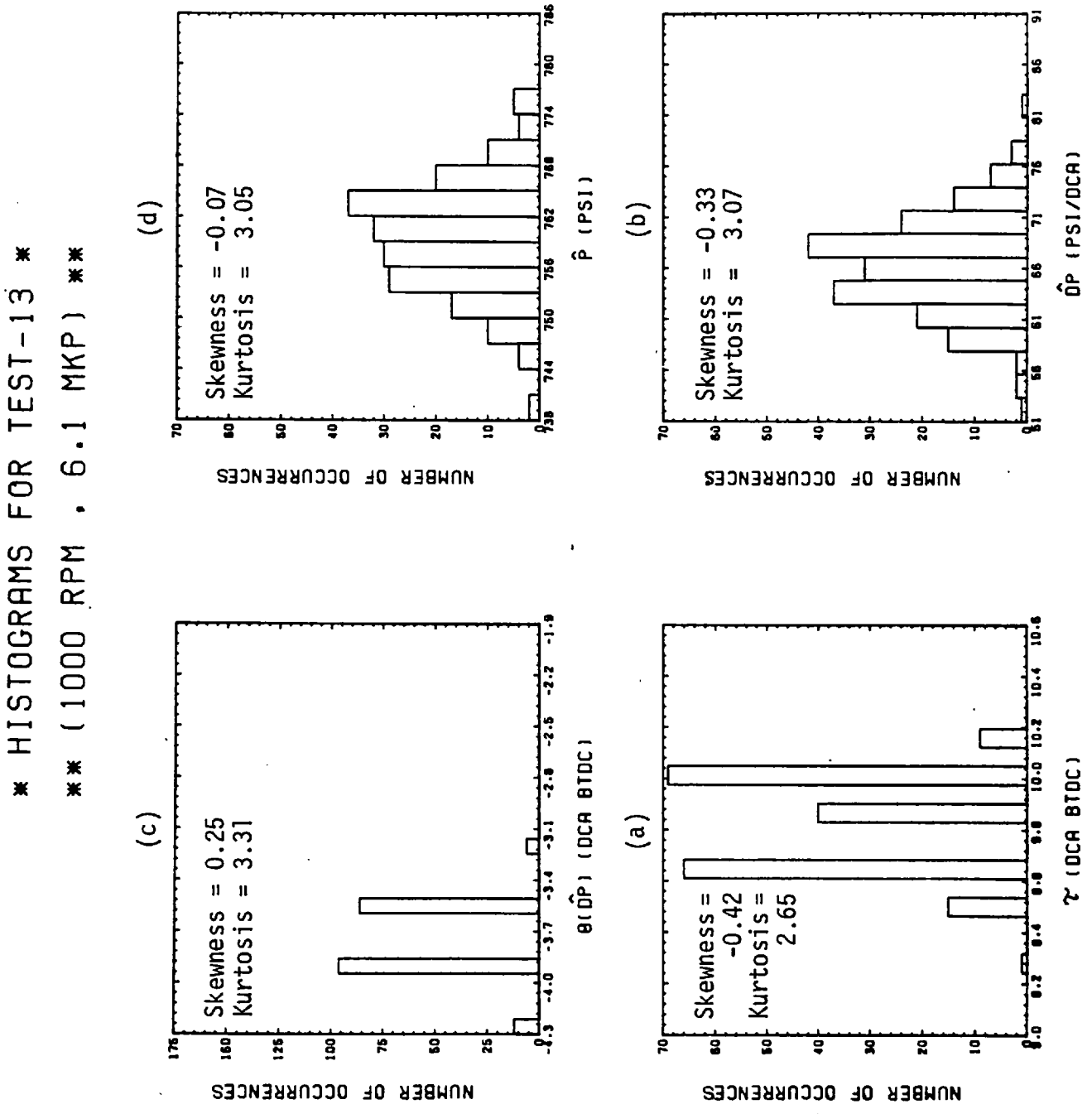


Figure 5.12: Histograms at low load-low speed conditions:

(a) histogram of starting angle of injection ($H(\tau)$)

(b) histogram of maximum rate of cylinder pressure rise ($H(d\hat{P})$)

(c) histogram of location of $d\hat{P}$ ($H(\theta(d\hat{P}))$)

(d) histogram of peak cylinder pressure ($H(\hat{P})$)

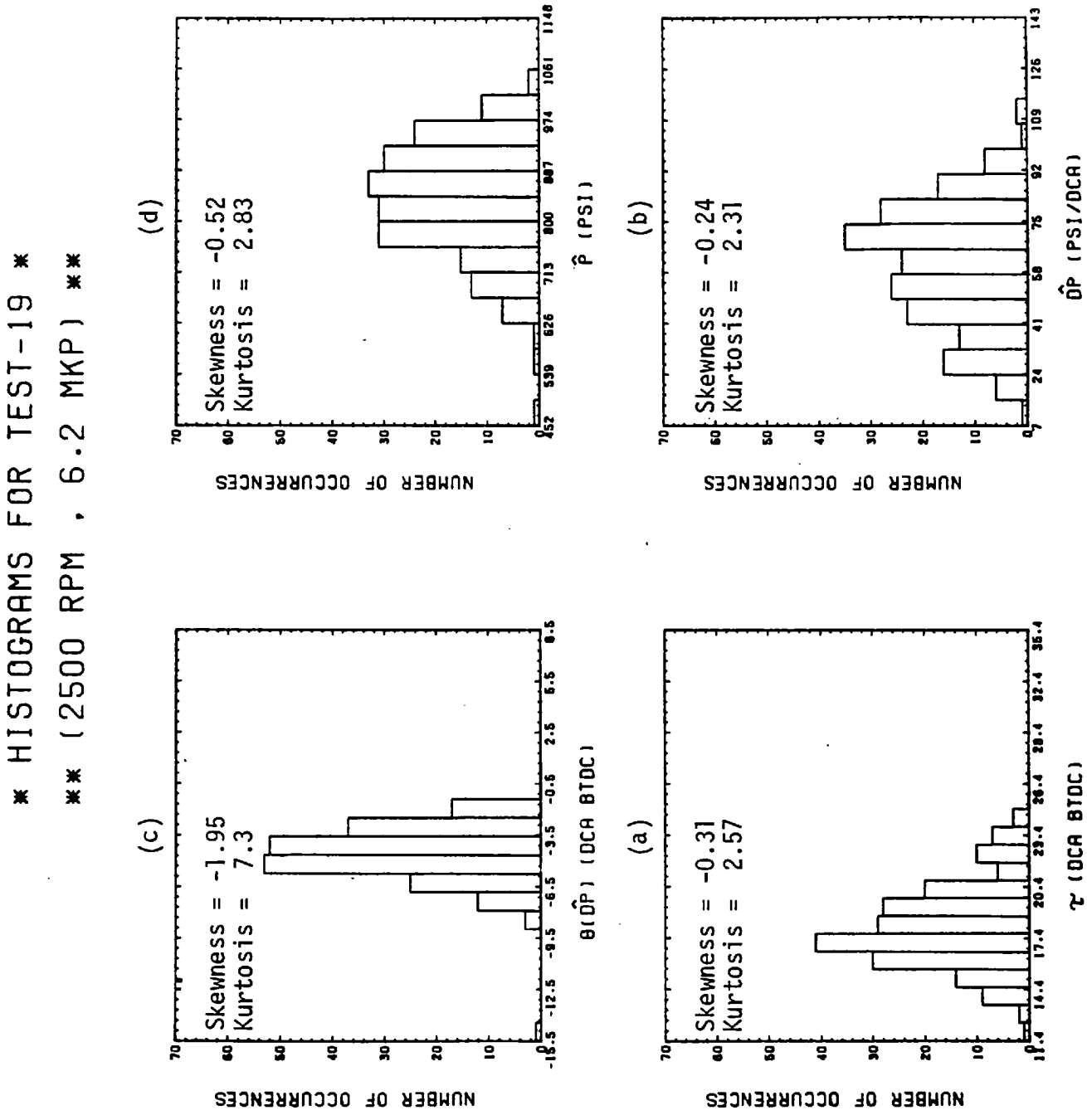


Figure 5.13: Histograms at low load-high speed conditions:

(a) histogram of starting angle of injection ($H(\tau)$)

(b) histogram of maximum rate of cylinder pressure rise ($H(\hat{dP})$)

(c) histogram of location of $\hat{dP}$ ($H(\theta(\hat{dP}))$)

(d) histogram of peak cylinder pressure ($H(\hat{P})$)

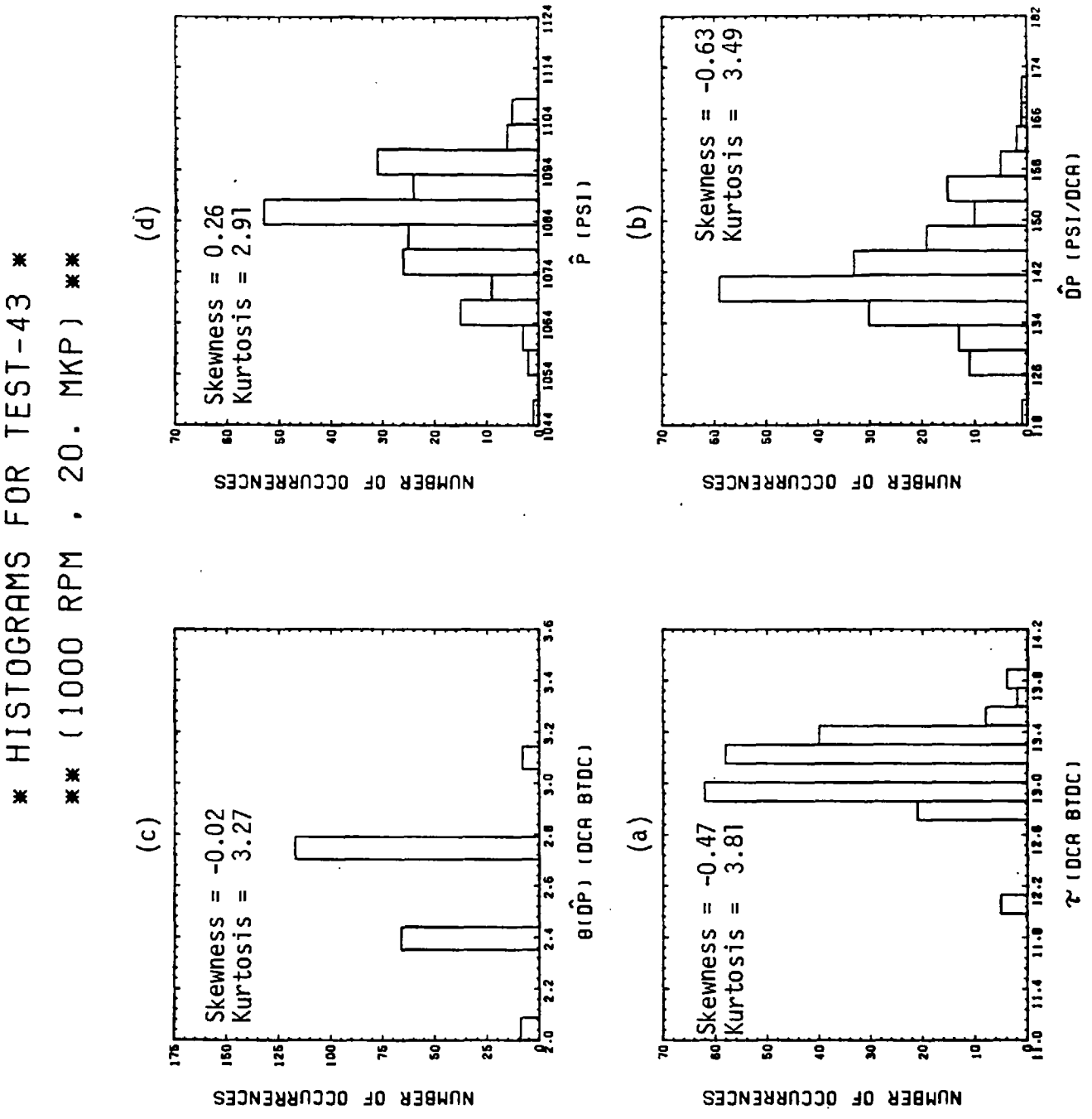


Figure 5.14: Histograms at high load-low speed conditions:

(a) histogram of starting angle of injection ($H(\tau)$)

(b) histogram of maximum rate of cylinder pressure rise ($H(d\hat{P})$)

(c) histogram of location of $d\hat{P}$ ($H(\theta(d\hat{P}))$)

(d) histogram of peak cylinder pressure ($H(\hat{P})$)

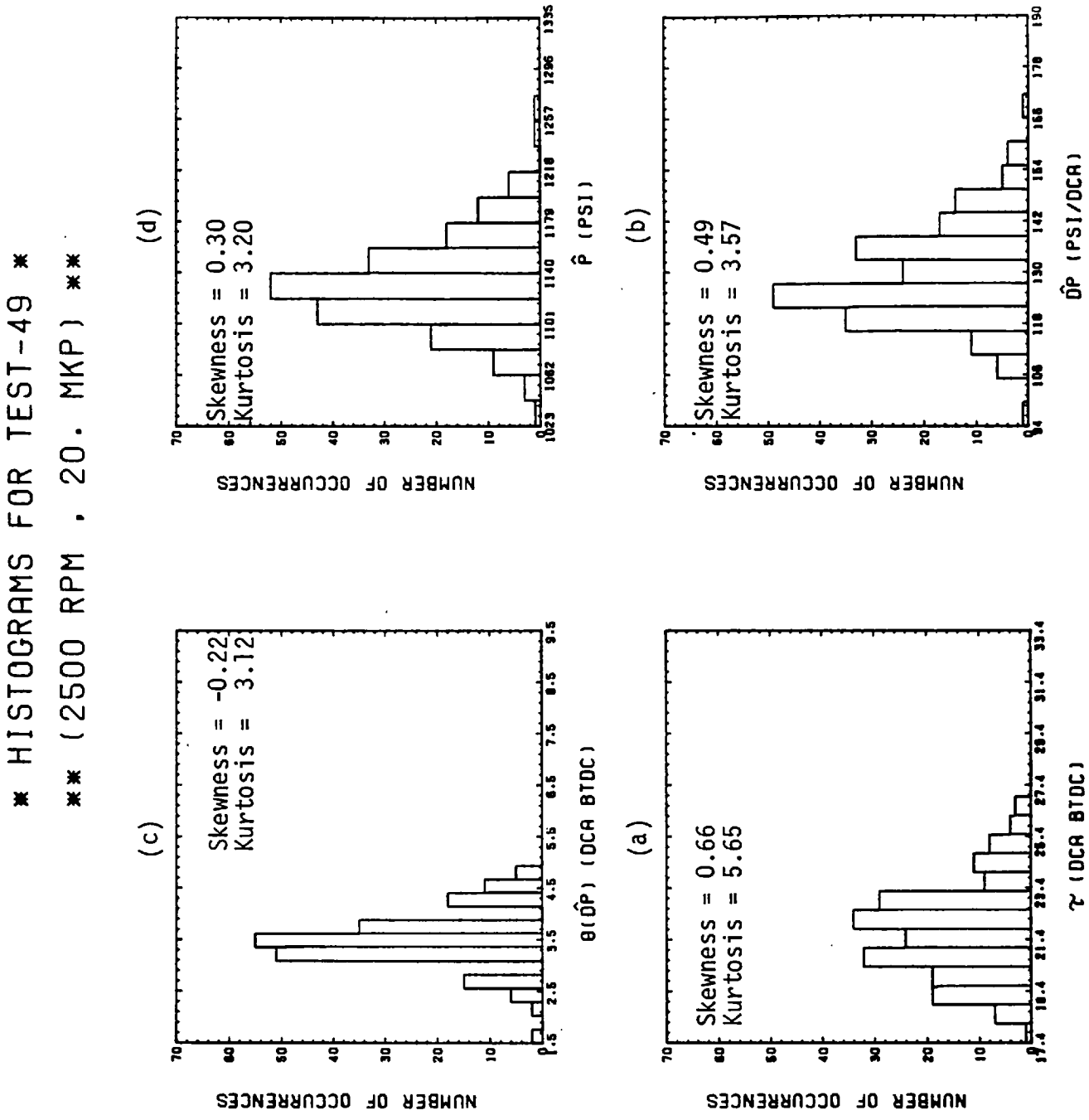


Figure 5.15: Histograms at high load-high speed conditions:

(a) histogram of starting angle of injection ($H(\tau)$)

(b) histogram of maximum rate of cylinder pressure rise ($H(\hat{dP})$)

(c) histogram of location of $\hat{dP}$ ($H(\theta(\hat{dP}))$)

(d) histogram of peak cylinder pressure ($H(\hat{P})$)

reflects combinations of two different normal distributions with their specific statistical properties. The combination of these two populations will then be conjectured as an almost distorted bell-shaped distribution, as shown diagrammatically in Figure 5.16.

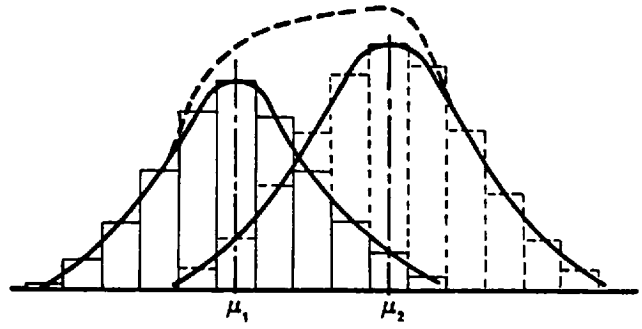


Figure 5.16: Distorted bell-shaped distribution obtained from two normal distributions

This is in agreement with the results of Curry (1963), indicating different populations for the knocking and non-knocking combustions. He also found somewhat similar histograms for the flame arrival time (which was used as a characterizing combustion parameter in his study) of knocking and non-knocking cycles. This phenomenon was not observed for other engine operating conditions as clearly as the case of low load-high speed which exhibited the highest range of variation.

5.2.2.3 Auto-correlograms

In Figure 5.7, auto-correlograms of τ, $\hat{dP}$, $\theta(\hat{dP})$ and $\hat{P}$ are shown for similar conditions (speed = 2500 RPM, load = 6.15 mkp). These diagrams demonstrate the values of each experimental set correlated

to each other. For example, the value of the auto-correlation of a single displacement indicates the effect of one cycle on the next cycle. On this basis, one can perform tests for analysing the engine characterizing parameters, and consequently showing the effect of one cycle on the following cycle using auto-correlation techniques. This auto-correlation can then be expressed to show the effect of residual gases inside the cylinder on cyclic variations.

Previous techniques for finding the effect of residual gases on cycle-to-cycle variation in petrol engines (Soltau (1960); Patterson (1966)) were found unsuitable for studying similar effects in diesel engines. This was because, in these studies, the charge was ignited at every fourth cycle (instead of every fourth stroke), and therefore the effect of scavenging was enhanced and, consequently, the effect of residual gases was insignificant due to the purging of the cylinders between firing cycles. Since diesel combustion is auto-igniting, arrangements for having one combustion in every two or four cycles is only possible by changes in the fuel injection system which are not desirable.

As shown in Figure 5.7, the auto-correlation of one cycle lag for $\hat{dP}$ or $\hat{P}$ is not insignificant, and therefore the effect of residual gases is considerable at the aforementioned conditions. This is in contrast with Wing's (1975) results previously discussed by the author (Razavi (1977)).

Although previous research (see Chapter 2 for references) indicated that the effect of residual gas on cyclic variation in petrol engines is insignificant, the results obtained here for a naturally aspirated diesel engine at a low load-high speed condition manifest a contrary phenomenon. This is because the auto-correlation

coefficient of $\hat{dP}$ for one or two cycles displacement is much higher than the value of 0.081 which is a critical value for the auto-correlation coefficient at 1% significance level. This high value of auto-correlation coefficient is not obviously due to insufficient sample data, but should indicate the influence of the residual gases on combustion cyclic variation.

Study of the auto-correlation of the dynamic injection provides a method of measuring the effect of the fuel injection of one cycle on later cycles. This can then be interpreted, in physical terms, as the effect of the drive backlash on the injection parameter's variabilities.

The oscillation of the auto-correlation of the engine time-series at certain operating conditions represents a bandpass white noise. Since the recorded signals are contaminated by high frequency noise, the parameters obtained from the unfiltered signals should show the same effect.

When the time-series tends to oscillate rapidly, there will be an oscillating auto-correlation which alternates in sign as it decays to zero, and the spectrum is dominated by high frequencies. Box & Jenkins (1970) showed that when the first order auto-regressive process modelled to the desired time-series:

$$\tilde{Z}_t = \Phi_1 \tilde{Z}_{t-1} + a_t \qquad (5.1)$$

where $\tilde{Z}_t$ = current value of the process

$\tilde{Z}_{t-1}$ = previous value of the process

a_t = white noise

the sign of Φ_1 determines the form of auto-correlation. The auto-

correlation function decays exponentially to zero when Φ_1 is positive, but decays exponentially to zero and oscillates in sign when Φ_1 is negative.

The nature of such time-series is shown by a simple example. In this test, every value of the time-series is subtracted from the previous value, thus producing a new time-series having *(N-1)* elements. If the sign of each element of this time-series is assumed to alternately positive and negative (or negative and positive), an oscillating auto-correlation would be generated because of existing high frequencies in the time-series.

This state of oscillating auto-correlation function with values of opposite sign in alternating cycles appeared at most of the operating conditions with high cyclic variations, which means every phenomenon causing this condition contributes to cycle-to-cycle variations. But, by varying the engine torque and the engine speed independently, no definite pattern was observed. Apart from the auto-correlograms shown in Figure 5.7 for the case which residual effect observed, the other auto-correlation results are not presented here because no correlation evidence was found.

5.2.2.4 Cross-correlograms

In Figure 5.8, cross-correlograms of τ, $\hat{dP}$, $\theta(\hat{dP})$ and $\hat{P}$ are shown for the same low load-high speed condition (speed = 2500 RPM, load = 6.15 mkp). The first correlogram exhibits cross-correlation coefficients between the dynamic injection, τ, and the maximum rate of cylinder pressure rise, $\hat{dP}$, over the range of - 6 to + 6 cycles. The second graph displays the correlogram relating the dependence of dynamic injection and the angle of occurrence of $\hat{dP}$, $\theta(\hat{dP})$. The third graph shows the cross-correlation between dynamic injection and peak cylinder pressure.

The negative sign of the dynamic injection, indicating degrees before top dead centre, gives rise to change in the sign of the correlation coefficients in these correlograms. However, the first graph of the correlation between τ and the minus value of $\hat{dP}$ is not affected. As can be seen from Figure 5.8 (bearing in mind the above considerations), there exists a high positive dependence between τ and $\hat{dP}$ or $\hat{P}$ or $\theta(\hat{dP})$. The analysis of cross-correlograms showed that only the cross-correlation coefficients of the order of - 1, 0 and + 1 were of significant interest. For delays of longer than two cycles, the correlation coefficients could only be interpreted as noise. The quantitative values of these dependences for different cycle displacements are also provided at the right hand side of these plots.

The overall results of cross-correlation coefficients of the maximum rate of cylinder pressure rise and dynamic injection for different operating conditions are demonstrated graphically in Figures 5.17 and 5.18. The chosen operating conditions (maximum variation of maximum rate of cylinder pressure rise) were established after monitoring the full range of operating conditions.

As shown in Figure 5.18, the zero order cross-correlation coefficients of τ and $\hat{dP}$ are plotted as a function of brake mean effective pressure (BMEP) for different speeds. As it can be seen from this figure, the cross-correlation coefficient increases up to a maximum value of 0.72 at 2250 rpm and 12 kW, and then it drops to a minimum value of - 0.52 for the highest power output. The mean value, the standard deviation and the coefficient of variation of dynamic injection and the maximum rate of cylinder pressure rise are demonstrated, respectively, as a function of BMEP in Figures 5.19 and 5.20.

By comparing the cross-correlation coefficient curve

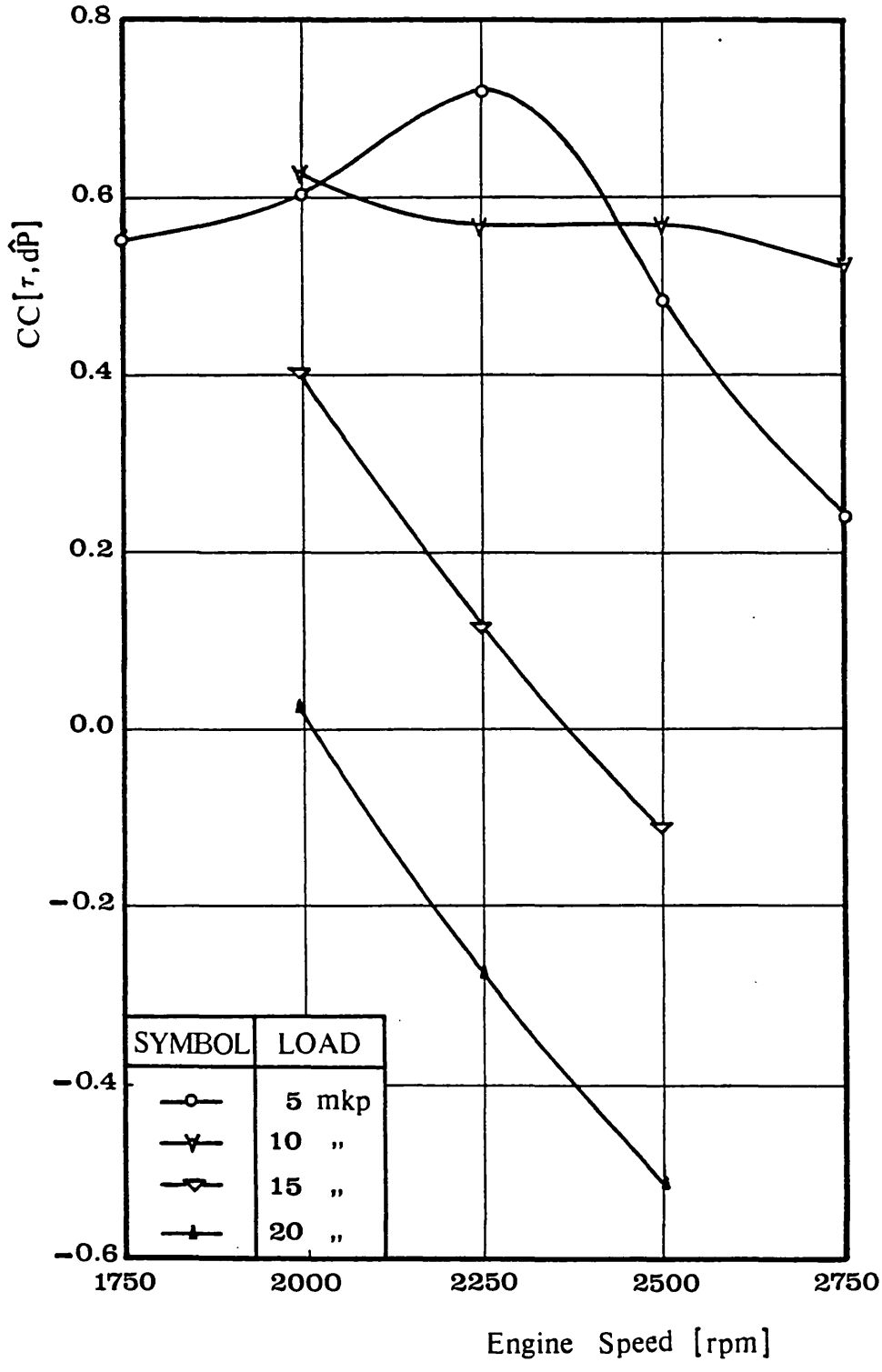


Figure 5.17: Cross-correlation coefficient (zero-order) between angle of injection and maximum rate of cylinder pressure rise as a function of speed for various torques

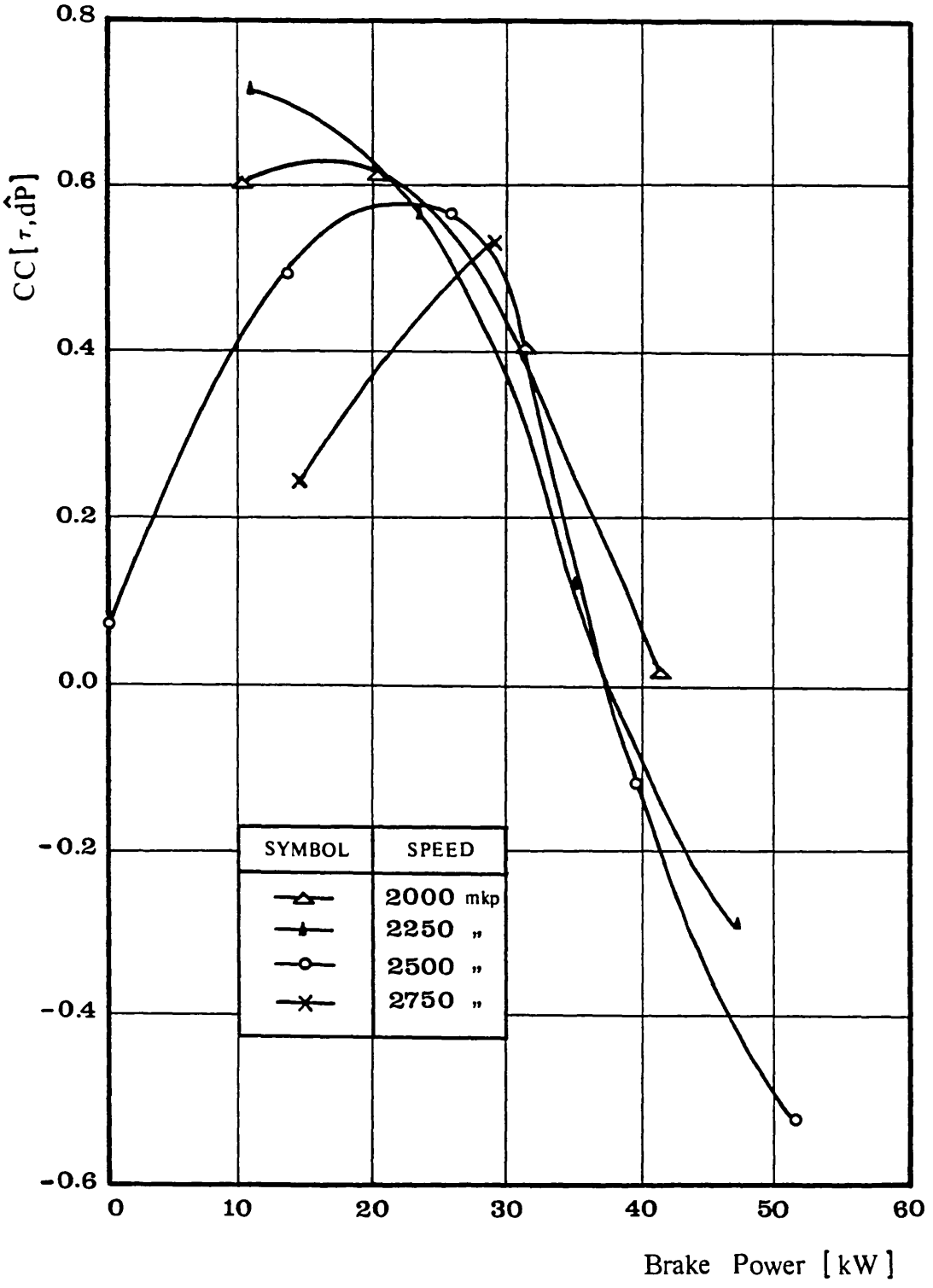


Figure 5.18: Cross-correlation coefficient (zero-order) between the angle of injection and maximum rate of cylinder pressure rise as a function of brake power for various speeds

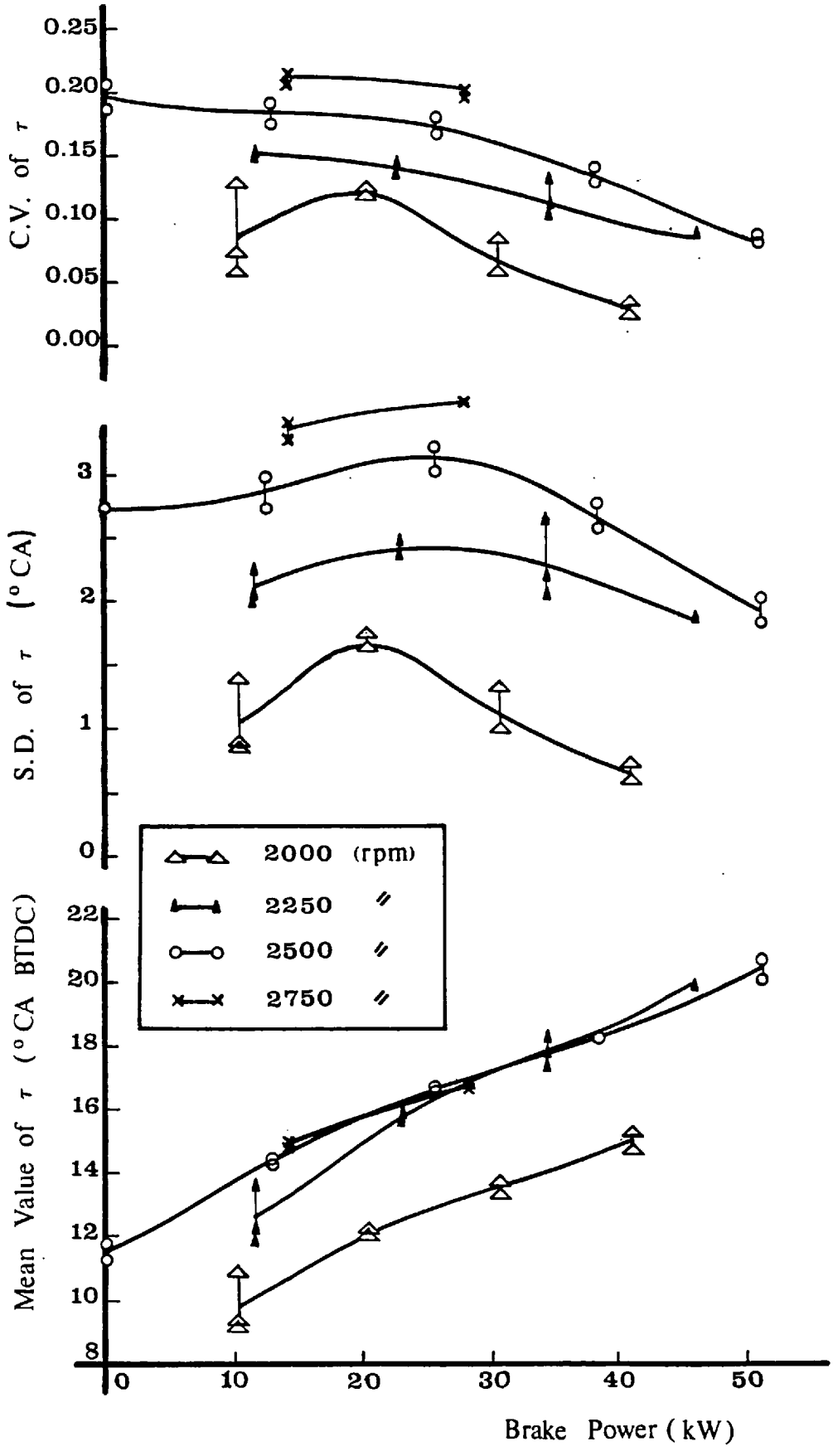


Figure 5.19: Mean value, standard deviation and coefficient of variation for starting angle of injection against brake power for different speeds

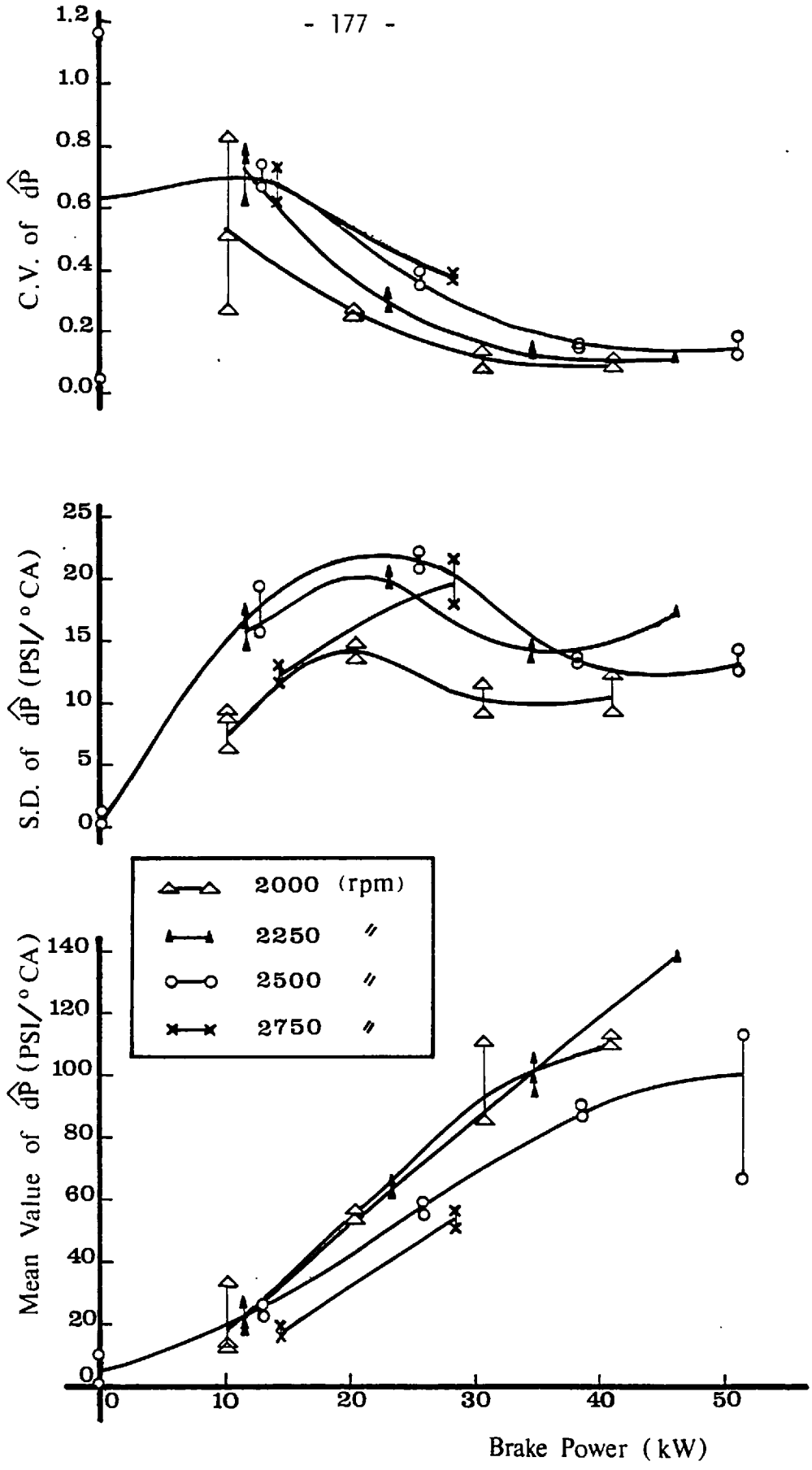


Figure 5.20: Mean value, standard deviation and coefficient of variation for maximum rate of cylinder pressure rise against brake power for different speeds

against BMEP with the standard deviation curves of τ and $\hat{dP}$ against BMEP for different speeds, the following conclusions can be deduced. (The discussion here is for 2500 RPM; the same argument can also be made for other speeds.)

i) From zero kW to 20 kW, the standard deviation of the maximum rate of cylinder pressure rise increases with the standard deviation of dynamic injection. During this period, there is an increasing positive cross-correlation coefficient between these two parameters.

ii) Between 20-30 kW, the standard deviations of both the dynamic injection and the maximum rate of cylinder pressure rise decrease. The result of this decrease in the cross-correlation curve is a declining positive correlation during this period.

iii) From about 30 kW to 52 kW, the standard deviation of the maximum rate of cylinder pressure rise starts to rise, despite the declining standard deviation of dynamic injection. This shows a negative correlation in the cross-correlation curve diagram.

5.2.3 Properties of Random Data

There are a number of parameters to describe the behaviour of random data which ideally should be determined over the infinite consecutive values of that variable. However, in practice, estimations of these parameters should be based on compromise of accuracy and economy.

By the classification of random data and by simplifying the assumptions, a great deal of unnecessary complicated data processing can be avoided and subsequently reduce the difficulty of analysis. Bendat & Piersol (1971) reported a classification of several important categories of random data.

The procedure for analysing properties of random data can be divided into two main categories: (i) properties of individual or ensembled average of sample records; and (ii) properties between different sample records. In the former analysis, we are dealing with the classification of a random process to evaluate stationarity, ergodicity, presence of periodicity and normality of data. To perform these analyses, the properties of these records (such as statistical parameters, auto-correlation, power spectral density and probability density function) are to be calculated.

The second category of analysis relating to the collection of sample records comprises the correlation analysis between each of two or more sets of records, and different tests (the F test and the Bartlett test) relating to the homogeneity* of variances. This checks whether the variations can be underlain in homogeneity of the data. If, for example, two variances are obtained using two different engine loadings with all other engine variables held constant and an F test indicates that they could be considered equal, then one could conclude that engine load did not affect the variances. On the other hand, if the hypothesis is rejected, then engine loading would be considered as the reason for the

---

* The homogeneity is an indication of some degree of certainty as to whether the resultant standard deviations are the same or not. (For more details, see Section 5.2.3.3 on the homogeneity of sampled data.)

significantly different variances. When the number of variances exceeds two, then Bartlett's test should be employed.

5.2.3.1 Stationarity, ergodicity, normality and periodicity of random data

The concept of an ensemble of time-series is the basis for the definition of stationarity and ergodicity in stochastic processes. An ensemble of m-series, $k = 1, 2, \ldots, m$ each T-time long, is shown in Figure 5.21 for a continuous time-series. If the properties of time-series do not change with the absolute time, they are called stationary (time invariant).

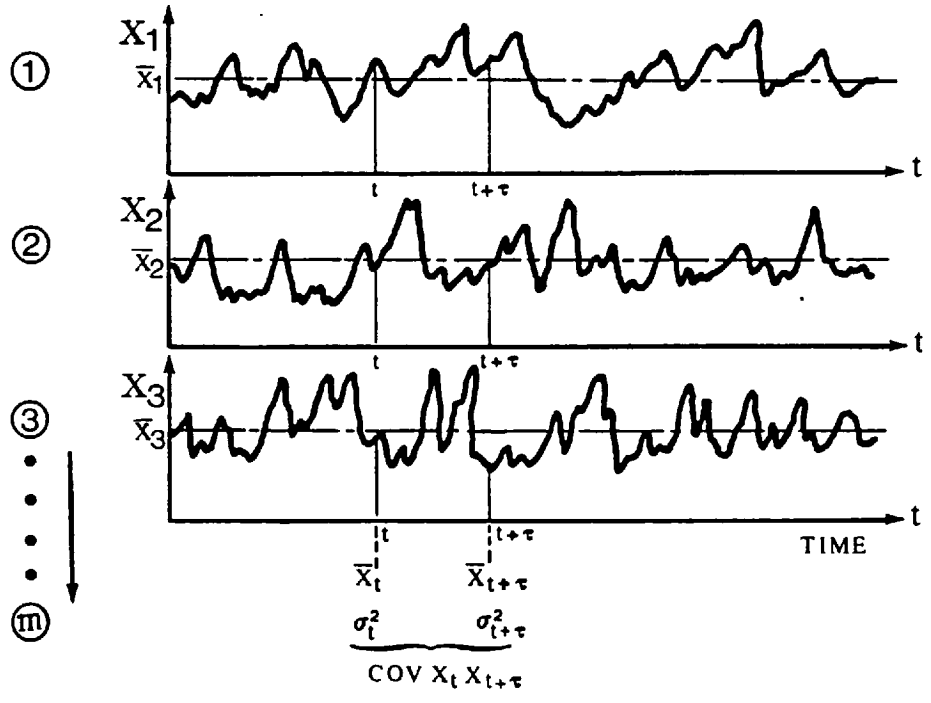


Figure 5.21: Ensemble of series for defining stationarity and ergodicity

At any time t, the mean value $\bar{x}_t$ may be determined over the ensemble by summing the instantaneous values divided by the total values summed:

$$\bar{x}_t = \frac{1}{m} \sum_{k=1}^{m} x_k(t) \tag{5.2}$$

Similarly, the mean value at the position $(t+\tau)$ is:

$$\bar{x}_{t+\tau} = \frac{1}{m} \sum_{k=1}^{m} x_k(t+\tau) \tag{5.3}$$

The auto-correlation function of $x(t)$ and $x(t+\tau)$ is:

$$R_x(t, t+\tau) = \frac{1}{m} \sum_{k=1}^{m} x_k(t)\, x_k(t+\tau) \tag{5.4}$$

If mean values of $\bar{x}_t$ and $\bar{x}_{t+\tau}$ converge with the probability unity to the same population mean, μ, in the case for $m \to \infty$ (which means $\bar{x}_t$ = constant), then the time-series $x(t)$ is said to be stationary in the mean or first order stationary (weakly stationary). If the series is stationary both in the mean and in the auto-correlation*, the series is said to be second order stationary. If all higher moments are time invariant, then the process is higher order stationary (strong stationary). If, also, a stationary process has a normal distribution, then the stationary process will be of a higher order stationary (Yevjevich (1972)).

If the properties of a stationary process are time-averaged over a period T, then parameters of each particular series of the ensemble of series, given here as the k-series, k = 1, 2, ..., m, are:

---

* If the auto-correlation defined in equation (5.4) is independent of the position t, but dependent on the lag τ for $m \to \infty$ ($R_x(t, t+\tau) = R_x(\tau)$), then the time-series is said to be stationary in the auto-correlation (co-variance).

$$\bar{x}_k = \frac{1}{T}\int_o^T x_t \, dt \tag{5.5}$$

$$R_x(t,t+\tau,k) = \frac{1}{T}\int_o^T x_k(t)\, x_k(t-\tau)\, dt \tag{5.6}$$

If the mean value and auto-correlation function are identical, regardless of the sample function of the ensemble from which they are obtained (it means $\bar{x}_k$ = constant, and $R_x(t,t+\tau,k) = R_x(\tau,k)$), the process is said to be ergodic.

The test of stationarity confirms the acceptability of the degree of accuracy in the prediction of time-series properties over the applied length of sample record. To find out whether the sampled data are stationary, different methods can be used. If basic physical factors underlying the phenomenon are time invariant, then the stationary state of the resulting data can generally be accepted without a further study. The procedure used in the present work to check whether the sample values had any non-stationary trend was a run test. A description of this test is given in the next section. This test was carried out only for a few sample records because, generally, a large number of cycles (1000) were considered to assure stationarity of the data. Thus, the results confirmed the validity of using computational subroutines (auto-correlation, cross-correlation, etc.) which were based on equations (C1.10) to (C1.13) for stationary signals. Some accompanying tests were carried out to study the stationarity, normality and also to detect any periodic components buried in the signals. Power spectral density is the best tool for detecting any periodic components in sampled data. They will appear as sharp peaks in the spectral density with theoretically represent delta functions in the power spectral density function. The auto-

correlation function also gives similar information. Moreover, the graphical presentation of probability density function (the histogram) with the help of skewness and Kurtosis analyses were used to test samples of stationary random data for normality. Figures 5.22 to 5.25 show the auto-correlation and power spectral density of the starting angle of injection and the maximum rate of cylinder pressure rise at certain operating conditions. In the case of Figure 5.23, a dominant frequency of 7.75 Hz ($f = k f_d/m = 140 \times 8.33/160 = 7.75$ Hz) can be easily distinguished for the maximum rate of cylinder pressure rise data. This abnormality was previously shown in the form of the presentation of $\hat{dP}$ over 1000 cycles in Figure 5.5(a) and in the form of a histogram of $\hat{dP}$ in Figure 5.11(a).

In spite of the fact that any hypothesis for describing the behaviour of the various engine parameters could be either proved or rejected by using only a single technique, nevertheless, different methods were employed to assess the validity of each method in these particular applications.

5.2.3.2 Run test

The run test is a method for establishing confidence intervals to show whether results are independent random observations of the same random variable. The run test can be easily performed by classifying the sample data into two mutually exclusive categories which may be identified simply by plus (+) or minus (-). These two categories can be simply distinguished by comparing each element of the sample data with its median value*. A run is defined as a sequence of identical

---

* The median is defined as the middle value when the given observations are arranged in order of magnitude.

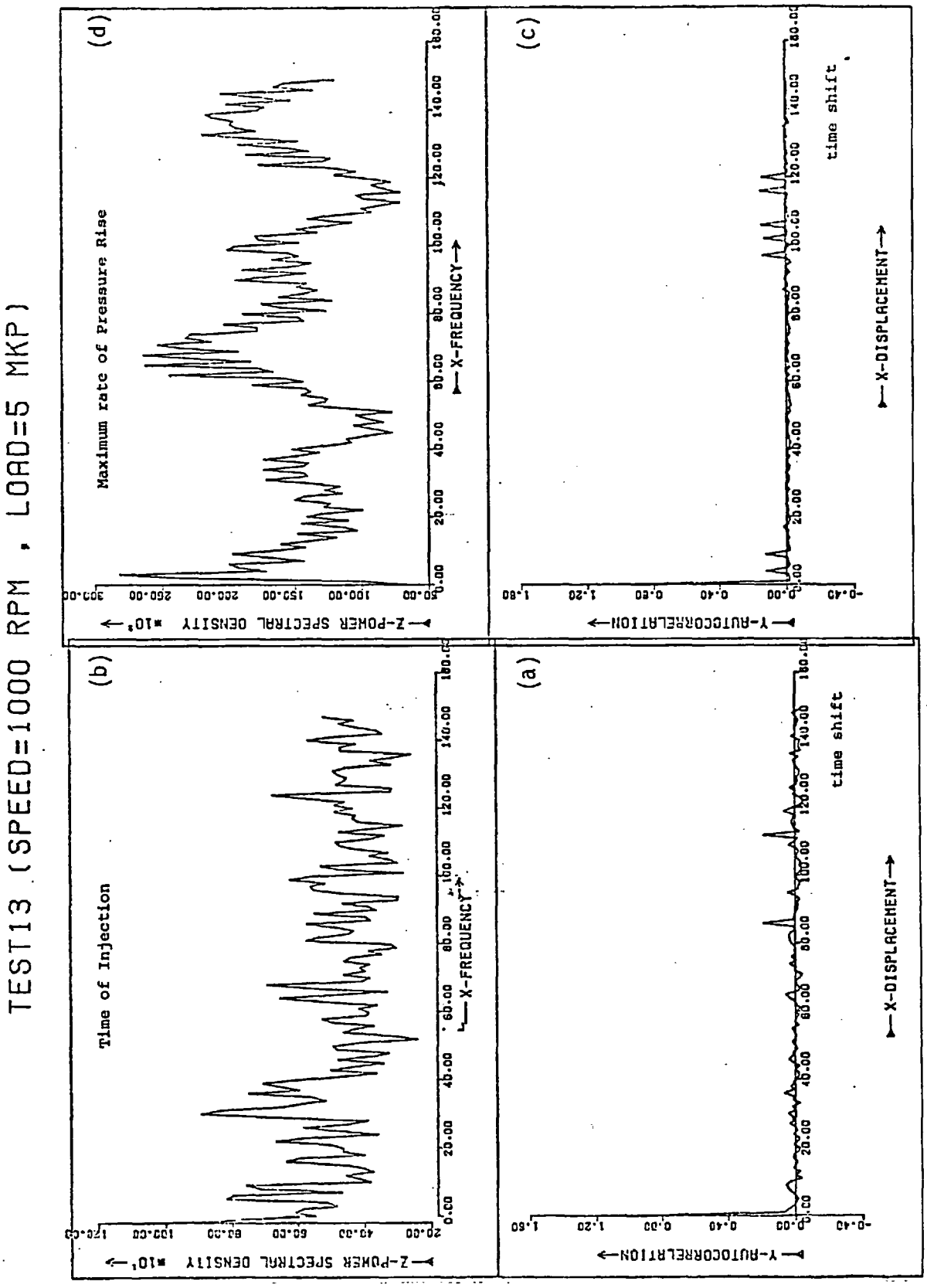


Figure 5.22: Auto-correlation and power spectral density of starting angle of injection and maximum rate of cylinder pressure rise at a speed of 1000 rpm and a load of 5 mkp

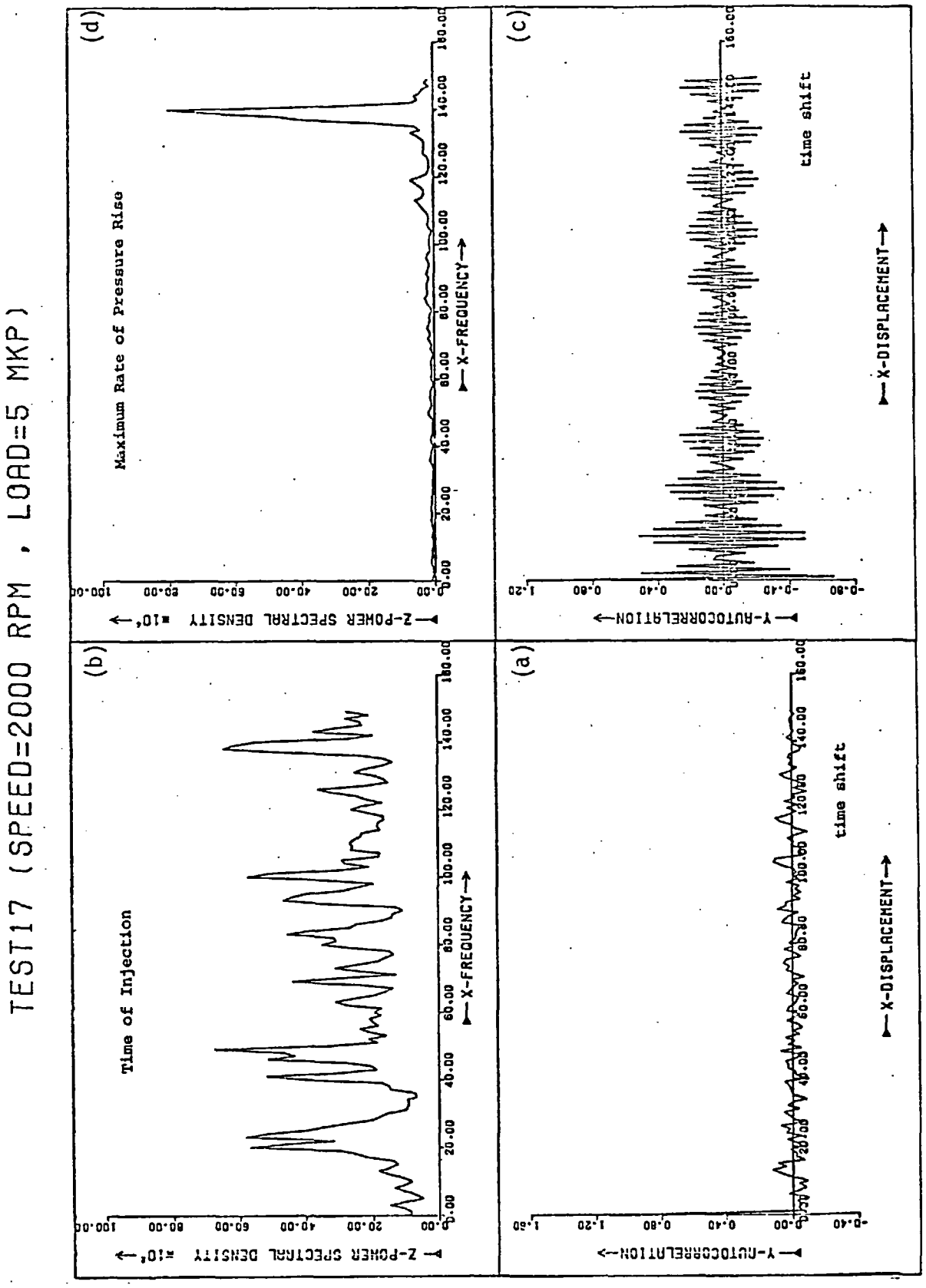


Figure 5.23: Auto-correlation and power spectral density of starting angle of injection and maximum rate of cylinder pressure rise at a speed of 2000 rpm and a load of 5 mkp

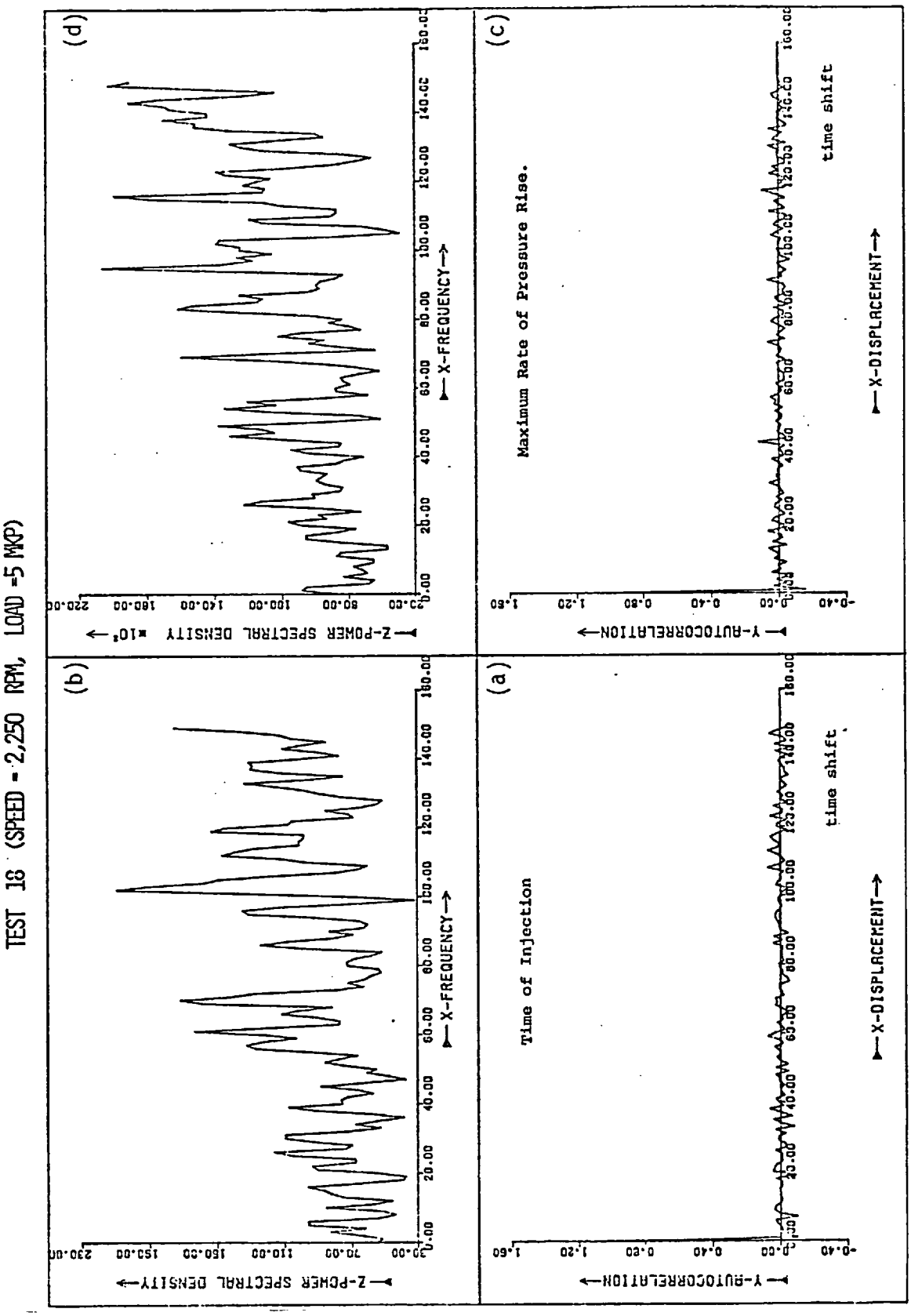


Figure 5.24: Auto-correlation and power spectral density of starting angle of injection and maximum rate of cylinder pressure rise at a speed of 2250 rpm and a load of 5 mkp

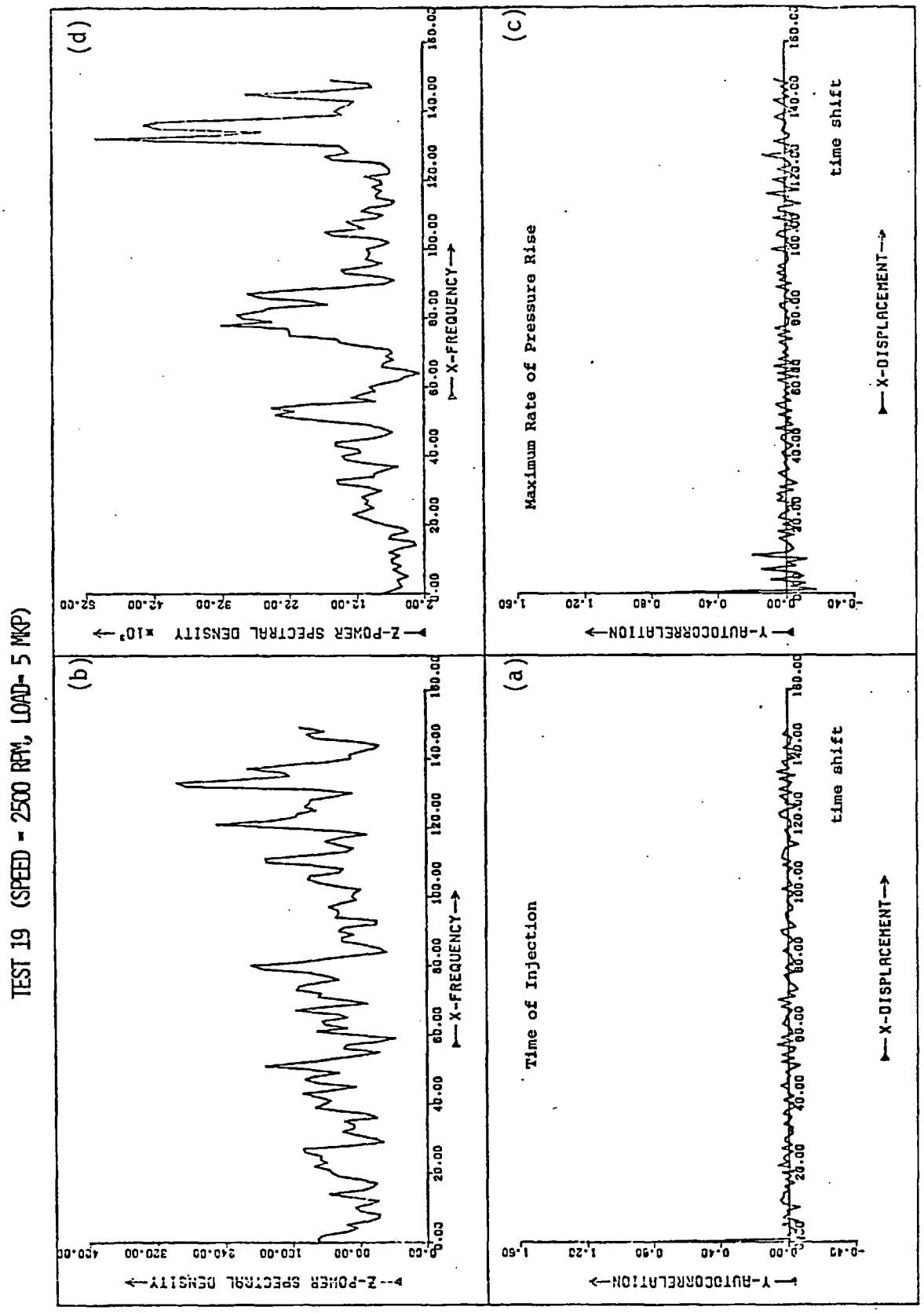


Figure 5.25: Auto-correlation and power spectral density of starting angle of injection and maximum rate of cylinder pressure rise at a speed of 2500 rpm and a load of 5 mkp

observations that is followed by a different observation or no observation at all. If a sequence of N observations are independent observations of the same random variable, then the probability of (+) observations equals the probability of (-) observations, the number of runs in the sequence having a sampling distribution as given in Table 5.2 (Bendat & Piersol (1971)).

The hypothesis of existence of a trend can be accepted or rejected at any desired level of significance, α, by comparing the observed runs with the tabulated values of interval between $r_{n;1-\alpha/2}$ and $r_{n;\alpha/2}$, where $n = N/2$. If the observed runs fall outside the interval, the hypothesis is accepted at the α level of significance. Otherwise, the hypothesis is rejected implying that the sample data is a sequence of independent random observations of the random variable.

Table 5.3 presents the number of runs which occurs in a sequence of 50 sampled observations of the maximum rate of cylinder pressure rise at the engine speed of 1000 RPM and engine load of 6 mkp. The median value was found to be 461.5 for 50 observations. All values greater than 461.5 were identified by a plus sign (+) and all with a value less than 461.5 were identified by a minus sign (-). The results are hence classified in Table 5.3. Hence, for runs represented by 50 observations with α level of significance, $\alpha = 0.05$, the acceptance region for being independent data is given by Table 5.2:

$$r_{n;1-\alpha/2} < r < r_{n;\alpha/2}$$

$$r_{25;0.975} = 18 \quad ; \quad r_{25;0.025} = 33$$

This is reasonable since $r = 30$ falls within the range between 18 and 33,

TABLE 5.2

Percentage Points of Run Distribution

Values of $r_{n;\alpha}$ such that Prob $[r_n > r_{n;\alpha}] = \alpha$, where $n = N_1 = N_2 = N/2$

	α					
$n = N/2$	0.99	0.975	0.95	0.05	0.025	0.01
5	2	2	3	8	9	9
6	2	3	3	10	10	11
7	3	3	4	11	12	12
8	4	4	5	12	13	13
9	4	5	6	13	14	15
10	5	6	6	15	15	16
11	6	7	7	16	16	17
12	7	7	8	17	18	18
13	7	8	9	18	19	20
14	8	9	10	19	20	21
15	9	10	11	20	21	22
16	10	11	11	22	22	23
18	11	12	13	24	25	26
20	13	14	15	26	27	28
25	17	18	19	32	33	34
30	21	22	24	37	39	40
35	25	27	28	43	44	46
40	30	31	33	48	50	51
45	34	36	37	54	55	57
50	38	40	42	59	61	63
55	43	45	46	65	66	68
60	47	49	51	70	72	74
65	52	54	56	75	77	79
70	56	58	60	81	83	85
75	61	63	65	86	88	90
80	65	68	70	91	93	96
85	70	72	74	97	99	101
90	74	77	79	102	104	107
95	79	82	84	107	109	112
100	84	86	88	113	115	117

TABLE 5.3

Typical Run-Test Presentation

Number	$\hat{dP}$ (ADC No.)	+ = above M^* - = below M	Number	$\hat{dP}$ (ADC No.)	+ = above M^* - = below M
1	463	1 +	26	462	17 +
2	460	-	27	459	18 -
3	459	2 -	28	465	19 +
4	456	-	29	457	20 -
5	462	3 +	30	463	+
6	455	4 -	31	463	+
7	466	5 +	32	465	21 +
8	456	6 -	33	465	+
9	462	7 +	34	465	+
10	466	+	35	461	-
11	458	8 -	36	461	22 -
12	449	-	37	459	-
13	463	9 +	38	463	23 +
14	455	10 -	39	461	24 -
15	465	11 +	40	462	25 +
16	459	-	41	459	26 -
17	456	12 -	42	458	-
18	461	-	43	473	+
19	463	13 +	44	463	+
20	463	+	45	471	27 +
21	460	14 -	46	464	+
22	462	15 +	47	469	+
23	461	-	48	459	28 -
24	457	16 -	49	464	29 +
25	461	-	50	461	30 -

* Median value = 461.5

Number of runs = 30

For $n = N/2 = 25$ and $\alpha = 0.05$ significant:

$$r_{n;1-(\alpha/2)} = r_{25;0.975} = 18$$

$$r_{n;\alpha/2} = r_{25;0.025} = 33$$

which indicates that there is no evidence of an underlying trend in the sampled data.

The analysis of data at different engine operating conditions showed that, although the run test provides a simple method to establish the existing trend in data, this will not be suitable when the data reveals a high frequency variation. This is so because the run test always indicates the existing trend for these data which may be false within the sampling period.

5.2.3.3 Homogeneity of variances

The F test and the Bartlett test were employed to examine the equality of two or more variances, respectively, and hence to determine the existence of homogeneity between different sample data.

In general, the F test simply attempts to find the F ratio (variance ratio) between the variances of two sets of data and compare it with tabulated values of F distribution for different levels of significance. This variance ratio is defined by:

$$F = \frac{\sigma_1^2}{\sigma_2^2} \qquad \text{where} \qquad \sigma_1^2 > \sigma_2^2 \tag{5.7}$$

If the calculated value of F is greater than the tabulated value, the probability that the difference between the two variances is haphazard and is smaller than the specified level of significance. On this basis, the validity of the hypothesis of equal variances can be assessed. If the hypothesis is accepted and the variances are considered to be equal, the best estimate of standard deviation is obtained by averaging these variances. However, if the hypothesis is rejected, the variances cannot be attributed to corresponding changes in the other variables which

produce these variations.

This technique has been previously employed satisfactorily by Barton et al (1970) in a study of cyclic variations of petrol engines. To cite an example, the F test provides a basis for comparing the degree of variability in different sets of data which are recorded from an engine process.

The F test was used here to show whether the warm-up effect of the engine has an appreciable significance in the variability of sampled characterizing parameters. Table 5.4 shows the mean values and variances of dynamic injection and maximum rate of cylinder pressure rise, and also the variance ratio for different operating conditions.

TABLE 5.4

Test Number	Speed (rpm)	Load (mkp)	Number of Samples	τ (ADC No.)	σ^2_τ	$\hat{dP}$ (ADC No.)	$\sigma^2_{\hat{dP}}$
19A	2500	5	200	35.34	51.30	469.9	1056.25
19B	2500	5	200	34.94	62.67	463.6	1636.20
F Value	$F_\tau = 62.67/51.30 = 1.221$; $F_{\hat{dP}} = 1636.20/1056.25 = 1.549$						
From Table	$F_{n_1,n_2;0.01} = 1.39$; $F_{n_1,n_2;0.05} = 1.26$						
27A	2000	10	200	41.54	16.85	424.6	610.58
27B	2000	10	200	41.24	19.01	429.2	523.95
F Value	$F_\tau = 19.01/16.85 = 1.128$; $F_{\hat{dP}} = 610.58/523.95 = 1.165$						
From Table	$F_{n_1,n_2;0.01} = 1.39$; $F_{n_1,n_2;0.05} = 1.26$						

As shown, the F values obtained from the statistical tables for 5% and 1% significance are 1.26 and 1.39, respectively (Bendat & Piersol (1971)).

In the case of Test 19, the variance ratio for $\hat{dP}$ (= 1.549 > 1.39) describes the variability of the variances which may be interpreted as the effect of the engine warming-up parameter. In contrast, the variance ratios of τ (= 1.128 < 1.26) and $\hat{dP}$ (= 1.165 < 1.26) for Test 27 does not show significant variabilities (Table 5.4). Therefore, the two sets of data (Test 27A and Test 27B) are taken as homogeneous. Consequently, the effect of warming-up is appreciable for combustion characterizing parameters, but has little effect on the fuel injection parameters.

The Bartlett test, being a special application of the chi squared (χ^2) test, is essentially similar to the F test, but the equality of more than two variances is determined.

If there are estimates (σ_i^2), each having f_i degrees of freedom, the Bartlett test criterion can be formulated as follows (Sredecor & Cochram (1967)):

$$M = (2.3026) \left[\left(\sum_{i=1}^{n} f_i \right) \log \overline{\sigma^2} - \sum_{i=1}^{n} f_i \log \sigma_i^2 \right] \tag{5.8}$$

where:

$$\overline{\sigma^2} = \frac{\sum_{i=1}^{n} f_i \sigma_i^2}{\sum_{i=1}^{n} f_i} \tag{5.9}$$

The quantity of $\chi^2 = M/C$ is approximately distributed as χ^2 (chi squared distribution) with $(a-1)$ degree of freedom, and C is defined by:

$$C = 1 + \frac{1}{3(a-1)} \left[\sum_{i=1}^{n} \frac{1}{f_i} - \frac{1}{\sum_{i=1}^{n} f_i} \right] \tag{5.10}$$

If the calculated value of χ^2 is greater than the tabulated values at a specified level of significance, the variance is considered as non-homogeneous. It is worth mentioning that the Bartlett test is sensitive to the normality of the data (especially positive Kurtosis), thereby it may yield erroneous verdicts on heterogeneity.

Tables 5.5, 5.6 and 5.7 show three samples of the Bartlett test which were carried out to demonstrate the homogeneity of the variances, and are described as follows:

i) Table 5.5 shows the homogeneity of seven test variances, all carried out at 5 mkp load and different engine speeds to study the effect of speed on variability of variances. These results describe non-homogeneity of the variances as $\chi^2 = 6721.19 >> 1105.14$, thus indicating that the engine speed contributes notably to the factors affecting cycle-to-cycle variations.

ii) Table 5.6 shows the results for a similar test, which attempts to discover the effect of load on variabilities of variances. The standard deviation of the characterizing parameter ($\hat{dP}$ here) were obtained at constant speed (2500 rpm) and different loading conditions. The heterogeneity of the variances ($\chi^2 = 4115.88 >> 1105.14$) indicates that the effect of loading on the combustion cyclic dispersions is significant.

iii) Table 5.7 demonstrates the results of the Bartlett method on three identical tests carried out at a

TABLE 5.5

Test Number	Speed (rpm)	Load (mkp)	Number of Samples	$\hat{dP}$ (ADC No.)	$\sigma_{\hat{dP}}$ (ADC No.)	σ_i^2	$\log \sigma_i^2$
1	1000	5	1000	456.1	4.114	16.92	1.228
2	1250	5	1000	440.3	5.25	27.56	1.440
3	1500	5	1000	453.1	7.31	53.43	1.727
4	2000	5	1000	464.2	14.65	214.62	2.331
5	2250	5	1000	480.2	30.21	912.64	2.960
6	2500	5	1000	469.9	32.50	1056.25	3.023
7	2750	5	1000	477.7	29.48	869.07	2.939
					Total	3150.49	15.648

$$\overline{\sigma_i^2} = \frac{\sum_{i=1}^{n} \sigma_i^2}{n} = \frac{3150.49}{7} = 450.07$$

$$\log \overline{\sigma_i^2} = 2.653$$

$$M = (2.3026)(999)\,[7\,(2.653) - 15.648] = 6723.76$$

$$C = 1 + \frac{a+1}{3\,a\,f} = 1 + \frac{8}{3 \times 7 \times 999} = 1.00038$$

$$\chi^2 = M/C = \frac{6723.76}{1.00038} = 6721.19$$

Tabulated values of χ^2:

for 5% significance, $\chi^2 = 1073.36 < 6721.19$

for 1% significance, $\chi^2 = 1105.14 < 6721.19$

So, the variances are non-homogeneous.

TABLE 5.6

Test Number	Speed (rpm)	Load (mkp)	Number of Samples	$\hat{dP}$ (ADC No.)	$\sigma_{\hat{dP}}$ (ADC No.)	σ_i^2	$log\ \sigma_i^2$
1	2500	0	1000	495.0	2.79	7.78	0.891
2	2500	5	1000	469.9	32.50	1056.25	3.023
3	2500	10	1000	394.6	43.11	1858.47	3.269
4	2500	15	1000	332.3	27.45	753.50	2.877
5	2500	20	1000	284.7	30.22	913.24	2.960
					Total	4589.24	13.020

$$\overline{\sigma_i^2} = \frac{\sum_{i=1}^{n} \sigma_i^2}{n} = \frac{4589.24}{5} = 917.84$$

$$log\ \overline{\sigma_i^2} = 2.962$$

$$M = (2.3026)(999)\ (5\ (2.962) - 13.02) = 4117.53$$

$$C = 1 + \frac{a + 1}{3\ a\ f} = 1 + \frac{6}{3 \times 5 \times 999} = 1.0004$$

$$\chi^2 = M/C = \frac{4117.53}{1.0004} = 4115.88$$

Because $\chi^2 = 4115.88 >> 1105.14$ (χ^2 for 1% significance), the variances, therefore, are non-homogeneous.

TABLE 5.7

Test Number	Speed (rpm)	Load (mkp)	Number of Samples	$\hat{dP}$ (ADC No.)	$\sigma_{\hat{dP}}$ (ADC No.)	σ_i^2	$log\ \sigma_i^2$
1	2250	15	1000	334.1	27.36	748.56	2.874
2	2250	15	1000	321.6	25.50	650.25	2.813
3	2250	15	1000	342.1	25.53	651.78	2.814
					Total	2050.59	8.501

$$\overline{\sigma_i^2} = \frac{\sum_{i=1}^{n} \sigma_i^2}{n} = \frac{2050.59}{3} = 683.53$$

$$log\ \overline{\sigma_i^2} = 2.834$$

$$M = (2.3026)(999)\ [3\ (2.834) - 8.501] = 7.52$$

$$C = 1 + \frac{a + 1}{3\ a\ f} = 1 + \frac{4}{3 \times 3 \times 999} = 1.00044$$

$$\chi^2 = M/C = \frac{7.52}{1.00044} = 7.52$$

Because $\chi^2 = 7.52 << 1073.36$ (χ^2 for 5% significance), the variances, therefore, are homogeneous.

speed of 2250 rpm and a load of 15 mkp. As expected, homogeneous variances were obtained (as $\chi^2 = 7.52 << 1073.36$), while all the working parameters remained constant. This also specifies that all differences in the variances can be explained by the random nature of the data.

5.3 DYNAMIC MODELLING RESULTS

As previously described in Section 3.2, dynamic modelling was set up to study the rôle of perturbations in fuel injection system characteristics on the overall performance of a direct injection diesel engine. The dynamic modelling program was fed with two sets of data. One contained the engine specifications and operating conditions, and the other represented the perturbation in the desired parameters of the fuel injection system. In most cases, in order to simplify the interpretation of the results, it was attempted to change only one parameter of the injection system characteristic at a time (cycle), assuming other parameters to be constant. For example, when the starting degree of injection, τ, was varied for every cycle, the assumption of constant injection duration and constant quantity of injected fuel had to be imposed. Some predictions were made where two parameters were varied simultaneously, but they are discussed separately later in this chapter.

It should be mentioned here that the magnitude of the cyclic variations (standard deviation of varying parameter) plays an important rôle in our consideration because the postulation of a constant mean value for each variable in the model can only be justified if we are certain that the variations are within prescribed limits. When these variations

are large (coefficient of variation exceeds 8-10%), the effect of these variations will then be important and should be considered in any evaluation of the results. Figure 5.26 demonstrates typical dynamic modelling prediction results of peak cylinder pressure and maximum rate of cylinder pressure rise for 100 consecutive cycles at Test 49 (speed = 2500 rpm, and load = 20.2 mkp). The dynamic injections were either sampled experimentally (in the case of Figure 5.26) or generated analytically (in the case of Figure 5.27) and fed as perturbing input data to the dynamic modelling prediction program.

The principal interest here is to find the functional dependences of the fuel injection characterizing parameters on the combustion characterizing parameters. To determine these dependences, $\hat{dP}$, $\theta(\hat{dP})$, $\hat{P}$ and $\hat{dm}_{fb}$ were obtained and plotted versus the dynamic injection, τ, or the quantity of fuel injected, m_f, depends on which one has been perturbed. Figure 5.28 is a typical demonstration of functional dependences of $\hat{dP}$, $\theta(\hat{dP})$, $\hat{P}$ and $\hat{dm}_{fb}$ on the dynamic injection at the Test 19 operating conditions. Graphs (a), (b), (c) and (d) in this figure display $\hat{dP}$, $\theta(\hat{dP})$, $\hat{P}$ and $\hat{dm}_{fb}$ versus τ or m_f (in the case of Figure 5.29), respectively.

The functional dependences of the dynamic injection, τ, and the quantity of injected fuel, m_f, on $\hat{P}$, $\hat{dP}$, $\theta(\hat{dP})$ and $\hat{dm}_{fb}$ are plotted non-dimensionally in most of the figures. In these graphs, all the parameters are divided by the mean value of the same variable, and thus comparison of the variation of different parameters with different dimensions can be made in a satisfactory manner.

5.3.1 Perturbing Input Data

At first, attempts were made to generate a function performing oscillating auto-correlations similar to those obtained from the time-

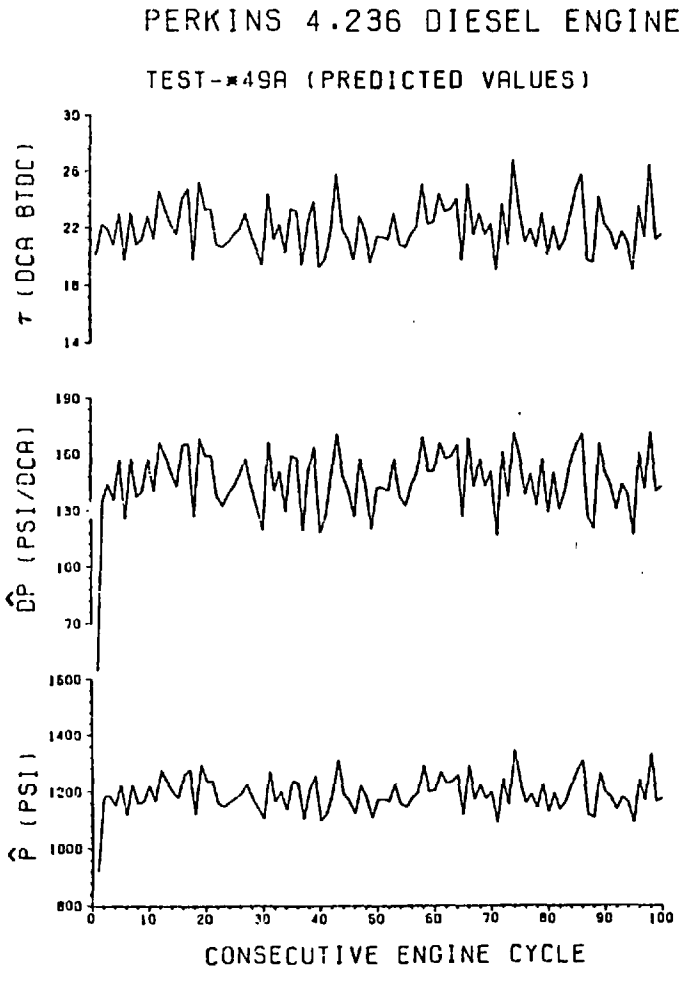


Figure 5.26: Dynamic modelling prediction results when generated random values of τ are used as a perturbing parameter (speed = 2500 rpm; load = 20.2 mkp)

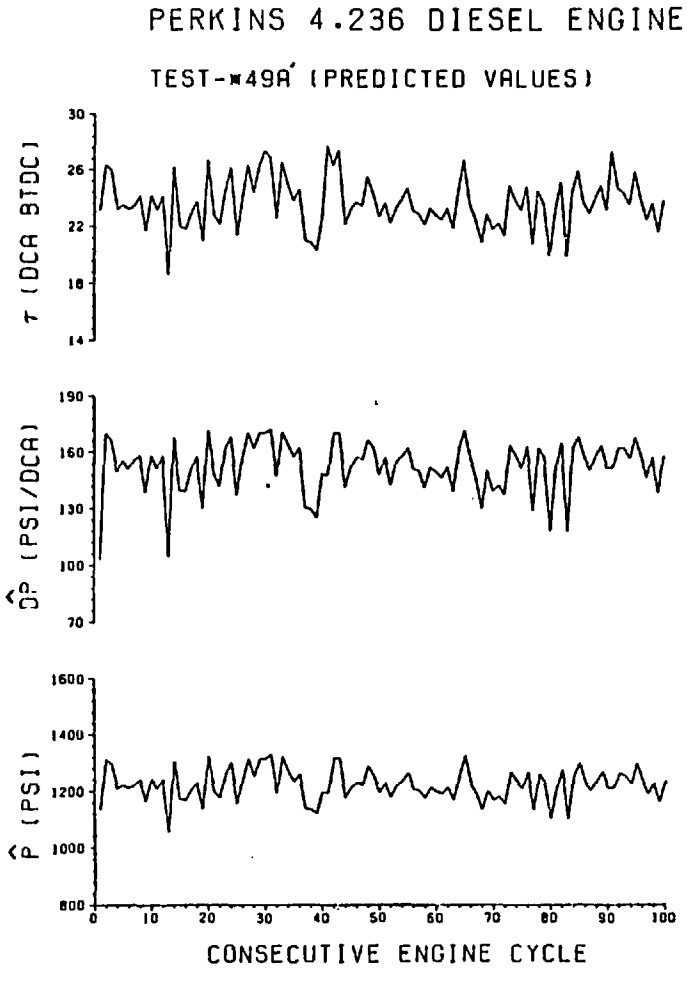


Figure 5.27: Dynamic modelling prediction results when experimental values of τ are used as a perturbing parameter (speed = 2500 rpm; load = 20.2 mkp)

series of certain engine data (Figure 5.7 shows typical oscillating auto-correlations obtained from time-series from different diesel engine parameters). The result could then have been used in dynamic modelling as the perturbing values. Many functions, including sinusoidal, exponential, pseudo random binary sequences, Bessel functions and various combinations of these, were accordingly applied.

As a result of this survey, some functions were found for representing the nearest mathematical models of empirical data obtained at an engine speed of 2000 rpm and an engine load of 5 mkp. The way these functions were obtained was tentative, and thus it was not possible to generate functions having more similar properties of the time-series without involving extended trial-and-error searching.

The more advanced method used by Box & Jenkins (1970) to generate a time-series using different stochastic models (auto-regressive model, moving average model, auto-regressive integrated moving average model) was not attempted for the same reason. Using the Box & Jenkins method, the whole process of finding the model coefficients has to be repeated at every engine operating condition. On the other hand, it was found that generating a relatively accurate time-series for using in dynamic modelling will not usually be required. With this in mind, it was decided to use an available standard subroutine for generating random values having specified normal distributions, mean value and standard deviations. Later, the experimental values recorded for each time-series could be used to check the probable deviations. Therefore, random values as perturbing input data were generated by the G05AEF subroutine (the NAG library subroutine (1977)) which produce pseudo random numbers with indicated distributions.

Although various potential distributions exist, in practice, a

relatively small number of these models have come to prominence. In the present work, only the normal distribution was considered and the reason underlying this assumption was firstly due to its desirable mathematical characteristics (a large body of knowledge exists about the normal distribution and also the central limit theorem* (Cramer (1946))), and secondly due to its satisfactory agreement with experimental reality.

The specified mean value and standard deviation of each variable was calculated by running the PERFU2 program. The results are shown in Table 5.8. The generated values of the result and the simulated values were thereafter fed to the dynamic model.

TABLE 5.8

Test	Speed (rpm)	Load (mkp)	τ (^{o}CA BTDC)	σ_{τ} (^{o}CA)	m_f (lb/cyc/cyl $\times 10^5$)	σ_{m_f} (lb)
13	998.0	6.15	9.6	0.6	3.27	0.30*
19	2508.0	6.38	18.1	2.1	4.13	0.55*
43	1004.0	20.20	13.1	0.8	7.93	0.60*
49	2508.0	20.70	21.8	1.75	8.92	0.80*

* These standard deviations are rough estimates of the quantity of injected fuel variations obtained by Pires (1973).

---

* This theorem shows that the sum of variables of any distribution whatsoever tends to be normally distributed if a sufficient number of them are added together.

5.3.2 Planning of Tests

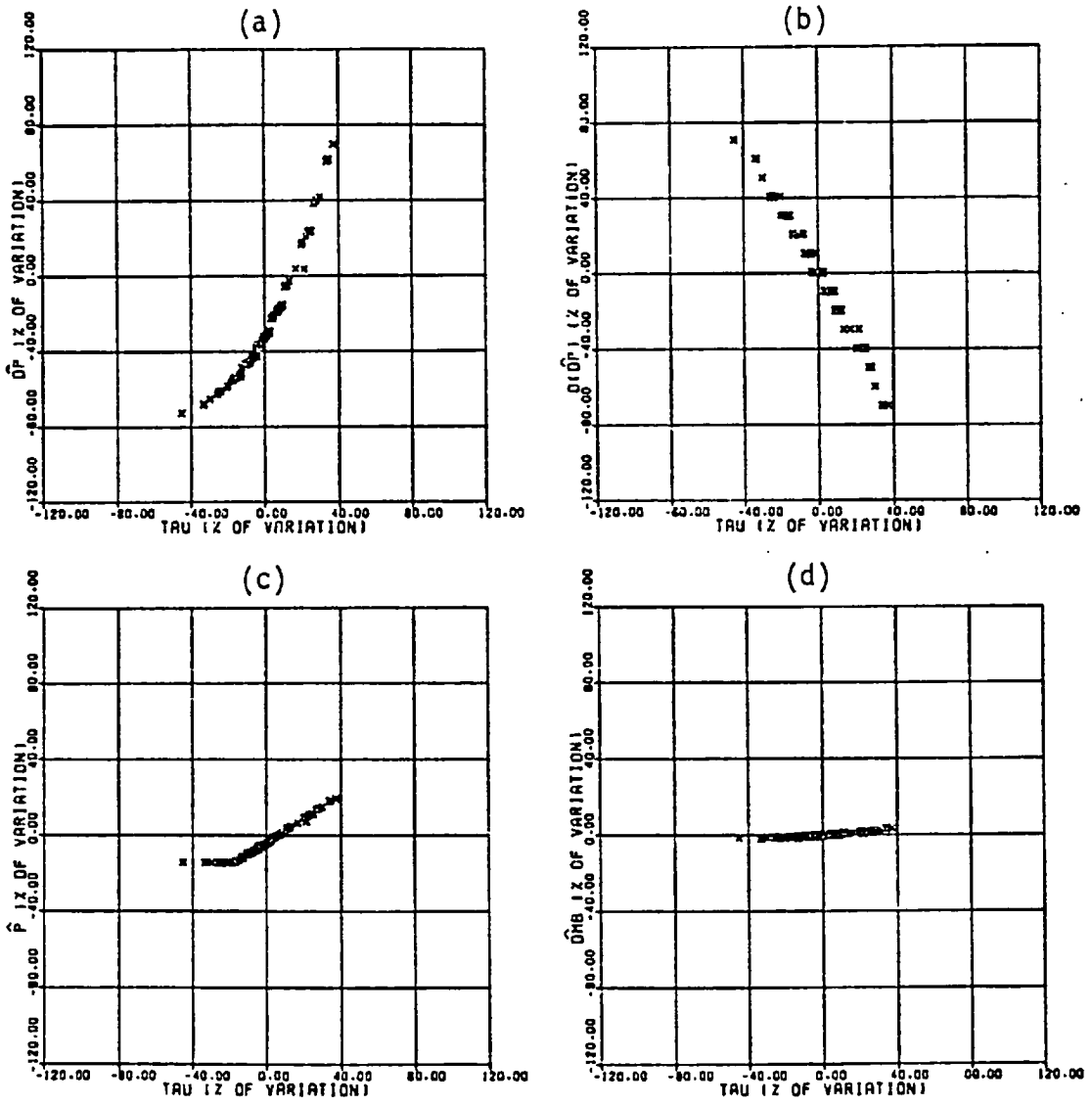
Limiting computational time to realistic proportions required careful planning of experiments. The solution chosen was to carry out the full prediction analysis and experimental program at four engine operating conditions: low load at low speed (Test 13); low load at high speed (Test 19); high load at low speed (Test 43); and high load at high speed (Test 49). The particular load/speed values were selected from initial laboratory experiments which indicated regions of higher than average cyclic variations. These load/speed combinations are fully specified in Table 5.8.

Analyses were carried out on this model using four different classifications of input data (physical data were assumed to be a combination of a static component (mean value) and a dynamic or fluctuating component), as follows:

(a) Random values generated for the starting angle of injection, τ, having a normal distribution, specified mean values and standard deviations corresponding to the measured values at each particular operating condition. Figure 5.28 shows the prediction values of $\hat{dP}$, $\theta(\hat{dP})$, $\hat{P}$ and $\hat{dm}_{fb}$ from the dynamic modelling program for Test 19 in which the generated random values were fed as dynamic injection perturbing values.

(b) Random values generated for the quantity of injected fuel, m_f, having specified normal distribution, mean values and standard deviations. The prediction values of the combustion characterizing parameters at the operating conditions of Test 19 are demonstrated in Figure 5.29.

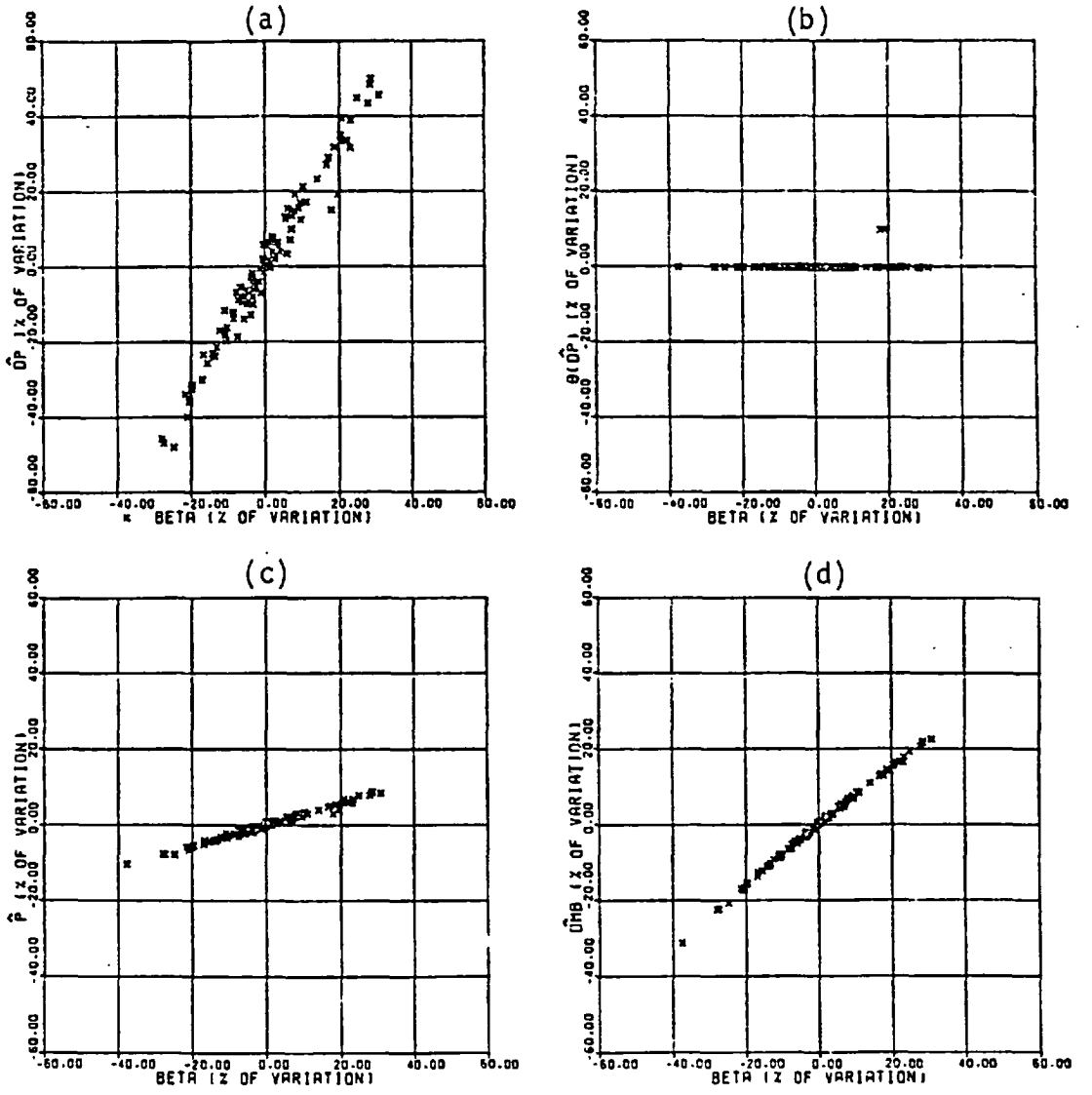
** PERKINS 4.236 DIESEL ENGINE
** TEST-19A (SPEED = 2500.0 RPM)
** (LOAD = 6.1 MKP)



** TAU - STARTING DEGREE OF INJECTION (DCA BTDC)
** GENERATED RANDOM DATA FOR TAU
** FROM G05AEF(18.1.2.1) NAG SUBROUTINE
** FIRST ARGUEMENT IS MEAN VALUE (DCA BTDC)
** SECOND ARGUEMENT IS STANDARD DEVIATION (DCA)

Figure 5.28: Dynamic modelling prediction results: Generated random data for starting angle of injection as a perturbing parameter

** PERKINS 4.236 DIESEL ENGINE
** TEST-19B (SPEED = 2500.0 RPM)
** (LOAD = 6.2 MKP)



** BETA - QUANTITY OF FUEL INJECTED (LB/CYC./CYL.)
** GENERATED RANDOM DATA FOR BETA
** FROM GO5AEF(4.13E-05,0.55E-05) NAG SUBROUTINE
** FIRST ARGUEMENT IS MEAN VALUE (DCA BTDC)
** SECOND ARGUEMENT IS STANDARD DEVIATION (DCA)

Figure 5.29: Dynamic modelling prediction results: Generated random values for quantity of fuel injected as a perturbing parameter

(c) Random values generated for the starting angle of injection and the quantity of fuel injected, both having specified normal distribution, mean values and standard deviations, and being uncorrelated. Figure 5.30 shows the values of $\hat{dP}$, $\theta(\hat{dP})$, $\hat{P}$ and $\hat{dm}_{fb}$ which are plotted against dynamic injection values when both τ and m_f are perturbed.

(d) Experimental data obtained for the starting angle of injection, τ. Figure 5.31 is a demonstration of the dynamic modelling prediction results when experimental data were sampled and fed to the prediction program as perturbing input data.

5.3.3 Discussion on the Predicted Results

The most important process affecting the cyclic variation in diesel engines is the phasing of the combustion due to the variation in ignition delay which was shown to be influenced by varying engine parameters, especially the dynamic injection. This phasing of the combustion consequently affects the rate of combustion to a greater or lesser extent, depending on the position of the top dead centre. As expected, an early start of injection produces a higher maximum cylinder pressure, a higher maximum rate of cylinder pressure rise, a higher maximum rate of fuel burning, and an early maximum rate of cylinder pressure rise (Figure 5.26). In general, an early start of injection would increase both the maximum pressure and thermal efficiency, since the combustion process approaches a constant volume process, the constant lines being steeper on the TS diagram.

A possible confusion in analysing the plots obtained for the

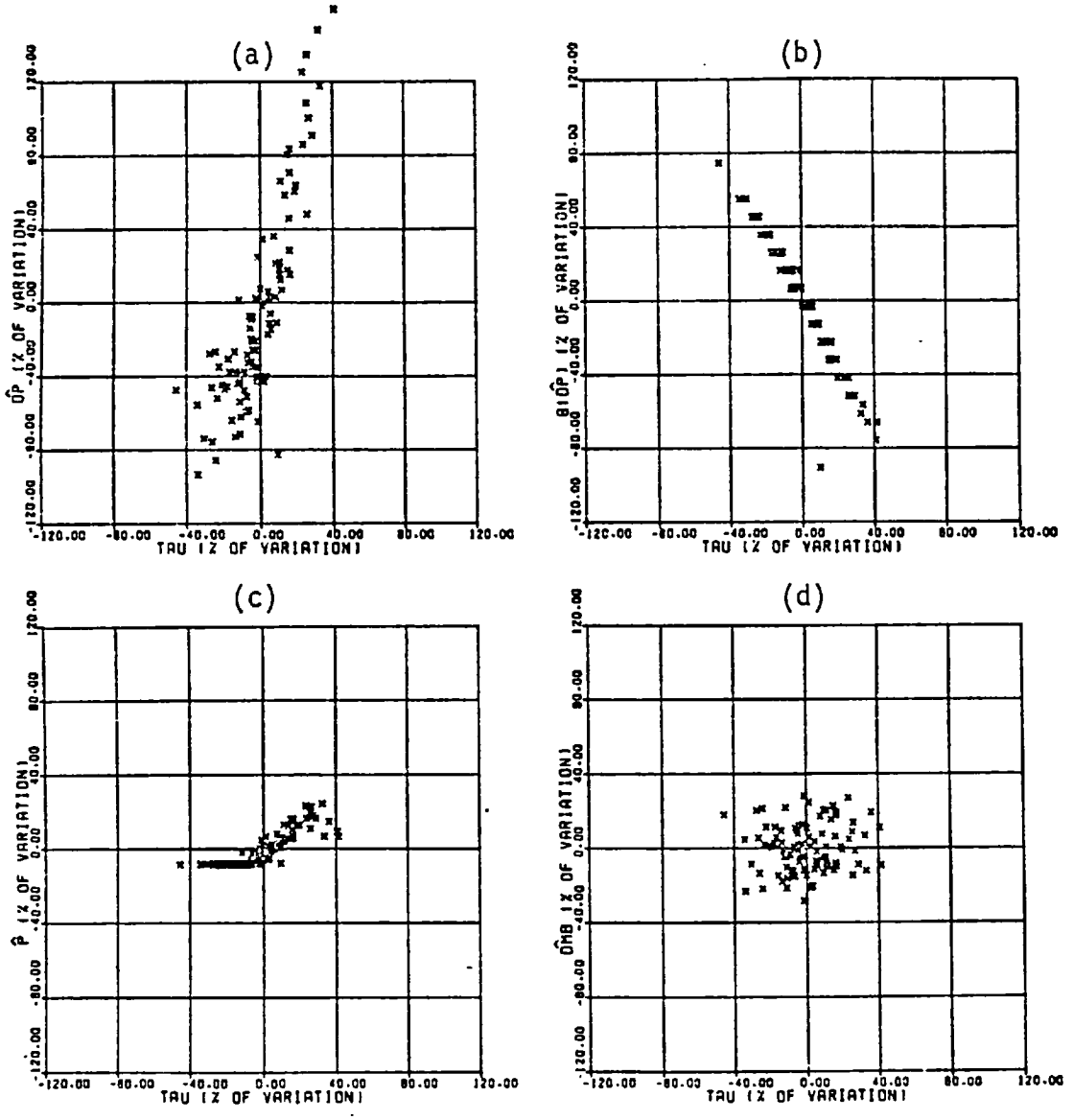


Figure 5.30: Dynamic modelling prediction results: Starting angle of injection and quantity of fuel injected perturbing simultaneously by generated random values

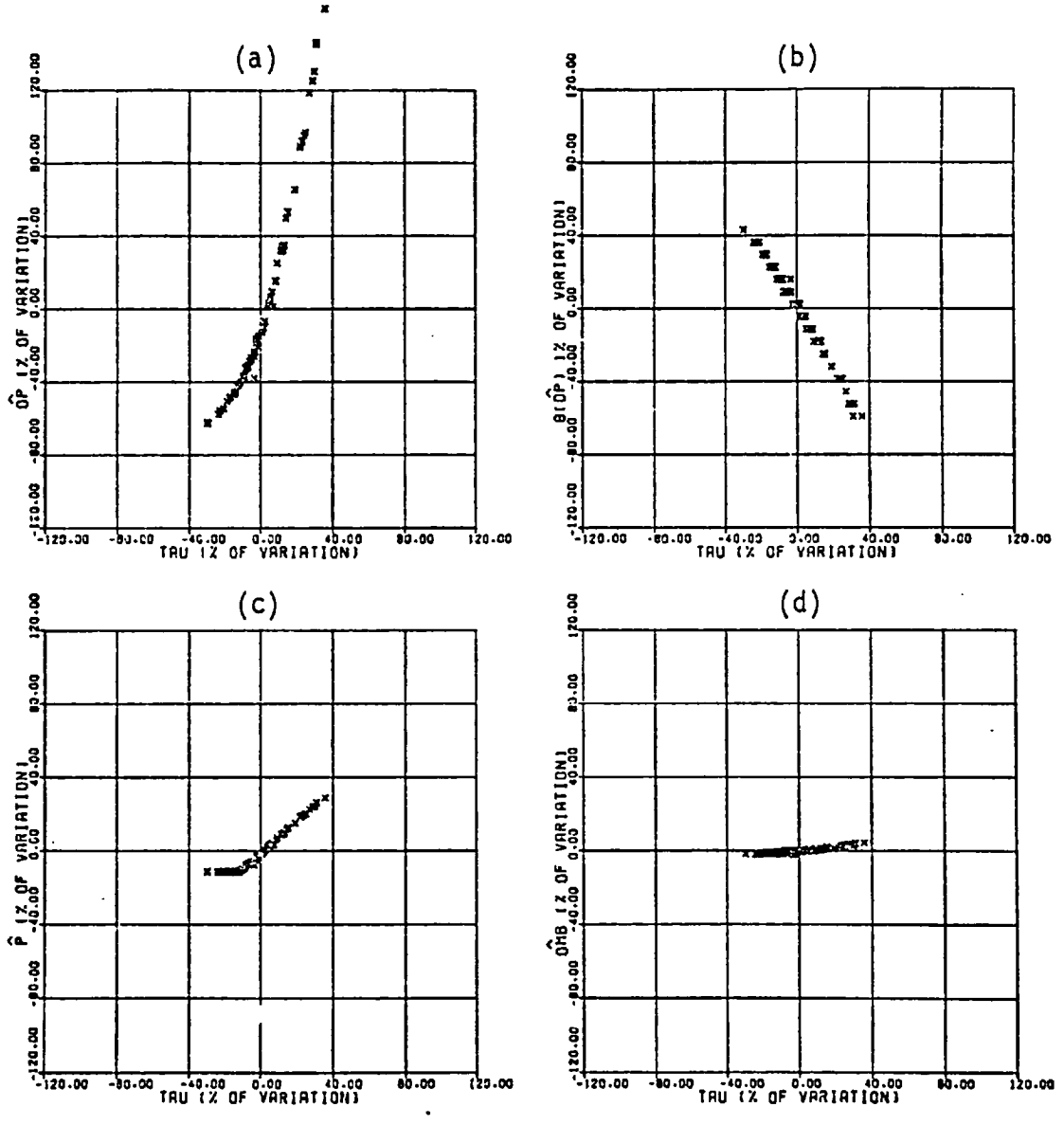


Figure 5.31: Dynamic modelling prediction results - experimental values for starting angle of injection used as perturbing parameters at given operating conditions

high speed-low load combination should be clarified. Figures 5.28, 5.30 and 5.31 show a region of constant peak cylinder pressure. This occurs when the peak cylinder pressure due to combustion is less than that due to compression and the computer program correctly indicates the compression pressure as the peak pressure for that cycle.

A further discrepancy arising from the computational procedure results in discontinuities in the plots of $d\hat{P}$ and $\hat{dm}_{fb}$. This results from the particular sampling interval used in the prediction program, this normally being 1^{0} of engine crank angle. In Figure 5.32(a), (b) and (c), the interval was changed to 0.2^{0} CA to examine the possible advantages of smaller intervals with regard to the resultant overall accuracy and smoothness of the data. The effect is clearly shown in Figures 5.32(b) and 5.32(d).

One or more odd points appearing in these graphs, which do not follow the general trend, pertain to calculation of the first few cycles. These singularities are probably caused by inaccurate definition of the initial condition prescribed for the first cycle.

By increasing the quantity of injected fuel, the maximum rate of burning increases, and consequently $d\hat{P}$ and $\hat{P}$ become greater. However, the variation in location of the maximum rate of cylinder pressure, $\theta(d\hat{P})$, appears to have little significance. In Figure 5.33(b), the chosen interval of 1^{0} CA is too great to show up the trivial changes of $\theta(d\hat{P})$ due to changes in ignition delay.

To further clarify the results, $d\hat{P}$ and $\hat{P}$ were plotted on the same plane versus τ and m_f for different operating conditions. This enables us to study the variation of these parameters with changes of speed and load (Figures 5.34 to 5.37).

On increasing the load, $d\hat{P}$ becomes greater, which is the result

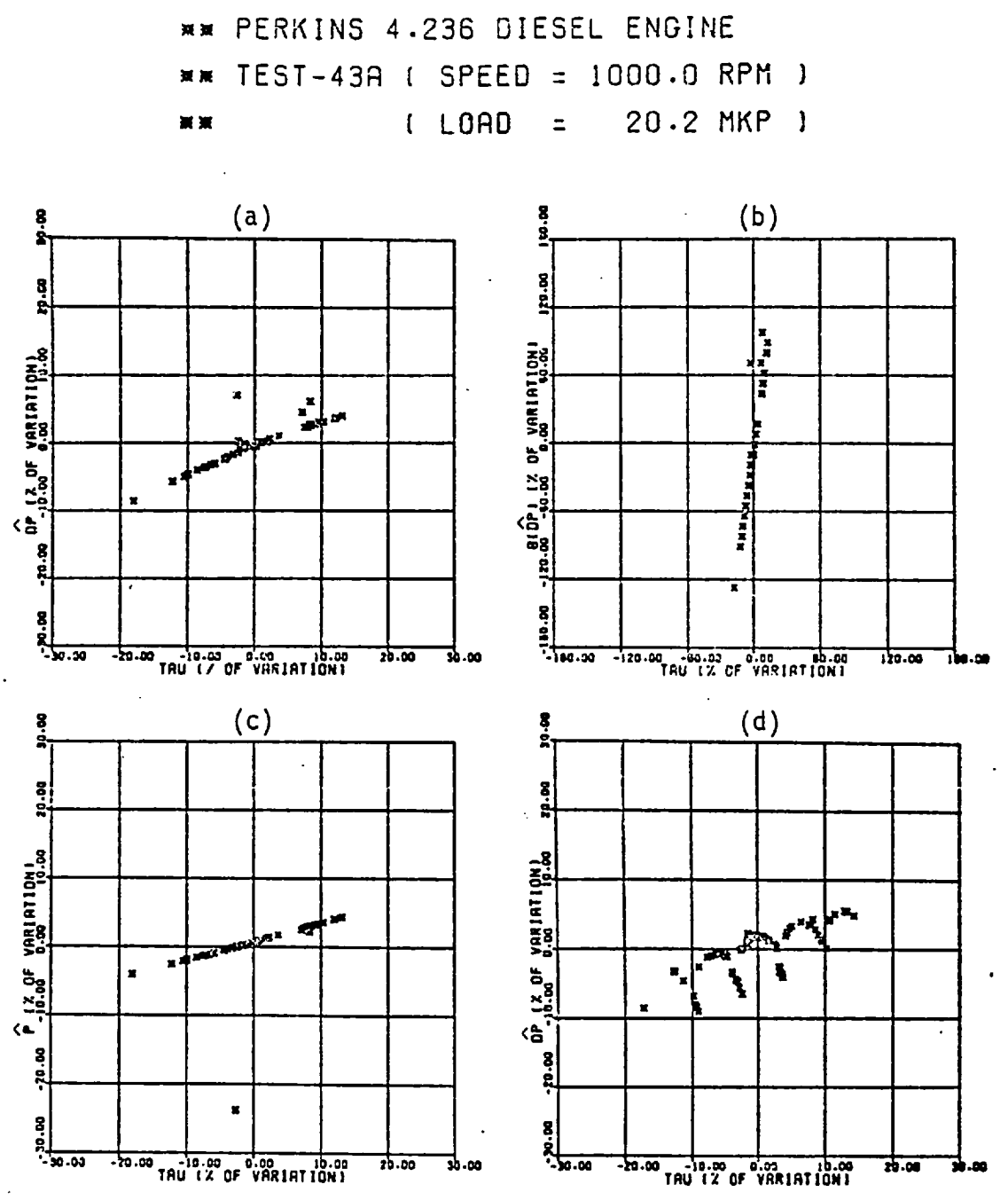
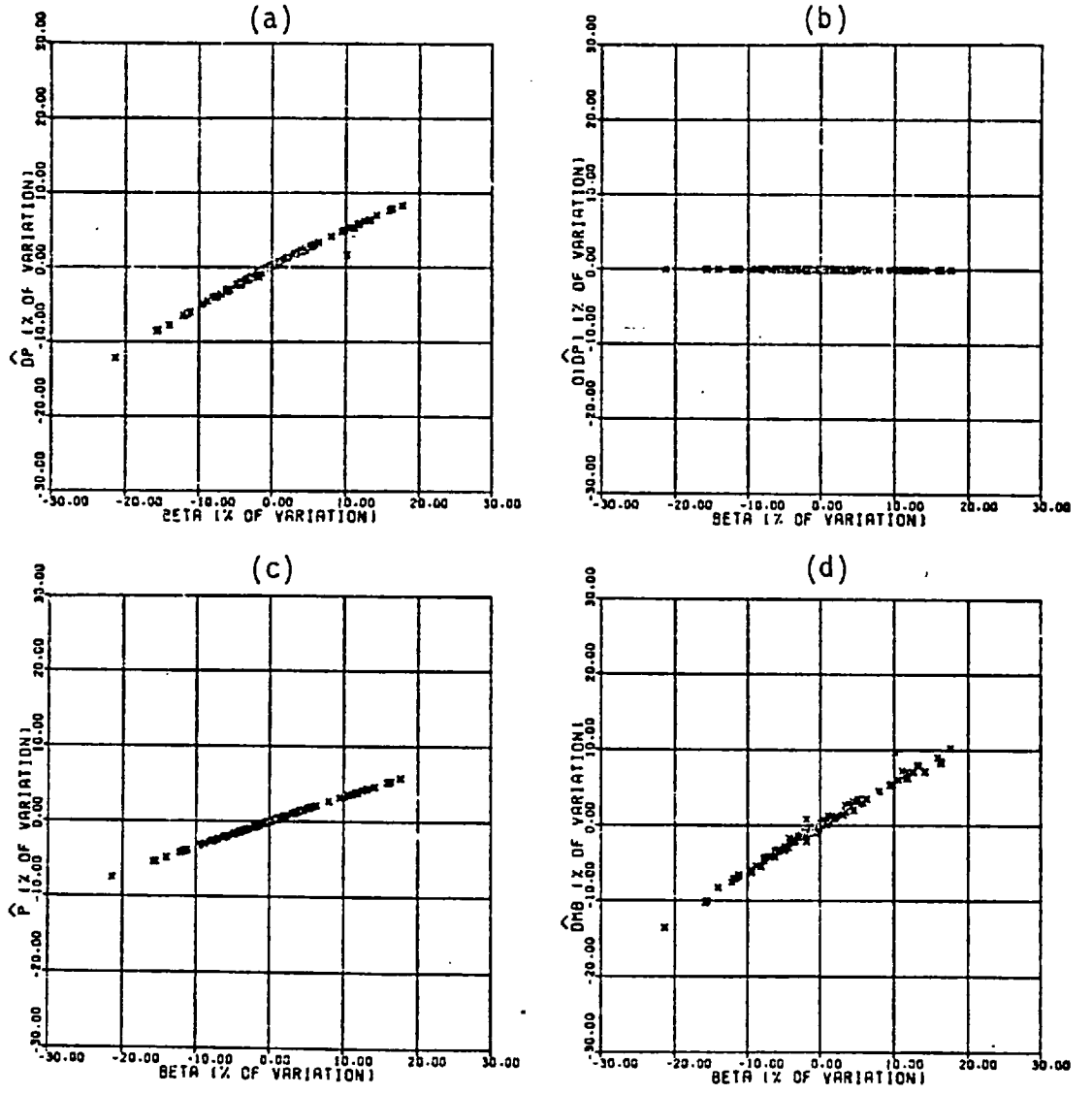


Figure 5.32: Significance of reduced interval in dynamic modelling prediction results when perturbed values were small

** PERKINS 4.236 DIESEL ENGINE
** TEST-436 (SPEED = 1000.0 RPM)
** (LOAD = 20.2 MKP)



** BETA - QUANTITY OF FUEL INJECTED (LB/CYC./CYL.)
** GENERATED RANDOM DATA FOR BETA
** FROM G05AEF(7.93E-05,0.60E-05) NAG SUBROUTINE
** FIRST ARGUEMENT IS MEAN VALUE (DCA BTDC)
** SECOND ARGUEMENT IS STANDARD DEVIATION (DCA)

Figure 5.33: Dynamic modelling prediction results: Generated random values for quantity of fuel injected as a perturbed parameter

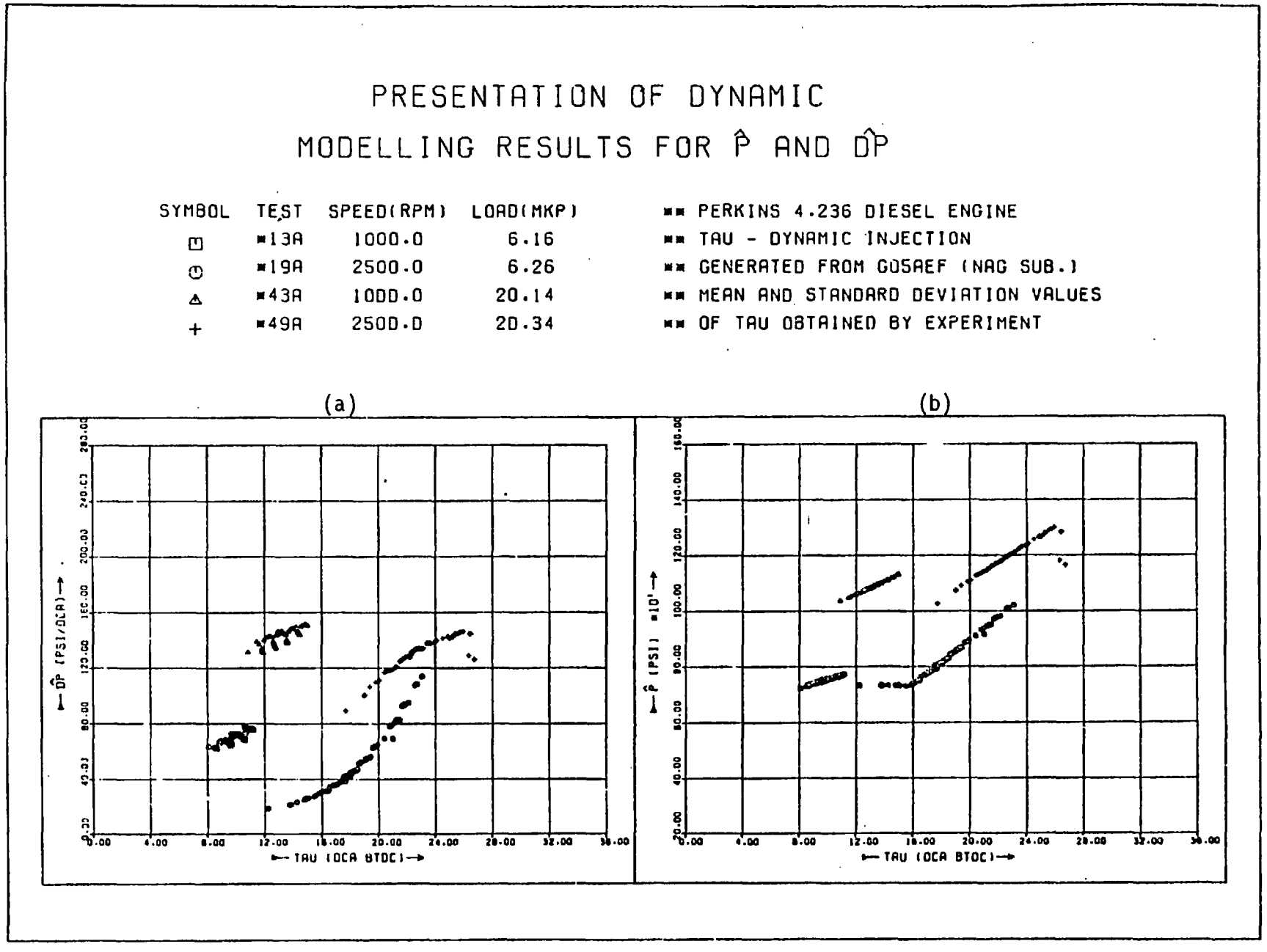


Figure 5.34: Generated random values for starting angle of injection (τ) as a perturbing parameter

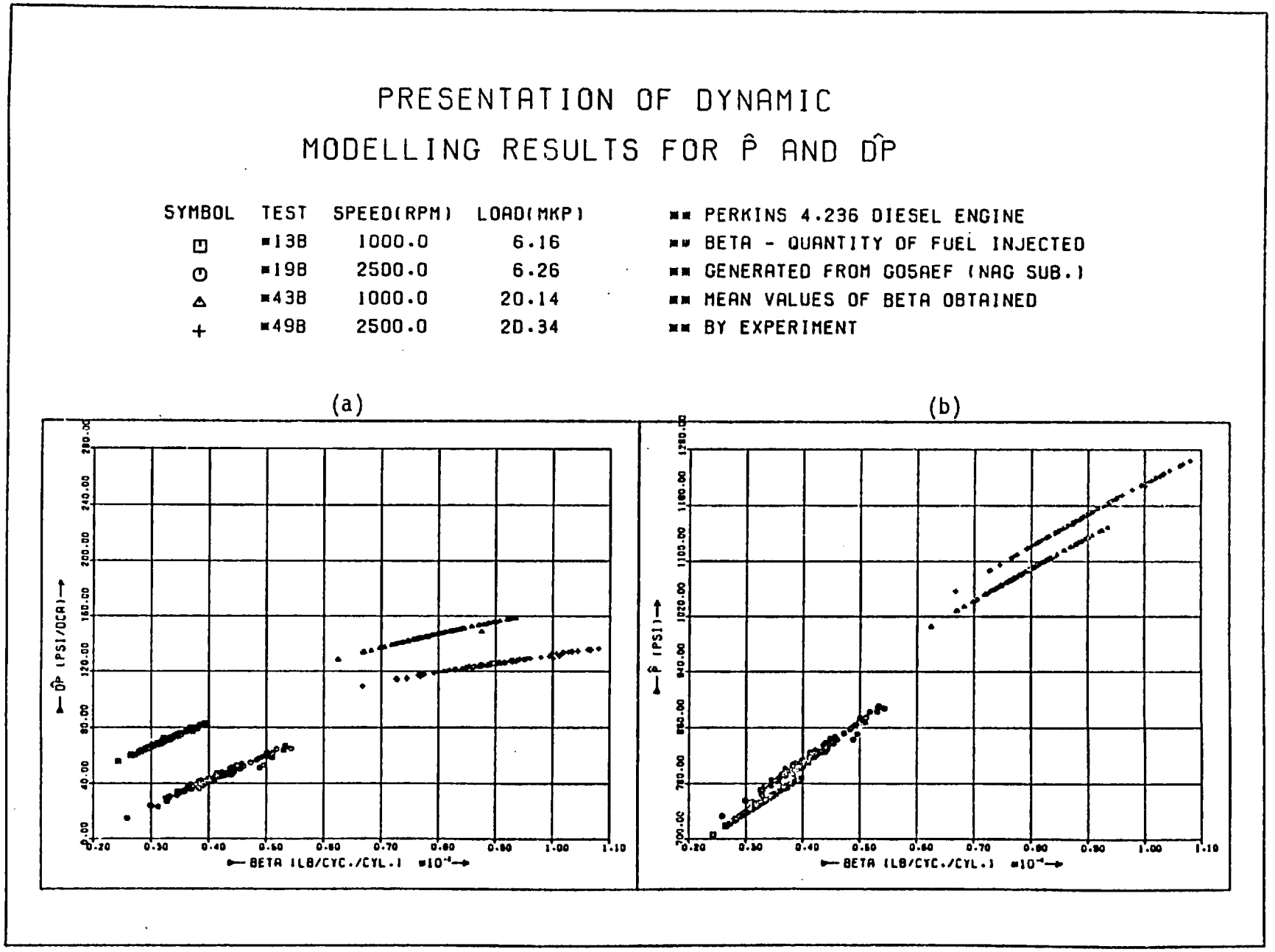


Figure 5.35: Generated random data for quantity of fuel injected (m_f) as a perturbing parameter

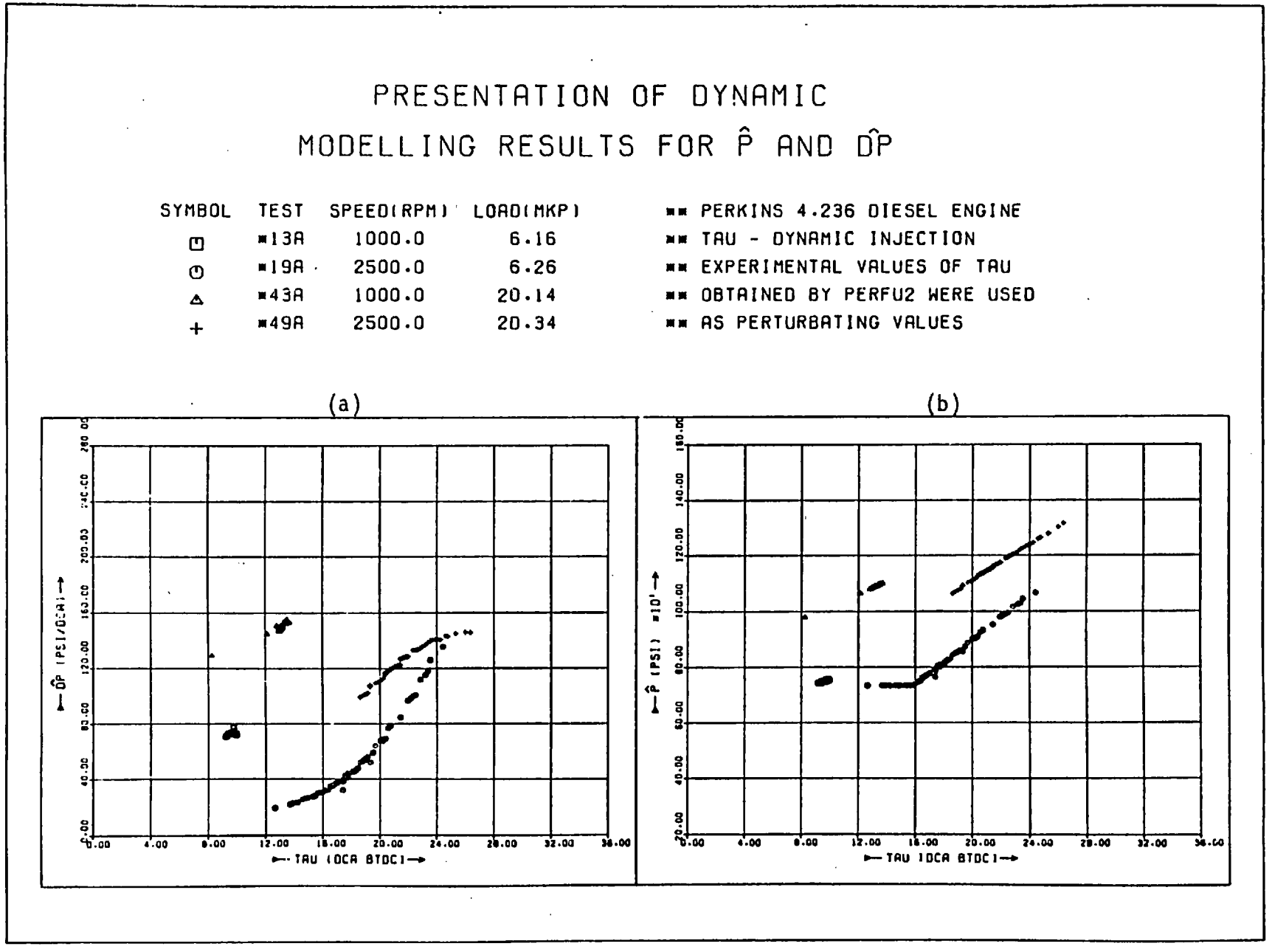


Figure 5.36: Experimental data for starting angle of injection (τ) as a perturbing parameter

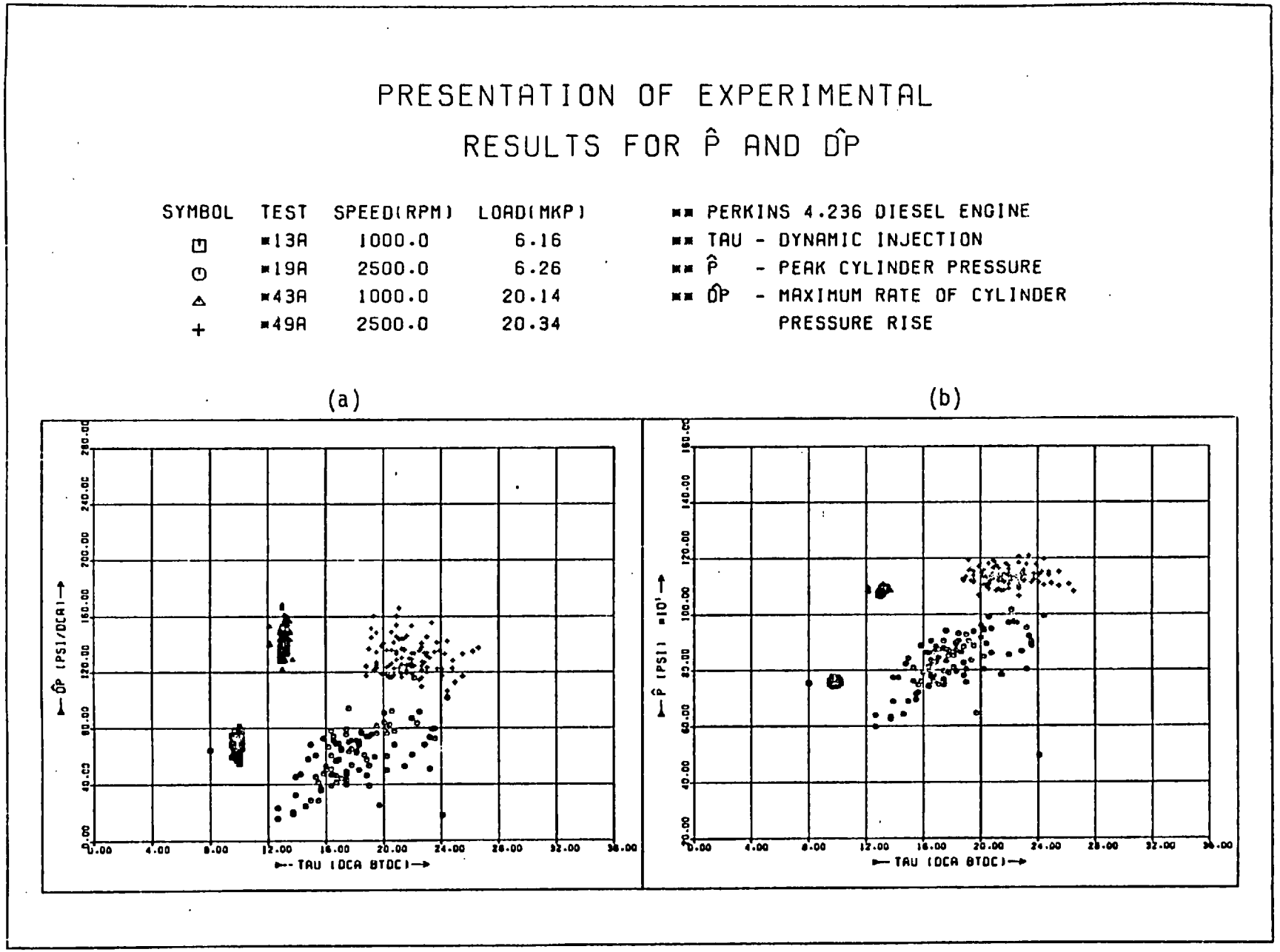


Figure 5.37: Experimental data for given operating conditions

of an earlier start of injection (the characteristics of the distributor type injection pump show an advance with increase in torque) and higher quantity of fuel injected. As the maximum rate of cylinder pressure rise depends on the maximum rate of heat release, and this also depends itself on the amount of fuel injected during the delay period, and therefore all the changes of $d\hat{P}$ due to the operating parameters can be viewed in terms of the injection process and the effect of different parameters on ignition delay. Furthermore, by increasing the speed, although variation of $d\hat{P}$ does not follow a specific trend, except for low speed conditions where speed increase results in a $d\hat{P}$ decrease since the ignition delay also decreases (Figure 5.34(a)). This behaviour is due to:

(a) The wall temperature becoming higher;

(b) The injection pressure becoming greater, consequently giving better atomization;

(c) Turbulence becoming greater.

The determination of the functional dependence between the input and output variables resulting from the dynamic modelling is essential to the interpretation of experimental results. The following explanatory examples form the basis of such an analysis:

i) Consider the conditions in which different values of independent (input) and dependent (output) variables form a straight line on the input-output plane (Figure 5.38(a)). This indicates that a linear dependence should exist between the two variables. If the results presented in a non-dimensional form are described by a straight line with a slope of 45^{o}, then the independent and dependent variables can be

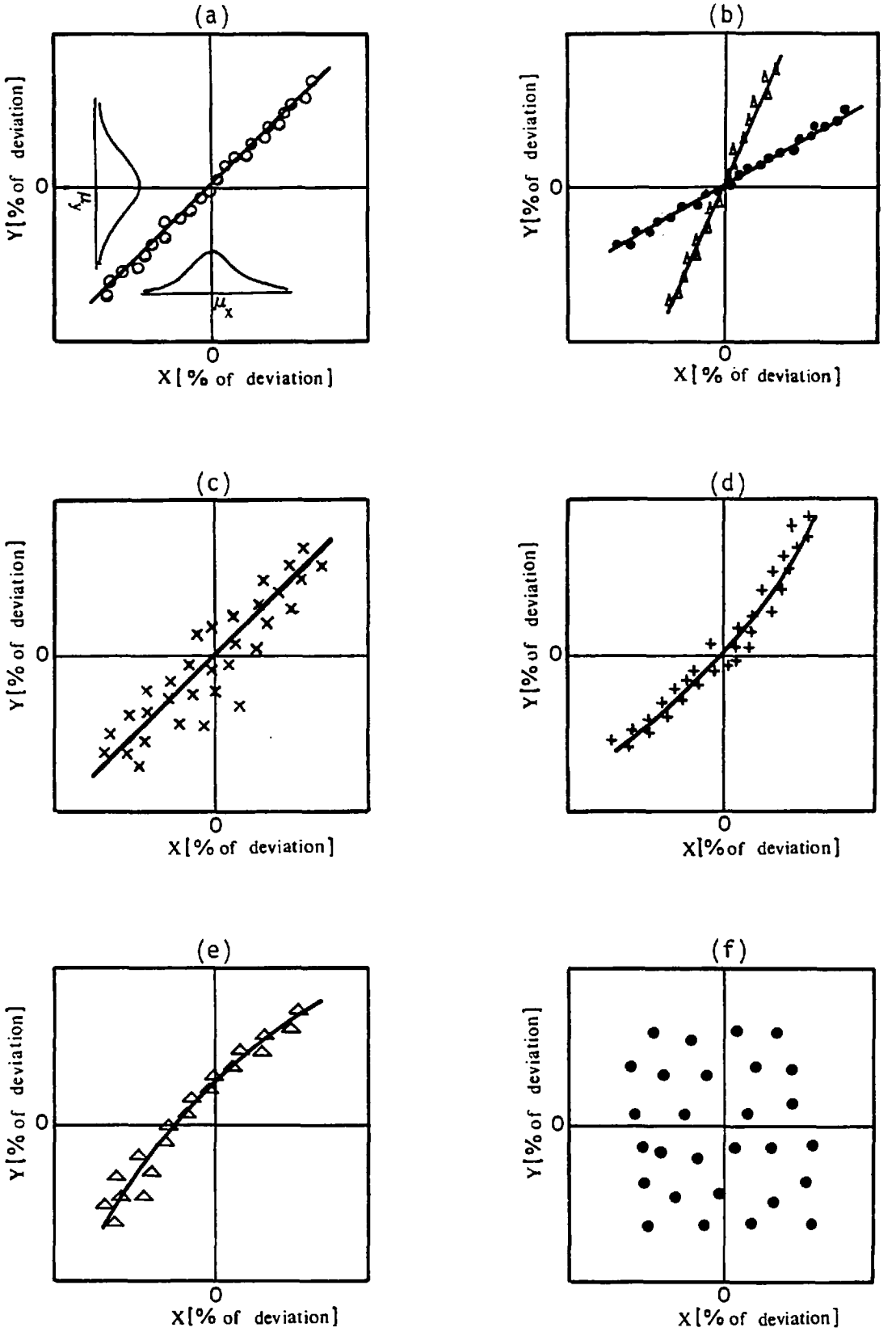


Figure 5.38: Different functional dependences for X and Y (scale of axes are in percentages of the deviations from their mean values):

X = independent variable

Y = dependent variable

characterized by an identical distribution function. In general, it can be noted that if the dependent variable is described by a normal distribution with a non-dimensional standard deviation, σ_1, then the independent variable can be similarly described by a normal distribution having a different non-dimensional standard deviation, σ_2. If the line of functional dependence obtained produces a slope of less than 45^0 with the dependent variable axis, then $\sigma_2 < \sigma_1$, or otherwise, if this slope is greater than 45^0, we have $\sigma_2 > \sigma_1$ (Figure 5.38(b)).

On the basis of this analysis, if a functional dependence with a slope of greater than 45^0 is obtained between the combustion characterizing parameters ($\hat{P}$, $\hat{dP}$, $\theta(\hat{dP})$, $\hat{dm}_{fb}$) and fuel injection system parameters (τ or m_f), then it can be seen that the combustion development has a positive influence on the cyclic cylinder pressure fluctuation. Similarly, a functional dependence with a slope of less than 45^0 reveals that the dependent variable is not influenced significantly by variation of the independent variable.

Figure 5.38(b) demonstrates the dependence of $\theta(\hat{dP})$ versus τ in which a slope of about 60^0 with the independent variable axis, indicating that τ has an appreciable influence on the variation of $\theta(\hat{dP})$.

ii) Assume that the values of dependent and independent variables are scattered randomly around a straight line on the input-output plane (Figure 5.28(c)). Statistically speaking, this behaviour implies that a linear dependence should exist between the two variables (apart from the cases where the line of functional dependence produces a slope of 0^0 or 90^0 with the dependent variable axis). However, the presence of scatter in a dynamic modelling analysis implies a more important phenomenon, that is the effect of one cycle on the next cycle. Generally, the scatter is

produced when, for a fixed value of the independent variable, different values for the dependent variable is obtained. This can only be interpreted as the result of different initial conditions reflecting the relation between the previous cycle on the current cycle. The extent of dispersion obtained is therefore an indication of the influence of one cycle (the initial conditions) on the following cycle.

The dynamic modelling results obtained for the variables $\hat{dP}$, $\hat{P}$ and $\hat{dm}_{fb}$ reveals that the degree of scatter increases with increasing cyclic variation and, as previously discussed in Section 5.2.2.3, this normally demonstrates the effect of residual gases on the performance of the subsequent cycles. Since normally a small scatter is produced, it is therefore reasonable to assume that this influence is relatively limited (Figures 5.29 and 5.33).

iii) Consider the conditions in which the functional dependence produced in the input-output plane is not of a linear nature (Figure 5.38(d)). In this case, if the independent variable is described by a normal distribution, then the dependent variable manifests a definite skewness from the normal distribution. As shown in Figure 5.39, an upward curvature implies a positive skewness, while a downward curvature is described by negative skewness. Figure 5.34(a) shows the variation of $\hat{dP}$ versus τ for various engine operating conditions. It can be seen that discrete in-curved and out-curved lines with varying inclinations are produced for different loading. Statistically, positive curvature implies positive skewness, while a negative curvature produces a negative skewness for the dependent variable. As demonstrated at low load, a positive skewness in τ causes a negative skewness in $\hat{dP}$, while a negative skewness in τ at high load creates a positive skewness in $\hat{dP}$. The absolute

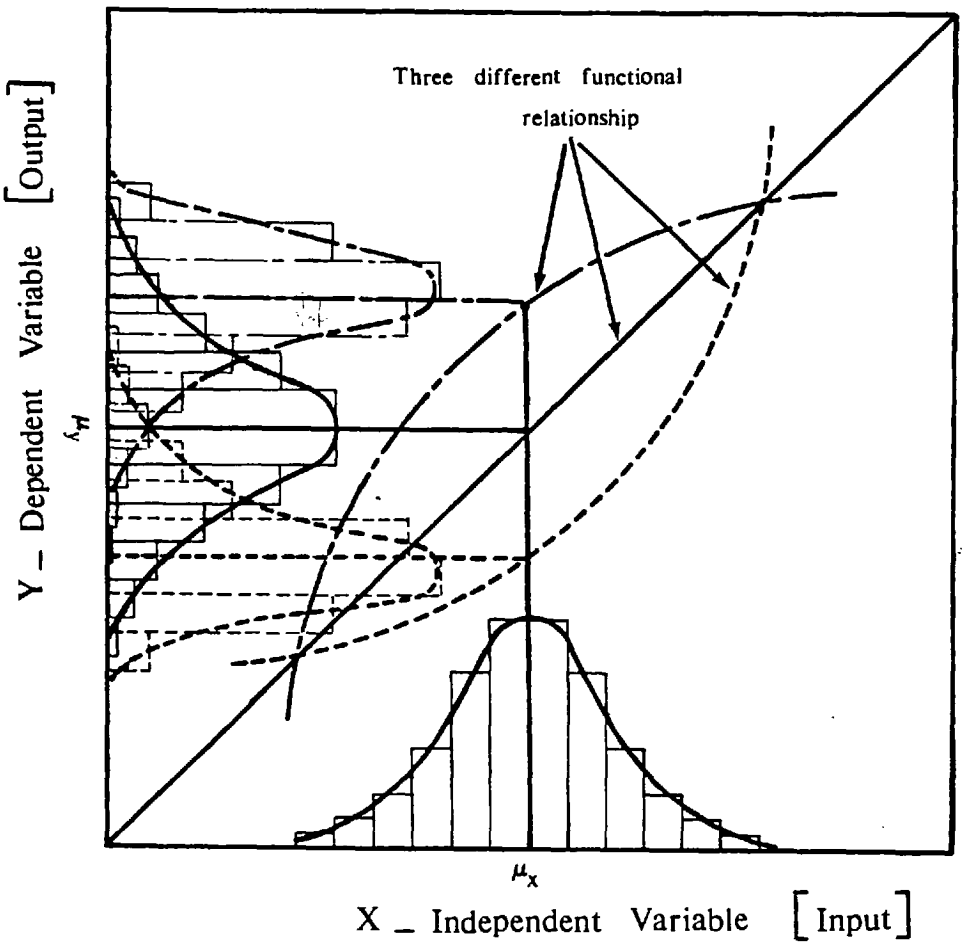


Figure 5.39: Effect of different curvature of functional dependences on the output histograms

magnitude of this skewness, in general, can be considered as an index of the symmetry of histograms which reflects the deviation from normality of the variables analysed. As indicated by Bendat & Piersol (1971), if the histograms of input and output of a system are normally distributed, the system can then be considered as linear.

iv) Consider the case where the functional dependence between the

dependent and independent variables does not pass through the origin of the coordinates, as shown in Figure 5.38(e). The distance from the origin then reveals the effect of cyclic variation on the mean value of the dependent variable. This is so because the mean value of the independent variable does not coincide with the mean of the independent variable, causing a definite intercept with the Y-axis.

The effect of cyclic variation on the maximum rate of cylinder pressure rise is shown in Figure 5.28(a). As demonstrated, the functional dependence produced does not pass through the origin and, therefore, it can be concluded that the mean values of these variables do not coincide. On the basis of this observation, the preference of dynamic modelling with reference to the averaging technique is clear. This aspect of functional dependence will be further discussed in the following section.

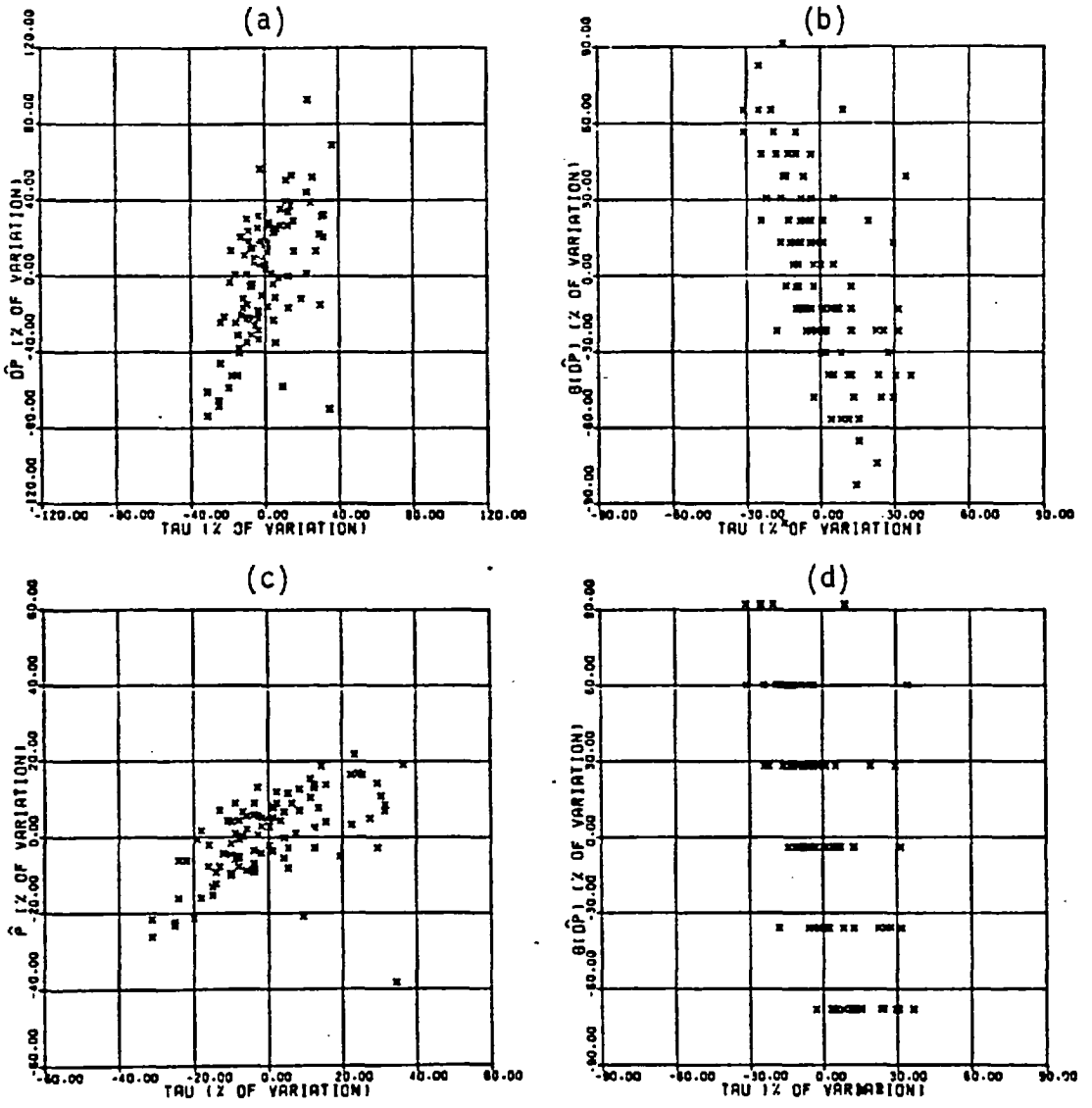
v) Finally, if the data are scattered on the input-output plane (Figure 5.38(f)) and a functional dependence cannot be defined, then it is clear that no correlation should exist between the pair of variables analysed. Figure 5.30(d) is an example, showing that no correlation exists between the starting angle of injection and the maximum rate of fuel burning at given operating conditions.

5.3.3 Analyses and Comparison of Predicted and Experimental Results

Figures 5.37 and 5.40 show the experimental measurements. If these values are compared with the computer-predicted results, some obvious discrepancies will be detected.

Regression analysis was considered to be the best method of

** PERKINS 4.236 DIESEL ENGINE
** TEST-190 (SPEED = 2500.0 RPM)
** (LOAD = 6.2 MKP)



** EXPERIMENTAL RESULTS FOR TAU, $\hat{P}$, $\hat{dP}$, $\theta(\hat{dP})$
** RESULTS OBTAINED BY PERFU2 PROGRAM
** TAU - STARTING DEGREE OF INJECTION (DCA BTDC)
** TWO PLOTS OF $\theta(\hat{dP})$ VERSUS TAU RELATED TO
** DIFFERENT RATE OF SAMPLING

Figure 5.40: Experimental data presented graphically as:

(a) $F(\hat{dP}, \tau)$

(b) $F(\theta(\hat{dP}), \tau)$

(c) $F(\hat{P}, \tau)$

(d) $F(\theta(\hat{dP}), \tau)$

carrying out a detailed comparison between the predicted and experimental values. In fact, the regression analysis* was essential, since the scatter in the experimental values does not permit a meaningful direct comparison with the computed predictions. In order to simplify this analysis, linear regression was used. However, in certain conditions, when the linear regression method did not yield a satisfactory description of the data, a non-linear regression had to be employed.

For linear regression analysis of the data, the coefficients of regression, standard error of these coefficients, correlation coefficients and population standard deviations of all the predicted and experimental data were calculated. The outputs of the regression analysis for one of the test conditions (Test 19) are given in Appendix C2 and also the results shown graphically in Figure 5.41 in which the confidence intervals of every regression line are displayed.

Examining the graphs in Figure 5.41, the width of confidence intervals of the experimental data are seen to be generally wider than those of the predicted data. It is clearly seen that the dispersion of the experimental data is larger than the predicted values. However, by varying the two parameters τ and m_f simultaneously, a large dispersion in the predicted values is obtained which is generally closer to the experimental results (Figure 5.30). A higher dispersion, however, does not automatically mean a better result if the other statistical parameters do not coincide with those of the experimental results (the parameters which are considered to be important in defining the system are the mean value, coefficient of variation, histogram for every variable, and correlation coefficient between input and output).

---

* For details of the regression analysis, see Appendix C2.

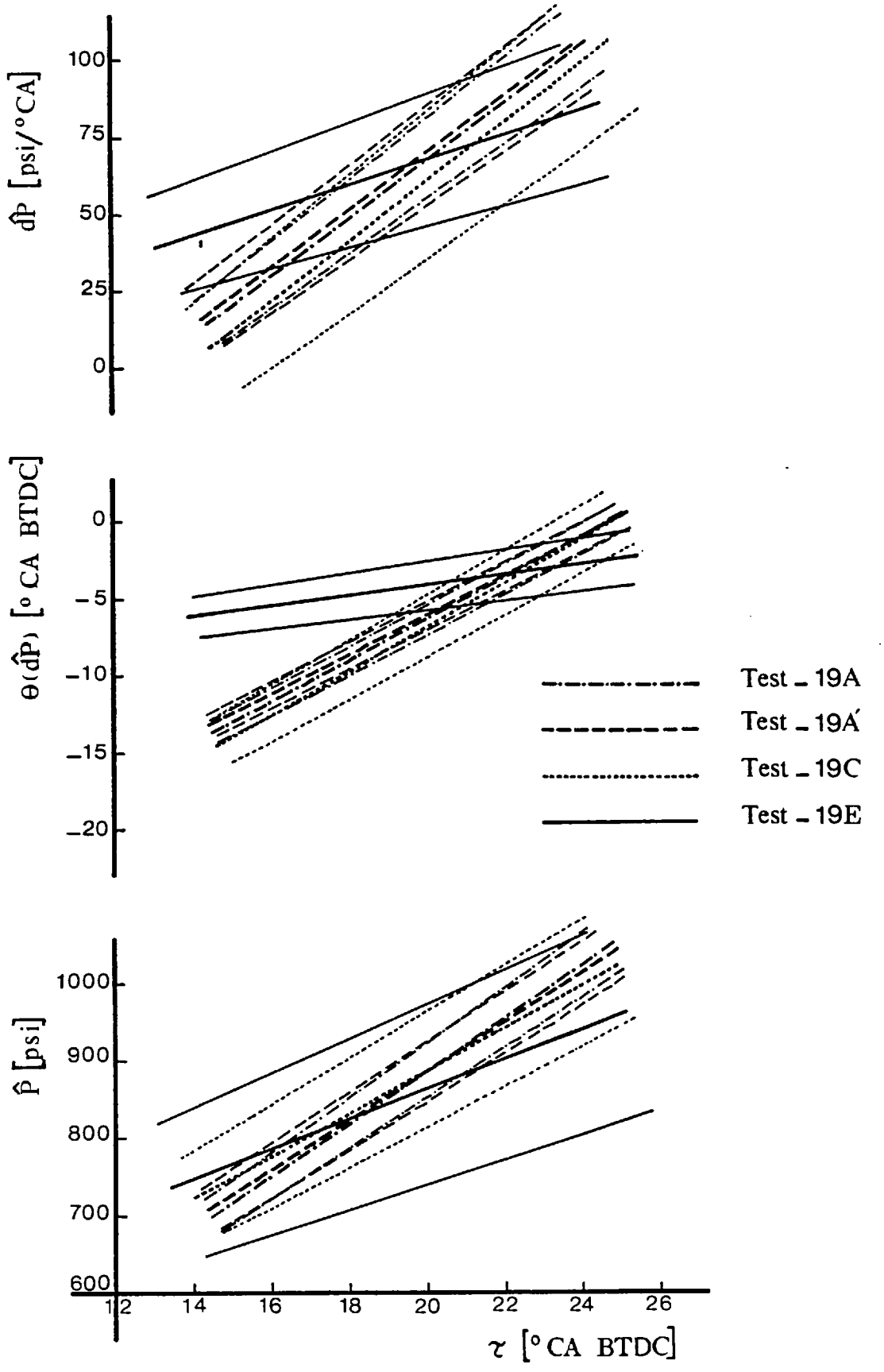


Figure 5.41: Linear regression for $\hat{dP}$, $\theta(\hat{dP})$ and $\hat{P}$ against τ (speed = 2500 rpm; load = 6.38 mkp):

Test 19A = τ perturbed with generated random values
Test 19A'= τ perturbed with experimental data
Test 19C = τ and m_f perturbed simultaneously with generated random values
Test 19E = experimental data

When linear regression is employed for two variables, the correlation coefficient between them, CC (i.e. cross-correlation between the starting angle of injection, τ, and the maximum rate of cylinder pressure rise, $\hat{dP}$), as presented in Table 5.9, can be interpreted in three ways. Firstly, as a measure of the amount of improvement (in terms of reducing the total error) due to the regression line; secondly, as a measure of the closeness of fit to the regression line to the points; and thirdly, as a measure of the degree of linearity of the scatter. As an example, in the case of Test 19E when $CC(\tau,\hat{dP}) = 0.56$, it can be argued that this parameter represents either (i) the true degree of linear dependence between τ and $\hat{dP}$, or (ii) a weaker closeness of fit compared to the predicted value $CC(\tau,\hat{dP}) = 0.98$, or (iii) that only 30% of variability of the observation data have been explained by the regression line (since $CC^2 \simeq 0.3$).

The statistical properties of $\hat{dP}$, $\theta(\hat{dP})$ and $\hat{P}$ of Test 19 which have been calculated with the aid of the dynamic modelling program are presented in Table 5.10.

Additional significant variables, such as $\hat{dP}$, $\theta(\hat{dP})$ and $\hat{P}$, have been evaluated for cases where there was no variation in the injection system characteristics. Comparing these two sets of data, it can be seen that when there is no such variation, $\hat{dP} = 44.3$ (psi/^{o}CA), but with 12% coefficient of variation for τ, the mean value for $\hat{dP}$ becomes 50.71 (psi/^{o}CA) (a 14.4% increase in the mean value for $\hat{dP}$, a 5.67% decrease in the mean value for $\theta(\hat{dP})$, and a 2.23% increase in the mean value for $\hat{P}$).

The physical interpretation of the above can be briefly summarized as follows: At the chosen engine operating conditions, the considerable variations in the injection system characteristics have an influence on the cyclic variation of the combustion process. The results

TABLE 5.9

Classified Correlation Coefficients for Different Tests

Description of Tests	Test Number	Speed (rpm)	Load (mkp)	Number of Cycles Sampled	$CC(\tau, d\hat{P})$	$CC(\tau, \theta(d\hat{P}))$	$CC(\tau, \hat{P})$	$CC(\tau, d\hat{m}_{fb})$
Experimental Results	13E	998	6.15	1000 100	0.08 0.097	- 0.33 - 0.19	0.28 0.097	- -
	19E	2508	6.38	1000 100	0.65 0.56	- 0.65 - 0.60	0.66 0.54	- -
	43E	1004	20.2	1000 100	0.015 0.18	- 0.04 - 0.11	0.01 0.20	- -
	49E	2508	20.7	1000 100	- 0.15 - 0.12	- 0.39 - 0.49	- 0.01 - 0.03	- -
Dynamic Modelling Results (Experimental Values for τ)	13A	1000	6.0	100	0.55	- 0.41	0.99	0.87
	19A	2500	6.0	100	0.95	- 0.99	- 0.97	0.94
	43A	1000	20.0	100	0.84	- 0.89	0.99	0.03
	49A	2500	20.0	100	0.97	- 0.99	0.99	0.08
Dynamic Modelling Results (Generated Random Values for τ)	13A	1000	6.0	100	0.83	- 0.96	0.92	0.22
	19A	2500	6.0	100	0.95	- 0.96	0.97	0.96
	43A	1000	20.0	100	0.72	- 0.84	0.94	0.20
	49A	2500	20.0	100	0.90	- 0.97	0.99	0.44

TABLE 5.10

All Tabulated Results Related to Test 19

(Speed = 2500 rpm and Load = 6.38 mkp)

Variables / Tests	τ (^{o}CA BTDC)	$\hat{dP}$ (psi/^{o}CA)	$\theta(\hat{dP})$ (^{o}CA ATDC)	$\hat{P}$ (psi)
(i) Mean value (Variation in τ exists)	18.1	50.716	8.48	827.26
Standard deviation	2.17	27.82	3.59	92.79
(ii) Mean value (No variation)	18.1	44.3	8.98	809.0
Percentage of difference between (i) and (ii)	0	14.4 %	5.67%	2.23%
Predicted values of CV*	12.0 %	54.85 %	42.7 %	11.2 %
Experimental values of CV*	12.0 %	32.3 %	31.1 %	11.5 %

* CV = coefficient of variation = $\frac{\text{standard deviation}}{\text{mean value}} \times 100$

confirm that the most important parameter to be studied in the cycle-to-cycle variation of a diesel engine is $\hat{dP}$, which shows the highest coefficient of variation.

Predicted and experimental coefficients of variations of $\hat{dP}$, $\theta(\hat{dP})$ and $\hat{P}$ are given in Table 5.10. Amongst these coefficients, the predicted values of $\theta(\hat{dP})$ and $\hat{P}$ are in good agreement with the experimental results. However, the experimental coefficient of variation for $\hat{dP}$ (32.3%) compared to the predicted one (54.85%) is only fairly reasonable.

On studying the experimental and predicted data obtained at each operating condition, it is realized that the principal difference lies in the magnitude of the degree of dependence of the starting angle of injection and the maximum rate of cylinder pressure rise. The model, being a device to describe the dispersion of the output data with respect to the variation of the input, deterministically predicts a high correlation coefficient and will tend towards the correlation coefficient of the experimental data, where the degree of randomness of these parameters becomes smaller at low load-high speed conditions (Modarres-Razavi (1973)). On the other hand, where there exists no statistical correlation between τ and $\hat{dP}$, the whole concept of the cycle-to-cycle variation due to the changes of the τ is not valid.

Figures 5.42(a), (b) and (c) demonstrate different cross-correlograms obtained for different dynamic modelling tests. Figure 5.42(a) shows the results when the generated values of τ are fed to the dynamic modelling as input. When the experimental values of τ are fed to the system, the results are presented in Figure 5.42(b). Figure 5.42(c) shows the results when generated perturbations of τ and m_f are employed together. If these diagrams are compared with the cross-correlogram obtained at identical experimental conditions (Figure 5.8(a)),

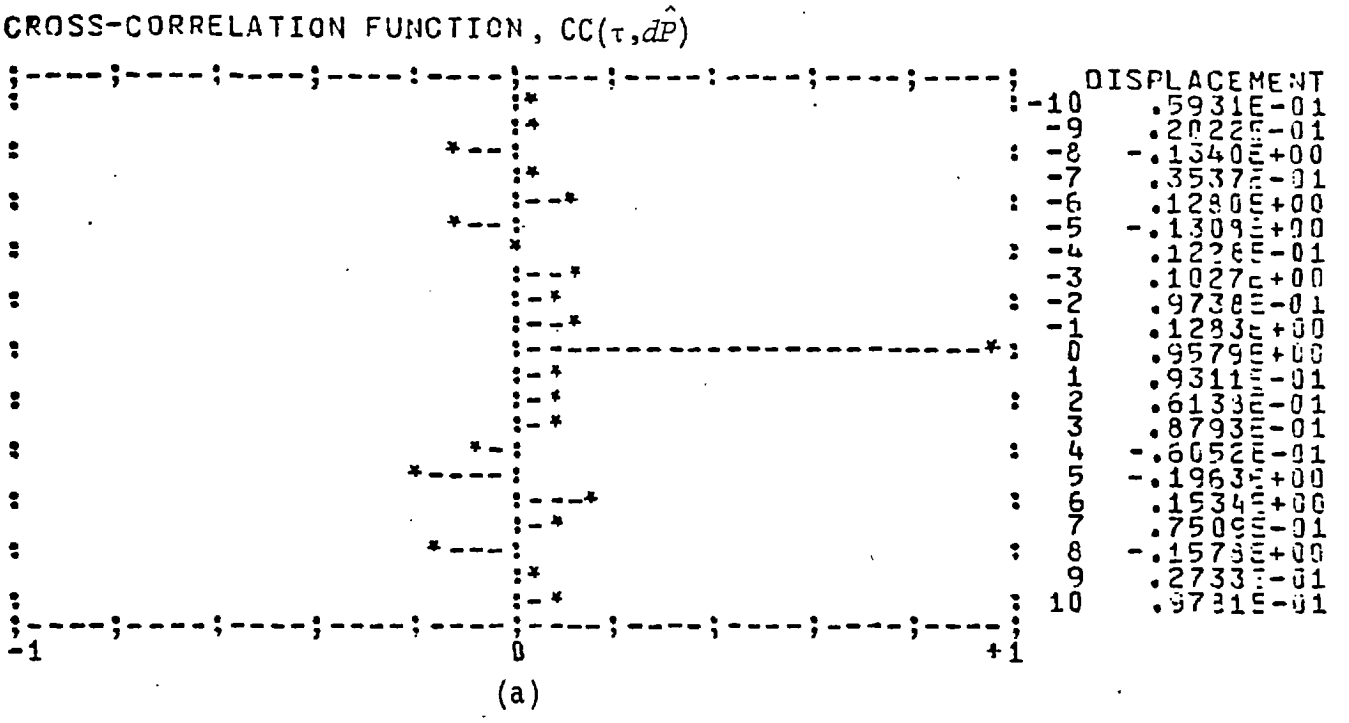


Figure 5.42: Cross-correlogram between predicted values of $\hat{dP}$ and generated values for τ at Test 19 (speed = 2500 rpm; load = 6.18 mkp)

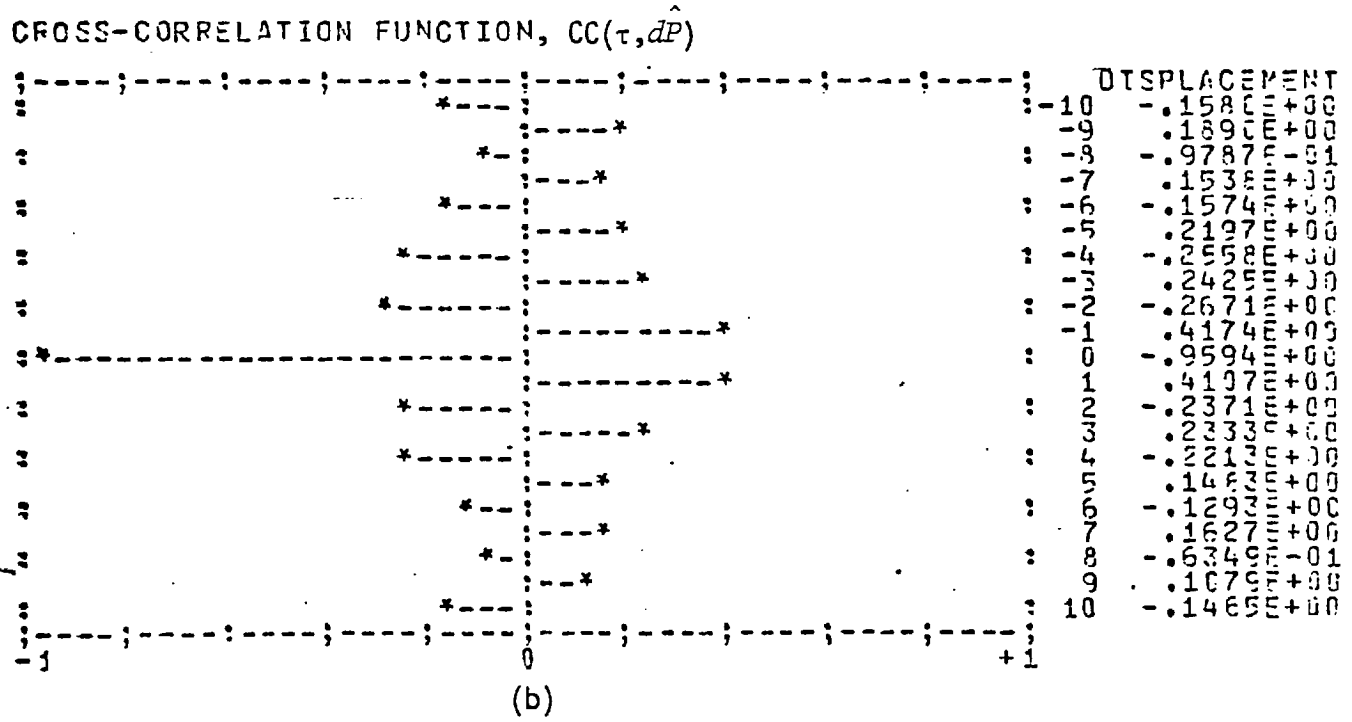
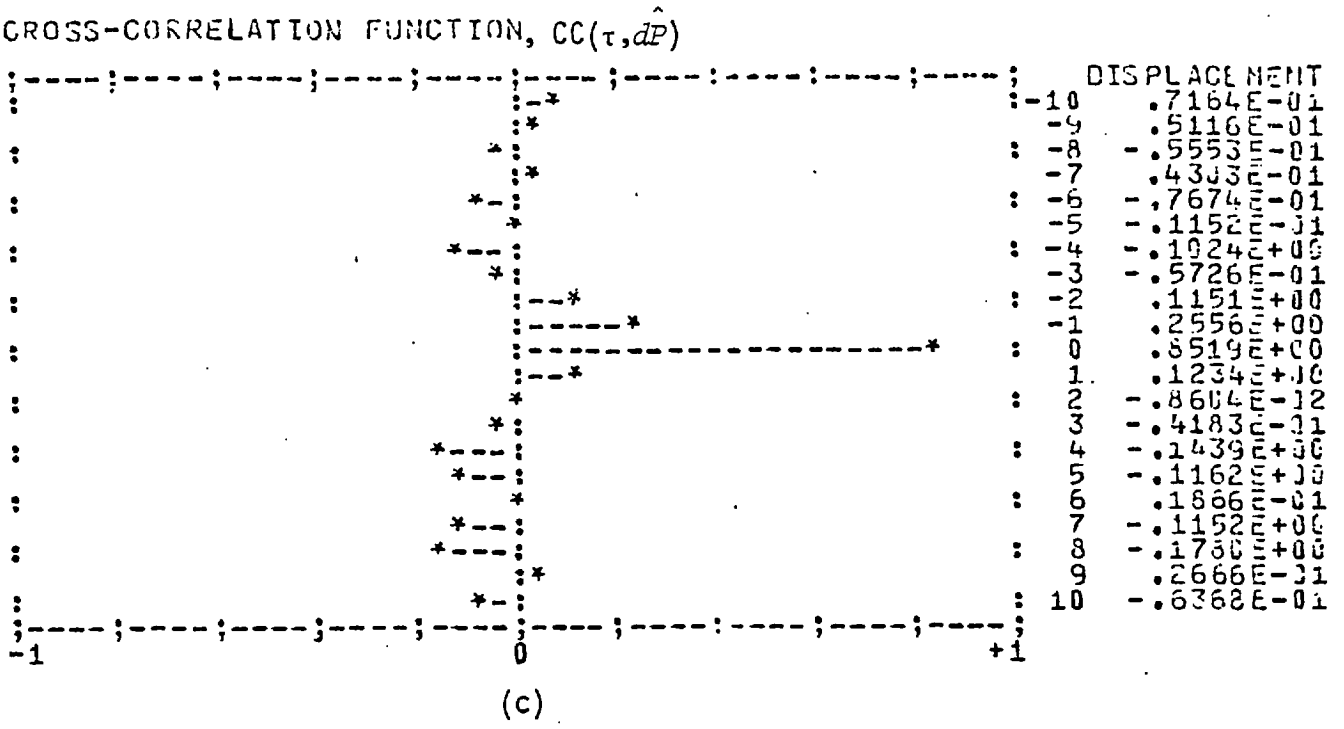


Figure 5.42: Cross-correlogram between predicted values of $\hat{dP}$ and minus values of experimental data for τ at Test 19 (speed = 2500 rpm; load = 6.18 mkp)



(c)

Figure 5.42: Cross-correlogram between predicted values of maximum rate of cylinder pressure rise and generated values of starting angle of injection when both dynamic injection and quantity of fuel injected were perturbed simultaneously at Test 19 (speed = 2500 rpm; load = 6.18 mkp)

then a distinct dissimilarity is observed. However, it is worth mentioning that the result presented in Figure 5.42(c) demonstrates a comparatively closer similarity with the experimental data.

5.4 THE BEHAVIOUR OF THE CHARACTERIZING PARAMETERS

The different characterizing parameters which were considered to be important in the present work will be briefly discussed under the two following categories:

(a) Characterizing parameters of the fuel injection process.

(b) Characterizing parameters of the combustion process.

5.4.1 Characterizing Parameters of the Fuel Injection Process

Among different characterizing parameters of the fuel injection process, the following are the most common in the study and design of fuel injection systems: static injection, dynamic injection, duration of injection, amount of fuel injected, maximum fuel-line pressure, maximum needle lift, and nozzle opening pressure.

For any combustion model which attempts to correlate the rate of heat release and the rate of injection, it is essential to have an estimate of at least three injection parameters (i.e. the starting angle of injection, the duration of injection, and the quantity of injected fuel), even assuming the most simple model for the fuel injection process (i.e. constant injection rate). The importance of these three parameters (τ, m_f, δ) is clear, not only as the characterizing parameters of the fuel injection process, but also for the important role of each parameter in the development of the combustion process.

5.4.1.1 Starting angle of injection (dynamic injection)

The extent of cyclic variation in the timing of the start of injection has been discussed elsewhere (e.g. Modarres-Razavi (1973); Wing (1975)). These studies showed that the dynamic injection variation from cycle to cycle is particularly noticeable at higher engine speeds, as shown in Figure 5.19, over the whole operating range of engine loads. Figure 5.19 shows the mean value, standard deviation and coefficient of variation of dynamic injection at various operating conditions. As can be seen, the mean value of the dynamic injection advances with increasing brake power, but does not considerably change at speeds higher than 2400 rpm. This is because of the variable static injection of the rotary fuel injection pump (DPA) with its built-in speed advance unit. As reported by Howes (1969), the characteristics of the standard rotary pump (DPA) is fixed such that the static timing advances linearly at a rate of about 14^{o} CA by increasing the engine speed from 1000 rpm to 2400 rpm, and then it remains fairly constant up to the maximum speed of the engine (about 2800 rpm). The standard deviations of the dynamic injection were often found to exceed 0.7^{o} CA at speeds higher than 2000 rpm and may eventually reach a value of about 3.3^{o} CA at the most severe condition.

The technique employed here to measure the injection timing is essentially based on the fuel-line pressure diagram rather than using a more common method which considers the needle lift diagram. The dynamic injection was assumed to be at the angular position at which the maximum rate of fuel-line pressure occurs. The fuel-line pressure at this position was compared with the nozzle opening pressure in order to find out whether the pressure is sufficient to lift the needle of the injector.

The standard deviation of the dynamic injection was

consequently calculated by analysing the distribution of 1000 consecutive values being sampled rapidly from the fuel-line pressure diagram by an on-line computer. The results for the standard deviations of dynamic injection presented here are in good agreement with those given by Wing (1975), but substantially differ from the results presented by Grigg* (1977). The method employed by Grigg for the estimation of the standard deviation of the dynamic injection was based on the one quarter of the scatter of the dynamic injection for twenty repeat shots of the needle lift diagram. The discrepancy in the results can either be due to the different technique employed or arises from the different performance of the injection pumps. This has also been reported by Grigg, who relates the scatter to the wearing of the drive system on our engine, causing excessive backlash in the pump drive. For a clear understanding of the underlying reason for this discrepancy, further investigation of the effect of different measurement methods on the estimation of the starting angle of injection is required.

Although the assumption of dynamic injection, being normally distributed, was accepted for the dynamic modelling technique, firstly due to similar bell-shaped distributions for a wide range of operating conditions, and secondly for simplicity of the generating input perturbations and the analysis of dynamic modelling prediction results, nevertheless, statistically speaking, the distributions of dynamic injection are not normal and slight skewness (positive and negative) and

---

* Data supplied by CAV shows the standard deviations of dynamic injection are much less than the values measured and presented here for the same model of fuel injection pump. Under certain operating conditions, these values are even less than one third of the measured values.

Kurtosis (positive or negative) can be recognized. This observation is in agreement with the general conclusion stated by Grigg that "... the distribution of injection timing is not normal anyway". In general, his analysis of 20 samples was not adequate to indicate the overall distribution of dynamic injection random data, and therefore his results could not show how much these distributions deviated from normal distributions. The histogram of dynamic injection at an engine speed of 2500 rpm and an engine load of 10 mkp in Figure 5.43 is an example showing how close these distributions might be to the normal distributions.

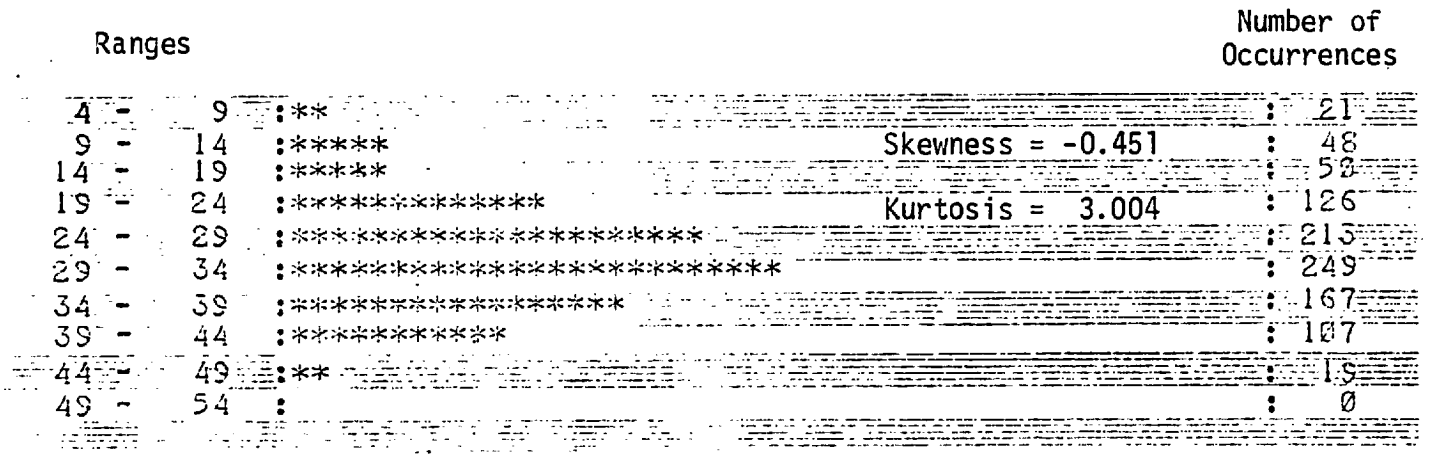


Figure 5.43: Histogram of dynamic injection at engine speed of 2500 rpm and engine load of 10 mkp

Dynamic injection is by far the most important factor affecting the development of the combustion process, and consequently the cyclic variations of diesel engines. Statistical analysis of the experimental results generally implies that certain correlations exist between the dynamic injection and the other fuel injection variables with the combustion characterizing parameters. This point is further clarified by using the diesel engine simulation program, where the effect of variation in the fuel injection process on the combustion characterizing

parameters was confirmed. For example, Figure 5.28 shows that in Test 19 (speed = 2500 rpm and load = 6 mkp) for a 1^{o} CA advance of the dynamic injection, the peak cylinder pressure will rise about 3%, the maximum rate of cylinder pressure rise will rise to 11%, and there will be about a 1.6^{o} CA advance in the angle of maximum rate of cylinder pressure rise occurrence. The reason for such influence lies in the effect of dynamic injection on the ignition delay period which partly controls the development of the combustion process. Grigg (1976) remarks that, thermodynamically, the effect of the period of heat replease in a diesel engine on efficiency is less than that of the timing of the heat release, and thus supports the significance of injection timing on the combustion process. Also, the effects of this parameter on smoke, unburned hydrocarbons, nitrogen dioxide and noise are considerable. The nature of this correlation can be illustrated as follows: If the dynamic injection advances, the ignition delay period increases and thus the amount of fuel and air premixed becomes greater, resulting in a higher rate of heat release. This behaviour eventually causes a reduction in smoke and an increase in peak cylinder pressure, maximum rate of cylinder pressure rise, nitric oxide concentration and noise.

5.4.1.2 Quantity of injected fuel

The extent of cyclic variation in the quantity of injected fuel has been investigated by Pires (1973). In his work, the area under the needle lift diagram has been assumed to be proportional to the amount of the fuel injected. Since the coefficient of discharge of the nozzles varies with the position of the injector needle during the injection, and also the difference between the fuel-line pressure and the pressure inside the cylinder affects the amount of the fuel injected, the

area under the needle lift diagram only approximately represents the quantity of the fuel injected. From these studies, Pires has concluded that there is a strong correlation between the variation of the quantity of fuel injected and the maximum rate of cylinder pressure rise in the same cycle, especially at the high speed-low load region. This is in agreement with the results described in the present work, since a strong correlation exists between the different fuel injection characterizing parameters almost over the whole range of engine operating conditions.

The variations of the combustion characterizing parameters against the amount of injected fuel is shown diagrammatically in Figure 5.35. As shown, the rate of heat release in a diesel engine is strongly dependent on the quantity of fuel injected during the delay period. Also, the functional dependence between the variation of the quantity of fuel injected and the variations of the characterizing parameters is almost linear. This means that the variations of the quantity of injected fuel (assumed to be normally distributed) will not result in any form of skewed distribution in the variations of the combustion characterizing parameters.

5.4.1.3 Duration of injection

The preliminary investigation has shown that accurate measurement of the duration of injection cannot be satisfactorily made for the purpose of statistical analysis. The difficulty particularly arises in measuring the end of injection either from the fuel-line pressure diagram or the needle lift diagram due to parasitic oscillation of the injector at the completion of injection. Faced with this problem, it was decided that it would be more profitable to demonstrate the relative signficance of variations in this parameter compared to the variation of

other fuel injection characterizing parameters with the aid of the diesel engine simulation program. As the Marzouk model of combustion does not correlate the duration of injection to the development of combustion, the CAV model (see Appendix A3) was employed for this reason.

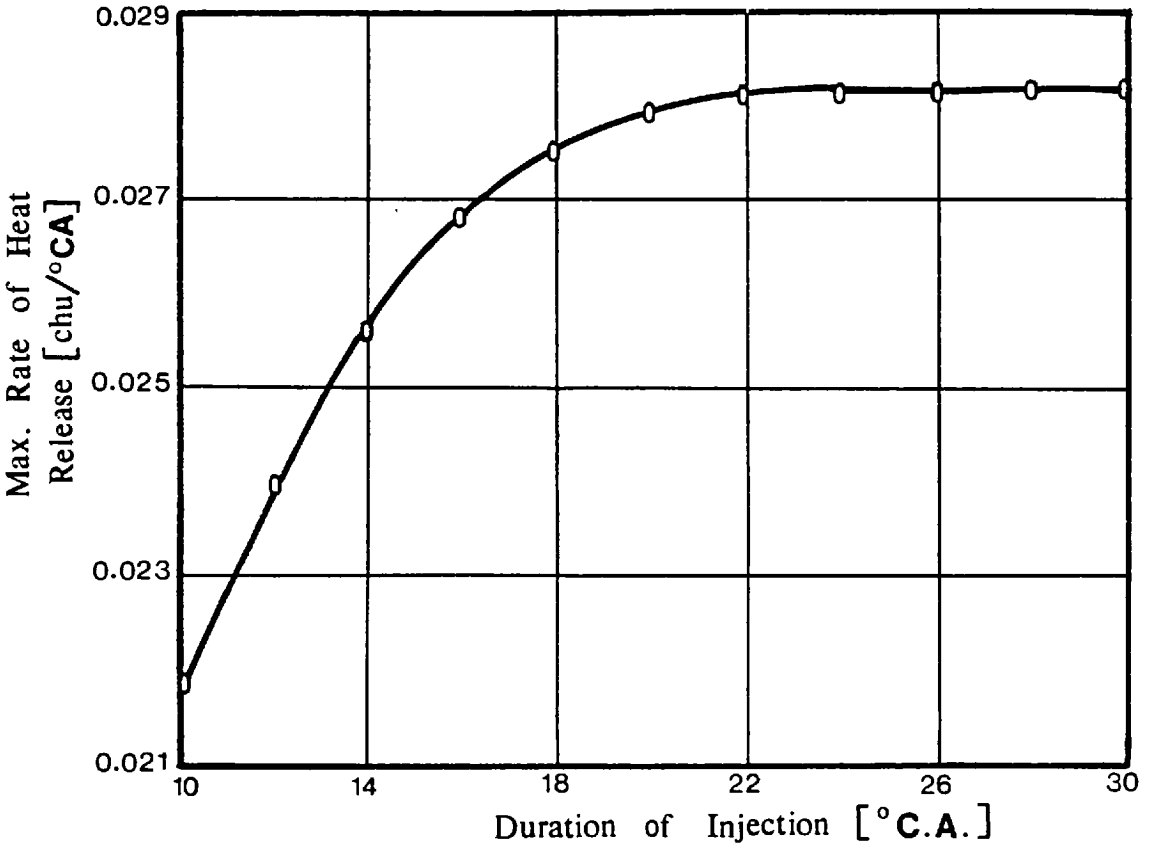


Figure 5.44: Variation of the maximum rate of heat release to the duration of injection

Figure 5.44 shows the variation of the maximum rate of cylinder pressure rise versus the changes in injection duration. As it shows, an increase in the duration of injection results in a noticeable rise in the maximum rate of cylinder pressure variations; however, this rise is limited and there is a definite value beyond which the changes in the parameter do not affect the combustion development.

5.4.2 Combustion Process Characterizing Parameters

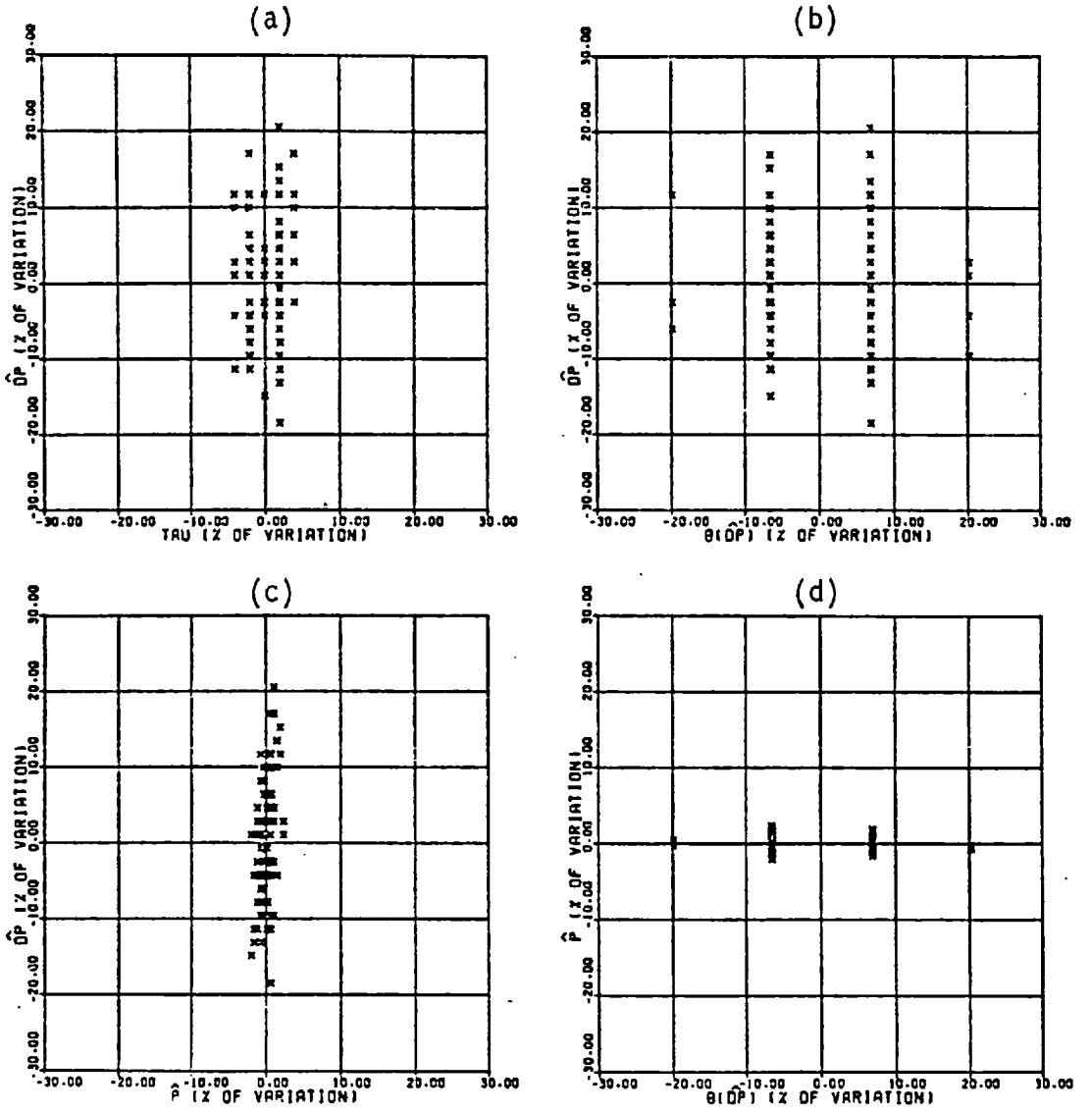
Among the various factors characterizing the combustion process, the following parameters are commonly used, particularly as the indicators of cycle-to-cycle variations in internal combustion engines:

(a) Peak cylinder pressure.
(b) Maximum rate of cylinder pressure rise.
(c) Angle of peak cylinder pressure occurrence.
(d) Angle of occurrence of maximum rate of cylinder pressure rise.
(e) Duration of combustion.
(f) Peak cylinder temperature.
(g) Maximum rate of burning fuel.
(h) Indicated mean effective pressure, etc.

In the present study, only the three parameters $\hat{P}$, $\hat{dP}$ and $\theta(\hat{dP})$, which are the best indicative factors for evaluating the cyclic variation, have been considered.

The cyclic variation of peak cylinder pressure and the maximum rate of cylinder pressure rise under different operating conditions in internal combustion engines are well established phenomena (Barton et al (1970) for petrol engines; and Wing (1975) for diesel engines). The Barton et al results for petrol engines showed that a nearly one-to-one linear association exists between $\hat{P}$ and $\hat{dP}$. As reported by Wing, a similar correlation may well be detected for diesel engines but the magnitude of the correlation will not be as high for the whole range of operating conditions. Similar correlations were found between $\hat{P}$ and $\theta(\hat{dP})$ and also between $\hat{dP}$ and $\theta(\hat{dP})$ (Figures 5.45 to 5.48 demonstrate the existing correlations between experimental values of these parameters for

** PERKINS 4.236 DIESEL ENGINE
** TEST-13E (SPEED = 1000.0 RPM)
** (LOAD = 6.1 MKP)



** EXPERIMENTAL RESULTS FOR TAU.$\hat{P}$.$\hat{\Delta P}$.θ($\hat{\Delta P}$)
** ARE PRESENTED TO SHOW THE DEPENDENCE OF THE
** 1- (TAU AND $\hat{\Delta P}$) . ** 3- ($\hat{P}$ AND $\hat{\Delta P}$)
** 2- (θ($\hat{\Delta P}$) AND $\hat{\Delta P}$) , ** 4- (θ($\hat{\Delta P}$) AND $\hat{P}$)
** TAU - STARTING DEGREE OF INJECTION (DCA BTDC)

Figure 5.45: Experimental results at low load-low speed conditions indicating the existing correlation between different combustion characterizing parameters

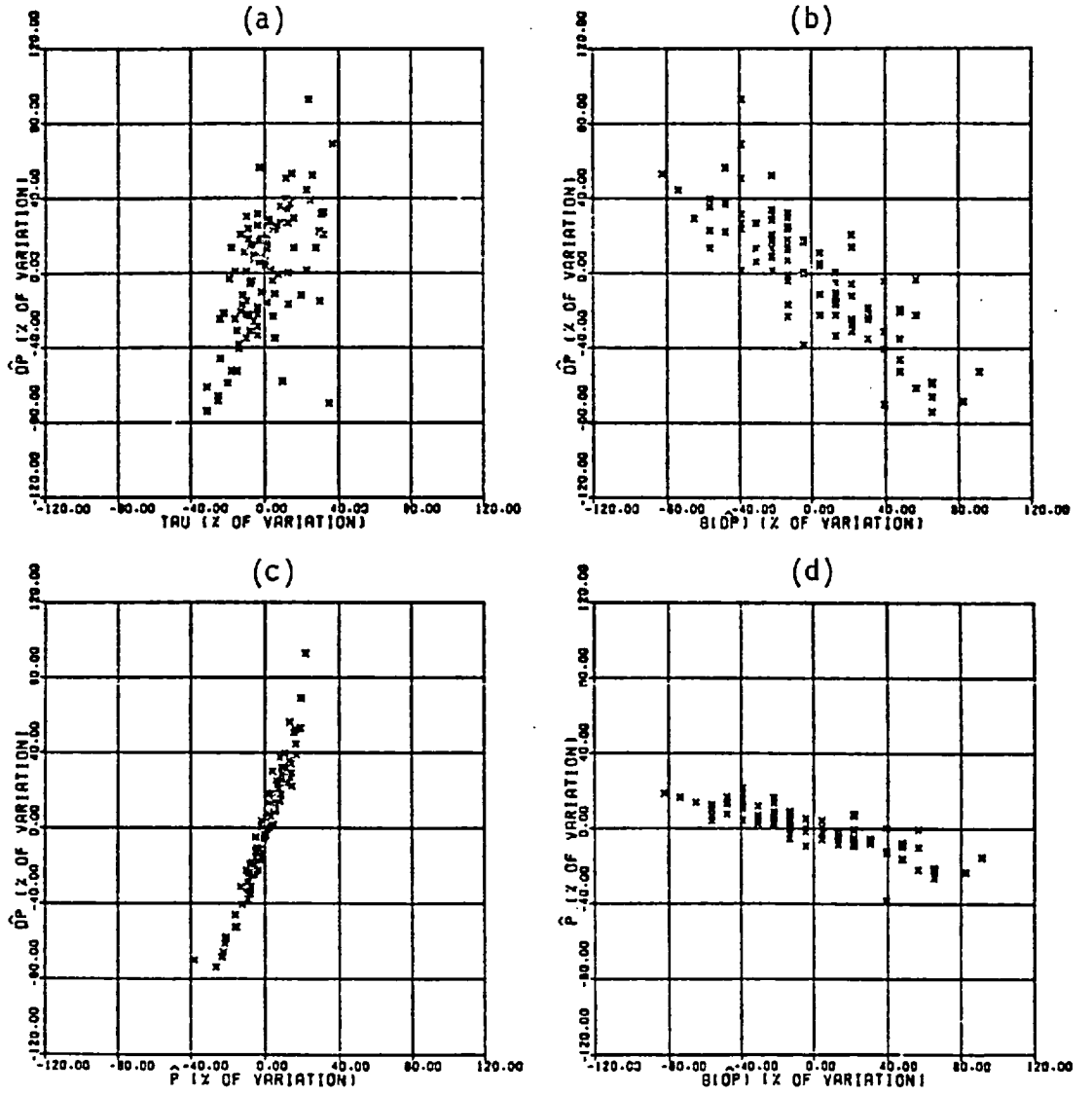


Figure 5.46: Experimental results at low load-high speed conditions indicating the existence of strong correlations between different combustion characterizing parameters

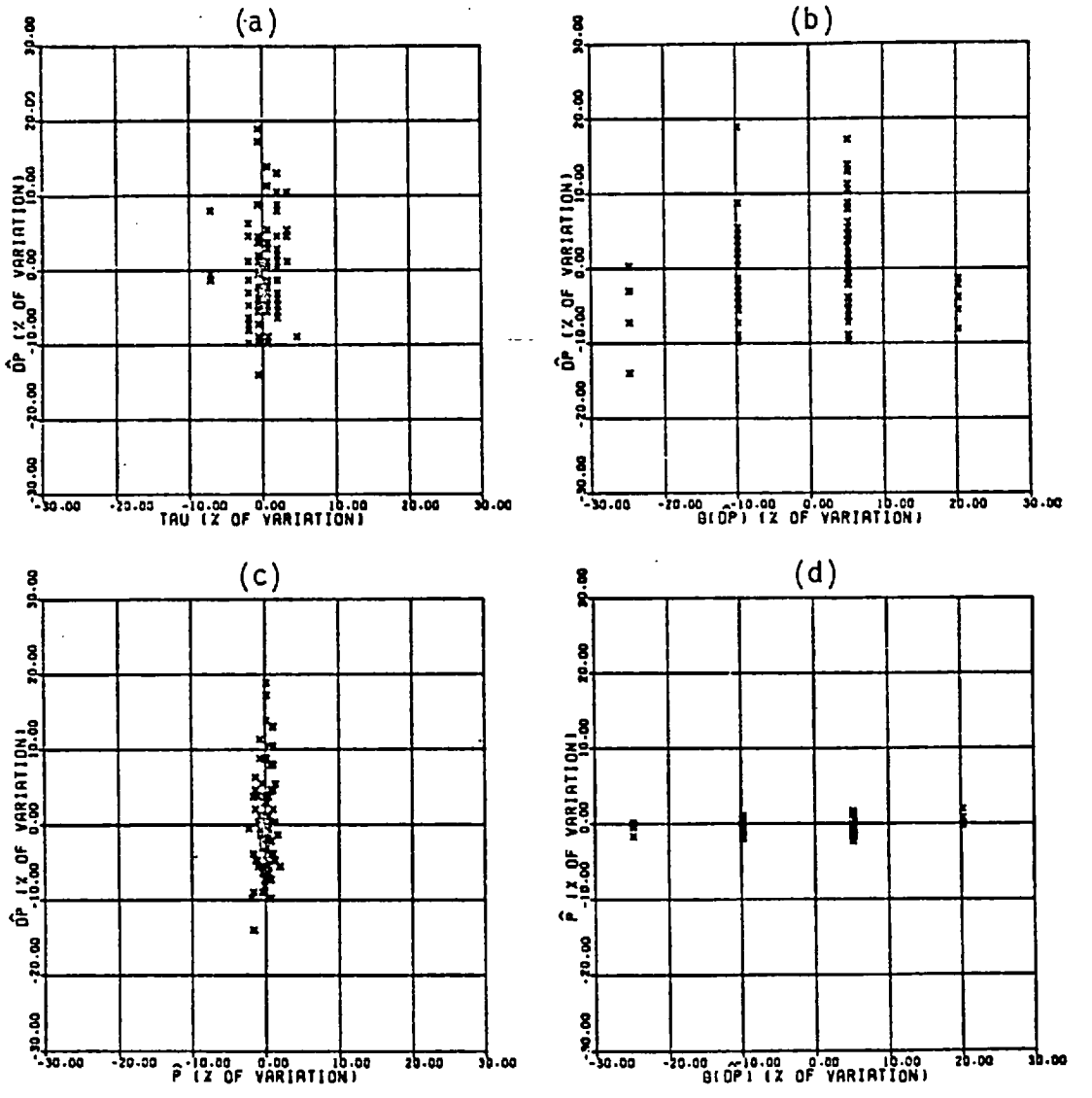


Figure 5.47: Experimental results at high load-low speed indicating the existing correlation between different combustion characterizing parameters

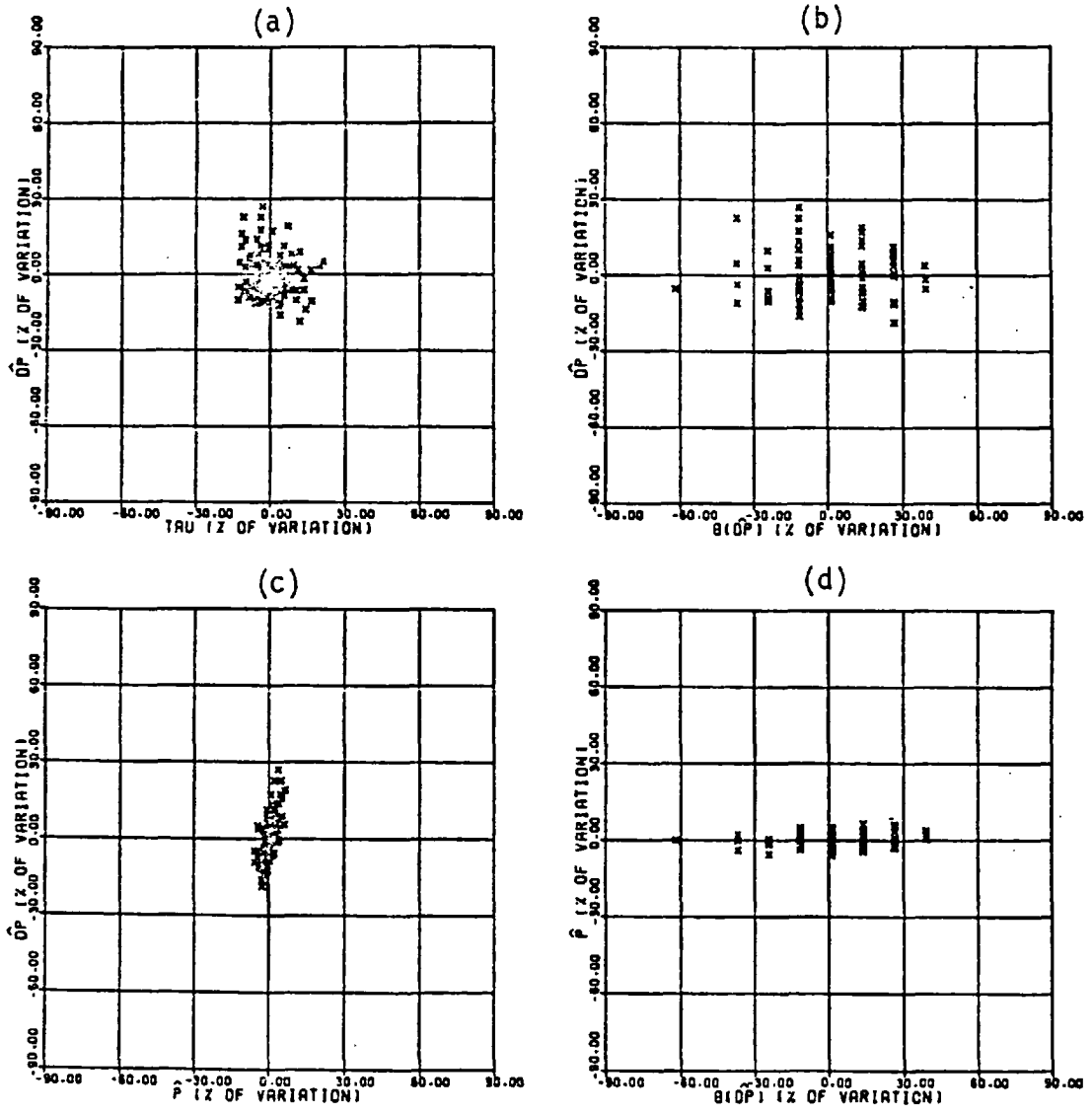
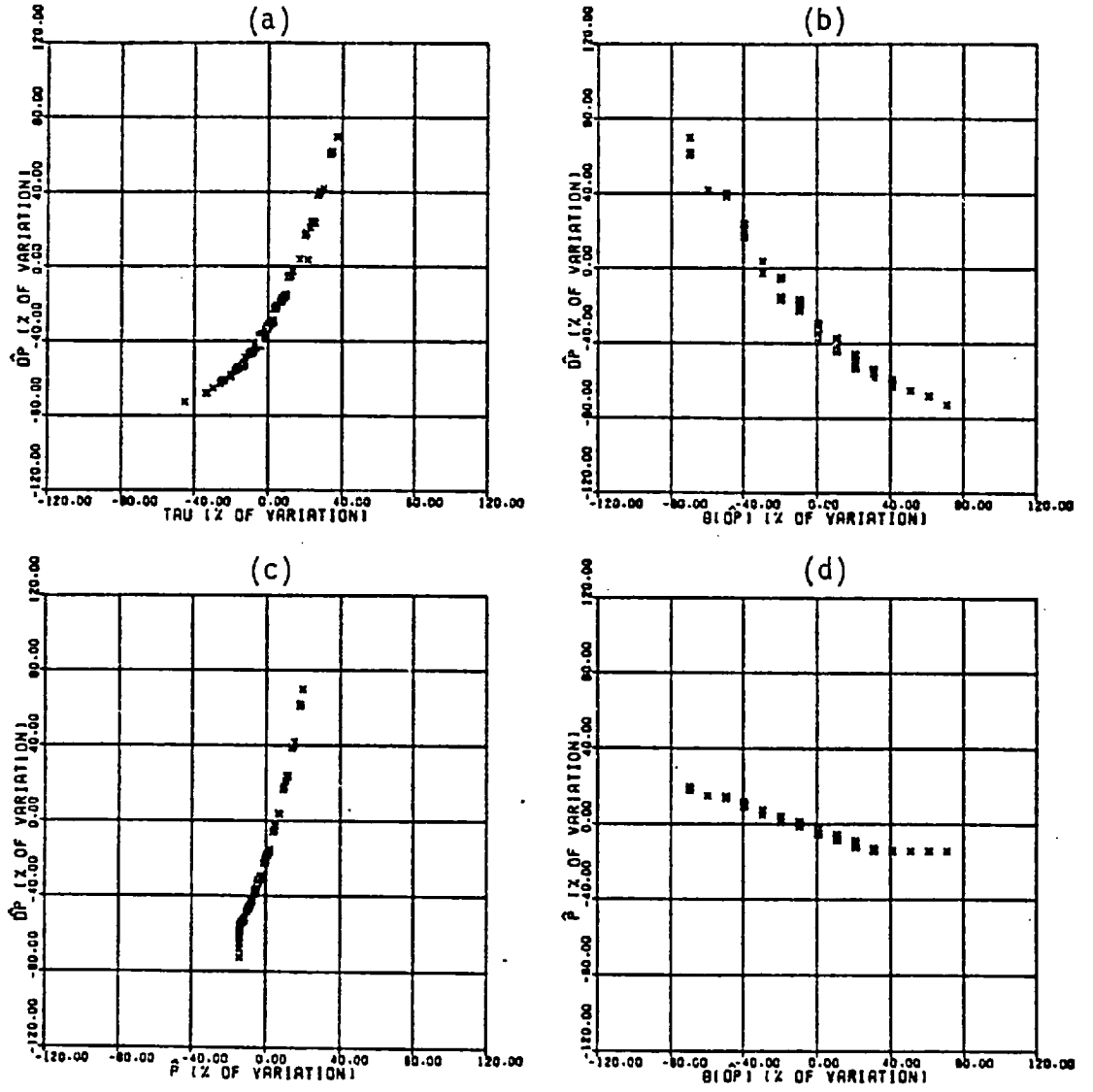


Figure 5.48: Experimental results at high load-high speed conditions indicating the existing correlation between different combustion characterizing parameters

Tests 13E, 19E, 43E and 49E. The predicted correlations between τ and $\hat{dP}$, $\hat{P}$ and $\hat{dP}$, $\theta(\hat{dP})$ and $\hat{dP}$, and $\theta(\hat{dP})$ and $\hat{P}$ for the case of Test 19E is presented graphically in Figure 5.49). Moreover, among the possible correlations between each pair of $\hat{P}$, $\hat{dP}$ and $\theta(\hat{dP})$, the maximum correlation was obtained between the peak cylinder pressure and the occurrence of the maximum rate of cylinder pressure rise. This is because the $\hat{P}$ is equivalent to the integrated values of the rate of cylinder pressure rise, $\hat{dP}$, and thus its sensitivity to the location of the maximum rate of cylinder pressure rise with reference to the top dead centre is more conspicuous. The results reported here also indicate that, while an increase in engine speed causes an appreciable increase in the variations of $\hat{P}$ ($\sigma_{\hat{P}}$), a change of engine load does not often produce a noticeable variation. This can be explained by the fact that injection initiation and ignition delay (which both are functions of the operating conditions) affect the rate and phasing of the premixed burning in particular and the combustion development as a whole. Therefore, generally speaking, any retardation in ignition point (due to increases of engine speed or any other working variables) results in $\hat{P}$ occurring after top dead centre; the clearance volume above the piston will rapidly increase while, simultaneously, the heat released during the period of $\theta(\hat{P})$ will decline. The cumulative effect of these phenomena will force $\hat{P}$ to decline sharply and thus the changing ratio of $\hat{P}$ becomes large causing an increase in the standard deviation of $\hat{P}$.

By studying the variations of the maximum rate of cylinder pressure fluctuations with speed and load in compression ignition engines (Figure 5.37) and comparing them with the results obtained for spark ignition engines, it can be concluded that the effect of rate of combustion on the cyclic variation is comparatively smaller for CI engines. In SI

** PERKINS 4.236 DIESEL ENGINE
** TEST-19F (SPEED = 2500.0 RPM)
** (LOAD = 6.1 MKP)



** PREDICTED RESULTS FOR TAU, $\hat{P}$, $\hat{\Delta P}$, $\theta(\hat{\Delta P})$
** ARE PRESENTED TO SHOW THE DEPENDENCE BETWEEN
** 1- (TAU AND $\hat{\Delta P}$) , ** 3- ($\hat{P}$ AND $\hat{\Delta P}$)
** 2- ($\theta(\hat{\Delta P})$ AND $\hat{\Delta P}$) , ** 4- ($\theta(\hat{\Delta P})$ AND $\hat{P}$)
** TAU - STARTING DEGREE OF INJECTION (DCA BTDC)

Figure 5.49: Dynamic modelling prediction results for low load-high speed conditions. Correlations between different combustion characterizing parameters

engines, a fast combustion is normally less prone to cyclic variations than slower combustions and therefore every engine parameter which causes an increase in the maximum rate of cylinder pressure also engenders a reduction in the cyclic variations (Soltau (1960)). This behaviour was not, however, maintained at all operating conditions in the diesel engine examined here since the mean value of $\hat{dP}$ was highly influenced by the engine load and to a smaller extent by the engine speed, while the cyclic variations (standard deviation of $\hat{dP}$, $\sigma_{\hat{dP}}$) was shown to be affected more by engine speed than by engine load (Figure 5.20). Hence, it can be concluded that the mixture motion, vibration of the drive, engine noise and other possible contributing parameters to the cyclic variations have a greater significance on cyclic variation than the combustion development itself.

5.5 GENERAL DISCUSSION OF THE RESULTS

The following remarks attempt to explain the causes of deviations between predicted and measured values:

i) Combustion model accuracy: Although it would be desirable to employ a precise combustion model which considers all the relevant phenomena taking place in the engine during this period, present models fall short in certain aspects and do not yield the overall accuracy required for this study.

ii) In order to simplify analysis of the results and to keep computational time within reason, it is impractical to vary more than one parameter at a time (τ or m_f in this case), and consequently requires the assumption that other parameters of

the injection system which may change remain constant during each cycle. In the case of Test 19C, when the simultaneous changes of two parameters (τ and m_f) were studied, a more reasonable result was achieved.

iii) As has been shown diagrammatically in Figure 3.1, the effect of the engine on the injection system has been ignored. It can be argued that this effect has been considered already to a certain extent, especially where experimental values have been employed to describe the variation in the injection system, but to completely define this reverse interaction further experiments would be necessary, using an independent pump drive (e.g. by coupling the injection pump to an electric motor instead of driving the pump from the engine itself).

iv) All coefficients employed in the model have been considered to remain constant while variations were introduced to the system. This is probably a reasonable assumption for small perturbations, but will certainly lead to gross errors in some of the extreme cases considered here.

v) Data errors: The experimental data (cylinder pressure measurements, etc.) naturally contain an element of electrical noise which is especially noticeable on those results which have been highly amplified and electronically differentiated. Further noise on the measurements derives from the use of an analogue to a digital converter. The variable "rounding error" from this device was avoided as far as possible by selecting

engine regions where the degree of cyclic variation was highest. Further precautions against noise were the use of the highest quality instrumentation throughout and the use of averaging and curve smoothing techniques where appropriate. The number of cycles over which measurements were taken was found to be critically significant in determining certain values (e.g. instantaneous engine speed) and was carefully considered for each case.

vi) The measured standard deviations of the starting angle of injection were much higher than data supplied by CAV (Grigg (1977)). In some conditions, these values are more than three times greater. Discussions with the manufacturer of this injection equipment have lead to the conclusion that, because of the completely different experimental techniques utilised, a detailed study of the performance of several injection pumps would be necessary to clarify this point.

CHAPTER 6

CONCLUSIONS

6.1 INTRODUCTION

In this project, an attempt has been made to investigate the probable relation between the variations of fuel-injection system parameters and combustion cyclic fluctuations. The dynamic modelling technique was developed as the means of studying the response of different combustion characterizing parameters to known perturbations in the fuel-injection system characterizing parameters.

Two points must be made before the conclusions of this study are presented:

(a) There is no real basis for comparison between most of the results and conclusions reported in this thesis and those reported elsewhere. This is because previous studies have been concerned only with petrol engines and also have based their results on different characterizing parameters to those chosen here.

(b) The limitation of working with one particular engine and attempting to generalize the findings and apply them to other operating conditions and engines is recognized. Furthermore, these conclusions apply only to the naturally aspirated direct injection diesel engine with rotary fuel pump.

6.2 CONCLUSIONS

Discussion of the results in the last chapter shows that, within the scope of the experimental work, the following conclusions, indicating the nature of the variations of injection system parameters and combustion characterizing parameters, can be derived:

(i) The variations of the combustion characterizing parameters ($\hat{P}$, $\hat{dP}$, $\theta(\hat{dP})$) and fuel-injection system parameters (τ, m_f) are random in nature and stationary over the period of 1000 cycles. This means that, although the values of these time-series vary from one cycle to another, the statistical distribution of these parameters are repeatable and almost constant over a large number of samples under steady-state operating conditions.

(ii) The variations in starting angle of injection, maximum rate of cylinder pressure rise, peak cylinder pressure and the angle of occurrence of the maximum rate of cylinder pressure rise are all directly influenced by the engine speed. This influence is particularly strong at high speeds. Changes in engine load do not, however, have the same effect on these variations. Moreover, its influence is not a monotonic function.

(iii) Over the wide range of experiments undertaken, variations of the combustion characterizing parameters were consistently higher than those of the fuel-injection system fluctuations. These two sets of variations are related to each other and changes in one affects the other. But, since injection occurs before combustion, the influence of the variations in fuel injection

system parameters on the combustion cycle-to-cycle variations is much stronger than the reverse case, which can, of course, only influence the next cycle.

(iv) Variations in the process of fuel injection do not appear to depend on the effects of any other cycle. They are related only through the drive backlash and cylinder pressure variations of each individual cycle.

(v) Similarly, variations in the process of combustion do not usually depend on the effects of other cycles. They depend on the intake, compression, combustion process (with a lesser degree of influence compared to that for SI engines) and fuel injection process variations of each individual cycle.

(vi) Apart from the high speed-low load conditions, the effects of residual gases on the cycle-to-cycle variations are unmeasurable.

(vii) The maximum correlation between variations of the fuel injection process and combustion process existed in the region of the high speed-low load operating conditions. Within the range of 5-10 mkp load, the cross-correlation coefficients of experimental results between the fuel injection system parameter (τ) and combustion characterizing parameters ($\hat{P}$, $\hat{dP}$, $\theta(\hat{dP})$) show maximum positive linear dependence. But, with increasing engine load, and less so with increasing engine speed, these correlations sharply weaken. Particularly for higher brake horsepowers, the

cross-correlations tend to zero and even indicate negative correlation.

(viii) Statistical analysis of the results obtained from each experiment can reveal the existence of any irregularities. It was thus shown that some of the extremely high variations in the combustion process from cycle-to-cycle could have been caused by the existence of either some form of misfiring or a combination of knocking and non-knocking combustion or the effect of residual gases in the region of low load-high speed.

(ix) The functional relationship of the cycle-to-cycle variations to the injection system characteristics has been established for different operating conditions with the aid of a dynamic modelling technique. Having these functional relationships, it is possible to calculate the statistical properties of the relevant variables ($\hat{dP}$, $\theta(\hat{dP})$, $\hat{P}$, $\hat{dm}_{fp}$) in relation to the variations of injection system parameters. The method used in this study can be extended to calculate the statistical distribution of the formation of nitric oxide in a diesel engine when its direct cycle-to-cycle measurement is not possible. This logical extension of the analysis of the injection and combustion system would, however, be limited due to the currently available nitric oxide predictions programs.

(x) It has been shown experimentally and confirmed analytically that $\hat{dP}$ is the most effective parameter to describe the cycle-to-cycle variation in a diesel engine, and that the variation in

injection system characteristics has a significant effect on the average value of $\hat{dP}$.

(xi) Of all the variables describing the fuel injection process, it is the starting time of injection that is found to have the most marked effect on combustion pressure fluctuations.

(xii) The theoretical correlations between dynamic injection and peak cylinder pressure, maximum rate of cylinder pressure rise and angle of occurrence of $\hat{dP}$ were found to be much higher than the experimental values. The reasons for this discrepancy have been discussed previously in Section 5.5.

It should also be mentioned that the construction of a dynamic modelling technique was not for engine simulation prediction purposes, since this would prove to be very expensive, but for a detailed investigation of the nature of the correlation between fuel injection system and combustion variations.

In short, through this work, the investigation of the extent of the influence of injection system characteristics on cycle-to-cycle combustion variations demonstrates the usefulness and validity of the dynamic modelling technique.

6.2 SUGGESTIONS FOR FUTURE WORK

An improvement in the dynamic modelling technique can be obtained by putting perturbations in all the fuel injection system parameters, taking into account the actual correlations that exist between these variations (these perturbations could be simulated from experimental measurements).

Because of the existence of large deviations between the experimental and predicted correlations, it would be necessary to make improvements to the combustion models so that correlations between the injection system process and the combustion process can be made with better accuracy. Hence, no suggestions can sensibly be made for the extension of theoretical work on dynamic modelling techniques.

There are, however, a number of suggestions which can be made regarding improvements to the experimental approach. One such improvement would be the use of an electrical fuel pump instead of the engine driven pump. This would help to show the effect of unsteadiness in the pump drive on the variation in fuel injection system parameters and consequently in combustion variations. The second suggestion is a thorough investigation into the different methods of measuring the starting time of injection, i.e. from the derivative of the needle lift diagram, from the difference between cylinder pressure and fuel-line pressure diagrams, etc. The other investigation which could also help to clarify measurement of the characteristics of the fuel-injection system and consequently the performance of the engine would be to separately study the effects of component tolerances of different parts of the fuel injection system on the variations of these parameters.

APPENDIX A1

FORMULAE FOR THE INTERNAL ENERGY AND THE GAS CONSTANT

The equilibrium thermodynamic properties of the products of combustion diesel fuel (assumed to be $C_n H_{2n}$) and air were expressed analytically in the form of:

$$U = U(T,P,F) \tag{A1.1}$$

$$R = R(T,P,F) \tag{A1.2}$$

As for the case of a naturally aspirated diesel engine running at the steady-state condition, only the lean fuel/air mixture ($F < 1$) is expected, and therefore the following formulae for the lean fuel/air mixture were taken from Krieger & Borman (1966) which were based on the concept of absolute internal energy, and are:

(i) Internal Energy

(a) For $T < 2600^{o}R$ (no dissociation):

$$U^* = A(T) - B(T)\,F \tag{A1.3}$$

where:

$$A(T) = 0.16528\,T + 5.1979\,(10)^{6}\,T^2 + 3.9016\,(10)^{-9}\,T^3 - 9.3632\,(10)^{-13}\,T^4 + 6.3156\,(10)^{-17}\,T^5 \tag{A1.4}$$

$$B(T) = 1311.0 - 1.3623\,(10)^{-2}\,T - 1.2605\,(10)^{-5}\,T^2 + 1.587\,(10)^{-9}\,T^3 - 8.2022\,(10)^{-14}\,T^4 \tag{A1.5}$$

(b) For $T > 2600^{o}R$ (dissociation):

$$U = U^* + \exp\,(e_1 + e_2 + e_3) \qquad \text{(A1.6)}$$

where:

$$e_1 = 10.41066 + 7.85125\,F - 3.71257\,F^3 \qquad \text{(A1.7)}$$

$$e_2 = (-27.00107 - 28.5087\,F + 17.30375\,F^3)(1000/T) \qquad \text{(A1.8)}$$

$$e_3 = \left[0.154226\,F^3 - 0.38656\,F - 0.10329 + (0.21289\,F - 0.026574)\,(1000/T)\right] \ln\,(P) \qquad \text{(A1.9)}$$

(ii) Gas Constant

For $T < 2600^{o}R$ (no dissociation):

$$R^* = 0.0685548 + 0.004788\,F \qquad \text{(A1.10)}$$

and for $T > 2600^{o}R$ (dissociation):

$$R = R^* + \exp\,(e_4)/1000 \qquad \text{(A1.11)}$$

where:

$$e_4 = \left[11.98 - 45.796\,(1000/T) - 0.4354\,\ln\,(P)\right] F + 0.2977\,\ln\,(F) \qquad \text{(A1.12)}$$

In all the above equations:

P = pressure (psia)

T = temperature (^{O}R)

F = f/f_s, equivalence ratio

U^* = undissociated internal energy (Btu/lbm)

U = internal energy (Btu/lbm)

R^* = gas constant for undissociated products (Btu/lbm^{O}R)

R = gas constant (Btu/lbm^{O}R)

APPENDIX A2

CALCULATION OF APPARENT RATE OF HEAT RELEASE

The apparent rate of heat release can be calculated from the energy equation by assuming that burning takes place incrementally as a homogeneous combustion and thus acts as a uniform heat source. The first law of thermodynamics can, therefore, be written in the form:

$$\frac{d(MU)}{dt} = -P\frac{dV}{dt} + \sum Q_i + h_f\frac{dM}{dt} \tag{A2.1}$$

As described by Krieger & Borman (1966), using the equation of state ($PV = MRT$) and the equivalence ratio ($F = f/f_s$) at any instant $F = F_o + ((M/M_o) - 1)((1 + f_o)/f_s)$, $\dot{M}$, the mass burning rate, can be derived from equation (A2.1):

$$\frac{1}{M}\frac{dM}{dt} = \frac{-\frac{RT}{V}\frac{dV}{dt} - \frac{\partial U}{\partial P}\frac{dP}{dt} + \frac{1}{M}\sum Q_i - C\,(B)}{U - h_f + D\frac{\partial U}{\partial F} - C\,(1 + \frac{D}{R}\frac{\partial R}{\partial F})} \tag{A2.2}$$

$$B = (\frac{1}{P}\frac{dP}{dt} - \frac{1}{R}\frac{\partial R}{\partial P}\frac{dP}{dt} + \frac{1}{V}\frac{dV}{dt}) \tag{A2.3}$$

$$C = \frac{T\frac{\partial U}{\partial T}}{(1 + \frac{T}{R}\frac{\partial R}{\partial T})} \tag{A2.4}$$

$$D = \frac{(1 + f_o)}{f_s}\frac{M}{M_o} \tag{A2.5}$$

Equation (A2.2) was solved numerically to obtain $\dot{M}$ as a function of time (or crank angle). The Adams-Moulton's Predictor-Corrector Method*

---

* Predictor formula: $y_{n+1}^{(o)} = y_n + \frac{h}{24}(55 f_n - 59 f_{n-1} + 37 f_{n-2} - 9 f_{n-3})$

Corrector formula: $y_{n+1}^{(k)} = y_n + \frac{h}{24}(9 f(x_{n+1}, y_{n+1}^{(k-1)}) + 19 f_n - 5 f_{n-1} + f_{n-2})$

(Conte (1965)) was used to solve the above equation.

Experimental values for cylinder pressure and the rate of cylinder pressure rise, and expressions for internal energy and gas constant of the products and unburned mixture (given in Appendix A1) were used in the above equation. The Eichelberg correlation (equation (3.18)) was used for calculating the approximate heat transfer coefficient. The trapped mass in the cylinder was calculated from the volumetric efficiency which was obtained from polynomial fit based on the published Parkins data (Jones (1966)). The required data and polynomial fit based on them are presented in Table A2.1.

The calculation was carried out for approximately every 1/3 of a degree of crank angle. Experimental values used for cylinder pressure were the mean values of 128 cylinder pressure diagrams.

As it is well known, combustion cyclic variations exist in diesel engines (especially naturally aspirated diesel engines) as well as petrol engines, but in to a lesser degree. Although cycle averaging reduces the effect of cyclic variations, and also attenuates random high frequency oscillations, nevertheless, the recorded mean cylinder pressure, and especially the rate of cylinder pressure rise diagrams, will still not be smoothed and consequently there will be unsmoothed rate of heat release diagram when these raw data are used in the apparent heat release calculations. Especially during combustion, the shock waves will cause a high oscillation in the rate of cylinder pressure rise, as shown in Figure A2.1. Therefore, for having a smoothed rate of heat release diagram, smoothed cylinder pressure and rate of cylinder pressure rise diagrams are needed. In order to obtain smooth cylinder pressure and rate of cylinder pressure rise diagrams, a spline function subroutine (Streit & Borman (1971)) was used to preclude noise and shock effects from

TABLE A2.1

Number	Engine Speed Ω_e (rpm)	Volumetric Efficiency (%)		Deviation from the Given Values
		Given Values by Jones (1965)	Smoothed Values Obtained by Polynomial*	
1	1000.0	81.20	81.2014	- 0.0014
2	1400.0	81.75	81.7163	0.0337
3	1500.0	81.90	81.9415	- 0.0415
4	2000.0	83.12	83.1056	0.0144
5	2500.0	83.72	83.7580	- 0.0080
6	2800.0	83.80	83.7974	0.0026

* Fitted polynomial to the given volumetric efficiency by Jones (1965):

$$\eta_v = 0.885126\ (10)^2 - 0.184424\ (10)^{-1}\ \Omega_e + 0.154\ (10)^{-4}\ \Omega_e^2 - 0.477233\ (10)^{-8}\ \Omega_e^3 + 0.50353\ (10)^{-12}\ \Omega_e^4$$

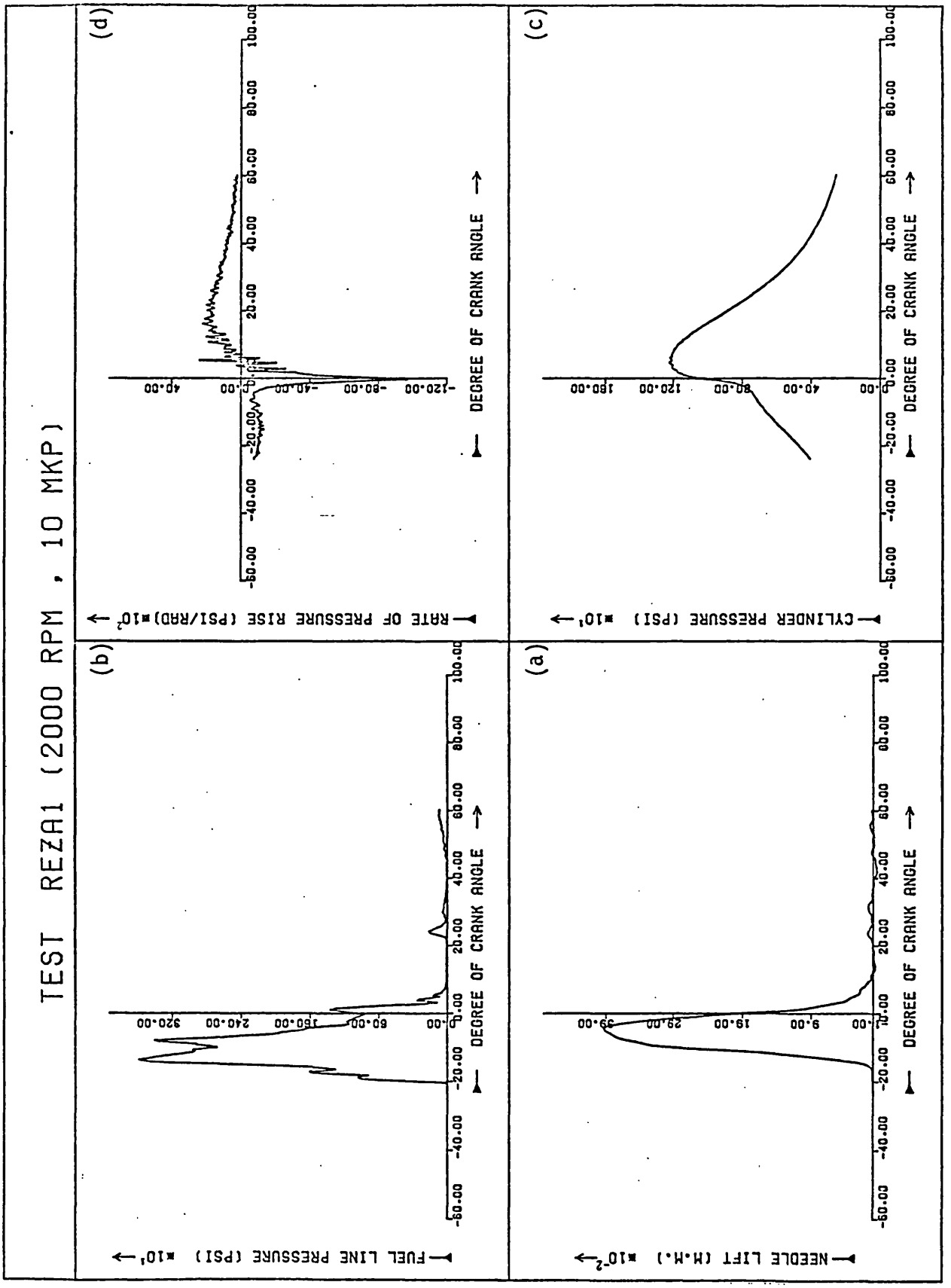


Figure A2.1: Typical unsmoothed diagrams for showing the shock waves on rate of cylinder pressure diagram

the signals. The recorded standard deviations of the cylinder pressure diagram, as reported, were needed in using this spline function.

The more the curve is smoothed, the more the value of its maximum is reduced, and consequently the maximum value of rate of heat release will be decreased. This effect, which has been reported by Marzouk & Watson (1976), was shown diagrammatically for the rate of cylinder pressure rise diagram in Figure A2.2. Figure A2.3 shows the smoothed cylinder pressure, the rate of cylinder pressure rise, the rate of heat release and the cumulative heat release curves obtained from this method for given operating conditions.

The results obtained were also compared with the results obtained by Watson & Marzouk (1974) and Khan, Greeves & Whithmore (1972) for the same engine.

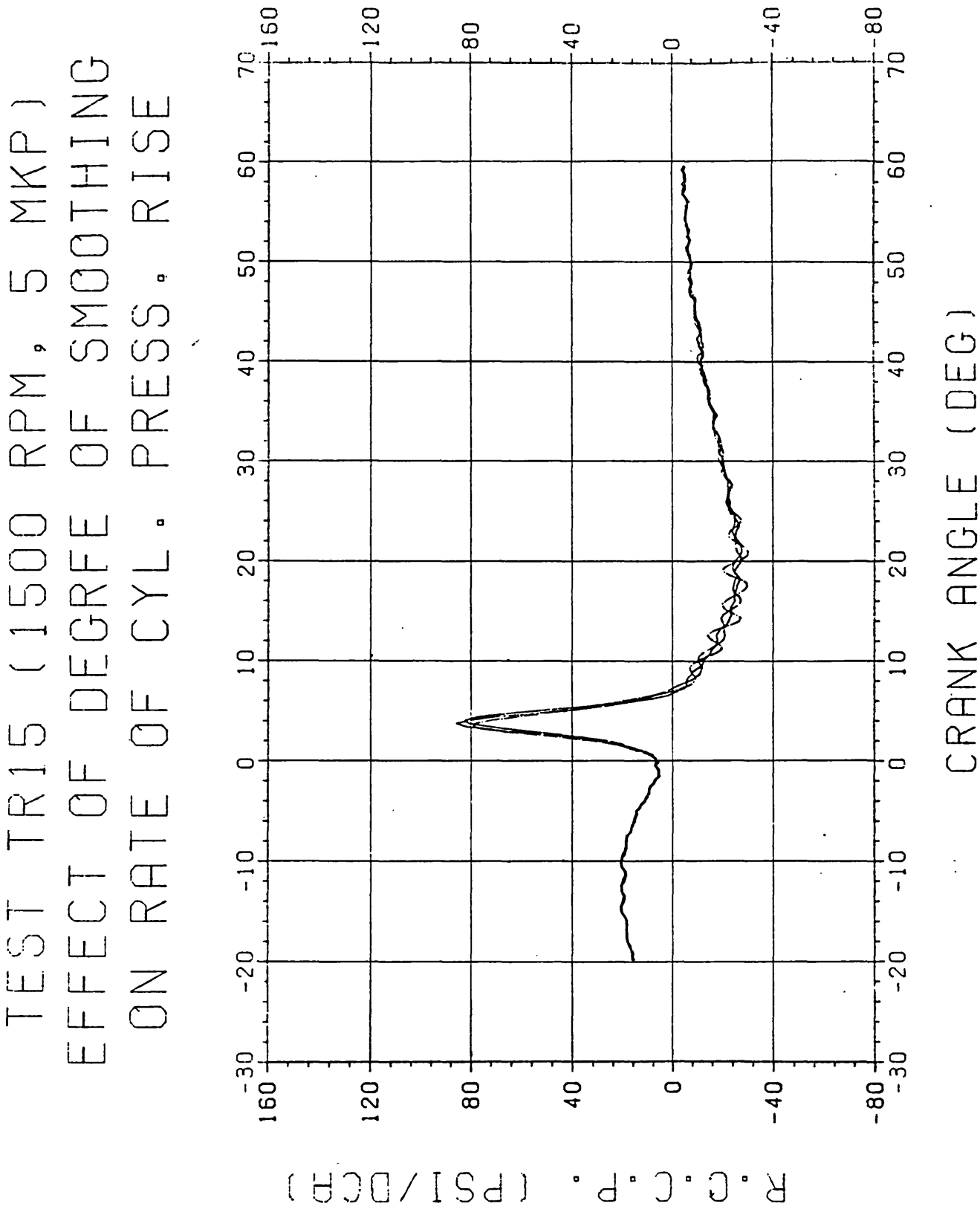


Figure A2.2: Effect of different degree of smoothing on the rate of cylinder pressure rise diagram

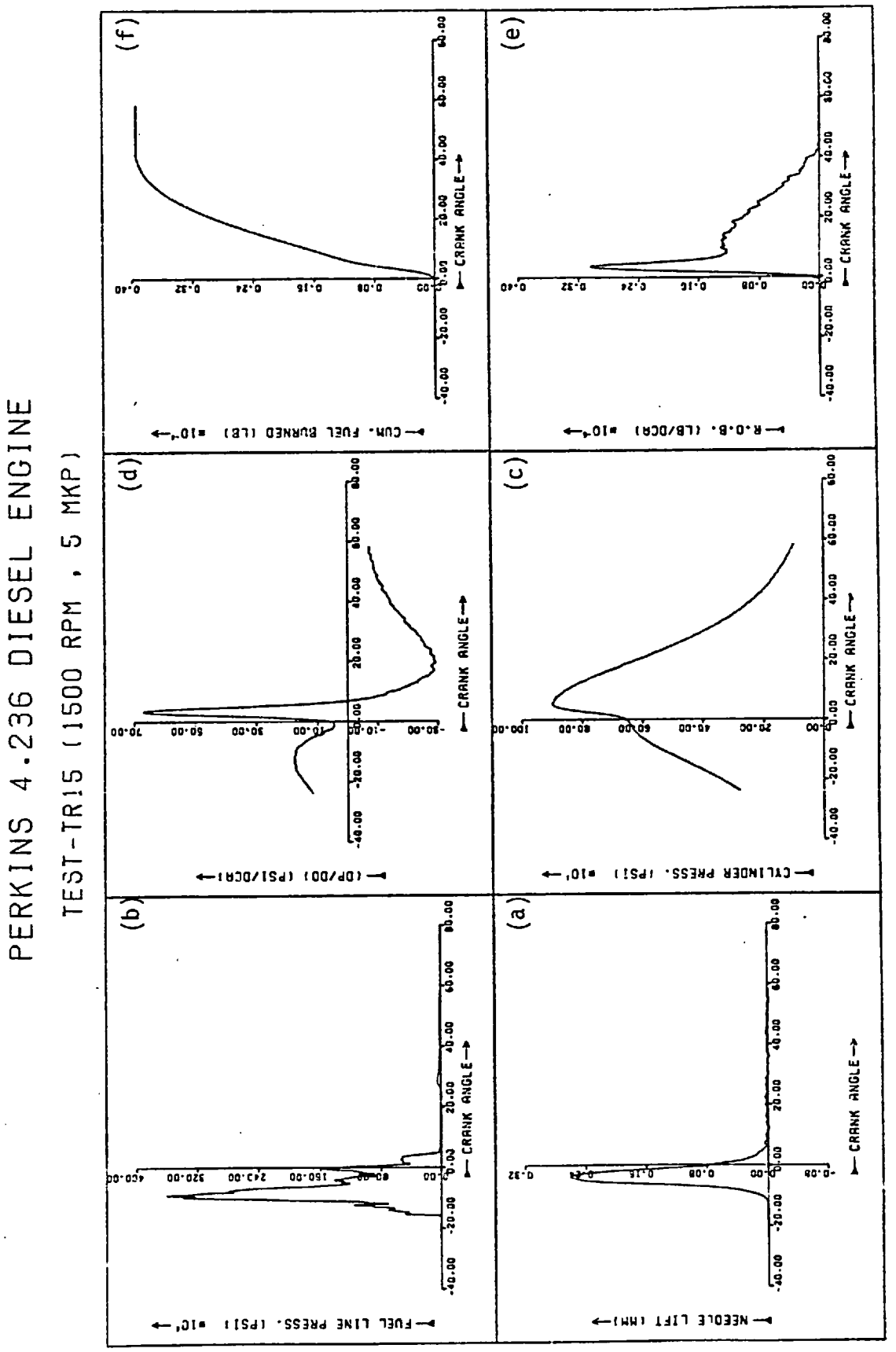


Figure A2.3: Experimental results at given operating conditions:

(a) Needle lift diagram
(b) Fuel-line pressure diagram
(c) Smoothed cylinder pressure diagram
(d) Smoothed rate of cylinder pressure rise diagram
(e) Apparent rate of heat release diagram
(f) Cumulative rate of heat release

APPENDIX A3

The CAV model is based on the assumption that air entrainment is controlled initially by a free jet, after impingement by a wall jet, and then intimate fuel/air mixing within the jets is controlled by turbulent diffusion. The amount of air entrainment can be predicted from a fuel jet model presented by Khan, Greeves & Whitmore (1972).

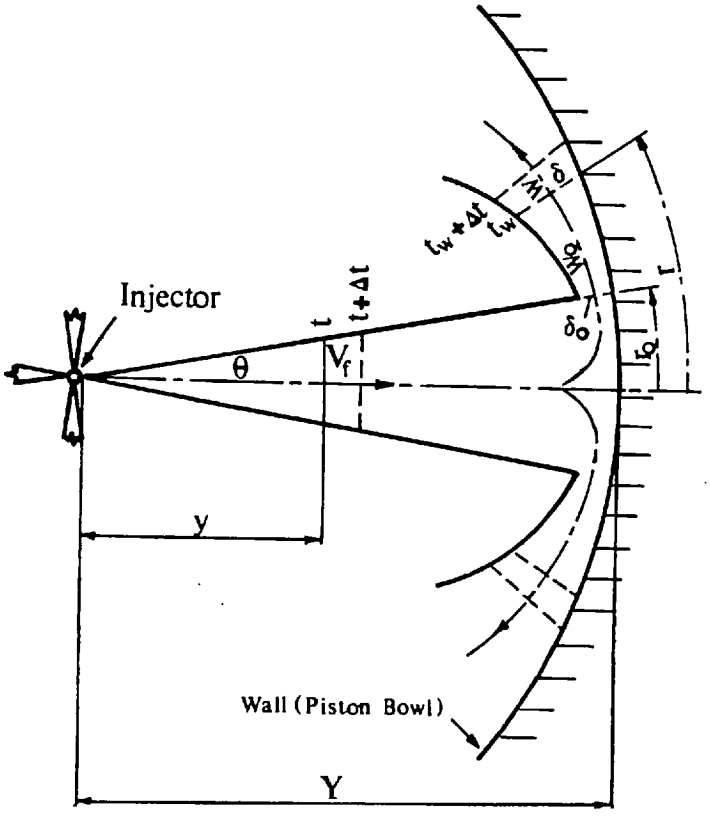


Figure A3.1: Fuel spray free jet and wall jet air entrainment model

A brief description of this model follows:

The injected fuel forms a free jet and, after impingement, it forms an axisymmetric wall jet (Figure A3.1). The rate of injection is assumed to be constant and the position of the free jet is governed by Schweitzer's

(1938) penetration equation:

$$y^2 = 1.042 \frac{10^6 D_n P_{inj}^{\frac{1}{2}} t}{Z} \qquad \begin{cases} 0 < y < Y \\ 0 < t < t_Y \end{cases} \tag{A3.1}$$

where y = penetration of free jet front (cm)

D_n = nozzle hole diameter (cm)

P_{inj} = injection pressure (atm)

t = time since beginning of injection (s)

Z = ratio of gas density relative to air at NTP

Y = impingement distance (cm)

t_Y = time for impingement (s)

The velocity of the jet tip can be obtained by differentiating equation (A3.1), $v = dy/dt$, and the time of impingement can be calculated by substituting impingement distance in equation (A3.1).

A square velocity profile of the jet front is assumed and the application of the momentum equation along the free jet axis gives the jet cone angle:

$$\tan^2\theta = 1.09\, Z \times 10^{-3} \tag{A3.2}$$

It is assumed that the variations of air entrainment are due to increases in the cone volume of the free jet. Therefore:

$$\Delta A \ (free\ jet) = \frac{\pi}{3} \rho_a \tan^2\theta \left[\frac{1.042 \times 10^6 P_{inj}^{\frac{1}{2}} D_n}{Z}\right]^{3/2} \times$$

$$\times \left[(t + \Delta t)^{3/2} - t^{3/2}\right] \tag{A3.3}$$

where A = mass of air entrained (gr)

ρ_a = gas density in cylinder (gr/cm^3)

θ = cone half angle

The above equation for the free jet is only valid under the conditions of $0 < t < t_Y$, i.e. from the beginning of injection up to impingement.

For calculating the air entrainment on the wall jet, the following assumptions have been made: the transition time, air entrainment during this transition, and the loss of kinetic energy in the direction of flow are all neglected. The velocity and the flow areas immediately before and after transition are the same. Thus, the initial conditions for the jet wall become:

$$r_o = T \tan \theta \tag{A3.4}$$

$$\delta_o = Y \frac{\tan \theta}{2} \tag{A3.5}$$

$$W_o = \frac{dY}{dt} \text{ at } y = Y \tag{A3.6}$$

$$Q_o = \pi Y^2 W_o \tan^2\theta \tag{A3.7}$$

where r_o = initial wall jet radius (cm)

δ_o = initial jet thickness on wall (cm)

W_o = initial velocity on the wall (cm/s)

Q_o = initial volume flow in wall jet (cm^3/s)

The velocity, jet thickness and volume flow on the wall can be calculated by assuming a square velocity profile for the jet front (Glauert (1956)):

$$W = W_o \left(\frac{r}{r_o}\right)^{-1.06} \tag{A3.8}$$

$$\delta = \delta_o \left(\frac{r}{r_o}\right)^{1.006} \tag{A3.9}$$

$$Q = 2\pi\, r\, \delta\, W = Q_o \left(\frac{r}{r_o}\right)^{0.946} \tag{A3.10}$$

The jet front velocity, $W = dr/dt$, and equation (A3.10) can be integrated to give:

$$\left(\frac{r}{r_o}\right)^{2.06} = \frac{t_w}{t_o} \tag{A3.11}$$

$$t_o = \frac{r_o}{2.06\, W_o} \tag{A3.12}$$

$$t_W = t + t_o - t_Y \tag{A3.13}$$

where t_o = initial reference time in wall jet (s)

t_W = current reference time in wall jet (s)

The increment in jet volume, and therefore in air entrainment caused by the wall jet, can now be evaluated by substituting equations (A3.10) and (A3.11) in equation (A3.14):

$$\Delta A\ (wall\ jet) = \rho_a \int_t^{t+\Delta t} Q\, dt \tag{A3.14}$$

$$\Delta A\ (wall\ jet) = \frac{\pi\, \rho_a\, Y^2\, W_o^2\, \tan^2\theta}{1.459\, t_o^{0.459}} \left[(t_W + \Delta t)^{1.459} - t_W^{1.459}\right] \tag{A3.15}$$

For any time t from the beginning of injection, equation (A3.1) can be used to determine whether or not the free jet has impinged. Using

equation (A3.3) or equation (A3.15), the increment of air entrainment in each time interval is calculated. After the injection period, it is assumed that the jet continues to proceed as before, and the corresponding reduction in jet volume is calculated by subtracting the vacuum at the back of the jet. The air entrainment for the jet back can be calculated from equations (A3.3) and (A3.15) by replacing t with $(t-t_p)$, where t_p is the injection period. The net increment in air entrainment is therefore:

$$\Delta A = \Delta A \text{ (jet front)} - \Delta A \text{ (jet back)} \qquad \text{(A3.16)}$$

To take into account the effects of the air charge motion due to piston motion or port induced swirl, an air entrainment ratio was introduced:

$$\Delta A \text{ (actual)} = E_r \, \Delta A \text{ (stagnant)} \qquad \text{(A3.17)}$$

The macro-mixed quantities of air and fuel within the jet boundary, as determined by ΔA and X, are assumed to be micro-mixed according to the equations given by Grigg & Syed (1969):

$$\dot{M}_a = D_i \, V_f \, (A - M_a) \qquad \text{(A3.18)}$$

$$\dot{M}_f = D_i \, V_f \, (m_f - M_f) \qquad \text{(A3.19)}$$

where M_a = mass of micro-mixed air (gr)

D_i = diffusivity constant (cm^{-1})

V_f = jet front velocity (cm/s)

m_f = fuel injected (gr)

M_f = mass of micro-mixed fuel (gr)

Heat release is computed from the micro-mixed quantities of fuel, M_f, and air, M_a.

The first phase of the combustion is dealt with empirically as follows. Experimental values of injection delay are used, and the rate of heat release follows a triangle rate law with a six or eight degree crank angle base, as long as premixed fuel and air is present.

Figure R5 is a typical heat release diagram obtained by the CAV model. From the results obtained using this model, it was found that for naturally aspirated diesel engines, the second hump in the rate of heat release diagram due to diffusion burning is much higher than the real one (Figure A3.2). Another factor was therefore introduced to decrease the air entrainment due to the wall jet which controls the second hump:

$$\Delta A \text{ (wall jet)} = F_W \, \Delta A \text{ (calculated)} \qquad \text{(A3.20)}$$

Values of diffusivity constant which control the rate of heat release were needed to be determined for the operating conditions under the test. These values were functions of engine speed and air swirl ratio. Thus, having one experimental heat release diagram at each speed, the heat release can be predicted for other injection rates, injection timing and fuellings.

An attempt was made to simulate the experimental rate of injection by the CAV model, but the attempt was not successful.

Since the results published in Khan et al (1972) compare the cumulative heat release with the experimental results and no comparison is made with the rate of heat release, it is difficult to discern the defects of the model, as shown in Figure A3.2. Although, by introduction of the F_W, air entrainment ratio and diffusivity constant, the CAV model

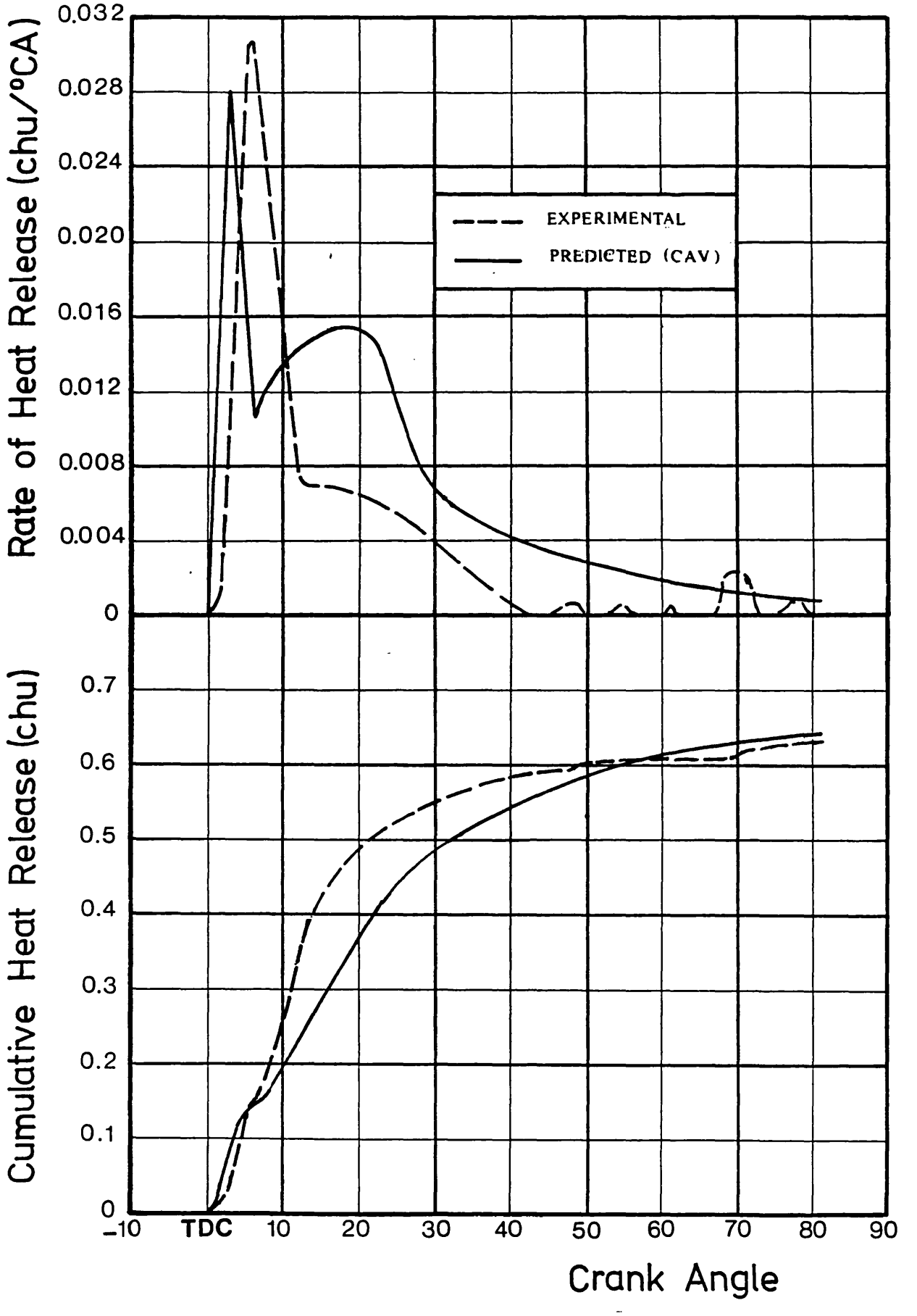


Figure A3.2: CAV predicted results for rate of heat release and cumulative heat release for a speed of 2000 rpm and a load of 5 mkp operating conditions

can be modified, nevertheless the efforts needed for finding the best values for these constants at each operating condition, and also the degree of empiricism involved, justifies substitution of this model by the Marzouk model (see Section 3.4.2).

APPENDIX A4

This appendix describes the method used to optimize the values of a_1, a_2 and a_3 over a wide range of operating conditions. By taking the logarithms of both sides of equation (A4.1), the equation will convert to a linear equation with regard to a_1, a_2 and a_3 as the variables:

$$ID_i = a_1 \exp (a_2/T_{mi})/P_{mi}^{a_3} \tag{A4.1}$$

$$\ln ID_i = \ln a_1 + \frac{a_2}{T_{mi}} - a_3 \ln P_{mi} \tag{A4.2}$$

For optimum values of these parameters, the sum of squares deviation of each calculated value to the real ones should be minimum. This can be mathematically written as:

$$s = \sum_{i=1}^{n} \left[D_i - a - \frac{b}{T_{mi}} - c \ln P_{mi} \right]^2 \tag{A4.3}$$

where s = the sum of squares deviation errors; and also:

$$D_i = \ln ID_i \quad ; \quad a = \ln a_1 \quad ; \quad b = a_2 \quad ; \quad c = -a_3$$

For minimizing the variation of s due to the variation of a_1, a_2 and a_3, we can write the following three equations:

$$\frac{\partial s}{\partial a} = \sum_{i=1}^{n} - \left[D_i - a - \frac{b}{T_{mi}} - c \ln P_{mi} \right] = 0 \tag{A4.4}$$

$$\frac{\partial s}{\partial b} = \sum_{i=1}^{n} - \frac{1}{T_{mi}} \left[D_i - a - \frac{b}{T_{mi}} - c \ln P_{mi} \right] = 0 \tag{A4.5}$$

$$\frac{\partial s}{\partial c} = \sum_{i=1}^{n} - \ln P_{mi} \left[D_i - a - \frac{b}{T_{mi}} - c \ln P_{mi} \right] = 0 \qquad \text{(A4.6)}$$

After some manipulation, the linear system equations (A4.7) can be derived from the three equations (A4.4), (A4.5) and (A4.6):

$$\begin{bmatrix} n & \sum_{i=1}^{n} \frac{1}{T_{mi}} & \sum_{i=1}^{n} \ln P_{mi} \\ \sum_{i=1}^{n} \frac{1}{T_{mi}} & \sum_{i=1}^{n} \frac{1}{T_{mi}^2} & \sum_{i=1}^{n} \frac{\ln P_{mi}}{T_{mi}} \\ \sum_{i=1}^{n} \ln P_{mi} & \sum_{i=1}^{n} \frac{\ln P_{mi}}{T_{mi}} & \sum_{i=1}^{n} \ln^2 P_{mi} \end{bmatrix} \times \begin{bmatrix} a \\ b \\ c \end{bmatrix} = \begin{bmatrix} \sum_{i=1}^{n} D_i \\ \sum_{i=1}^{n} \frac{D_i}{T_{mi}} \\ \sum_{i=1}^{n} D_i \ln P_{mi} \end{bmatrix} \qquad \text{(A4.7)}$$

In order to find a, b and c, and consequently a_1, a_2 and a_3, the three linear system equations (A4.7) should be solved. Kramer's method for solving linear system equations was used and a subroutine called HAL was written on the basis of this method (Conte (1965)).

The program which was written to calculate the optimum value for a_1, a_2 and a_3 first reads the total number of tests and then the ignition delay, mean temperature and pressure during the delay, and the engine speed for every test. Subroutine HAL is called after each of the sums of the matrices elements are calculated. The program of calculating the sums of the matrices elements is called subroutine SIG2. Programs SIG2 and HAL are provided at the end of this appendix. The values of these constants are printed after writing all the input data received by the program.

Figure 3.6(c) shows the comparison of predicted and experimental ignition delays.

The optimization program has been checked with the results obtained

from another program written based on an analytical solution for only three test points, whereby an optimization procedure is needed. For this case, a_1, a_2 and a_3 can be found by the following equations:

$$a_3 = \frac{T_a (T_c - T_b) \ln (\frac{ID_a}{ID_b}) - T_c (T_b - T_a) \ln (\frac{ID_b}{ID_c})}{T_c (T_b - T_a) \ln (\frac{P_b}{P_c}) - T_a (T_c - T_b) \ln (\frac{P_a}{P_b})} \qquad \text{(A4.8)}$$

$$a_2 = \frac{T_b T_a}{T_b - T_a} \ln \left[\frac{ID_a}{ID_b} (\frac{P_a}{P_b})^{c_3} \right] \qquad \text{(A4.9)}$$

$$a_1 = \frac{ID_a (P_a)^{c_3}}{\exp (c_2/T_a)} \qquad \text{(A4.10)}$$

Similar results for a_1, a_2 and a_3 from two different programs for each of the three test points will confirm the reliability of the written optimization program.

```
      SUBROUTINE SIG2(N,DI,RPM,TM,PM)
C     ***************************************
C     PROGRAM FOR CALCULATING THE COEFFICIENTS *
C     OF IGNITION DELAY CORRELATION (WOLFER)   *
C     BY THE AID OF EXPERIMENTAL DATA          *
C     DI=C1*EXP(C2/TM)/PM**C3                  *
C     TM = MEAN CYLINDER TEMPERTURE DURING     *
C          THE IGNITION DELAY ( K)             *
C     PM = MEAN CYLINDER PRESSURE DURING       *
C          THE IGNITION DELAY (BAR)            *
C     DI = IGNITION DELAY (MS)                 *
C     N  = NUMBER OF POINTS                    *
C     C1,C2,C3 ARE CONSTATS                    *
C     RPM= ENGINE SPEED                        *
C     THIS SUBROUTINE CALLS SUBROUTINE HAL     *
C     FOR SOLVING LINEAR SYSTEM EQUATIONS      *
C     26/2/76  [RMR]                           *
C     ***************************************
      DOUBLE PRECISION A(12)
      DIMENSION DI(20),RPM(20),TM(20),PM(20)
      DO 1 I=1,12
    1 A(I)=0.
      DO 2 I=1,N
      B=ALOG(PM(I))
      B1=ALOG(DI(I))
      A(1)=A(1)+1.
      A(2)=A(2)+1./TM(I)
      A(3)=A(3)+B
      A(4)=A(2)
      A(5)=A(5)+1./(TM(I)*TM(I))
      A(6)=A(6)+B/TM(I)
      A(7)=A(3)
      A(8)=A(6)
      A(9)=A(9)+B*B
      A(10)=A(10)+B1
      A(11)=A(11)+B1/TM(I)
    2 A(12)=A(12)+B1*B
      CALL HAL(A)
      RETURN
      END

      SUBROUTINE HAL(A)
      DOUBLE PRECISION A(12),DD,DX1,DX2,DX3
C     ***********************************************
C     PROGRAM FOR SOLVING A THREE LINEAR SYSTEM     *
C     EQUATION BY CRAMER'S METHOD                   *
C     THIS SUBROUTINE IS CALLED BY SUBROUTINE SIG2  *
C     1/3/76  [RMR]                                 *
C     ***********************************************
      DD=A(1)*(A(5)*A(9)-A(6)*A(8))-A(2)*(A(4)*A(9)-A(6)*A(7))+A(3)*(A(4
     1)*A(8)-A(5)*A(7))
      DX1=A(10)*(A(5)*A(9)-A(6)*A(8))-A(2)*(A(11)*A(9)-A(6)*A(12))+A(3)*
     1(A(11)*A(8)-A(5)*A(12))
      DX2=A(1)*(A(11)*A(9)-A(6)*A(12))-A(10)*(A(4)*A(9)-A(6)*A(7))+A(3)*
     1(A(4)*A(12)-A(11)*A(7))
      DX3=A(1)*(A(5)*A(12)-A(11)*A(8))-A(2)*(A(4)*A(12)-A(11)*A(7))+A(10
     1)*(A(4)*A(8)-A(5)*A(7))
      WRITE(6,85)DD,DX1,DX2,DX3
   85 FORMAT(//4(D14.6,2X)/)
      X1=DX1/DD
      X2=DX2/DD
      X3=DX3/DD
      WRITE(6,7)(A(I),I=1,12)
    7 FORMAT(3(D14.6,2X))
      WRITE(6,4)X1,X2,X3
    4 FORMAT(//3G14.6)
      C1=EXP(X1)
      C2=X2
      C3=-X3
      WRITE(6,66)C1,C2,C3
   66 FORMAT(1X,5HC1 = ,G14.6,1X,5HC2 = ,G14.6,1X,5HC3 = ,G14.6//)
      RETURN
      END
```

APPENDIX A5

The ideal adiabatic equation of PV^{γ} = constant does not hold during the compression for several reasons: (i) the increase of the specific heat coefficients of gases due to the rising temperature; (ii) impurity of air due to residual exhaust gases; (iii) heat losses to the combustion chamber. In practice, the adiabatic process is normally replaced by PV^{n} = constant (where n is an exponential parameter and its value changes according to the existing cylinder conditions).

Judge (1967) quoted a value of about 1.35 for n for direct injection engines at moderate speeds and with relatively higher values at higher engine speeds and relatively lower values at lower speeds. However, the best value of n at each engine operating condition can be computed by analysing the cylinder pressure diagram using the least square optimization program.

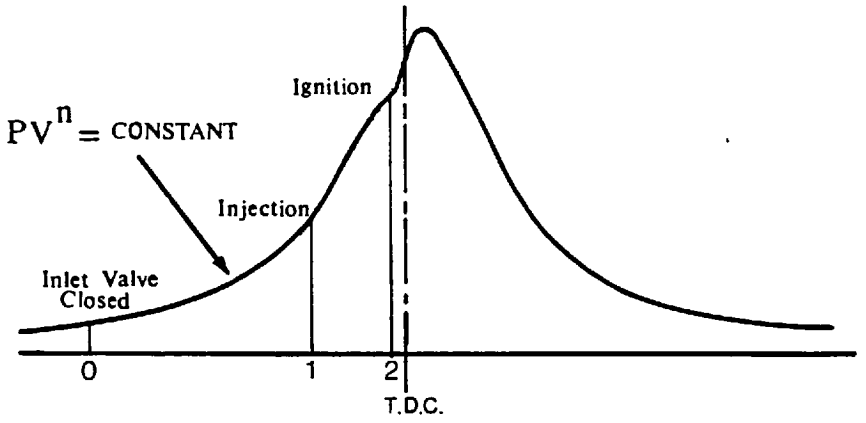


Figure A5.1: Typical cylinder pressure diagram

The equation PV^{n} = constant is applied for the compression process from the time of inlet valve closure to the instant of ignition occurrence.

Thus, for each point, we have (Figure A5.1):

$$P_o V_o^n = P_1 V_1^n = P_2 V_2^n = P_i V_i^n = C \qquad \text{(A5.1)}$$

where P = cylinder pressure

V = instantaneous cylinder volume

i = index designated to instants between inlet valve closure to the instant of ignition occurrence

On a log-log plot:

$$ln\ P_i + n\ ln\ V_i = ln\ C \qquad \text{(A5.2)}$$

$$s = \sum_{i=1}^{m} \left(ln\ P_i + n\ ln\ V_i - ln\ C \right)^2 \qquad \text{(A5.3)}$$

for having a least square deviation of $\partial s/\partial n = 0$, therefore:

$$\frac{\partial s}{\partial n} = \sum_{i=1}^{m} 2\ ln\ V_i \left(ln\ P_i + n\ ln\ V_i - ln\ C \right) = 0 \qquad \text{(A5.4)}$$

$$n = \frac{ln\ C \sum_{i=1}^{m} ln\ V_i - \sum_{i=1}^{m} ln\ V_i\ ln\ P_i}{\sum_{i=1}^{m} ln\ V_i^2} \qquad \text{(A5.5)}$$

A program called GAMMA based on the above equation, was written for calculating n, and therefore the values of n were found for different operating conditions with the aid of cylinder pressure diagrams.
Table 3.2 shows the values obtained for n for different operating conditions.

APPENDIX A6

The effective valve area is the product of the coefficient of discharge and the minimum valve area. Calculating the minimum valve flow area for the standard type valve, three different cases are recognized:

Case 1: This case is shown in Figure A6.1(a) and corresponds to a lift range of $0 < L/D_v < 25/D_v$ where a frustrum of a cone of slant height is perpendicular to the valve seat faces:

$$A_m = 2.22 * L\ (D_v + L/2) \tag{A6.1}$$

where A_m = minimum valve flow area

L = valve lift

D_v = valve diameter

S = distance as shown in figure

Case 2: The cone of minimum area is no longer perpendicular to the valve seat faces (Figure A6.1(b)):

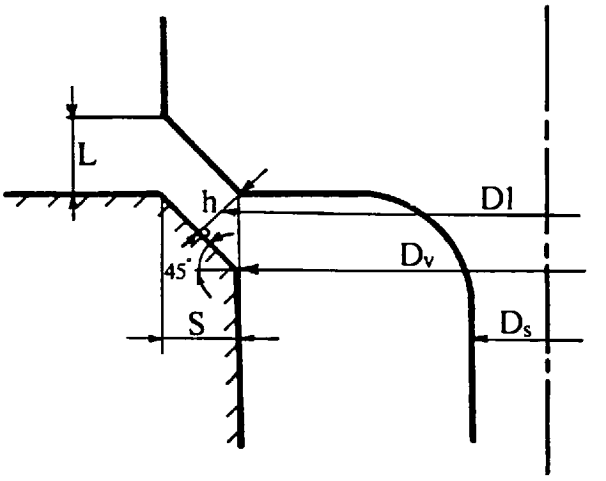
$$A_m = \pi\ (D_v + S)(L^2 + 2\ S^2 - 2\ L\ S)^{\frac{1}{2}} \tag{A6.2}$$

The lift range, which is a constraint for equation (A6.2), is given by the following inequality:

$$\frac{2S}{D_v} < \frac{L}{D_v} < \left\{\left[\frac{D_v^2 - D_s^2}{D_v + S}\right)^2 - S^2\right]^{\frac{1}{2}} + S\right\}/D_v \tag{A6.3}$$

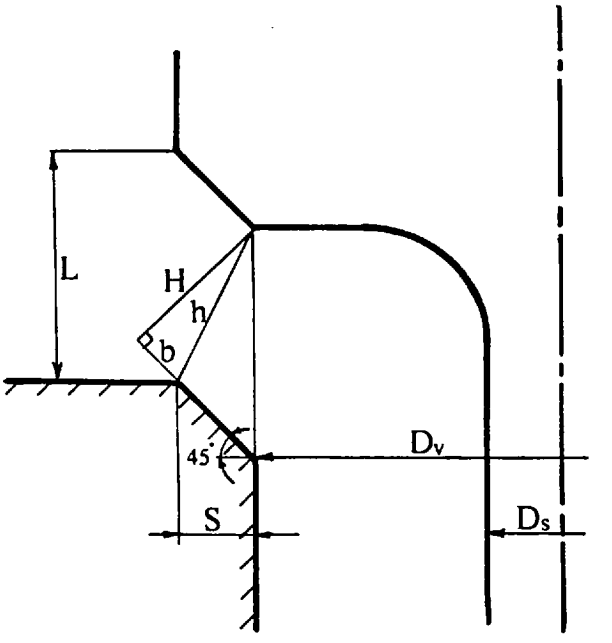
where D_s = stem diameter

Case 1: h is perpendicular to the valve seat faces



(a)

Case 2: h is not perpendicular to the valve seat faces



(b)

Case 3: $h > \frac{D_v - D_s}{2}$

Figure A6.1: Position of standard type valve for different lift

Case 3: In this case, the area of the valve minus the area of the valve stem is the minimum area:

$$A_m = \frac{\pi}{4} (D_v^2 - D_s^2) \tag{A6.4}$$

where:

$$\frac{L}{D_v} > \left\{ \left[\frac{D_v^2 - D_s^2}{D_v + S})^2 - S^2 \right]^{\frac{1}{2}} + S \right\} / D_v \tag{A6.5}$$

For calculating the effective valve area for the inlet and exhaust valves, a program was written based on equations (A6.1) to (A6.5). The geometry of the valves and valve lift diagrams were supplied by Perkins. The coefficients of discharge are based on the data given by Kastner, Williams & White (1963). Calculation of the coefficient of discharge was thus based on the following correlations which were obtained by curve fitting:

(a) For $L/D_v < 0.1$:

$$C_d = 1.0 - 0.77102 * (\frac{L}{D_v}) - 17.1207 + (\frac{L}{D_v})^2 + 128.309 * (\frac{L}{D_v})^3 \tag{A6.6}$$

(b) For $0.1 < L/D_v < 0.275$:

$$C_d = 0.953311 - 12.4012 * (\frac{L}{D_v}) + 190.885 * (\frac{L}{D_v})^2 - \\ - 981.403 * (\frac{L}{D_v})^3 + 1576.07 * (\frac{L}{D_v})^4 \tag{A6.7}$$

(c) For $L/D_v > 0.275$:

$$C_d = - 10.0075 + 131.763 * (\frac{L}{D_v}) - 620.603 * (\frac{L}{D_v})^2 + \\ + 1306.78 * (\frac{L}{D_v})^3 - 1030.27 * (\frac{L}{D_v})^4 \tag{A6.8}$$

Figure A6.2 illustrates the diagrams of the effective valve area for the inlet and exhaust valves based on the above correlations.

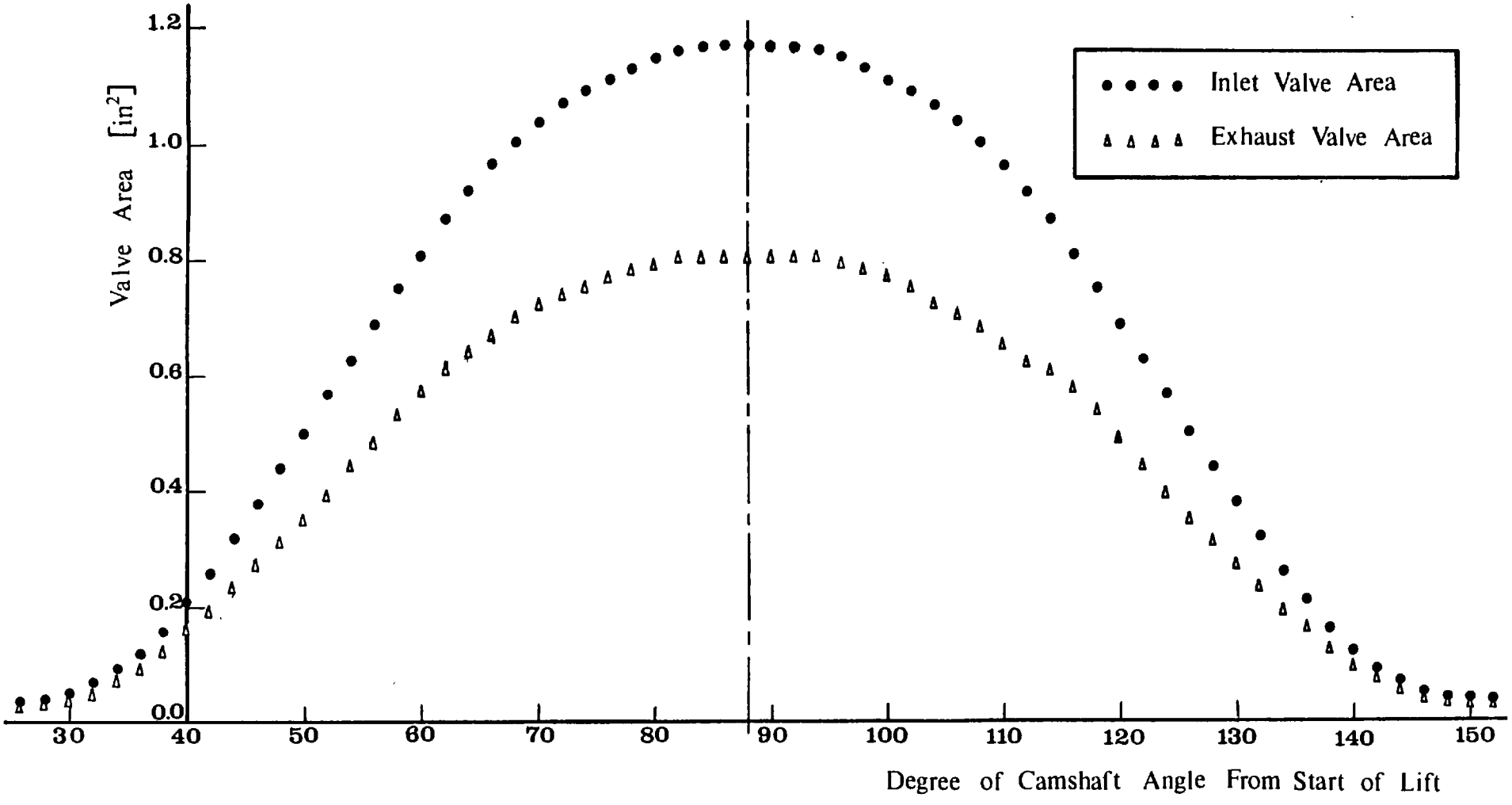


Figure A6.2: Effective valve area for inlet and exhaust valves

APPENDIX B1

SPECIFICATIONS OF THE ENGINE

Engine make and model		:	Perkins 4.236
Type		:	4-stroke, compression ignition, naturally aspirated
Combustion system		:	Direct injection
Number of cylinders		:	4
Firing order		:	1, 3, 4, 2
Compression ratio		:	16:1
Bore		:	3.875 in
Stroke		:	5 in
Swept volume		:	236 in^3
Maximum torque		:	193 lb.ft
Power		:	72 bhp maximum continuous
Speed range		:	500 - 2800 rpm
Valve timing:	IVO	:	19^o BTDC
	IVC	:	49^o ABDC
	EVO	:	52^o BBDC
	EVC	:	16^o ATDC
Fuel pump		:	CAV distributor type (DPA) with hydraulic governor
Injector type		:	CAV multi-hole type nozzle (4)
Static injection timing		:	26^o BTDC
Opening injector pressure		:	170 atm
Piston area		:	18.5 in^2
Exhaust valve area		:	1.62 in^2
Inlet valve area		:	2.38 in^2
Cylinder head area		:	10.79 in^2

Exhaust manifold volume	:	32.6 in^3
Inlet manifold volume	:	73.2 in^3
Piston bowl volume	:	3.35 in^3
Piston temperature*	:	270^oC
Exhaust valve temperature*	:	650^oC
Inlet valve temperature*	:	400^oC
Cylinder head temperature*	:	230^oC
Linear temperature*	:	125^oC
Water temperature*	:	100^oC
Specific weight of fuel	:	0.82 gr/cm^3

---

* Estimated component temperature data, supplied by Perkins, corresponds to the full load condition. For part load conditions, a pro-rata reduction of the temperature difference was assumed.

APPENDIX B2

(a) Specifications of Cylinder Pressure Transducers

Transducer make and model	:	Vibro-meter (AVL) 8Q P500 C
Type	:	Piezo-electric
Pressure range	:	Up to 500 kg/cm^2 or 7100 psi
Resolution	:	0.004 kg/cm^2 or 0.06 psi
Temperature range	:	Up to 240^{o}C or 465^{o}F
Sensitivity variation	:	0.01%/^{o}C
Cooling	:	4 - 5 gallons per hour
Capacity	:	3.1 pF
Natural frequency	:	100 kHz
Damping	:	0.35 log decrement

(b) Specifications of Fuel-Line Pressure Transducers

Transducer make and model	:	Vibro-meter (AVL) 31 DP 1200 E-2.5
Type	:	Strain gauge
Measuring elements	:	Strain gauge full bridge 120 ohms
Measuring range	:	1200 kg/cm^2 (17,000 psi)
Sensitivity	:	1 mV/V referred to full scale
Excitation voltage	:	Maximum 5 V
Non-linearity and hysteresis	:	< 0.5%
Operating temperature range	:	- 10 to + 90^{o}C (14 to 194^{o}F)
Temperature influence on zero point and sensitivity	:	0.04%/^{o}C
Overload	:	50% over full scale
Insulation resistance	:	1000 ohms

(c) Specifications of Needle Lift Transducers

Transducer make	:	They were built at the College
Type	:	Inductive
Natural frequency	:	100 kHz
Resistance	:	53.4 ohms
Inductance	:	940 μH
Output impedance	:	644 ohms

APPENDIX B3

(a) Specifications of Charge Amplifiers

Model	:	E 568
Output voltage	:	10 V
Output impedance	:	100 ohms
Input impedance	:	10^{11} ohms for short time constant
	:	10^{14} ohms for long time constant
Frequency response	:	DC to 150 kc/s
Linearity error	:	0.1%
Noise	:	1 mV

(b) Specifications of Operational Differential Amplifiers

Model	:	48 K (Analogue Device Company)
Rated output	:	± 10 V and ± 20 mA
Offset voltage versus temperature	:	± 15 V/^{o}C
Input impedance	:	10^{11} ohms
Input noise	:	3 μV
Frequency response	:	15 MHz

(c) Specifications of Carrier Amplifiers

Model	:	375 AVL
Carrier frequency	:	100 kHz
Impedance	:	600 ohms
Output voltage	:	12 V

APPENDIX B4

Program Listings

(a) PERFU2

(b) AVESTD

```
        .TITLE PERFU2
        .GLOBL .XXMON,PUNCHP
        .GLOBL STATIS,HISTOR,AUTOCR,CROSSC
        /*************************************
        /PROGRAM TO ACEPT DP/DT & P FROM      *
        /CYLINDER ONE                        *
        /FUEL LINE PRESSUER FROM CYLINDER ONE *
        /                                    *
        /INPUTS FROM ADC , ANALYSE, AND      *
        /STORE IN MEMORY (BLANK COMMON)       *
        /NO. OF CYCLES DEFINED BY OPERATOR    *
        /                                    *
        /INPUT 0 - FUEL LINE PRESS.          *
        /INPUT 1 - CYLINDER PRESS.           *
        /INPUT 2 - FUEL LINE PRESS.          *
        /INPUT 3 - RATE OF CYLINDER PRESS.   *
        /                                    *
        /ANALYSIS : FIND THE STARTING ANGLE OF *
        /           INJECTION , THE MAX (DP/DT) ,*
        /           THE LOCATION OF MAX (DP/DT) &*
        /           THE PEAK CYLINDER PRESSURE . *
        /                                    *
        /ASSIGN PP TO SIX                    *
        /                                    *
        /R.M.R. VERSION [V2]                 *
        /JUNE 1976                           *
        /ONE CYLINDER TEST VERSION           *
        /*************************************
TTO=-3
IN=0
OUT=1
        .IODEV -3
SYNC    .INIT TTO,OUT,RESTRT
        /PRINT IDENTIFIER
        .WRITE TTO,2,IDENT,20
        .WAIT TTO
        /
        /ROUTINE TO SET UP FINAL 4000        BB
        /WORD DATA BUFFER STORE
        .EBREL
RESTRT  LAC .XXMON
        DAC PTXX        /POINTER TO .XX
        .DEC
        LAC (-4000
        .OCT
        DAC COUNT4
        LAC (-1750      /1000 DEC.
        DAC COUNTX
ZERO    DZM* PTXX
        ISZ PTXX
        ISZ COUNT4
        JMP ZERO
        LAC .XXMON
        DAC PTXX
        /
        .DEFIN NEG,LOC
        CMA
        TAD (1
        DAC LOC
        .ENDM
        HLT
        700004          /CLOCK OFF
        /ADC OPERATING SUBROUTINE
ADC     LAC (DATA
        DAC DATAPT
        LAW -740
        DAC COUNTO
        DAC COUNT
        LAW -170        /120 DEC.
        DAC COUNT1
        LAW -74                              CC
        DAC COUNT2
        DAC COUNT3
        LAC (DATA
        DAC DATAPT
        DZM* DATAPT                          AA
        ISZ DATAPT
        ISZ COUNT
        JMP AA
AGAIN   LAC (DATA
        DAC DATAPT
        701112          /READ ADC & RESET
        701101          /FLAG
        JMP .-1
        701112          /READ ADC & RESET
        LAC (40         /FOUR CHANNEL MODE
        705604          /LOAD CHANNEL SELECTION
        705642          /CLEAR MEMORY
        LAC (740        /480 DEC
        705624          /SET COUNT TO 480
        705641          /FLAG TO INDICATE COMPLETION
        JMP .-1
        705642          /CLEAR & RESET
        705621          /SETUP REPLAY CYCLE
FLAG1   705601
        JMP .-1
        705612          /READ ADC & RESET
        DAC* DATAPT
        ISZ DATAPT
        ISZ COUNTO
        JMP FLAG1
        /END OF READING FROM ADC
        LAW -170
        DAC TIMI1
        DZM TIMI2       /CLEAR TIMI2
        DZM TIMI3       /CLEAR TIMI3
        DZM DIFU1       /CLEAR DIFU1
        LAC (DATA
        DAC ADDR
        LAC* ADDR       /AC=FLP1
        NEG HOLD        /HOLD=-FLP1
        ISZ ADDR        /NEXT ADDR IN DATA
        ISZ ADDR
        ISZ TIMI1       /& ITS LOCATION
        NOP
        LAC TIMI1
        SMA
        JMP CC
        LAC* ADDR       /AC=FLP2
        DAC LAST        /LAST=FLP2
        TAD HOLD        /AC=FLP2-FLP1
        DAC DIFU2
        LAC HOLD
        DAC CHECP       /CHECP=-FLP1
        LAC LAST
        NEG HOLD        /HOLD=-FLP2
        LAC DIFU2
        SPA
        JMP BB          /DISCARD NEG SLOPES
        LAC DIFU1       /CURRENT MAX SLOPE
        NEG DIFUO       /NEGATE
        TAD DIFU2       /AC=DIFU2-DIFU1
        SPA
        JMP BB
        LAC CHECP       /CHECK FOR CORRECT VALUE
        TAD (167
        SPA
        JMP .+2
        JMP BB
        LAC DIFU2
        DAC DIFU1       /NEW MAX SLOPE
        LAC TIMI1
        DAC TIMI2       /TIME OF NEW MAX SLOPE
        JMP BB
        LAW -73
        DAC TIMI1
        ISZ ADDR
        LAC* ADDR       /AC=P1
```

```
        NEG MAXP        /MAXP=-P1
        ISZ ADDR        /NEXT ADDR IN DATA
        ISZ ADDR
        LAC* ADDR       /AC=DP1
        NEG MAX1        /MAX1=-DP1
DD      ISZ ADDR
        ISZ ADDR
        LAC* ADDR       /AC=P2
        DAC DIFFP       /DIFFP=P2
        TAD MAXP        /AC=P2-P1
        SPA
        JMP .+5
        LAC DIFFP       /AC=P2
        NEG MAXP        /MAXP=-P2
        ISZ ADDR
        ISZ ADDR
        LAC* ADDR       /AC=DP2
        DAC DIFF2       /DIFF2=DP2
        TAD MAX1        /AC=DP2-DP1
        SMA
        JMP .+7
        LAC DIFF2
        NEG MAX1
        LAC TIMI1
        DAC TIMI3
        ISZ TIMI1
        JMP DD
EE      LAC TIMI2
        TAD (-54        /171-245=-54 IN OCTAL
        DAC* PTXX       /TIMI2 IN 1ST LOCATION
        ISZ PTXX
        LAC MAX1
        NEG MAX1
        DAC* PTXX       /MAX1(DP/DT) 2ND LOCATION
        ISZ PTXX
        LAC TIMI3
        TAD (47         /75-26=47 IN OCTAL
        DAC* PTXX       /TIMI3 3RD LOCATION
        ISZ PTXX
        LAC MAXP
        NEG MAXP
        DAC* PTXX       /MAXP 4TH LOCATION
        ISZ PTXX
        ISZ COUNTX      /ALL CYCLES READ?
        JMP ADC         /NO;GO TO NEXT CYCLE
        700044          /CLOCK RESTORE
        JMS* STATIS
        JMS* HISTOR
        JMS* AUTOCR
        JMS* CROSSC
        HLT
        JMS* PUNCHP
        /
        JMP RESTRT
        /
        /
IDENT   DATA-IDENT/2*1000
        0
        .ASCII '[ADC]'(07)(07)(07)(07)(15)(12)
DATA    .BLOCK 740
COUNT4;PTXX;;TIMI1;HOLD;DIFF2;MAX1;DIFF0
LAST;DIFU0;DIFU1;DIFU2;TIMI2;COUNT2;COUNT3
CHECP;COUNT1;COUNTX;DIFFP;COUNT0
TIMI3;MAXP;COUNT;DATAPT;ADDR
        .END
```

```
        .TITLE AVESTD
        .GLOBL FUNCH1,IVALUE,ISTEAD
        /*****************************************
        /PROGRAM FOR READING & CALCULATING       *
        /P,RP,FLP,NL FOR 128 CYCLES              *
        /STANDARD DIVIATION OF CYLINDER PRESSURE *
        /                                        *
        /MAY 1,1975  (RMR)                       *      CC
        /                                        *
        /CHANNEL SELECTION                       *
        /(1)= CYLINDER PRESSURE (P)              *
        /(2)= RATE OF CYLINDER PRESSURE (RP)     *
        /(3)= FUEL LINE PRESSURE (FLP)           *      DD
        /(4)= NEEDLE LIFT (NL)                   *
        /*****************************************
AVESTD  LAW -5
        DAC TEST$
        LAW -200        /-128 DEC.
        DAC CYCLES$
        DAC CYCLE1$
        HLT
        LAW -1700       /-960 DEC.
        DAC SAMPLE$
        LAC IVALUE
        DAC PT$
AA      DZM* PT
        ISZ PT
        ISZ SAMPLE
        JMP AA
        700004
AGAIN   LAW -1700
        DAC SAMPLE
        LAC IVALUE
        DAC PT
        701112          /READ ADC & RESET
        701101          /FLAG                   FLAG1
        JMP .-1
        701112
        LAC (40         /BIT 12 FOR FOUR CHANNEL
        705604          /LOAD CHANNEL SELECTION
        705642          /CLEAR MEMORY
        LAC (1700
        705624          /SET COUNT TO 960
        705641          /FLAG TO INDICATE COMPLETION
        JMP .-1                                 CORE
        705642          /CLEAR DATA STROBE
        705621          /SETS ADDRESS CLEAR
FLAG    705601
        JMP .-1
        705612          /READ
        TAD* PT
        DAC* PT
        ISZ PT
        ISZ SAMPLE
        JMP FLAG
        ISZ CYCLES
        JMP AGAIN

        700044          /CLOCK ON
        LAW -1700
        DAC SAMPLE
        LAC IVALUE
        DAC PT
BB      LAC* PT
        CLL
        LRS 7           /(XBAR)
        TCA
        DAC* PT         /(-4XBAR)
        ISZ PT
        ISZ SAMPLE
        ISZ PT
        ISZ SAMPLE
        ISZ PT
        ISZ SAMPLE
        ISZ PT
        ISZ SAMPLE
        JMP BB
        HLT
        LAW -360        /240 DEC.
        DAC SAMPL1$
        LAC ISTEAD
        DAC PTT$
        DZM* PTT
        ISZ PTT
        ISZ SAMPL1
        JMP CC
        700004  /CLOCK OFF
        LAW -200
        DAC CYCLES
        LAW -360
        DAC SAMPL1
        LAW -1700
        DAC SAMPLE
        LAC IVALUE
        DAC PT
        LAC ISTEAD
        DAC PTT
        701112          /READ
        701101          /FLAG
        JMP .-1
        701112
        LAC (20         /BIT 13TH IS FOR SINGLE INPUT
        705604
        705642
        LAC (360
        705624          /SET COUNT TO 240
        705641
        JMP .-1
        705642
        705621
        705601
        JMP .-1
        705612
        TAD* PT         /(X-XBAR)
        SPA
        TCA
        DAC CORE
        CLL
        LAC CORE
        MUL
        0
        SZA
        JMP .+3
        LACQ
        JMP .+2
        LAW (777777
        TAD* PTT        /PTT+(X-XBAR)**2
        DAC* PTT
        ISZ PT
        ISZ SAMPLE
        ISZ PT
        ISZ SAMPLE
        ISZ PT
        ISZ SAMPLE
        ISZ PT
        ISZ SAMPLE
        NOP
        ISZ PTT
        ISZ SAMPL1
        JMP FLAG1
        ISZ CYCLE1
        JMP DD
        700044          /CLOCK ON
        JMS* FUNCH1
        ISZ TEST
        JMP AVESTD
        .END
```

APPENDIX C1

I. Statistical Definitions

Any collection of data can be reduced and described by its statistical properties, using a computer program to compute these parameters. The following statistical definitions were used in the analysis of raw data.

(a) The first moment or average which is usually known as the arithmetic mean value and is given by:

$$\bar{x} = \frac{1}{N} \sum_{i=1}^{N} x_i \qquad \text{(C1.1)}$$

(b) The second moment or variance is defined by:

$$\sigma^2 = \frac{1}{N-1} \sum_{i=1}^{N} (x_i - \bar{x})^2 \qquad \text{(C1.2)}$$

(c) The standard deviation, which is expressed as:

$$\sigma = \sqrt{\sigma^2} = \left[\frac{1}{N-1} \sum_{i=1}^{N} (x_i - \bar{x})^2 \right]^{\frac{1}{2}} \qquad \text{(C1.3)}$$

(d) The standard error is given by:

$$e = \sigma/\sqrt{N} \qquad \text{(C1.4)}$$

(e) The skewness or degree of symmetry as defined by:

$$Sk = \frac{1}{N \sigma^3} \sum_{i=1}^{N} (x_i - \bar{x})^3 \qquad \text{(C1.5)}$$

(f) The Kurtosis or degree of peakedness as expressed by:

$$Kt = \frac{1}{N\,\sigma^4} \sum_{i=1}^{N} (x_i - \bar{x})^4 \qquad (C1.6)$$

(g) Histogram, which is one of the most common graphical representations of the statistical data. This graphic display of the frequency distribution is usually an appropriate method for facilitating the visualization of the underlying pattern that exists in the data. In this graph, the frequency of occurrence is normally measured on a vertical axis and the values of variables on the horizontal axis.

(h) Correlogram, which is the graphical presentation of the correlation function (auto-correlation or cross-correlation function). In this graph, the vertical axis shows the values of correlation coefficients, and on the horizontal axis the values of the sample period shift are defined.

II. Correlation Technique

A recognized method of measuring the similarity between two time-series is to multiply them together, ordinate by ordinate, and add products over the duration of the time-series. This method may be applied for either continuous or sampled signals.

(i) Auto-correlation: The auto-correlation function of a time-series, $x(t)$, is a graph of the similarity between the time-series, $x(t)$, and a delayed replica of itself, $x(t-\tau)$, as a function of the time shift. Hence, for stationary data, it can be written:

$$R_{xx}(t) = \lim_{T\to\infty} \frac{1}{T} \int_{0}^{T} x(t)\, x(t-\tau)\, dt \qquad \text{(C1.7)}$$

where R is the auto-correlation

T is the integrating (averaging) time

x is the waveform of the time function

τ is the delay or time shift

If $x(t)$ is a sampled signal ($\{x_n\}$, $n = 1, 2, \ldots, N$), then (when N is relatively large) equation (C1.7) can be approximated by:

$$\hat{R}_{xx}(rh) = \frac{1}{N - r} \sum_{n=1}^{N-r} x_n\, x_{n+r} \qquad r = 0, 1, \ldots, m \qquad \text{(C1.8)}$$

where rh is the displacement

r is the lag number

m is the maximum lag number

Since the magnitude of the individual samples can be large, the computer's task of evaluating the statistical correlation will be facilitated if the auto-covariance is used. The auto-covariance is simply obtained by averaging the product of deviation from the mean and can be expressed by:

$$\hat{R}_r = \frac{1}{N - r} \sum_{n=1}^{N-r} (x_n - \bar{x})\, (x_{n+r} - \bar{x}) \qquad \text{(C1.9)}$$

A normalised auto-correlation function is obtained by dividing the auto-covariance by the zero-order auto-correlation which is equal to the variance of the sample data. Thus, it can be expressed by:

$$AC_r(x) = \frac{\hat{R}_r}{\hat{R}_o} = \frac{1}{N-r}\frac{1}{\sigma_x^2}\sum_{n=1}^{N-r}(x_n - \bar{x})(x_{n+r} - \bar{x}) \qquad (C1.10)$$

In other words, the auto-correlation function of a series of random data describes the general dependence of the values of the time-series at any particular time to its values at another time. The auto-correlation function would therefore show how successive samples of a signal are related.

(ii) Cross-correlation: The cross-correlation function of two waveforms, $x(t)$ and $y(t)$, is a graph of similarity between $x(t)$ and the delayed $y(t)$, $y(t-\tau)$ as a function of delay, τ, between them. Hence, for stationary data, it can be written:

$$C_{xy}(\tau) = \lim_{T\to\infty}\frac{1}{T}\int_o^T x(t)\, y(t-\tau)\, dt \qquad (C1.11)$$

where C is the cross-correlation

T is the integrating (averaging) time

x is the time-series (waveform)

y is the time-series

τ is the delay or time shift

When $x(t)$ and $y(t)$ are sampled signals ($\{x_n\}$ and $\{y_n\}$, $n = 1, 2, \ldots, N$), then (N is relatively large) equation (C1.11) can be approximated by:

$$\hat{C}_{xy}(rh) = \frac{1}{N-r}\sum_{n=1}^{N-r} x_n\, y_{n+r} \qquad (C1.12)$$

where rh is the displacement

r is the lag number

m is the maximum lag number

Accordingly, the normalised cross-correlation function is obtained by the following equation:

$$CC_r(x,y) = \frac{\hat{C}_r}{\hat{C}_o} = \frac{1}{N-r}\frac{1}{\sigma_x \sigma_y}\sum_{n=1}^{N-r}(x_n - \bar{x})(y_{n+r} - \bar{y}) \qquad (C1.13)$$

As the auto-correlation function of a waveform can contain only those frequency components present in the waveform itself, the cross-correlation function of two waveforms contain only those frequencies common to both waveforms. The cross-correlation of two sets of data describes the general dependence of the values of one set of data on the other.

One of the advantages of the correlation analysis is that the aperiodic functions cannot affect the resultant auto-correlation or cross-correlation functions. Thus, signals hidden by noise can be detected.

III. Power Spectral Density

Frequency information can be obtained from an auto-correlation function by calculating the Fourier transforms of the auto-correlation curve. The result is an estimate of the power spectral density of the signal, commonly called the auto-spectral function. The term "power" used in this way implies a squaring and an averaging operation.

Spectral analysis is based on the theorem that any repetitive signal can be considered to be the sum of sinusoidal components whose frequencies

are integral multiples of the basic repetition frequency. For stationary data, the auto-correlation function and power spectral density function are related by a Fourier transform as follows:

$$G_x(f) = 2 \int_{-\infty}^{\infty} R_x(\tau)\, e^{-j2\pi f\tau}\, d\tau = 4 \int_{o}^{\infty} R_x(\tau)\, \cos 2\pi f\tau\, d\tau \qquad \text{(C1.14)}$$

For sampled data, a raw estimate of power spectral density function, $G_x(f)$, for an arbitrary frequency, f, in the range of $0 < f < f_c$ is defined by:

$$\tilde{G}_x(f) = 2h \left\{\hat{R}_o + 2 \sum_{r=1}^{m-1} \hat{R}_r \cos\left(\frac{\pi r f}{f_c}\right) + \hat{R}_m \cos\left(\frac{2m f}{f_c}\right)\right\} \qquad \text{(C1.15)}$$

where h is the time interval between samples

$\hat{R}_r$ is the estimate of auto-correlation at lag r

m is maximum lag number

$f_c = 1/2h$ is the cut-off frequency

$\tilde{G}_x(f)$ is a raw estimate of true value $G_x(f)$ at frequency f

If we calculate the $\tilde{G}_x(f)$ at $(m+1)$ discrete frequencies, where:

$$f = \frac{k f_c}{m} \qquad k = 0, 1, 2, \ldots, m \qquad \text{(C1.16)}$$

then:

$$\tilde{G}_k = \tilde{G}_x\left(\frac{k f_c}{m}\right) = 2h \left\{\hat{R}_o + 2 \sum_{r=1}^{m-1} \hat{R}_r \cos\left(\frac{\pi r k}{m}\right) + (-1)^k \hat{R}_m\right\} \qquad \text{(C1.17)}$$

and estimates of the smoothed power spectral density are given by:

$$\hat{G}_k = 0.23\,\tilde{G}_{k-1} + 0.54\,\tilde{G}_k + 0.23\,\tilde{G}_{k+1} \qquad \text{(C1.18)}$$

where $\hat{G}_k$ is the smoothed power spectral density.

Subroutine ASA (the STATMAT library subroutine (1965)) was used to calculate smoothed power spectral density based on equations (C1.16) to (C1.18).

In plotted power spectral density functions, the X-axes are scaled for the parameter k, which is related to the frequency by equation (C1.16). The power spectral density function technically supplies no new information over the auto-correlation since the two are Fourier transfer pairs, but it establishes the frequency composition of the data.

APPENDIX C2

REGRESSION ANALYSIS

Methods concerning prediction of the average value of one variable in terms of the known value of another variable come under the heading of "regression analysis". The relationship between the measured (observed) variables and those which are to be predicted by means of mathematical equations is useful to assess the validity and reliability of the regression coefficients. In any problem in which prediction is to be based on mathematical equations, the kind of curve fit through the experimental data should first be decided. In the simplest form, a linear relationship between two variables associated to a given value x, a value of y as defined by:

$$y = a + b\,x + \varepsilon \tag{C2.1}$$

where a and b are numerical constants.

In practice, however, data usually do not display a perfect linear relationship due to extraneous random effects or possibilities of distortions as a result of non-linearity. Nevertheless, if a linear relationship is assumed, the value of a and b can be defined in the way that the sum of squares deviation of the measured values y from the predicted values of y_c to be minimum. This procedure is called a least square fit and is expressed by the following relationships:

$$s = \sum_{i=1}^{n} (y_i - a - b\,x_i)^2 \tag{C2.2}$$

$$\frac{\partial s}{\partial a} = \frac{\partial s}{\partial b} = 0 \tag{C2.3}$$

By solving equation (C2.3), the values of a and b (regression coefficients) can be estimated:

$$a = \frac{\Sigma x^2 \, \Sigma y - \Sigma x \, \Sigma xy}{n \, \Sigma x^2 - (\Sigma x)^2} \tag{C2.4}$$

$$b = \frac{n \, \Sigma xy - \Sigma x \, \Sigma y}{n \, \Sigma x^2 - (\Sigma x)^2} \tag{C2.5}$$

The effectiveness of y_c (predicted value) as a representative value is determined by the extent to which any individual observation is dispersed in the overall distribution of y values. The dispersion of the individual y values around the regression line is measured by the standard error of estimate:

$$\hat{\sigma}_{y,x} = \sqrt{\frac{\Sigma (y - y_c)^2}{N - m}} \tag{C2.6}$$

By putting the computed values of y_c in the above equation, the above formula can be rewritten in the following form:

$$\hat{\sigma}_{y,x} = \sqrt{\frac{\Sigma y^2 - a \, \Sigma y - b \, \Sigma xy}{N - m}} \tag{C2.7}$$

where N is the total number of paired observations

m is the number of degress of freedom lost

The standard errors of a and b when estimated from the sample data are determined by:

$$\hat{\sigma}_b = \frac{\hat{\sigma}_{y,x}}{\sqrt{\Sigma (x - \bar{x})^2}} \tag{C2.8}$$

$$\hat{\sigma}_a = \hat{\sigma}_{y,x} \left[\frac{(\Sigma x^2)}{n \Sigma (x - \bar{x})^2} \right]^{\frac{1}{2}} \tag{C2.9}$$

The total error is obtained by the sum of explained error due to regression and unexplained error about regression. The mathematical expression for these errors can be written as follows:

$$SSR = \Sigma (y_c - \bar{y})^2 \tag{C2.10}$$

$$SSD = \Sigma (y - y_c)^2 \tag{C2.11}$$

$$SST = SSR + SSD = \Sigma (y - \bar{y})^2 \tag{C2.12}$$

where *SSR* is explained error (due to regression)

SSD is unexplained error (about regression)

SST is total error

The analysis of variance can be set up by calculating the *F*-value using the following equations:

$$F = \frac{MSR}{MSD} \tag{C2.13}$$

$$MSR = \frac{SSR}{DFR} \tag{C2.14}$$

$$MSD = \frac{SSD}{DFD} \tag{C2.15}$$

where *MSR* is mean square value due to regression

MSD is mean square value about regression

DFR = 1 is the degree of freedom due to regression

DFD = $N - 2$ is the degree of freedom about regression

Subroutine G02CAF (the NAG library subroutine (1977)) was used to perform regression analysis (applying linear regression based on the above equations). By using this subroutine, the following values were calculated for each set of data.

(i) Mean of independent variable ($\bar{x}$ based on equation (C1.1))

(ii) Mean of dependent variable ($\bar{y}$ based on equation (C1.1))

(iii) Standard deviation of independent variable (σ_x based on equation (C1.3))

(iv) Standard deviation of dependent variable (σ_y based on equation (C1.3))

(v) Correlation coefficient ($CC_r(x,y)$ based on equation (C1.13) for zero order r = 0)

(vi) Regression coefficient (b based on equation (C2.5))

(vii) Standard error of coefficient (σ_b based on equation (C2.8))

(viii) T value for coefficient ($T_b = b/\sigma_b$)

(ix) Regression constant (a based on equation (C2.4))

(x) Standard error of regression constant (σ_a based on equation (C2.9))

(xi) T value for constant ($T_a = a/\sigma_a$)

(xii) Sum of squares due to regression (SSR based on equation (C2.10))

(xiii) Sum of squares about regression (SSD based on equation (C2.11))

(xiv) Total sum of squares (SST based on equation (C2.12))

(xv) Mean square due to regression (MSR based on equation (C2.14))

(xvi) Mean square about regression (MSD based on equation (C2.15))

(xvii) F value (analysis of variance F based on equation (C2.13)).

Tables C2.1, C2.2, C2.3 and C2.4 demonstrate the regression analysis output for Test 19A, Test 19AP, Test 19C and Test 19E, respectively, at an engine speed of 2500 rpm and an engine load of 6.38 mkp.

TABLE C2.1(a): Regression Analysis of Test 19A

Speed = 2500 rpm; Load = 6.38 mkp

Generated values for τ

τ = starting angle of injection (^{o}CA BTDC)

$\hat{dP}$ = maximum rate of cylinder pressure rise (psi)

$\theta(\hat{dP})$ = location of $\hat{dP}$ (^{o}CA BTDC)

$\hat{P}$ = peak cylinder pressure

TAU	$\hat{DP}$	$\theta(\hat{DP})$	$\hat{P}$
.1755E+02	.9569E+01	-.1480E+02	.7224E+03
.2138E+02	.6245E+02	-.5800E+01	.9054E+03
.2097E+02	.6933E+02	-.5800E+01	.9174E+03
.1763E+02	.3826E+02	-.9800E+01	.7917E+03
.1797E+02	.4146E+02	-.9800E+01	.8085E+03
.1763E+02	.4107E+02	-.9800E+01	.8012E+03
.1790E+02	.4285E+02	-.3800E+01	.8109E+03
.1869E+02	.5187E+02	-.7800E+01	.8460E+03
.1588E+02	.3004E+02	-.1180E+02	.7366E+03
.1878E+02	.5319E+02	-.7800E+01	.8498E+03

REGRESSION ANALYSIS FOR TAU & $\hat{DP}$:

MEAN OF INDEPENDENT VARIABLE	=	18.179
MEAN OF DEPENDENT VARIABLE	=	49.667
STANDARD DEVIATION OF INDEPENDENT VARIABLE	=	2.176
STANDARD DEVIATION OF DEPENDENT VARIABLE	=	21.749
CORRELATION COEFFICIENT	=	.943
REGRESSION COEFFICIENT	=	9.422
STANDARD ERROR OF COEFFICIENT	=	.337
T-VALUE FOR COEFFICIENT	=	27.970
REGRESSION CONSTANT	=	-121.617
STANDARD ERROR OF CONSTANT	=	6.167
T-VALUE FOR CONSTANT	=	-19.720

ANALYSIS OF REGRESSION TABLE :

SOURCE	SUM OF SQUARES	D.F.	MEAN SQUARE	F-VALUE
DUE TO REGRESSION	41615.6947	1.	41615.6947	782.3057
ABOUT REGRESSION	5213.2279	98.	53.1962	
TOTAL	46828.9226	99.		

TABLE C2.1(b)

REGRESSION ANALYSIS FOR TAU & $\theta(\hat{DP})$:

MEAN OF INDEPENDENT VARIABLE	= 18.179
MEAN OF DEPENDENT VARIABLE	= -8.780
STANDARD DEVIATION OF INDEPENDENT VARIABLE	= 2.176
STANDARD DEVIATION OF DEPENDENT VARIABLE	= 3.015
CORRELATION COEFFICIENT	= .976
REGRESSION COEFFICIENT	= 1.352
STANDARD ERROR OF COEFFICIENT	= .031
T-VALUE FOR COEFFICIENT	= 43.997
REGRESSION CONSTANT	= -33.354
STANDARD ERROR OF CONSTANT	= .562
T-VALUE FOR CONSTANT	= -59.298

ANALYSIS OF REGRESSION TABLE :

SOURCE	SUM OF SQUARES	D.F.	MEAN SQUARE	F-VALUE
DUE TO REGRESSION	856.5935	1.	856.5935	1935.7372
ABOUT REGRESSION	43.3665	98.	.4425	
TOTAL	899.9600	99.		

REGRESSION ANALYSIS FOR TAU & $\hat{P}$:

MEAN OF INDEPENDENT VARIABLE	= 18.179
MEAN OF DEPENDENT VARIABLE	= 829.440
STANDARD DEVIATION OF INDEPENDENT VARIABLE	= 2.176
STANDARD DEVIATION OF DEPENDENT VARIABLE	= 77.500
CORRELATION COEFFICIENT	= .965
REGRESSION COEFFICIENT	= 34.353
STANDARD ERROR OF COEFFICIENT	= .949
T-VALUE FOR COEFFICIENT	= 36.195
REGRESSION CONSTANT	= 204.929
STANDARD ERROR OF CONSTANT	= 17.376
T-VALUE FOR CONSTANT	= 11.794

ANALYSIS OF REGRESSION TABLE :

SOURCE	SUM OF SQUARES	D.F.	MEAN SQUARE	F-VALUE
DUE TO REGRESSION	553227.9077	1.	553227.9077	1310.0640
ABOUT REGRESSION	41384.4920	98.	422.2907	
TOTAL	594612.3997	99.		

STOP

TABLE C2.2(a): Regression Analysis of Test 19AP

Speed = 2500 rpm; Load = 6.38 mkp

Experimental values for τ

TAU	$\hat{DP}$	$\Theta(\hat{DP})$	$\hat{P}$
.2406E+02	.2408E+02	-.7800E+01	.8102E+03
.1826E+02	.2778E+02	-.1080E+02	.7597E+03
.1738E+02	.3188E+02	-.1080E+02	.7649E+03
.1931E+02	.5196E+02	-.6800E+01	.8550E+03
.1773E+02	.4088E+02	-.8800E+01	.8014E+03
.1738E+02	.3792E+02	-.9800E+01	.7852E+03
.1908E+02	.4480E+02	-.8800E+01	.8166E+03
.1632E+02	.3218E+02	-.1090E+02	.7494E+03
.1738E+02	.3908E+02	-.9800E+01	.7893E+03
.1826E+02	.4601E+02	-.8800E+01	.8246E+03

REGRESSION ANALYSIS FOR TAU & $\hat{DP}$:

MEAN OF INDEPENDENT VARIABLE	=	18.058
MEAN OF DEPENDENT VARIABLE	=	30.716
STANDARD DEVIATION OF INDEPENDENT VARIABLE	=	2.712
STANDARD DEVIATION OF DEPENDENT VARIABLE	=	27.822
CORRELATION COEFFICIENT	=	.905
REGRESSION COEFFICIENT	=	9.283
STANDARD ERROR OF COEFFICIENT	=	.441
T-VALUE FOR COEFFICIENT	=	21.048
REGRESSION CONSTANT	=	-116.921
STANDARD ERROR OF CONSTANT	=	8.053
T-VALUE FOR CONSTANT	=	-14.519

ANALYSIS OF REGRESSION TABLE :

SOURCE	SUM OF SQUARES	D.F.	MEAN SQUARE	F-VALUE
DUE TO REGRESSION	62749.1448	1.	62749.1448	443.0209
ABOUT REGRESSION	13880.6471	98.	141.6393	
TOTAL	76629.7919	99.		

TABLE C2.2(b)

REGRESSION ANALYSIS FOR TAU & $\hat{B}(\hat{DP})$:

MEAN OF INDEPENDENT VARIABLE	=	18.058
MEAN OF DEPENDENT VARIABLE	=	-8.480
STANDARD DEVIATION OF INDEPENDENT VARIABLE	=	2.712
STANDARD DEVIATION OF DEPENDENT VARIABLE	=	3.595
CORRELATION COEFFICIENT	=	.970
REGRESSION COEFFICIENT	=	1.286
STANDARD ERROR OF COEFFICIENT	=	.032
T-VALUE FOR COEFFICIENT	=	39.594
REGRESSION CONSTANT	=	-31.705
STANDARD ERROR OF CONSTANT	=	.593
T-VALUE FOR CONSTANT	=	-53.457

ANALYSIS OF REGRESSION TABLE :

SOURCE	SUM OF SQUARES	D.F.	MEAN SQUARE	F-VALUE
DUE TO REGRESSION	1204.4649	1.	1204.4649	1567.6667
ABOUT REGRESSION	75.2951	98.	.7683	
TOTAL	1279.7600	99.		

REGRESSION ANALYSIS FOR TAU & $\hat{P}$:

MEAN OF INDEPENDENT VARIABLE	=	18.058
MEAN OF DEPENDENT VARIABLE	=	827.262
STANDARD DEVIATION OF INDEPENDENT VARIABLE	=	2.712
STANDARD DEVIATION OF DEPENDENT VARIABLE	=	92.799
CORRELATION COEFFICIENT	=	.938
REGRESSION COEFFICIENT	=	32.103
STANDARD ERROR OF COEFFICIENT	=	1.197
T-VALUE FOR COEFFICIENT	=	26.826
REGRESSION CONSTANT	=	247.560
STANDARD ERROR OF CONSTANT	=	21.849
T-VALUE FOR CONSTANT	=	11.330

ANALYSIS OF REGRESSION TABLE :

SOURCE	SUM OF SQUARES	D.F.	MEAN SQUARE	F-VALUE
DUE TO REGRESSION	750376.8342	1.	750376.8342	719.6497
ABOUT REGRESSION	102184.3421	98.	1042.6974	
TOTAL	852561.1763	99.		

TABLE C2.3(a): Regression Analysis of Test 19C

Speed = 2500 rpm; Load = 6.38 mkp

Generated random data for τ and m_f

TAU	$\hat{DP}$	$\hat{B}\langle\hat{DP}\rangle$	$\hat{P}$
.1755E+02	.1801E+02	-.1930E+02	.9435E+03
.2097E+02	.3871E+02	-.7800E+01	.8604E+03
.1797E+02	.2366E+02	-.1080E+02	.7758E+03
.1790E+02	.3084E+02	-.1080E+02	.8049E+03
.1588E+02	.2267E+02	-.1280E+02	.7704E+03
.1761E+02	.3336E+02	-.9800E+01	.8082E+03
.1221E+02	.2189E+02	-.1680E+02	.7702E+03
.1618E+02	.1502E+02	-.1190E+02	.7699E+03
.1737E+02	.2800E+02	-.1080E+02	.7845E+03
.1501E+02	.3047E+02	-.1380E+02	.7703E+03

REGRESSION ANALYSIS FOR TAU & $\hat{DP}$:

MEAN OF INDEPENDENT VARIABLE	=	18.288
MEAN OF DEPENDENT VARIABLE	=	41.393
STANDARD DEVIATION OF INDEPENDENT VARIABLE	=	2.300
STANDARD DEVIATION OF DEPENDENT VARIABLE	=	26.484
CORRELATION COEFFICIENT	=	.844
REGRESSION COEFFICIENT	=	9.715
STANDARD ERROR OF COEFFICIENT	=	.624
T-VALUE FOR COEFFICIENT	=	15.559
REGRESSION CONSTANT	=	-136.280
STANDARD ERROR OF CONSTANT	=	11.508
T-VALUE FOR CONSTANT	=	-11.842

ANALYSIS OF REGRESSION TABLE :

SOURCE	SUM OF SQUARES	D.F.	MEAN SQUARE	F-VALUE
DUE TO REGRESSION	49427.4723	1.	49427.4723	242.0375
ABOUT REGRESSION	20008.8468	98.	204.1719	
TOTAL	69436.3191	99.		

TABLE C2.3(b)

REGRESSION ANALYSIS FOR TAU & B($\hat{DP}$):

MEAN OF INDEPENDENT VARIABLE	= 18.288
MEAN OF DEPENDENT VARIABLE	= -9.205
STANDARD DEVIATION OF INDEPENDENT VARIABLE	= 2.300
STANDARD DEVIATION OF DEPENDENT VARIABLE	= 3.503
CORRELATION COEFFICIENT	= .930
REGRESSION COEFFICIENT	= 1.416
STANDARD ERROR OF COEFFICIENT	= .057
T-VALUE FOR COEFFICIENT	= 25.003
REGRESSION CONSTANT	= -35.104
STANDARD ERROR OF CONSTANT	= 1.044
T-VALUE FOR CONSTANT	= -33.627

ANALYSIS OF REGRESSION TABLE :

SOURCE	SUM OF SQUARES	D.F.	MEAN SQUARE	F-VALUE
DUE TO REGRESSION	1050.2114	1.	1050.2114	625.1408
ABOUT REGRESSION	164.6361	98.	1.6800	
TOTAL	1214.8475	99.		

REGRESSION ANALYSIS FOR TAU & $\hat{P}$:

MEAN OF INDEPENDENT VARIABLE	= 18.288
MEAN OF DEPENDENT VARIABLE	= 841.500
STANDARD DEVIATION OF INDEPENDENT VARIABLE	= 2.300
STANDARD DEVIATION OF DEPENDENT VARIABLE	= 76.740
CORRELATION COEFFICIENT	= .825
REGRESSION COEFFICIENT	= 27.526
STANDARD ERROR OF COEFFICIENT	= 1.905
T-VALUE FOR COEFFICIENT	= 14.449
REGRESSION CONSTANT	= 338.112
STANDARD ERROR OF CONSTANT	= 35.111
T-VALUE FOR CONSTANT	= 9.630

ANALYSIS OF REGRESSION TABLE :

SOURCE	SUM OF SQUARES	D.F.	MEAN SQUARE	F-VALUE
DUE TO REGRESSION	396763.9155	1.	396763.9155	208.7662
ABOUT REGRESSION	186250.7686	98.	1900.5180	
TOTAL	583014.6841	99.		

STOP

TABLE C2.4(a): Regression Analysis of Test 19E

Speed = 2500 rpm; Load = 6.38 mkp

Experimental data

TAU	$\hat{DP}$	$\Theta(\hat{DP})$	$\hat{P}$
.2408E+02	.1813E+02	-.6328E+01	.4950E+03
.1828E+02	.7062E+02	-.3867E+01	.8983E+03
.1740E+02	.4677E+02	-.5273E+01	.7966E+03
.1834E+02	.5965E+02	-.4219E+01	.8360E+03
.1775E+02	.5392E+02	-.5273E+01	.7901E+03
.1740E+02	.7540E+02	-.4219E+01	.8786E+03
.1811E+02	.6394E+02	-.3516E+01	.8524E+03
.1635E+02	.4677E+02	-.7031E+01	.7409E+03
.1740E+02	.7921E+02	-.3867E+01	.9048E+03
.1828E+02	.5058E+02	-.5273E+01	.7966E+03

REGRESSION ANALYSIS FOR TAU & $\hat{DP}$:

MEAN OF INDEPENDENT VARIABLE	=	18.081
MEAN OF DEPENDENT VARIABLE	=	60.122
STANDARD DEVIATION OF INDEPENDENT VARIABLE	=	2.712
STANDARD DEVIATION OF DEPENDENT VARIABLE	=	19.564
CORRELATION COEFFICIENT	=	.567
REGRESSION COEFFICIENT	=	4.088
STANDARD ERROR OF COEFFICIENT	=	.600
T-VALUE FOR COEFFICIENT	=	6.809
REGRESSION CONSTANT	=	-13.796
STANDARD ERROR OF CONSTANT	=	10.977
T-VALUE FOR CONSTANT	=	-1.257

ANALYSIS OF REGRESSION TABLE :

SOURCE	SUM OF SQUARES	D.F.	MEAN SQUARE	F-VALUE
DUE TO REGRESSION	12168.8883	1.	12168.8883	46.3589
ABOUT REGRESSION	25724.3353	98.	262.4932	
TOTAL	37893.2236	99.		

TABLE C2.4(b)

REGRESSION ANALYSIS FOR TAU & $\theta(\hat{DP})$:

MEAN OF INDEPENDENT VARIABLE	= 18.081
MEAN OF DEPENDENT VARIABLE	= -4.743
STANDARD DEVIATION OF INDEPENDENT VARIABLE	= 2.712
STANDARD DEVIATION OF DEPENDENT VARIABLE	= 1.473
CORRELATION COEFFICIENT	= .626
REGRESSION COEFFICIENT	= .340
STANDARD ERROR OF COEFFICIENT	= .043
T-VALUE FOR COEFFICIENT	= 7.956
REGRESSION CONSTANT	= -10.897
STANDARD ERROR OF CONSTANT	= .782
T-VALUE FOR CONSTANT	= -13.933

ANALYSIS OF REGRESSION TABLE :

SOURCE	SUM OF SQUARES	D.F.	MEAN SQUARE	F-VALUE
DUE TO REGRESSION	84.3479	1.	84.3479	63.3007
ABOUT REGRESSION	130.5846	98.	1.3325	
TOTAL	214.9325	99.		

REGRESSION ANALYSIS FOR TAU & $\hat{P}$:

MEAN OF INDEPENDENT VARIABLE	= 18.081
MEAN OF DEPENDENT VARIABLE	= 827.678
STANDARD DEVIATION OF INDEPENDENT VARIABLE	= 2.712
STANDARD DEVIATION OF DEPENDENT VARIABLE	= 95.328
CORRELATION COEFFICIENT	= .548
REGRESSION COEFFICIENT	= 19.261
STANDARD ERROR OF COEFFICIENT	= 2.970
T-VALUE FOR COEFFICIENT	= 6.485
REGRESSION CONSTANT	= 479.415
STANDARD ERROR OF CONSTANT	= 54.300
T-VALUE FOR CONSTANT	= 8.829

ANALYSIS OF REGRESSION TABLE :

SOURCE	SUM OF SQUARES	D.F.	MEAN SQUARE	F-VALUE
DUE TO REGRESSION	270129.9913	1.	270129.9913	42.0520
ABOUT REGRESSION	629523.2490	98.	6423.7066	
TOTAL	899653.2404	99.		

STOP

REFERENCES

ANDON, J., & MARKS, C. (1964)

"Engine Roughness - The Key to Lower Octane Requirement",

SAE Trans., Vol. 72, Paper 647A, pp. 636-658.

ANDREE, A., & PACHERNEGG, S.J. (1969)

"Ignition Conditions in Diesel Engines",

SAE Trans., Paper 690253, pp. 1082-1105.

AUSTEN, A.E.W., & LYN, W.T. (1960-61)

"Relation Between Fuel Injection and Heat Release in a Direct Injection Engine and the Nature of the Combustion Processes",

Proc. Inst. Mech. Engrs., No. 1, pp. 47-62.

BARTON, R.K., KENEMUTH, D.K., LESTZ, S.S., & MEYER, W.E. (1970)

"Cycle-by-Cycle Variations of a Spark Ignition Engine - A Statistical Analysis",

Paper 700488 presented at SAE Mid-Year Meeting, Detroit, May 1970.

BARTON, R.K., LESTZ, S.S., & MEYER, W.E. (1971)

"An Empirical Model for Correlating Cycle-by-Cycle Cylinder Gas Motion and Combustion Variations of a Spark Ignition Engine",

SAE Trans., Vol. 80, Paper 710163, pp. 695-707.

BENDAT, J.S., & PIERSOL, A.G. (1971)

"Analysis and Measurement Procedures of Random Data",

John Wiley & Sons Incorporated, New York.

BENSON, R.S., & PICK, R. (1974)

"Recent Advances in Internal Combustion Engine Instrumentation with Particular Reference to High-Speed Data Acquisition and Automated Test Bed",

SAE Trans., Paper 740695, Vol. 83, pp. 2569-2585.

BLOXHAM, R.D., JONES, T.F., MURGATROYD, W., & WING, R.D. (1972)
"Computer Control for IC Engines Development",
Chartered Mechanical Engineer, October 1972.

BOX, G.E.P., & JENKINS, G.M. (1970)
"Time-Series Analysis, Control and Forecasting",
Holden-Day Incorporated.

BROWN, W.L. (1967)
"Methods for Evaluating Requirements and Errors in Cylinder Pressure Measurement",
Paper 67008 presented at Automotive Eng. Congress, Detroit, January 1967.

BURGETT, R.R., LEPTICH, J.M., & SANGWAN, K.V.S. (1972)
"Measuring the Effect of Spark Plug and Ignition System Design on Engine Performance",
SAE Trans., Paper 720007, pp. 48-66.

CHAMBERLAIN, L.J. (1970)
"A Simple Discussion of Time-Series Analysis",
Time/Data AGR Company, November 1970.

*CHEN, S.K., & FLYN, T. (1965)
"Development of Compression Ignition Research Engine",
SAE Paper 650733.

CHEN, K.K., & KRIEGER, R.B. (1976)
"A Statistical Analysis of the Influence of Cyclic Variation on the Formation of Nitric Oxide in Spark Ignition Engines",
Combustion Science & Technology, Vol. 12, pp. 125-134.

---

* References which are marked by asterisks * refer to additional works which have not been consulted.

CLARKE, J.S. (1960-61)

"Initiation and Some Controlling Parameters of Combustion in the Piston Engine",

Proc. Inst. Mech. Engrs., No. 5, pp. 165-189.

COLE, D.E., & MIRSKY, W. (1968)

"Mixture Motion - Its Effect on Pressure Rise in a Combustion Bomb: A New Look at Cyclic Variation",

SAE Trans., Vol. 77, Paper 680766, pp. 2993-3007.

CONTE, S.D. (1965)

"Elementary Numerical Analysis",

McGraw-Hill Incorporated, International Student Edition.

CONTROL DATA 6000 SERIES COMPUTER SYSTEM (1965)

"Statistical Subroutine General Information Manual",

Subroutine ASA, STATMAT Subroutine Library, Control Data Corporation, U.S.A.

CRAMER, H. (1946)

"Mathematical Methods of Statistics",

Princeton University Press, U.S.A.

CURRY, S. (1963)

"A Three-Dimensional Study of Flame Propagation in a Spark Ignition Engine",

SAE Trans., Vol. 71, Paper 452-B, pp. 628-650.

DIGITAL EQUIPMENT CORPORATION (1972)

"PDP-15 System Reference Manual",

Maynard, Massachusetts, U.S.A.

DIGITAL PDP-8 HANDBOOK SERIES (1972)

"Introduction to Programming",

Digital Equipment Corporation, Vol. 1.

EICHELBERG, G. (1939)

"Some New Investigations on Old Combustion Engine Problems - III",

Engineering (London), Vol. 148, pp. 547-550.

*ESCHENBACH, R.C., & AGNEW, J.T. (1958)

"Use of Constant-Volume Bomb Technique for Measuring Burning Velocity",

Combustion & Flame, Vol. 2, pp. 273-285.

FISHER, R.V., & MACEY, J.P. (1975)

"Digital Data Acquisition with Emphasis on Measuring Pressure Synchronously with Crank Angle",

SAE Trans., Paper 750025.

GEE, D.E., & KARIM, G.A. (1966)

"Heat Release in a Compression Ignition Engine",

The Engineer, September 1966, pp. 473-479.

*GENERAL ELECTRIC COMPANY (1955)

"Properties of Combustion Gases/System: $C_n H_{2n}$- Air",

GEC Aircraft Gas-Turbine Development Department, Cincinnati, Ohio, U.S.A., Vols. 1 & 2.

GHOBADIAN, A. (1976)

"Some Preliminary Investigations into the Computer Simulation of Cyclic Dispersion in a Single Cylinder Spark Ignition Engine",

M.Sc. Thesis, University of Manchester Institute of Science and Technology.

GLAUERT, M.B. (1956)

"The Wall Jet",

J. Fluid Mech., December 1956.

GRIGG, H.C., & SYED, M.H. (1969-70)

"The Problem of Predicting Rate of Heat Release in Diesel Engines",

Proc. Inst. Mech. Engrs., Vol. 184, Pt. 3J, pp. 192-202.

GRIGG, H.C. (1976)

"The Rôle of Fuel Injection Equipment in Reducing 4-Stroke Diesel Engine Emissions",

SAE Trans., Paper 760126, Vol. 85, pp. 491-501.

GRIGG, H.C. (1977)

Discussion on the paper "The Rotary Fuel Injection Pump as a Source of Cyclic Variation in Diesel Engines and its Effect on Nitric Oxide Emissions",

Proc. Inst. Mech. Engrs.

HANSEL, J.G. (1970)

"A Turbulent Combustion Model of Cycle-to-Cycle Combustion Variations in Spark Ignition Engines",

Combustion Science & Technology, Vol. 2, pp. 223-225.

HANSEL, J.G. (1971)

"Lean Automotive Engine Operation - Hydrocarbon Exhaust Emissions and Combustion Characteristics",

SAE Trans., Paper 710164, pp. 708-722.

HARLAND, G.E., PAN'KO, M.A., GILL, K.F., & SCHWARZENBACH, J. (1969)

"Pseudo-Random Signal Testing Applied to a Diesel Engine",

Control, February 1969, pp. 137-140.

HEIZMAN, C.L. (1970)

"Signal Analysis with Digital Time-Series Analysers",

General Radio Experimenter, July/September 1970.

HENEIN, N.A., & BOLT, J.A. (1967)

"Ignition Delay in Diesel Engines",

Paper 670007 presented at Automotive Eng. Congress, Detroit, January 1967.

HENEIN, N.A., & BOLT, J.A. (1972)

"Kinetic Considerations in the Auto-Ignition and Combustion of Fuel Sprays in Swirling Air",

ASME Paper 72-DGP-4 presented at Diesel & Gas Turbine Power Conf., St Louis, U.S.A., April 1972.

HENEIN, N.A., & SINGH, T. (1974)

"Effect of Imposed Faults on a Distributor Injection System",

SAE Trans., Paper 740531.

HOWES, P. (1969)

"A Procedure for the Specification of Distributor Pumps for High Volume Production",

Paper 690602 presented at SAE Farm, Construction & Industrial Machinery Meeting, Milwaukee, U.S.A., September 1969.

JONES, P.E. (1966-67)

"Induction System Development for High Performance Direct Injection Diesel Engines",

Proc. Inst. Mech. Engrs., Vol. 180, Pt. 3N, p. 39.

JONES, T.F. (1970)

"The On-Line Control of a Diesel Engine",

M.Sc. Thesis, Imperial College, University of London.

JONES, T.F., & WING, R.D. (1975)

"On-Line Computer Control for Automatic Testing of IC Engines",

Conf. on Automatic Testing Technology, Inst. Elec. & Radio Engrs., April 1975.

JUDGE, A.W. (1967)

"High Speed Diesel Engines",

Chapman & Hall Limited, Sixth Edition.

KARIM, G.A. (1967)

"An Examination of the Nature of the Random Cyclic Pressure Variations in a Spark Ignition Engine",

J. Inst. Pet., Vol. 53, No. 519, pp. 112-120.

KARIM, G.A., & SARPAL, G. (1975)

"An Analytical Examination of the Rôle of Small Perturbations in Operating Parameters on Cyclic Pressure Variations in an Engine",

IECEC '75 Record, Paper 759027, pp. 159-161.

KASTNER, L.J., WILLIAMS, T.J., & WHITE, J.B. (1963-64)

"Popet Inlet Valve Characteristics and Their Influence on the Induction Process",

Proc. Inst. Mech. Engrs., Vol. 178, Pt. 1, p. 955.

KHAN, I.M., GREEVES, G., & WHITMORE, A.F. (1972)

"Further Development of Fuel Jet Model for Calculating Fuel-Air Mixing in Direct Injection Diesel Engines",

CAV Research Department, Internal Report, January 1972.

KRIEGER, R.B., & BORMAN, G.L. (1966)

"The Computation of Apparent Heat Release for Internal Combustion Engines",

ASME Paper 66-WA/DGP-4 presented at Winter Annual Meeting.

LANCASTER, D.R., KRIEGER, R.B., & LIENESCH, J.H. (1975)

"Measurement and Analysis of Engine Cylinder Pressure Data",

SAE Trans., Paper 750026, pp. 155-172.

LEE, Y.W. (1966)

"Statistical Communication Theory",

John Wiley & Sons, London.

LYN, W.T. (1963)

"Study of Burning Rate and Nature of Combustion in Diesel Engines", 9th Symposium on Combustion, Academic Press, New York.

LYN, W.T., & VALDMANIS, E. (1966-67)

"The Effects of Physical Factors on Ignition Delay", *Proc. Inst. Mech. Engrs.*, Vol. 181, Pt. 2A, No. 1.

MARZOUK, M., & WATSON, N. (1976)

"Program IMCOENG Manual", Imperial College, Internal Report.

MARZOUK, M., & WATSON, N. (1976)

"Some Problems in Diesel Engine Research with Special Reference to Computer Control and Data Acquisition", *Proc. Inst. Mech. Engrs.*, Vol. 190, 23/76, pp. 137-151.

MARZOUK, A.M. (1976)

"Simulation of Turbocharged Diesel Engine under Transient Conditions", Ph.D. Thesis, Imperial College, University of London.

MATSUOKA, S., YAMAGUCHI, T., & UMEMURA, Y. (1971)

"Factors Influencing the Cyclic Variation of Combustion of Spark Ignition Engines", Paper 710586 presented at SAE Mid-Year Meeting, Montreal, Canada, June 1971.

MODARRES-RAZAVI, M.R. (1973)

"Diesel Engine Fuel Injection Measurements - Study of Fuel-Line", M.Sc. Thesis, Imperial College, University of London.

MILKINS, E.E., WATSON, H.C., GOLDSWORTHY, L.C., & HALLWORTH, R.J. (1974)

"Cycle-by-Cycle Variability in Emissions of a Spark Ignition Engine", *SAE Trans.*, Paper 741034.

THE NAG (NUMERICAL ALGORITHMS GROUP) (1977)

"Subroutines G02CAF & G05AEF",

ICCC Bulletin 5.2/1, Fifth Version, August 1977.

OBERT, E.F. (1970)

"Internal Combustion Engine Analysis and Practice",

International Text Book Company, Scranton, Pennsylvania, U.S.A.,

Third Edition.

PARKS, P.C., & CLARKSON, B.L. (1964-65)

"Some Theory and Practice of Random Process Analysis",

Proc. Inst. Mech. Engrs., Vol. 179, Pt. 3H, pp. 105-115.

PATTERSON, D.J. (1966)

"Cylinder Pressure Variations - A Fundamental Combustion Problem",

SAE Trans., Vol. 75, Paper 660129, pp. 621-632.

PEDERSEN, P.S., & QVALE, B. (1974)

"A Model for the Physical Part of the Ignition Delay in a Diesel Engine",

SAE Trans., Paper 740716, pp. 2625-2638.

PETERS, B.D., & BORMAN, G.L. (1970)

"Cyclic Variations and Average Burning Rate in an SI Engine",

Paper 700064 presented at SAE Automotive Eng. Congress, Detroit, January 1970.

PIRES, R.M.M. (1973)

"Injection and Combustion Phenomena in a Direct Injection Diesel Engine - A Statistical Analysis",

M.Sc. Thesis, Imperial College, University of London.

RASSWEILER, G.M., & WITHROW, L. (1938)

"Motion Pictures of Engine Flames Correlated with Pressure Cards",

SAE Trans., Vol. 33, pp. 185-204.

RAZAVI, M.R.M. (1977)

Discussion on the paper "The Rotary Fuel Injection Pump as a Source of Cyclic Variation in Diesel Engines and its Effect on Nitric Oxide Emissions",

Proc. Inst. Mech. Engrs., Vol. 189, 50/75.

*RÖGENER, H. (1949)

"Entzündung von Kohlenwasserstoff-Luft Gemischen durch Adiabatische Verdichtung",

Zeitschrift für Elektro-Chemie, Vol. 53, No. 6, p. 389.

*SCHMIDT, F.A.F. (1938)

"Theoretische Untersuchungen und Versuche über Zündverzug und Klopfvorgang",

VDI-Forschungsheft, No. 392.

SCHWEITZER, P.H. (1938)

"Oil Sprays (An Investigation of Velocities and Penetrations)",

The Automobile Engineer, pp. 61-64.

SHAHED, S.M., CHIU, W.S., & LYN, W.T. (1975)

"A Mathematical Model of Diesel Combustion",

Proc. Inst. Mech. Engrs., Combustion in Engines Conf., Paper C94/75, July 1975, pp. 119-128.

SHIPINSKI, J., UYEHARA, O.A., & MYERS, P.S. (1968)

"Experimental Correlations Between Rate-of-Injection and Rate-of-Heat-Release in a Diesel Engine",

ASME Paper 68-DGP-11.

SHIPINSKI, J., MYERS, P.S., & UYEHARA, O.A. (1969-70)

"A Spray Droplet Model for Diesel Combustion",

Proc. Inst. Mech. Engrs., Vol. 184, Pt. 3J, pp. 28-35.

*SITKEI, G. (1963)

"Uber den Dieselmotorischen Zündverzug" (On the Ignition Delay in Diesel Engines),

MTZ, 24 Jg., Heft 6, pp. 190-194.

SNEDECOR, G.N., & COCHRAN, W.G. (1967)

"Statistical Methods",

The Iowa State University Pressure, U.S.A., Sixth Edition.

SOLTAU, J.P. (1960-61)

"Cylinder Pressure Variations in Petrol Engines",

Proc. Inst. Mech. Engrs., Vol. 2, pp. 99-117.

STREIT, E.E., & BORMAN, G.L. (1971)

"Mathematical Simulation of a Large Turbocharged Two-Stroke Diesel Engine",

SAE Trans., Paper 710076, Appendix E (Fitting of Experimental Data by Spline Function).

TANUMA, T., SASAKI, K., KANEKO, T., & KAWASAKI, H. (1971)

"Ignition, Combustion, and Exhaust Emissions of Lean Mixture in Automotive Spark Ignition Engines",

SAE Trans., Paper 710159, pp. 663-674.

VICHNIEVSKY, R. (1955)

"Combustion in Petrol Engines",

Proc. Joint Conf. on Combustion, IME/ASME, London, October 1955, pp. 288-299.

WATSON, H.C., GOLDSWORTHY, L.C., & MILKINS, E.E. (1976)

"Cycle-by-Cycle Variations of HC, CO, and NOx",

Paper 760753 presented at Automobile Eng. Meeting, Dearborn, October 1976.

WATSON, N., & MARZOUK, M. (1974)

"Apparent Rate of Heat Release for Perkins 4.236 Diesel Engine", Unpublished Report for Perkins.

*WIEBE, I.I. (1956)

"Halbempirische Formel für die Verbrennungs-Geschwindigkeit", *Verlag der Akademie der Wissenschaften der VdSSR*, Moscow, Russia.

WING, R.D., & MURGATROYD, W. (1972)

"Statistical Methods in the Study of Cyclic Variations in Diesel Engines",
Internal Report, Imperial College, University of London.

WING, R.D., & JONES, T. (1973)

"Perkins Software System",
Collected as an Internal Report, Thermal Power Section, Imperial College, University of London.

WING, R.D. (1975)

"The Rotary Fuel Injection Pump as a Source of Cyclic Variation in Diesel Engines and its Effect on Nitric Oxide Emissions", *Proc. Inst. Mech. Engrs.*, Vol. 189, 50/75, pp. 497-505.

WINSOR, R.E., & PATTERSON, D.J. (1973)

"Mixture Turbulence - A Key to Cyclic Combustion Variation", *SAE Trans.*, Paper 730086, pp. 368-383.

*WOLFER, H.H. (1938)

"Der Zündeverzug im Dieselmotor" (The Injection Delay in Diesel Engines), *VDI-Forschungsheft*, No. 392, pp. 15-24.

YEVJEVICH, V. (1972)

"Stochastic Process in Hydrology",
Water Resources Publications.

*ZIMMERMANN, K.D. (1962)

"Uber den Zündverzug bei der Dieselmotorischen Verbrennung",

Diss., Karlsruhe.

TSAO, K.C., MYERS, P.S., & UYEHARA, O.A. (1962)

"Gas Temperature During Compression in Motored and Fired Diesel

Engines",

SAE Trans., Vol. 70, p. 136.